EPA-600/R-05/035
AFRL-ML-TY-TR-2002-4506
January 2005

Final Report: Membrane-Mediated Extraction and Biodegradation of Volatile Organic Compounds from Air

Stephen W. Peretti and Robert D. Shepherd
North Carolina State University
Raleigh, NC 27695

Russell K. Clayton and David E. Proffitt
ARCADIS Geraghty & Milller
4915 Prospectus Drive
Durham, NC 27713

EPA Project Officer
Norman Kaplan
Office of Research and Development
National Risk Management Research Laboratory
109 T.W. Alexander Drive
Research Triangle Park, NC 27711

AIR FORCE RESEARCH LABORATORY
MATERIALS & MANUFACTURING DIRECTORATE
AIR EXPEDITIONARY FORCES TECHNOLOGIES DIVISION
139 BARNES DRIVE, STE 2
TYNDALL AFB FL 32403-5323

Report Documentation Page

Form Approved
OMB No. 0704-0188

1. REPORT DATE	2. REPORT TYPE	3. DATES COVERED
10 NOV 2001		**-**

4. TITLE AND SUBTITLE	5a. CONTRACT NUMBER
Membrane-Mediated Extraction and Biodegradation of VOCs from Air	**F08637-98-c-6002**
	5b. GRANT NUMBER
	5c. PROGRAM ELEMENT NUMBER **63716D**
6. AUTHOR(S) **Stephen Peretti; Robert Shepherd; Russell Clayton; David Proffitt**	5d. PROJECT NUMBER **3904**
	5e. TASK NUMBER **A3**
	5f. WORK UNIT NUMBER **3904A38B**
7. PERFORMING ORGANIZATION NAME(S) AND ADDRESS(ES) **ARCADIS Geraghty & Miller,4915 Prospectus Drive,Durham,NC,27713**	8. PERFORMING ORGANIZATION REPORT NUMBER **EPA-600/R-05/035**
9. SPONSORING/MONITORING AGENCY NAME(S) AND ADDRESS(ES)	10. SPONSOR/MONITOR'S ACRONYM(S)
	11. SPONSOR/MONITOR'S REPORT NUMBER(S)

12. DISTRIBUTION/AVAILABILITY STATEMENT
Approved for public release; distribution unlimited

13. SUPPLEMENTARY NOTES

14. ABSTRACT

This report describes feasibility tests of a two-step strategy for air pollution control applicable to exhaust air contaminated with volatile organic compounds (VOCs) from painting aircract. In the first step of the two-step strategy, the VOC-contaminated exhaust air passes over coated, polypropylene, hollow-fiber membranes while an involatile liquid (silicone oil, mineral oil, decanol, octanol) is pumped counter-current through the filters. The organic liquid captures the VOCs, and their concentration in the circulating liquid increases whenever exhaust air circulates. In the second step, the circulating organic loop passes through a second set of hollow-fiber membranes that support a culture of microorganisms, which remove and metabolize the VOCs, on their exterior surfaces. The concentration of VOCs in the circulating loop oscillates as the painting process starts and stops because VOC capture by the liquid is a fast process whereas removal and metabolization by microorganisms is a slow process. Despite constraints caused by limited availability of commercial membrane packages, adequate rates of removal and transport into and out of circulating octanol were shown to be adequate to support the proposed technology. Biodegradation was also qualitatively validated, although each of the organisms used in these tests selectively metabolized specific classes of solvents; however, other cultures or sequential treatment stages are expected to provide statisfactory removal. Scale-up revealed material incompatibility of the membranes and adhesives with octanol. Silicone oils and vegetable oils were briefly tested as the circulating organic liquid at the end of the project. Pressure drop also remains as an engineering challenge unless ventilation exhause rates are decreased.

15. SUBJECT TERMS

16. SECURITY CLASSIFICATION OF:			17. LIMITATION OF ABSTRACT	18. NUMBER OF PAGES	19a. NAME OF RESPONSIBLE PERSON
a. REPORT	b. ABSTRACT	c. THIS PAGE			
unclassified	**unclassified**	**unclassified**		**186**	

NOTICES

USING GOVERNMENT DRAWINGS, SPECIFICATIONS, OR OTHER DATA INCLUDED IN THIS DOCUMENT FOR ANY PURPOSE OTHER THAN GOVERNMENT PROCUREMENT DOES NOT IN ANY WAY OBLIGATE THE US GOVERNMENT. THE FACT THAT THE GOVERNMENT FORMULATED OR SUPPLIED THE DRAWINGS, SPECIFICATIONS, OR OTHER DATA DOES NOT LICENSE THE HOLDER OR ANY OTHER PERSON OR CORPORATION; OR CONVEY ANY RIGHTS OR PERMISSION TO MANUFACTURE, USE, OR SELL ANY PATENTED INVENTION THAT MAY RELATE TO THEM.

THIS TECHNICAL REPORT HAS BEEN REVIEWED AND IS APPROVED FOR PUBLICATION.

JOSEPH D. WANDER, Ph.D
Program Manager

GLEN T. SHEN, PhD
Chief, Weapons Systems Logistics Branch

DONALD R. HUCKLE, Col, USAF
Chief, Airbase Technologies Division

This report is published in the interest of scientific and technical information exchange and does not constitute approval or disapproval of its ideas or findings.

Do not return copies of this report unless contractual obligations or notice on a specific document requires its return.

Foreword

The U.S. Environmental Protection Agency (EPA) is charged by Congress with protecting the Nation's land, air, and water resources. Under a mandate of national environmental laws, the Agency strives to formulate and implement actions leading to a compatible balance between human activities and the ability of natural systems to support and nurture life. To meet this mandate, EPA's research program is providing data and technical support for solving environmental problems today and building a science knowledge base necessary to manage our ecological resources wisely, understand how pollutants affect our health, and prevent or reduce environmental risks in the future.

The National Risk Management Research Laboratory (NRMRL) is the Agency's center for investigation of technological and management approaches for preventing and reducing risks from pollution that threaten human health and the environment. The focus of the Laboratory's research program is on methods and their cost-effectiveness for prevention and control of pollution to air, land, water, and subsurface resources; protection of water quality in public water systems; remediation of contaminated sites, sediments and ground water; prevention and control of indoor air pollution; and restoration of ecosystems. NRMRL collaborates with both public and private sector partners to foster technologies that reduce the cost of compliance and to anticipate emerging problems. NRMRL's research provides solutions to environmental problems by: developing and promoting technologies that protect and improve the environment; advancing scientific and engineering information to support regulatory and policy decisions; and providing the technical support and information transfer to ensure implementation of environmental regulations and strategies at the national, state, and community levels.

This publication has been produced as part of the Laboratory's strategic long-term research plan. It is published and made available by EPA's Office of Research and Development to assist the user community and to link researchers with their clients.

Sally Gutierrez, Acting Director
National Risk Management Research Laboratory

EPA Review Notice

This report has been peer and administratively reviewed by the U.S. Environmental Protection Agency and approved for publication. Mention of trade names or commercial products does not constitute endorsement or recommendation for use.

This document is available to the public through the National Technical Information Service, Springfield, Virginia 22161.

Abstract

This report describes feasibility tests of a two-step strategy for air pollution control applicable to exhaust air contaminated with volatile organic compounds (VOCs) from painting aircraft. In the first step of the two-step strategy, the VOC-contaminated exhaust air passes over coated, polypropylene, hollow-fiber membranes while an involatile organic liquid (silicone oil, mineral oil, decanol, octanol) is pumped counter-current through the fibers. The organic liquid captures the VOCs, and their concentration in the circulating liquid increases whenever exhaust air circulates. In the second step, the circulating organic liquid loop passes through a second set of hollow-fiber membranes that support a culture of microorganisms, which remove and metabolize the VOCs, on their exterior surfaces. The concentration of VOCs in the circulating liquid loop oscillates as the painting process starts and stops because VOC capture by the liquid is a fast process whereas removal and metabolization by microorganisms is a slow process. Despite constraints caused by limited availability of commercial membrane packages, adequate rates of removal and transport into and out of circulating octanol were shown to be adequate to support the proposed technology. Biodegradation was also qualitatively validated, although each of the organisms used in these tests selectively metabolized specific classes of solvents; however, other cultures or sequential treatment stages are expected to provide satisfactory removal. Scale-up revealed material incompatibility of the membranes and adhesives with octanol. Silicone oils and vegetable oils were briefly tested as the circulating organic liquid at the end of the project. Pressure drop also remains as an engineering challenge unless ventilation exhaust rates are decreased.

Acknowledgments

This research was supported by the U.S. Department of Defense through the Strategic Environmental Research and Development Program (SERDP). This report was prepared under Contract Number 68-C-99-201 for the U.S. Environmental Protection Agency (EPA), Research Triangle Park, NC.

This final report describes work performed from 1 March 1998 to 30 January 2001. The Co-Principal Investigators were first Norman Kaplan then Jack Wasser of EPA's National Risk Management Research Laboratory (NRMRL) and Dr. Joe Wander of the Air Force Research Laboratory (AFRL/MLQ).

The authors particularly acknowledge the contributions and guidance of Bradley Smith and Dr. Robert Holst of the SERDP Program Office and the review panel members, without whose help this study would not have been possible.

Table of Contents

Table of Contents (continued)

Section **Page**

Index of Tables

Index of Figures

Blank Page

Executive Summary

A. Objective

The objective of this project was to examine the feasibility of capturing and destroying volatile organic compounds (VOCs) from process or storage exhaust air by extracting the VOCs through a coated, hollow-fiber membrane into an involatile liquid and then metabolizing them with bacteria residing on the exterior surface of a second, coated, hollow-fiber membrane.

B. Background

1. VOC Emissions from Large Aircraft-Painting Facilities

Implementation of the Clean Air Act in the form of the National Emission Standards for Hazardous Air Pollutants for aerospace coating operations (Aerospace Manufacturing and Rework Facilities NESHAP) imposed a requirement that large aircraft-painting operations either apply an emission control system to decrease the amount of VOC emitted to the atmosphere by at least a threshold amount (originally 81 percent) or apply coating materials that contain less than a specified (for each) threshold amount of VOCs. Strenuous efforts to develop competent low-VOC coatings have not been uniformly successful, and use of these compliant coatings generally involves compromises in coat quality and durability and in preparation, application, and curing time and effort.

By most standards, the option to control emissions is by far the superior approach because it preserves availability of coatings that have been optimized after decades of development and experience, because it involves no changes to the established painting methods and techniques, and because the amount of VOCs emitted are less than half that from an equivalent operation conducted with low-VOC coatings. However, ventilation of an aircraft-painting facility makes inefficient use of air by continuously ventilating the entire volume of a hangar while painting is conducted intermittently in a much smaller part of it, so the exhaust volume is large and the level of contamination is low. Both factors act to drive up the cost to decontaminate these exhausts by conventional VOC control methods.

The Strategic Research & Development Program (SERDP) issued Statement of Need CP-98, VOC Control Technology for Aircraft Painting and Depainting Facilities as a call for develop-ment and evaluation of alternative technologies that, alone or in combination with flow-reduction technologies (e.g., exhaust recirculation), would decrease the cost to control emissions of VOCs from aircraft

painting operations. Heat generation and loss in processes handling flow rates approaching 1M ft^3/min is commonly the main source of cost, fuel consumption, and greenhouse gas and airborne pollutant generation. As efforts to oxidize organic vapors by catalysis at low temperatures have found success only with such easily oxidized materials as aldehydes and thioethers, the most-promising avenue of development is through concentration of the VOCs prior to destruction. Recovery is possible as well but rarely economical for gross mixtures of solvents.

2. Membrane Extraction and Biotreatment

With appropriate modification of the structural polymeric surface, hollow-fiber membranes (HFMs) allow selective passage of molecules based on their physical properties. Significant research has examined separation and biotreatment of VOCs from air streams with varying degrees of success. A literature search performed during this project led to several pertinent conclusions regarding membrane configuration, materials of construction, extraction fluid, module operation and control of biofouling. These conclusions are summarized as follows:

1. Hollow fiber shell-and-tube membrane modules offer the highest possible surface-area-to-volume ratio, roughly an order of magnitude more than the nearest alternate, the spiral-wound configuration.
2. Asymmetric, composite membranes composed of a highly porous support membrane coated by a thin, nonporous, permselective film offer the most effective combination of perme-ability and selectivity.
3. For gas-liquid systems, it is most efficient to have the coating film contacted by the liquid phase and the pores filled by the gas. For instances where the coating film is the predominant mass transfer resistance, the fluid that fills the pores is less important.
4. The composition of the coating film is critical to performance. In decreasing order of permeability to organic vapors, it was found that poly[(1-trimethylsilyl)-1-propyne] (PTMSP) is greater than polydimethylsiloxane (PDMS) which is greater than polyalkylsulfone (PAS-16), other rubbery polymers are greater than fluoropolymers. Although PTMSP exhibits the highest permeability to organic vapors, its performance decays relatively rapidly over time, so it is not considered suitable for long-term commercial applications. PDMS is a rubbery polymer that, along with other silicone rubber derivatives, is the material of choice by researchers involved in organic vapor separations. PAS-16 is relatively uncharacterized but offers excellent properties as a rubbery polymer with local crystallinity.
5. Lower temperatures favor organic vapor separations.
6. Removal percentages in excess of 95 percent are possible with membrane extraction systems operated with gas–membrane contact times on the order of 20 seconds.
7. Low-vapor-pressure oils and alcohols (silicone oil, mineral oil, decanol, octanol) exhibit excellent solubility and permeability characteristics for organic vapor separation, with silicone

oil exhibiting optimal performance in composite membranes.

Peretti et al. have filed for a patent for the use of coated HFMs with involatile solvents to capture VOCs from furniture-finishing industries and to biodegrade the VOCs by a process of direct capture across a second HFM by bacteria colonizing the external surface.

Figure E-1 depicts the functional elements and flows in the Membrane Extraction and Biotreatment (MBT) process. Contaminated exhaust gas enters at the bottom left and is stripped of VOCs as it passes upward through an array of parallel HFMs. The stripped exhaust is released to the atmosphere, so the amount of VOC in the treated exhaust is the total amount released, and this amount defines the efficiency of the control device. An involatile solvent circulates inside the HFMs opposite to the direction of airflow, so the concentration of captured VOCs increases downward to the point of entry of the facility exhaust before entering the bottom of the membrane bioreactor (MBR).

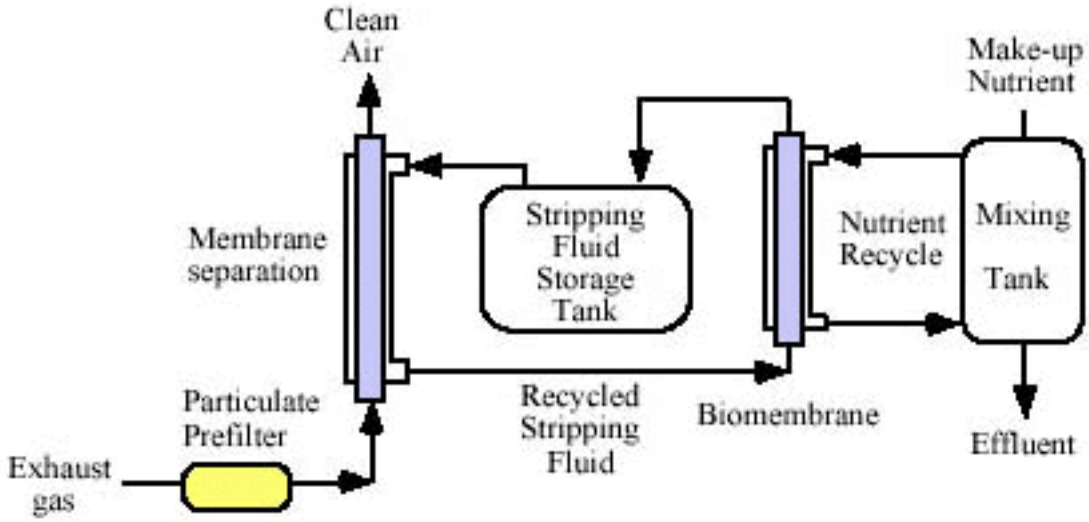

Figure E-1. MBT System Schematic

The MBR is a similar array of parallel HFMs surrounded by a nutrient medium circulated downward among the HFMs to sustain a culture of microorganisms adhering to their surface. The solvent and its load of VOCs rises inside the HFMs while the microorganisms capture and consume part of the VOCs. During periods of painting, VOCs will enter the system faster than the microorganisms can

consume them. The stripping fluid storage tank is a reservoir of fluid with an unreacted VOC concentration that increases gradually during painting and subsides during interludes between painting episodes. This distribution of peak load serves both to decrease the size of the MBR and to ensure a fairly constant rate of delivery of VOCs to the MBR.

Operating equations were derived to describe the membrane separation processes for a system with non-coated hollow fibers and using octanol as the stripping fluid. The final result for the separation/concentration unit was a design equation that relates concentration, partition coefficient, membrane surface area, and flow rate to an overall mass transfer coefficient, K_o. The K_o is based on the overall system driving force and is defined by a sum of resistances model. In the equation shown below for K_o in the separation/concentration unit, the concentration (C) subscripts A and O denote the air and octanol phases, and subscripts 1 and 2 represent inlet and outlet conditions, respectively. P is the air/octanol equilibrium partition coefficient, Q is the volumetric flow of the respective phases (cubic centimeters per second), and A_m is the membrane surface area (square centimeters).

$$K_O = \frac{\ln\left(\dfrac{\dfrac{C_{A2}}{P} - C_{O2}}{\dfrac{C_{A1}}{p} - C_{O1}}\right)}{A_m\left(\dfrac{1}{Q_O} - \dfrac{1}{Q_A P}\right)}$$

Experiments were initially conducted using individual pure VOCs that are typical components of paints to assess mass transfer rates and removal efficiencies. Studies progressed to include VOC mixtures and real military paint. Degradation of VOCs was measured for individual and mixed biofilm cultures. All of these experiments were necessary because both the separation and biotreatment processes are competitive among the species present.

C. Scope

This is the final technical report for SERDP project CP-1105, Membrane-Mediated Extraction and Biotreatment of VOCs. Results of the first half of the project have been presented at two national meetings. The associated long abstracts published in the respective meeting proceedings are included as Appendixes D and E.

D. Methodology

Initial evaluations of mass transfer coefficients for the membrane module were conducted by quantifying the removal of each individual VOC [*m*-xylene, toluene, methyl ethyl ketone (MEK)] from an air stream. Experiments were performed to determine the effect of airflow rate, stripping fluid flow rate, air stream VOC concentration, and stripping fluid VOC concentration on overall mass transfer coefficients. This early work was performed using the Celgard Liqui-Cell module. The focus of the separation/concentration process development was aimed at producing a module that provided high-efficiency removal of VOCs from the airstream at high air flow rates and low pressure drop.

E. Test Description

Numerous biotreatment experiments were conducted to determine efficacy of the proposed biotreatment module for enhanced VOC removal from the stripping fluid. These studies included the following:

- Screening experiments to identify organisms able to degrade paint VOCs
- Liquid–liquid stripping efficiency of MEK with and without a biofilm present
- Degradation of individual and mixed VOCs with individual and mixed organism biofilms
- Growth of degraders and degradation of single and mixed VOCs to determine strain characterization, substrate range, metabolic regulation, and organism interactions
- Capacity of dual organisms in staged reactors to degrade mixtures of differently soluble VOCs

F. Results and Discussion

The Celgard Liqui-Cell membrane module, or contactor, was used in the early bench-scale experiments. Because of the difference in pressures between the air and stripping fluid sides of the HFMs, some leakage of stripping fluid into the air occurred. Because it is not economically feasible to pressurize the air side to prevent this leakage, the application of a thin coating of a VOC-permeable coating to the HFMs, preferably on the inside of the fibers to maximize mass transfer was considered. Acceptable coated fibers and modules were not commercially available, and work with a number of vendors to provide a suitable contactor proved to be unsuccessful. An in situ coating technique for the Celgard contactor was developed but was found to be too time consuming as a cost-effective approach.

A secondary issue regarding cost-effective contactor design was the relatively high pressure required to drive the air through the Celgard module. Discussions were held with module vendors to develop an efficient separation/concentration module with non-porous coated fibers and low pressure drop. Applied Membrane Technologies (AMT) was selected to provide a cross-flow module design with fibers externally coated with plasma-polymerized silicone rubber. The coating was found to perform

adequately, but the fibers themselves elongated when exposed to the octanol stripping fluid. This led to the substitution of silicone oil as the stripping fluid. Upon developing a feasible module design, pilot testing was performed to validate its performance.

Two basic sizes were tested. Bench scale tests using 1 and 2 modules were done using the Celgard microporous hollow-fiber membrane module coated with perfluorodimethyldioxole and tetrafluoro-ethylene (PDD-TFE). Pilot scale studies with paint vapors were done using the AMT module coated with silicone rubber in arrangements of 2 and 10 modules. Test flow rates up to 200 crm provided contact times of less than 0.1 sec with the coated membrane.

In the bench-scale testing, VOC removal rates ranged between 4.4 percent and 73.7 percent. Higher air side flow, lower oil flow, and lower VOC inlet concentrations were generally associated with lower removal rates. Pilot-scale test results were variable and sometimes difficult to understand. Average VOC removal rates were 34–80 percent, while removal of individual compounds ranged from17 to 82 percent. As in the bench-scale testing, MEK proved to be the most difficult compound to extract from the air. A major problem with the cross-flow modules occurred when leaking modules allowed the fibers to become wetted with the less-viscous silicone oil, causing fiber elongation and subsequent voids between some fibers and matting of others. This resulted in poor contact with the air stream and reduced VOC removal rates. Time and funding limitations prevented actions to address these issues. These problems resulted in a reduction in planned pilot scale stream from 500 cfm to 200 cfm.

G. Conclusions

The membrane-supported biofilm modules successfully removed VOCs from the recirculating stripping fluid stream. Degradation of the aromatic compounds investigated (toluene, *m*-xylene) was achieved; these compounds were not observed in the aqueous phase above the biofilm. MEK biodegradation is problematic, appearing to be partially inhibited by toluene and *m*-xylene. Further studies are required to ascertain the underlying mechanism.

A fully-integrated pilot system was not successfully demonstrated. Although the test results did not meet the research goal of 85-95%, the MBT concept showed potential for being developed into a technically feasible process. However, the MBT concept has been shown to offer several attractive benefits:

- Continuous biotreatment of VOCs directly from the stripping fluid avoids the mechanical complexities of sequential medium transfers found in most concentrate-and-treat designs (e.g., air-to-adsorber-to-lower-volume-air-stream, and thence to final treatment).
- Continuous recirculation of captured VOCs through the biotreatment module provides

complete destruction of captured VOCs.

- Modularity of the MBT unit allows linear scaling of a large system by connection of *n* units in parallel
- Modularity of the MBT unit allows amplification of the net capture-and-removal efficiency by connection of two or more units in series.

H. Recommendations

Several serious obstacles remain before a practical MBT system can be applied to a painting operation:

- Available materials of construction must be compatible with each other (fiber, coating, assembly adhesives), with the stripping fluid, with the microorganisms, and with the VOCs to be treated.
- Manufacturing techniques for membrane modules must advance enough to allow cost effective fabrication of low-pressure drop, high efficiency, leak-free modules.
- Microbiological cultures must be identified that can coexist and metabolize all of the VOCs to be treated at practical rates.
- Some engineering relief may be possible, but the ventilation system must be able to accommodate a fairly large pressure loss (>25 in. H_2O) across the HFM array, consistent with acceptable process economics.

Additional fundamental and applied research is needed to fill out the understanding of these processes. Design and eventual commercial availability of properly configured and scaled hollow-fiber membrane modules must occur before MBT or related technologies can be implemented on a practical scale. Finally, this technology will be compatible only with processes that can tolerate a moderate pressure (>20 in. H_2O) loss through its control system, for example, low flow high concentration sources.

1.0 Objective

The objective of this project was to examine the feasibility of developing a practical VOC control method using coated, hollow-fiber membranes to extract organic vapors from ventilation exhaust streams into a circulating pool of an involatile liquid and to deliver the organics at a buffered rate to a biofilm adhering to the exterior surface of a separate, coated membrane.

1.1 Background

This project was performed in response to the Statement of Need for FY98 SERDP, Com-pliance New Start Number 2 (CPSON2), entitled, "VOC Control Technology for Aircraft Painting and Depainting Facilities." Painting and coating operations present a number of environmental problems and economic challenges. Volatile organic compounds (VOCs) and other hazardous air pollutants (HAPs) are present in all currently used coatings. The toxic compounds include metals, metal oxides, and VOCs. Many of these compounds are either direct or indirect health threats; VOCs are ozone precursors and may be designated as toxic, and many metals and metallic oxides are identified on toxic compound lists. In response to the Clean Air Act Amendments of 1990, VOCs and HAPs in coatings are being reduced, thereby reducing emissions of ozone precursors and toxic compounds from painting operations. However, additional controls are mandated in specific instances, such as aircraft booths. The National Emissions Standard for Hazardous Air Pollutants (NESHAP) specific to aircraft painting will force the DoD to either implement volatile hazardous air pollutant (VHAP) control technology or replace existing coating formulations. Because efforts to develop replacement coatings have met with only mixed success, implementation of control technology appears to be the most-promising near-term solution.

Control technology cost primarily depends on contaminated airflow rates. Paint spray booth exhausts are high-volume streams because an obsolete OSHA standard requiring a minimum velocity of 100 ft/min) through all booth section areas remains in the public record. Conventional booth design approaches include no provision for adjusting flowrate, relying instead on using a high flowrate with clean filters that will remain above the 100-fpm threshold after the filters are dirtied. If controls are required for VOC destruction, the necessary equipment must be sized for the maximum exhaust flow rate. As a result, typical booths emit large volumes of air contaminated with dilute concentrations of VOCs and HAPs. Many current technologies treat the VOCs within the entire gas volume directly, leading to large-volume incineration, absorption, or biofiltration systems. These technologies are extremely expensive in terms of both capital and operating expenses. Also, they often generate hazardous byproduct streams that must be further treated. The system evaluated in this research was designed to both minimize the treated volume and to concentrate the VOCs within that treated volume in order to reduce the size and cost of the ultimate control device. These

advantages would make this VOC treatment option applicable across a broad range of spray booth sizes.

Such a VOC control system could eliminate a significant portion of toxic materials emissions from DoD installations. Past data regarding aircraft service reported in *Air Force Times* indicate that 5 of the top 10 air discharges that triggered Toxic Release Inventory reporting thresholds from 131 DoD installations were typical paint constituents. Significant reduction of these emissions in a cost-effective manner is important to DoD's adherence to the 1995 Aerospace NESHAP for Aerospace Manufacturing and Rework Facilities and to its meeting existing and evolving limits for VOC emissions in ozone nonattainment areas.

1.1.1 Membrane BioTechnology Development Background

During initial Membrane BioTechnology (MBT) development, tests were performed to assess the ability of hollow-fiber membrane contactors to separate VOCs from an air stream. A membrane separation system was constructed to allow contact of VOC- laden air streams with octanol inside a Hoechst-Celanese Liqui-Cel hollow-fiber module. The entire membrane separation system used in initial experiments is shown schematically in Figure 1. A stripping fluid, octanol, was passed through the unit's shell space while air flowed through the fibers. The two phases contacted in counter-current cross flow. The octanol reservoir was recycled to the module, but air passed through the system only once. Air flow rates were varied from 10 to 40 L/min, giving a minimum gas/membrane contact time of 0.004 seconds based on the inside volume of the hollow fibers. The air-side pressure drop ranged from 0.5 to 2.0 psi, and the total surface area available for mass transfer was 1.4 m^2.

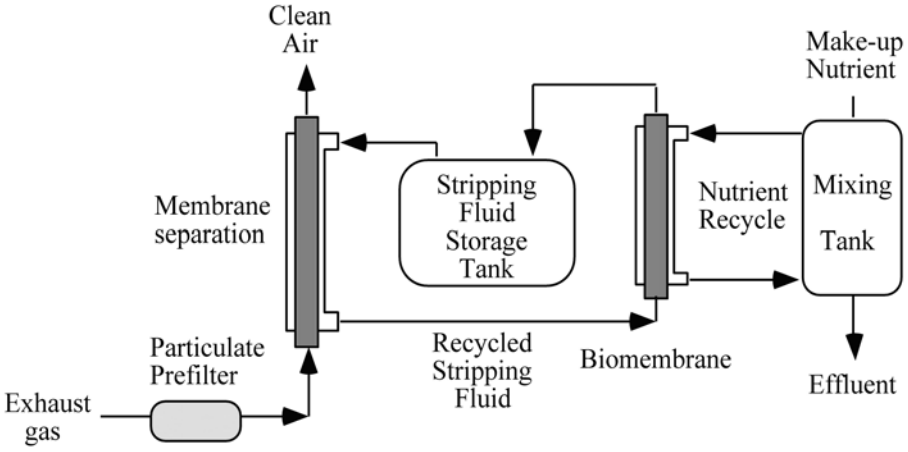

Figure 1. MBT System Schematic

Biological degradation experiments were conducted with naturally occurring microorganisms isolated from soil samples removed from a site contaminated with gasoline. Using a mixed consortium of organisms isolated in liquid culture from soil samples removed from this site, degradability of model compounds from each of the species found in furniture exhaust gases was examined (Table 1). Following completion of these initial studies, organism subcultures were generated for specific compounds. By enrichment of the initial gasoline-adapted consortium in individual flasks with isobutyl acetate (IBA), methanol (MeOH), methyl ethyl ketone (MEK), methyl isobutyl ketone (MIBK), *m*-xylene, and *p*-xylene, respectively, consortia capable of degrading each compound were developed.

Table 1. Compounds Successfully Biodegraded

Acetone	Benzene
Diethylene glycol ethyl ether	Ethylene glycol butyl ether
Formaldehyde	Ethanol
Isobutyl isobutyrate	Isobutyl acetate (IBA) *
Methyl ethyl ketone (MEK) *	Methanol
Methyl *n*-amyl ketone	Methyl isobutyl ketone (MIBK) *
n-Butyl alcohol *	Styrene
Toluene *	*m*-Xylene *
o-Xylene *	*p*-Xylene *

* Indicates compounds common to DoD painting operations

One pure culture, designated MX-2, was established on *m*-xylene and another, PX-2, was established on *p*-xylene. Other consortia which grew on either IBA, MEOH, MEK, or MIBK consisted of approximately three different organisms each. Maximum growth rates for the isolated consortia were determined in shake flask studies containing low-ionic-strength buffer solution supplemented with the appropriate carbon source. Growth rates obtained with *m*-xylene in the presence of additional carbon sources and with pure octanol are given in Table 2.

The partition coefficient is defined as the ratio of concentrations of a given compound in two phases (octanol/air and octanol/H_2O) at equilibrium. Before beginning work with Liqui-Cel membrane modules, partition coefficient experiments were performed to investigate the equilibrium distribution of *m*-xylene, MEK, and MIBK between phases for stripping fluid/air and stripping fluid/aqueous systems. Octanol was chosen as the stripping fluid. Values of the partition coefficient at different temperatures are given in Table 3.

Table 2. Growth Rates of MX-2 with Modified Carbon Sources

Carbon Source	Specific Growth Rate[a]	Degradation Rate[b]
m-Xylene	0.46 hr^{-1}	3.60×10^{-10} mg/(hr-cell)
m-Xylene + 0.2% MeOH	0.45 hr^{-1}	3.57×10^{-10} mg/(hr-cell)
m-Xylene + 0.2% EtOH[c]	0.40 hr^{-1}	2.34×10^{-10} mg/(hr-cell)
m-Xylene + 500 ppm[d] octanol	0.46 hr^{-1}	3.60×10^{-10} mg/(hr-cell)
500 ppm octanol (no *m*-xylene)	0.20 hr^{-1}	not applicable

[a] The specific growth rates are reported as the rate of change of cell dry mass divided by the cell dry mass.

[b] The degradation rate is the rate of removal of *m*-xylene (in mg per mL of medium per hour) divided by the cell density (in cells per mL).

[c] Ethyl alcohol.

[d] Mass/mass

Table 3. Partition Coefficient Values

Temp.	Partition Coefficient [octanol]/[air]			Partition Coefficient [octanol]/[water]		
	***m*-Xylene**	**MEK**	**MIBK**	***m*-Xylene**	**MEK**	**MIBK**
6 °C	9865	2181	NA[a]	NA	NA	NA
22 °C	7978	1634	22,045	NA	NA	NA
31 °	7703	1344	8721	1021	33	2.1

[a] NA=not analyzed

Experiments were also conducted to examine the range of compounds degradable by enzymes present in the *meta*- and *para*-xylene-degrading organisms. As shown in Table 4, these organisms successfully removed many compounds that are typically difficult to biodegrade. Higher values for oxygen uptake indicate a compound is being more rapidly degraded.

An additional set of experiments was run to evaluate alternative stripping fluids because commercially available octanol is fairly expensive. Partition coefficients were determined for *m*-xylene in corn oil, sunflower seed oil, and mineral oil at 31 °C. The respective partition coefficients ([oil]/[air]) were 8283, 8244, and 7284, comparable to that of octanol. These oils cost about one-fourth that of octanol.

Table 4. Oxygen Uptake Rates for Various VOCs

Compound	Oxygen Uptake, mmol/min-mg Total Cell Protein	
	Strain PX-2	Strain MX-2
p-Xylene	0.34	1.21
m-Xylene	0.31	0.82
o-Xylene	NA	0.31
Toluene	0.17	0.18
Benzene	0.13	0.27
Styrene	0.47	0.55
Benzoic acid	2.34	0.66
Catechol	5.19	1.23
3-Methylcatechol	1.50	1.17
4-Methylcatechol	4.35	0.92
Protocatechuic acid	0.00	0.32

1.1.2 Treatment Process Concept

In the Membrane BioTreatment (MBT) system, organic volatiles are first separated from the air stream, concentrated, and then completely metabolized by microorganisms. Selective removal and concentration of VOCs from the exhaust stream enables significant reduction in the volume directed to the final control device, dramatically reducing equipment size and costs. The system allows for independent optimization of each process. One process removes organics from the air, and the other process biodegrades them. The system relies on micro-porous hollow-fiber membrane contactors to mediate the extraction and concentration of vapors from the air into an organic stripping fluid and to provide a physical support for degradative microorganisms. A schematic of the MBT system appears in Figure 1.

Exhaust gases laden with VOCs pass first through a particle filter, which removes solid particles and any residual atomized droplets of coatings. Next, the gases enter a membrane separation/concentration (S/C) unit composed of bundles of microporous, hydrophobic fibers. In the S/C unit, vaporized HAPs and VOCs (represented as dark particles) are transferred from the exhaust gases into a stripping-fluid medium (potentially octanol, silicone oil, sunflower seed oil, etc.), as shown in Figure 2. The stripping fluid is chosen to have low volatility, low water solubility, and high (fluid/air) partition coefficients for the VOCs. The medium serves as a pollutant sink and allows accumulation of significant HAP/VOC concentrations.

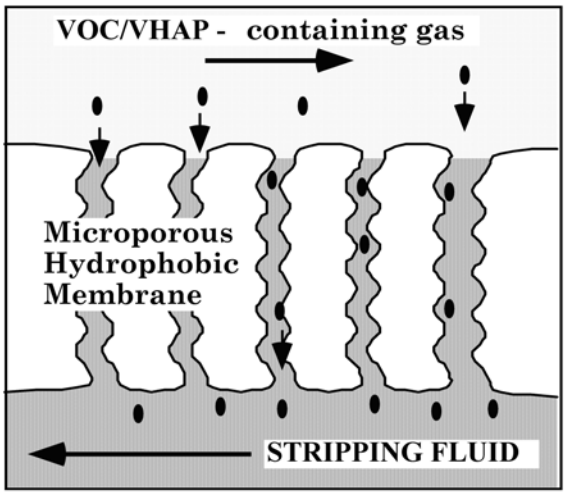

Figure 2. VOC Extraction in the S/C Unit

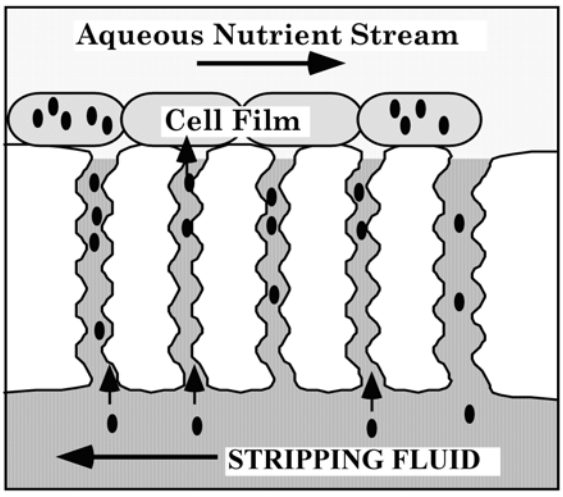

Figure 3. Bioextraction of VOCs

Upon exiting the S/C unit, the stripping fluid is delivered to a biomembrane unit. There, the stripping fluid circulates past one side of another microporous membrane with VOC-degrading bacteria in a film on the opposite side of the membrane. Figure 3 illustrates diffusion of VOCs through the membrane pores (filled with stripping fluid) into the biofilm, in which they are selectively and completely metabolized by the bacteria. The solvent is then collected in a storage vessel and ultimately recycled through the S/C. When hydrocarbon pollutants are treated, outputs from the overall MBT System are clean air, carbon dioxide, and a mixture of water and nonhazardous cell mass.

In the design of a full-scale system for a military paint spray booth, further economic gains can be realized by reducing the contaminated air volume through the application of partitioned recirculation. This patented technology was developed through EPA and Air Force funding to reduce the cost of VOC control by minimizing the treated volume. This technology takes advantage of the fact that, in horizontal-flow booths, the lower segment of a paint booth exhaust contains more highly concentrated VOCs, and conversely, the upper segment exhaust contains lower VOC concentrations. This characteristic allows both the recirculation of a significant portion of the exhaust (30 to 90 percent) without adverse health and safety implications, and a comparable reduction in the size of the required VOC control device. Adding on this technology enables a two-step reduction in the volume of VOC-contaminated streams to be treated: first, partitioned recirculation concentrates the VOCs into a smaller air volume; and second, the S/C unit concentrates the VOCs in a proportionally smaller volume of stripping fluid for biodegradation.

MBT offers potential unique advantages due to the nature of the control technology and the impact

of implementation on coating operations. Advantages include the following:

- **High VOC destruction:** Naturally occurring bacteria consume pollutants as food for growth and energy.
- **Non-Pollutant-Generating Process:** MBT is a clean process with no hazardous by-products.
- **Optimized Rates of Removal and Degradation:** Having separate processes for removal and destruction of pollutant compounds allows each to be designed and operated for maximum efficiency, and equipment size is minimized.
- **Adaptability:** MBT is fully adaptable to individual sites. S/C units are modular, which allows the pollutant-removal process to be tailored to site-specific operations, facilities, and regulatory permit requirements. Selection and optimization of suitable micro-organisms ensures effective degradation of site-specific HAPs and VOCs.
- **Extended Equipment Life:** Each module of the S/C units may be changed on an individual basis, and extra modules may be built into the system and/or kept on site to make replacement easier.
- **Operating Flexibility:** The stripping fluid storage vessel allows the MBT system to operate continuously to control intermittent processes. For example, some coating operations are single-shift, resulting in eight hours of waste generation followed by 16 hours of down time. In other instances, painting facilities may be off line for days or even weeks. The storage tank mitigates the interruptions in waste generation—that is, the tank *uncouples waste generation from biotreatment*, which allows the biotreatment process to operate at optimal levels regardless of spray booth schedules. A VOC feedstock can be manually introduced to maintain the bacterial colonies during extended interludes between painting episodes.
- **Cost-Effective Treatment:** Original estimates indicated that this system would be significantly less costly than other typical VOC control systems for medium and large paint spray booths.

1.2 Scope

This is the final technical report describing a 2-year project supported by the Strategic Environmental Research and Development Program [SERDP].

2.0 Technical Objectives

The overall objective of this small, pilot project was to validate and extend development of a potentially cost-effective VOC control system for painting facilities that meets the requirements of the Aerospace Coatings NESHAP—81 percent reduction in VOCs from noncompliant coatings. This was believed to be feasible by combining the partitioned recirculation technique for flow reduction with a novel process that concentrates VOCs for biological treatment. The project was designed as a two-phase activity consisting of bench- and pilot-scale efforts. The objective of the project in phase I was to demonstrate that membrane-supported extraction, coupled with membrane-supported biotreatment, is a technically feasible VOC treatment process for DoD painting emissions. In phase II, the objective was to establish the technical and econo-mical efficacy of this process to treat actual aircraft painting emissions. The original concept was to use the paint booth facilities at Tyndall AFB as the pilot test site, but that option was abandoned after technical difficulties caused delays and added costs. Secondary goals of Phase II included both attention to the effects of particulate fouling on membrane transfer performance and dissemination of information about the technology by identifying all DoD sites and organizations that could benefit from this technology and distributing appropriate technology transfer materials to them.

The original cost estimates for the technology were based on lab-scale performance. In support of project technical objectives and economic feasibility, it was necessary to answer the following critical questions:

1. Under conditions of 85–95 percent reduction of VOC emissions, what are the mass transfer rates of VOCs present in DoD painting and depainting operations (e.g., MEK, MIBK, xylenes, toluenes)
    a) from air to organic solvent via membrane?
    b) from organic solvent to aqueous phase via membrane?
2. What are the contact times needed to achieve the above mass transfer rates?
3. Can a membrane-supported biofilm be stably maintained?
4. What are the degradation rates of the above-cited VOCs?
5. Using commercially available membrane units for design purposes, what is the projected cost of treatment in
    a) dollars per cubic feet per minute of air treated?
    b) dollars per unit of VOC removal?

    The design is to be based on modules capable of controlling streams from 20,000 to 300,000 ft^3/min of exhaust treated at typical VOC concentrations found in DoD operations.
6. What is the impact of particle and particle-bound contaminants such as isocyanates on membrane performance? How does this impact filtration requirements?

Answers to these questions were the subject of this project and were necessary to scale-up and design the process and to determine process economics. Preliminary targets for mass transfer rate were 10^{-4} cm/sec for VOCs from air and 3×10^{-10} mg/cell-hr for VOC degradation rate.

3.0 Results at Bench-Scale

Details of progress in the bench-scale development phase (prior to pilot-testing) are described in two publications, "Membrane-Mediated Extraction and Biodegradation of VOCs from Air," reviewed and accepted 2/25/00, which was presented at the 2000 Spring National Meeting of the American Institute of Chemical Engineers (AIChE), and "Membrane Biotreatment of VOC-Laden Air," reviewed and accepted 5/1/00, which was presented at the 2000 Annual Conference of the Air & Waste Management Association (AWMA).

3.1 Development of Coated Modules

The project approach outlined in the Work Plan was initiated but was soon altered based on early findings. One significant area of study, which was not the subject of the technical papers, was in situ coating of fibers in Celgard Liqui-Cell modules. Because significant back pressure was required on the air side of the contactors to prevent oil seeping through the pores, it was deter-mined that coated fibers were necessary to make the process cost competitive, but acceptable coated fibers were commercially unavailable. Celgard did not manufacture any contactors with coated fibers, so work continued on testing the performance and ease of application of several coatings on smaller, bench-scale Celgard contactors. Significant effort was aimed at identifying or developing a suitably coated (nonporous polymer coating on a porous polypropylene sub-strate) separation/concentration membrane module. Discussions with Compact Membrane Systems (CMS) led to the acquisition and testing of a module coated on the inside of the lumens (hollow fibers) with an amorphous copolymer composed of perfluorodimethyldioxole and tetrafluoroethylene (PDD–TFE). Although PDD–TFE would not have optimum transfer charac-teristics, CMS was the only vendor identified and judged to be capable of applying in situ coatings to the inside of the lumens, and they would agree to work with only this material. Methyl ethyl ketone (MEK) and *m*-xylene were the VOCs used to test air to octanol VOC mass transfer performance. Three conditions were examined in duplicate for each compound, for a total of 12 experiments. Air flow rate and VOC concentration were experimental variables while absorbent (octanol) flow was held constant. Experimental conditions were chosen to emulate previous work with a Celgard Liqui-Cel module containing hollow fibers coated on their outside surface with PDD–TFE. The results of the tests (see Table 5) were similar to those of previous tests using a module coated with PDD–TFE on the outside of the lumens. These results indi-cated that the major resistance to mass transfer in modules coated with PDD–TFE may be in the coating. Because PDD–TFE does have a relatively high resistance to mass transfer of VOCs, the need for a better polymeric coating is needed to improve process economics.

Table 5. PDD-Coated Membrane Results

Mass Transfer Coefficients					
PDD-Coated Membranes, Shell-Side (outside) Coating					
Compound Transferred	Air Stream			Solvent Stream	
	Concentration (ppm)	Flow (L/min)	Loading[a] (ppm/s)	Concentration (mg/L)	K_0 (10^{-5} cm/s)
m-xylene	44	28	120	6.2	0.85
	50		130	6.2	0.91
	110	28	290	6.2	0.96
				6.0	1.0
	64	60	370	6.3	1.3
	275		1600	5.9	1.6
MEK	270	28	720	550	0.7
	750	28	2000	105	2.0
	1050	60	6000	1200	9.4
	2200	30	5500	980	4.3
PDD-Coated Membranes, Tube-side (inside) Coating					
m-xylene	40	28	110	4080	0.1
	230	60	1300	4300	2.0
	280	60	1600	850	2.7
MEK	470	28	1300	8500	-4.0
	2800	60	16,000	9500	2.0
	5000	28	13,000	5500	5.3

Removal Efficiencies				
PDD-Coated Membranes, Shell-Side Coating				
Compound Transferred	Air Concentration (ppm)	Air Flow (L/min)	Loading (ppm/s)	Removal Efficiency (%)
toluene	800	105	8000	74
	900	60	5100	76
	1300	30	3700	78
MEK/toluene	500	60	2800	80
	250	60	1400	60
	850	30	2400	80
	650	30	1900	70

Other activities aimed at acquiring a suitable coated module followed. Bend Research, Inc., supplied two prototype hollow-fiber modules for wet testing of the microporous Rayon fibers typically used in their scalable, high-flow, low-pressure-drop "box module" configuration. Results of the wet testing indicated that the pore size was too large for use in the system.

Chemica Technologies was contracted to coat a sample of the Celgard polypropylene fiber, and several small patches of coated material were received and tested as a VOC mass-transfer medium at North Carolina State University (NCSU). The results indicated satisfactory VOC transfer, but the coating partially delaminated from the substrate. Discussions continued with Chemica to assess their ability to improve coating adherence to internal lumen walls, but no satisfactory resolution was reached.

Celgard recommended a polyalkyl sulfone (PAS-16) and supplied some PAS-16 as well as a method for in situ fiber coating, the only option available for coating the Celgard module. With advice from Celgard and Anatrace, the PAS-16 manufacturer, a significant in-house effort with to coat the inside of the lumens with the PAS-16 polymer was begun. The coating attempts were based on Celgard's suggested method, which involved pumping a dilute polymer solution through the lumens while pulling vacuum on the shell side of the module. This was followed by rinsing and drying, followed by annealing the inside of the lumens with warm nitrogen (~60 °C). Variations in solvent, concentration of polymer, amounts of nonsolvent additives, operating conditions, annealing procedures, and drying and cleaning protocols were used. In initial attempts using tetrahydrofuran (THF) as a solvent (suggested by Celgard), the polymer did not dissolve completely, causing plugging in many of the lumens. Discussions with Anatrace and Celgard provided several new ideas, which included substituting toluene as the solvent, heating, blending, filtering, and centrifuging to improve solubility. After several trials, two of the four general approaches tried seemed to show promise toward achieving the desired results. These four approaches are summarized in Table 6.

Table 6. Fiber Coating Technique Development

TEST TYPE	SOLVENT	NON-SOLVENT	PAS-16 CONC. (%)	VACUUM (in. Hg)	CLEANING	DRYING	ADVANTAGES	DISADVANTAGES
1	THF	—	0.5 – 2	0 – 29.5	THF/Acetone mix to N_2-only purge	1–12 psi N_2 20 – 60 °C	Initial recommended solvent Compatible with module mat'l	Poor solvent for PAS Relatively expensive
2	Toluene	—	1 – 5	0 – 29.5	THF/Acetone mix to N_2-only purge	1–12 psi N_2 20 – 60 °C	Good PAS solvent Can be mixed with propanol to precipitate PAS	Drying more difficult More clogged lumens Unsatisfactory permeability results
3	Toluene	Propanol 40 – 45%	~1	0 – 19	Nitrogen	1–12 psi N_2	Fewer clogged lumens Faster drying Predictable permeability results	
4	Toluene	Propanol added to shell side	~2	0	Nitrogen	1–12 psi N_2	Precipitated PAS in pores	Difficult to control fluid permeation

To test for complete coating of the porous substrate, Anatrace suggested pressurizing one side of the membrane module with a mixture of nitrogen and carbon dioxide. Since carbon dioxide is seven times more permeable to PAS-16 than nitrogen, an analysis of the permeate could be used to determine whether coating was complete. Since that procedure is fairly difficult and time consuming to conduct, a simpler surrogate procedure was selected, at least for the initial tests as the coating procedure was being refined. This procedure is a permeation test in which nitrogen is admitted into the lumen side of the modules. The flow rate of nitrogen penetrating the lumen walls and escaping through the shell side was measured. A new module allows ~21 L/min flow at a selected pressure. Coating attempts conducted during this research exhibited flows ranging from 21 (uncoated) to less than 0.35 L/min. A module, flow tested at 0.35 L/min of nitrogen, was then tested and found to perform, in terms of mass transfer rate, much like the PDD–TFE-coated module. Since the PAS-16 coating is known to be more permeable to the VOCs tested than PDD–TFE, coating thickness was suspected to be excessive. Samples of lumens were cut out and viewed using a scanning electron microscope. The samples indicated a coating thickness of ~15 to 20 μm on the inside of the lumens; ~1 μm is the goal for coating thickness. Samples of a module that allowed nitrogen permeation at ~0.7 L/min showed a coating thickness of ~7 to 10 μm. From these preliminary tests, it is estimated that the proper permeability may be in the 1-to-1.5-L/min flow range to achieve a 1-to-2-μm-thick coating. It became evident that, although a reasonably successful technical exercise, this path would be time-consuming and would not validate a cost-effective approach.

Many discussions were held with commercial companies to determine the best approach to developing a separation/concentration module with a quality nonporous coating and a low-pressure drop. Proposals were solicited from Celgard, Bend Research, and Applied Membrane Technologies (AMT) for bench-scale modules and commitments to support the project with future larger-scale modules. Bend Research and AMT responded with proposals, and AMT was eventually selected as the manufacturer of choice.

3.2 Membranes Coated with Silicone Rubber

During searches for coated fiber modules, a company (AMT) was found that had developed modules for several water-stripping applications based on a coated fiber. They were asked to consider our application, and they offered a small, cylindrical module to be used for initial testing. The parallel-flow, stainless steel, cylindrical-membrane module was filled with fibers coated on the exterior with plasma-polymerized silicone rubber at a nominal thickness of 1 μm. Upon inspection prior to testing, a concern was raised because of the unknown effectiveness of the air-to-fiber contact area. AMT suggested that contact efficiency issues could be eliminated in a cross-flow module. Therefore, though the cylindrical parallel-flow design of the existing AMT module did not lend

itself to high efficiency, it was used in preliminary testing to gather data for the design of a cross-flow module.

Five 48-minute tests were conducted with air flowing through the shell side of the module: three were conducted using *m*-xylene as the pollutant, and two were conducted with MEK. Results are presented in Table 7. The airflow was typically 60 L/min, and VOC removal ranged from 56 to 83 percent with average overall mass transfer coefficients, K_o, of 4.4×10^{-6} to 5.0×10^{-5} cm/sec.

Table 7. Air-in-Shell Tests – Cylindrical Parallel-Flow AMT Module

Characteristic	*m*-xylene 1	*m*-xylene 1	*m*-xylene 1	MEK 1	MEK 2
Air flow (L/min)	60	60	60	28	60
Avg. inlet VOC air concentration (molar ppm)	65	190	185	186	1350
Average VOC removal (%)	56	77	70	83	78
Average mass transfer coefficient, K_0 (cm/sec)	4.40×10^{-6}	8.30×10^{-6}	1.20×10^{-5}	2.10×10^{-5}	5.00×10^{-5}

In commercial operation, one may expect that contaminated air will flow through the shell side of a cylindrical design while the stripping fluid is pumped through the tube, or lumen side. The initial set of tests on the AMT cylindrical module was run in this manner. Because of the distri-bution and contact shortcomings encountered, AMT suggested that a second series of tests be conducted with the air flowing through the fibers. Therefore, a second set of tests was run with the air flowing through the fibers and octanol on the shell side. Twelve runs were conducted using *m*-xylene as the pollutant. These shorter (34-min) tests were conducted with airflow rates through the lumens ranging from 5.6 to 10.3 L/min at pressure drops from 11.5 to 20 inches H_2O (292 to 508 mm H_2O). Results are shown in Table 8. Each mass transfer rate reported in this table is an average of samples taken at four time points and has a variance of 0.17.

The K_o values (6.0×10^{-7} to 5.1×10^{-6} cm/sec) for this set of runs were consistently and signif-icantly lower than for the air-in-shell results. As airflow decreases or as inlet concentrations increase, average VOC removal (overall) increases, but K_o, which is affected by other physical factors, may be impacted negatively. High removal efficiencies (93 and 97 percent) were achieved with octanol in the shell, and high mass transfer coefficients (2.1×10^{-5} and 5.0×10^{-5}) were achieved with air in the shell.

Table 8. Octanol-in-Shell Tests – Cylindrical Parallel-Flow AMT Module

Parameter	MX7	MX8	MX9	MX10	MX11	MX12	MX13	MX14	MX15	MX16	MX17	MX18
Air-side pressure drop [in. (mm) H_2O]	11.5 (292)	11.0 (279)	11.5 (292)	11.0 (279)	16.0 (406)	16.0 (406)	16.5 (419)	16.0 (406)	20.0 (508)	20.0 (508)	20.0 (508)	20.0 (508)
Air flow [L/min]	5.6	5.6	5.6	5.6	8.6	8.6	8.6	8.6	10.3	10.3	10.3	10.3
Avg inlet VOC air concentration [molar ppm]	68	84	261	684	92	125	457	499	76	105	274	697
Average VOC removal [%]	91	91	80	97	51	44	93	89	60	52	73	85
Average K_o [cm/s]	1.60 $\times 10^{-6}$	1.90 $\times 10^{-6}$	8.20 $\times 10^{-7}$	2.30 $\times 10^{-6}$	8.60 $\times 10^{-7}$	6.00 $\times 10^{-7}$	3.60 $\times 10^{-6}$	2.50 $\times 10^{-6}$	5.10 $\times 10^{-6}$	1.20 $\times 10^{-6}$	1.60 $\times 10^{-6}$	2.00 $\times 10^{-6}$

One problem encountered in all extraction experiments was swelling of the membrane material. Occasionally, this was accompanied by "sweating" of the octanol through the membrane. It will be necessary to evaluate alternate stripping fluids as a means to ameliorate this problem.

The information from this testing was used in the decision to develop a cross-flow module designed and manufactured specifically for this project by AMT (See Figure 4). This module contained roughly 2.3 m^2 of available membrane surface packaged in a module with air contact dimensions of roughly 3.5 × 10 × 1.0 inches (88.9 × 254 × 25.4 mm). Manufacturing methods required manufacturing in pairs, so the minimum two modules were procured.

Differences in design between the cross-flow and radial modules required a different potting material to seal the fibers into the end caps and plans were to use a urethane. This urethane material had not been previously used in applications with octanol, so limited tests were done to determine chemical compatibility. Initial results were only partially successful, showing softening of the urethane in longer periods of exposure. Using heat accelerated curing and longer setup times improved performance. These concerns and subsequent extended testing trials delayed the beginning of VOC tests. The urethane manufacturer concurrently investigated these issues, but they were unwilling to develop entirely new compounds and were unable to create small batches of existing materials to test. Few options were readily available.

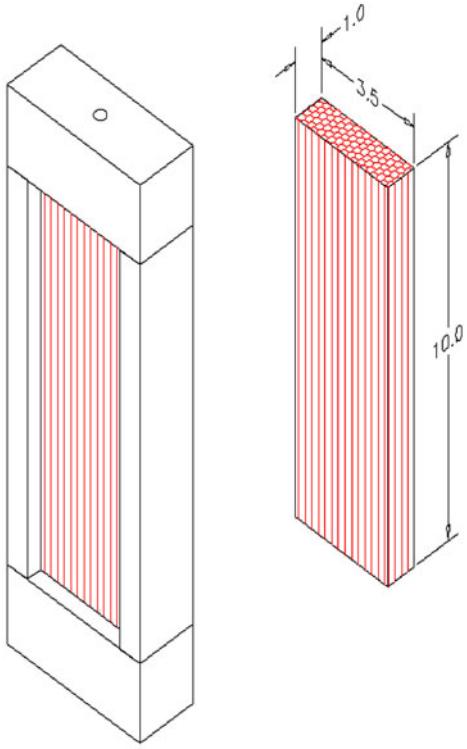

Figure 4. AMT Cross-Flow Module – Overall Dimensions in Inches

After assembly of the modules, they were pressure-tested to prove compatibility with octanol. This was expected to be an easy test to pass because no compatibility issues surfaced with the radial module. However, during the test, elongation swelling of the polypropylene fibers was encountered in the new module. At this point, further testing was done with single fibers to prevent destroying the remaining module. It was also determined that, after removing the octanol and cleaning the module, the fibers returned to their original length. A number of tests were completed with single fibers exposed to octanol, and it was found that the stretching was limited to about 5 percent of total length. Three different manufacturers' fibers were tested; all produced similar results.

Disassembly and testing by AMT resulted in destroying one of the two modules that were built.

While a solution to the fiber stretching was being sought, the other module was received from AMT for inspection and airflow testing to determine how the cross-flow module performed in comparison to the goal of low pressure drop. The module was mounted in the custom steel transition sections, and a variable-speed blower and electrical controls were connected for the test. The results indicate that the module was able to pass 20 ft^3/min of air at 0.62 inch H_2O pressure drop and 72 ft^3/min at less than 4.0 inches H_2O pressure drop. Limitations of the test apparatus prevented using higher air flows. The goal for flow vs. pressure drop was 10 ft^3/min at less than 20 in H_2O, so this design greatly exceeded this goal. With such a low pressure drop, multiple modules could be arrayed in series to increase VOC transfer performance, if needed. Inspection of the module and velocity profiles measured at the face of the fibers indicated that some bypass was created on the long sides where the fibers lay parallel to the polycarbonate housing. To address this problem, AMT proposed to create a seal along the two sides to limit the bypass. The fibers also exhibited some tendency to vibrate during the test, especially at the midpoint of the fiber bundle. AMT provided a modification to reduce or eliminate this vibration. At the end of the test, the module was returned to AMT for the modifications.

As indicated in Figure 5, the air pressure drop is negligible for this module, even at high flow rates. These results represent an order-of-magnitude improvement in pressure drop performance, relative to the cylindrical module containing identically coated fibers.

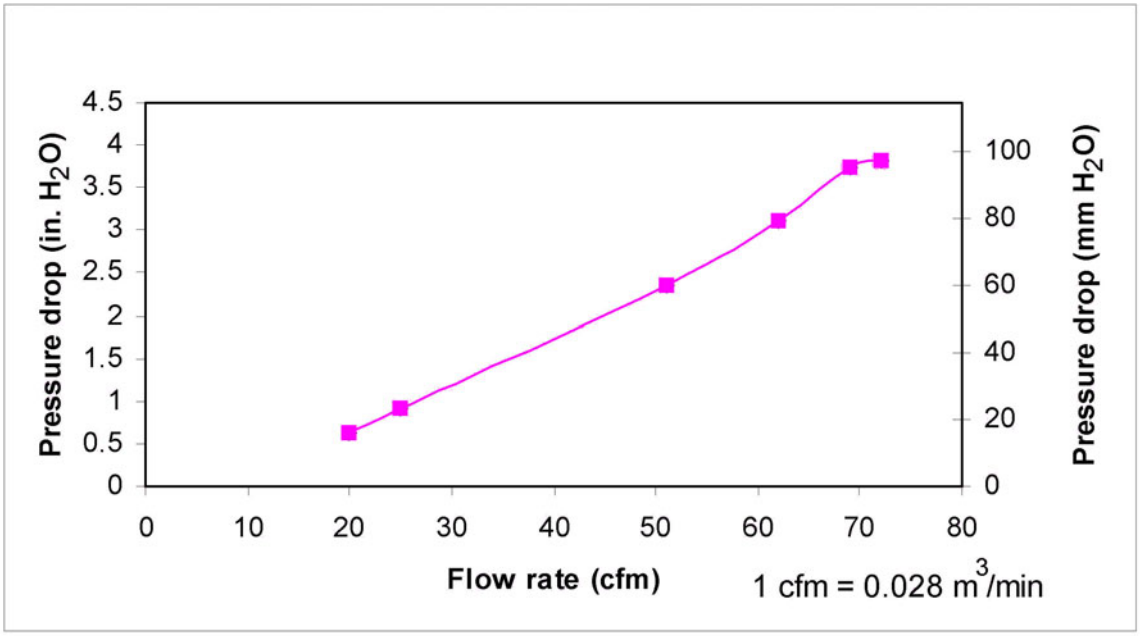

Figure 5 Pressure Drop for AMT Cross-Flow Module

The two approaches were available to address the fiber-swelling problem are (1) modify the housing in such a way that its length could be adjusted after the initial exposure to octanol, thereby re-tensioning the fibers, and (2) to use a stripping fluid other than octanol. The first method for fixing the stretching problem would involve redesigning the module to allow for post octanol length adjustment; this was abandoned due to complexity and an increased leakage risk. Alternate stripping fluids, including silicone oil and canola oil, were considered. Canola oil was seen as the most-economic alternative, but it lacked the chemical purity needed during analysis for extracted compounds. AMT then tested the fiber material with silicone oil in the same manner that had been used to measure the length changes after exposure to octanol. Single-fiber tests showed that fiber stretching was not evident after exposure to silicone oil, so a decision was reached to pursue switching to silicone oil. A change to silicone oil required repeating some of the initial octanol testing to verify partition coefficients at different temperatures for the com-pounds of interest. Potential toxicity to the bacteria also required investigation.

The AMT cross-flow module was returned for slight modifications and more tests using silicone oil in place of the octanol. The tests using silicone oil were successful; no swelling was seen, as had occurred in the case of octanol. AMT then returned the module after modifications were made, and a final decision was reached that further work on the separation contactor module would be done using silicone oil stripping fluid. An oil of viscosity slightly less than that of octanol (5 cs) was ordered and received. The single module was set up in a new apparatus for bench-scale testing using a simulated paint stream.

3.3 Experimental Structure

The bench scale S/C and biomembrane units were evaluated separately during the testing of the cross-flow separation contactor module. During the bench-scale testing, oil doped with the four target compounds was used in biomembrane effectiveness studies at N.C. State. During the final three months of the project, the used oil from the pilot-scale testing separation contactor system at ARCADIS was taken to N.C. State for biomembrane testing.

VOC mass transfer experiments require real-time sampling and analysis of VOC concentrations in inlet and outlet air and sampling of the stripping-fluid-reservoir VOC concentration for offline analysis. The VOC stream was created by a custom system configured as shown in Figure 6. The VOC-laden air stream is created by first injecting the four-component liquid mixture into a fitting that is heated by a small electric heater. This forces complete volatilization of the mixture before it is progressively diluted with filtered air until finally being force-mixed by a fan in the mixing box. During the mass transfer experiments, module inlet-stream VOC concentration was set via adjustments to the syringe pump delivery and airflow rates. Silicone oil flows were adjusted by a

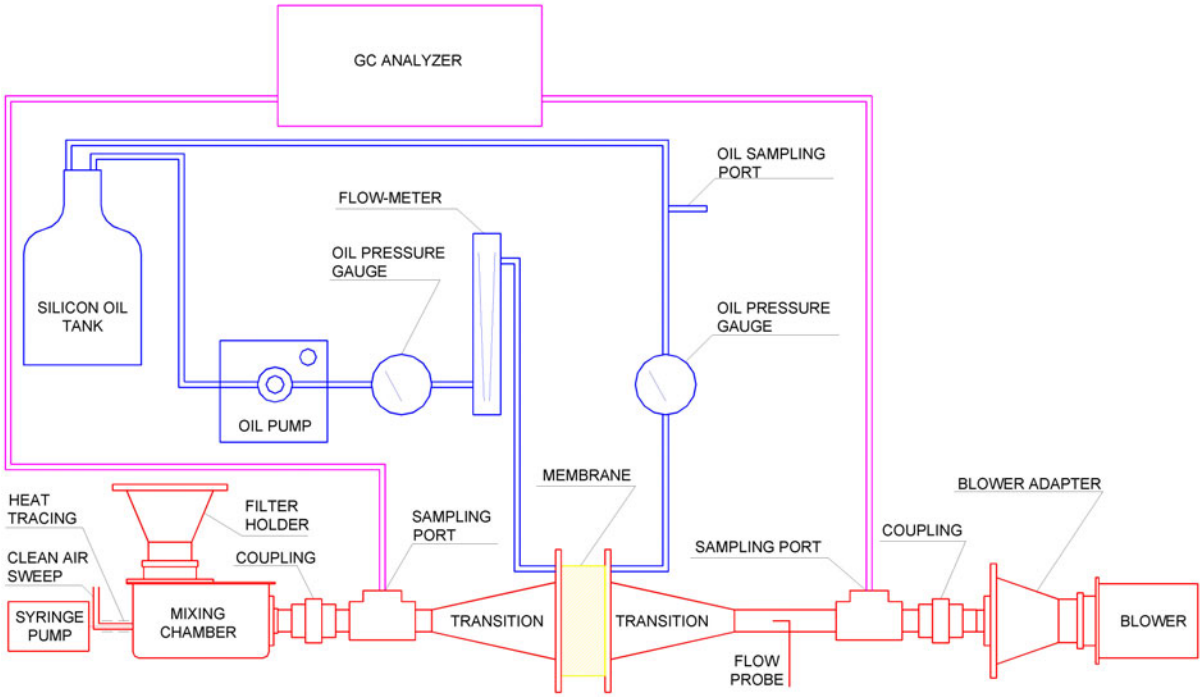

Figure 6. Separation Module Bench-Scale Test Apparatus

pump-speed setting and were read on a rotameter. The system was allowed 5–10 minutes to stabilize before testing began. Once the experiment began, samples of the air at the inlet and outlet of the module (two air samples) were taken at approximately 2½-minute intervals and analyzed online by a gas chromatograph with a flame ionization detector (GC/FID). Oil samples were also withdrawn via syringe from an oil-sampling port located between the module outlet and the oil reservoir. These oil samples were taken at 5–10-minute intervals. The oil samples were then stored, headspace-free, at 3 °C for later analysis by GC. Analysis of air-side data resulted in a separation contactor removal efficiency, and oil-side analysis permitted a mass balance analysis of the system and determination of the oil condition from test to test.

3.3.1 MBT Bench-Scale Separation Contactor

A schematic of the bench-scale system separation contactor is shown in Figure 6 and a process flow schematic is presented as Figure 7.

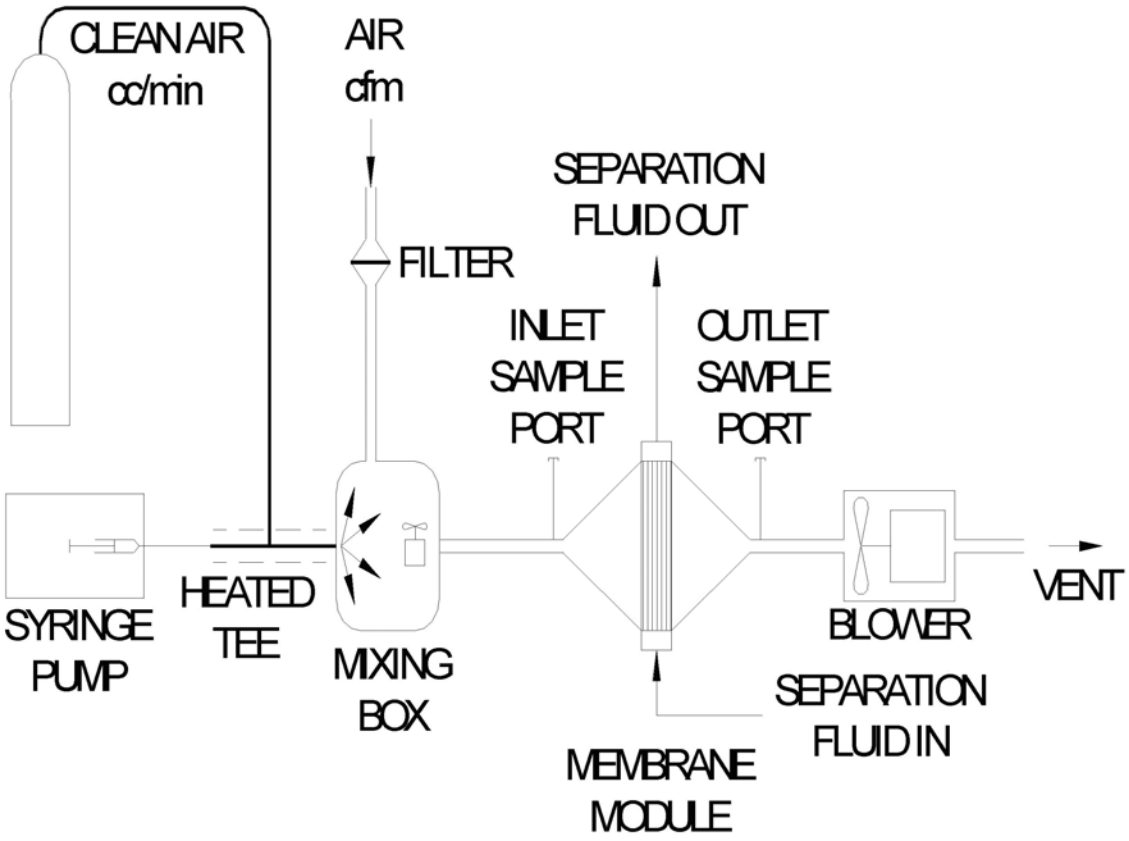

Figure 7. Process Schematic of Separation Module Bench-Scale Apparatus

3.3.2 Pilot Testing

A schematic of the complete MBT system appears as Figure 1 in Section 1.1.1. A process such as a paint booth produces a dilute stream of VOCs in air. After particles are filtered from the stream, it enters an S/C unit, which employs bundles of microporous hydrophobic fibers with the VOC-laden air and stripping fluid flowing across and through the fibers, respectively. The VOCs are transferred from the exhaust gases into the stripping fluid medium. The stripped air that leaves this unit is taken to an exhaust stack. After the circulating silicone stripping fluid leaves the S/C unit, it is delivered to a biomembrane unit is stored in an intermediate storage vessel. In the biomembrane unit, the stripping fluid is circulated past one side of another microporous membrane module that has a film of VOC-degrading bacteria on the opposite side of the membrane. VOCs diffuse through the membrane pores and are selectively and completely metabolized by the bacteria. The stripped solvent is then collected in a storage vessel and recycled through the S/C unit. Outputs from the overall MBT system are clean air, carbon dioxide, and a mixture of water and nonhazardous cell mass.

A diagram of the pilot-scale system is shown in Figure 8. The pilot-scale system differed from the bench-scale description in a number of details, including that the system was much larger and that the stream was created from spraying actual coatings from a paint spray gun pointed at a target in a small tabletop paint booth. The coating used for these experiments were acquired from an Air Force refinishing facility, and its components were determined from Material Safety Data Sheets (MSDS). However, paints are not composed of pure compounds, and industrial versions of listed compounds (e.g., MEK) are typically a mix of many compounds. Also, com-ponents below 1 percent are not required to be listed on an MSDS. Therefore, the capture efficiency was measured by using a total hydrocarbon analyzer on the upstream and downstream air streams rather than by speciation with a GC/FID. For these same reasons, a hydrocarbon analyzer is the instrument typically used to measure paint booth control equipment destruction efficiency in commercial operations. Based on previous work at NCSU, it was assumed that the separation contactor module could display selective removal behavior. To look for module compound preferences, samples were also taken for analysis with a GC/mass spectrometer (MS). These samples were taken on charcoal sorbent tubes at input and output locations adjacent to the sampling ports for the total hydrocarbon analyzer and were analyzed against a list of typical paint compounds, including those listed in Table 9. The oil analysis was done the same as for the bench scale. Testing followed the matrix outlined in Table 10.

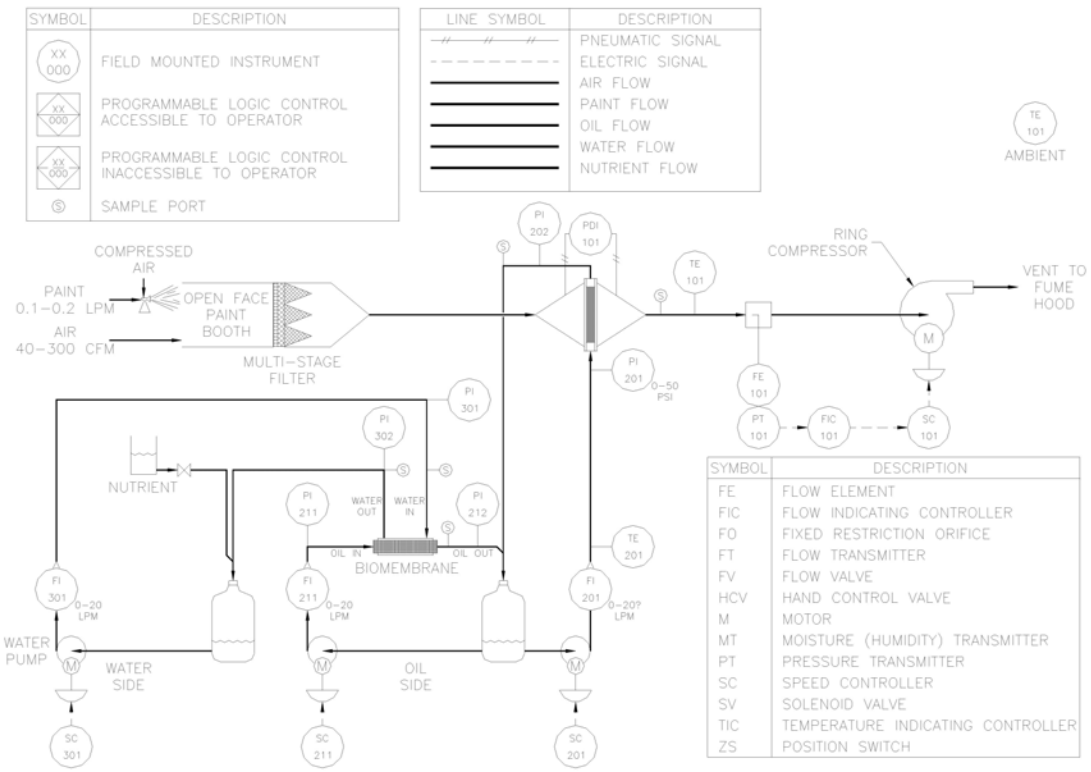

Figure 8. Pilot-Scale System Design

Table 9. Tertiary Mixtures in the Air Stream

Mixture Component	% VOCs in Paint by Volume	% VOCs in Paint by Weight
Bench Scale		
Xylene	8.7	7.5
MEK	18.6	15
Ethylbenzene	2.9	2.5
Butyl Acetate	11.3	10
Pilot Scale		
Paint (Aerospace Coating)	63.95	50

Table 10. Typical Flow Rates Used During Testing

Test Air Flow (ft^3/min)	Input VOC Concentration (ppm)		
	100	200	400
Bench Scale			
2	X	X	X
4	X	X	X
8	X	X	X
16	X	X	X
Pilot Scale			
20	X	X	X
100	X	X	X
200	X	X	X

4.0 Results/Data

The following sections present the results of the experiments performed during this study. Pertinent data from bench- and pilot-scale tests can be found in Appendices B and C, respec-tively.

4.1 Separation Module Tests

Separation module tests, described below, was performed in a number of bench- and pilot-scale modules.

4.1.1 Bench-Scale Tests

Eighteen successful tests, summarized in Table 11, were completed using a variety of air flow rates, VOC loadings, and oil conditions. Average removal efficiencies varied from 4.4 to 73.7 percent, and peak removal rates exceeded 79 percent twice for *ortho*-xylene. A question was raised about the performance of the GC after test nine, so the steps were expanded to include pre and post test calibrations. Preparation of calibration standards had also been inconsistent prior to this test, so alternate methods were found to improve consistency. For this reason, there is more confidence in the results from tests 12 and higher, but tests did just as well with 17 percent of the loading. Nevertheless, the results show important trends and general information. Higher loadings, such as in Test 2, improved inlet/outlet removal efficiency. Typical paint booth operations will have emissions in the range of 200 to 350 ppm, so most of the tests were run within that range. Higher air flow rates were used in a few tests to determine if increased turbulence improved performance, but it appeared that any such performance increase was negated by shortened contact time, resulting in lower removal efficiencies. Two modules arranged in series improved performance over a single module. Higher oil flow resulted in higher removal rates, but leaks resulted if this flow were set too high, indicating that materials and the module structure required improvements. Although overall removal efficiencies for individual compounds were as high as 79 percent, VOC removal rates were highly variable; MEK removal was often well below acceptable values, especially considering its prevalence in military coatings. Even though MEK removal was often at or close to zero, the other three compounds were consistently removed and were relatively comparable from test to test.

The first module received from AMT was the one not damaged during the initial testing. After a few trial runs with the lab apparatus, the module was tested for VOC removal efficiency. As a starting point, pressures and flows were chosen based on previous bench-scale investigations at NCSU using the uncoated fibers of the Celgard module. Oil flow was set at 1.0 L/min and air flow at 2.0 ft^3/min. It became apparent after two tests that the module was leaking oil, and swelling of an internal silicone rubber bridge was creating packs and voids in the fibers. This substantially reduced the

Table 11. Summary of Bench-Scale VOC Tests

Test	Date	Number of Modules	Air Flow (ft^3/min)	Oil Flow (L/min)	Approx. Inlet Load (ppm)	Tests Since Last Oil Change	Removal Rate (%)				
							MEK	*n*-Butyl Acetate	Ethyl-Benzene	*o*-Xylene	Avg.
1	4/27/00	1	2.0	1.0	450	0	18.5	47.9	19.6	50.4	34.1
2	4/27/00	1	0.5	1.0	2100	1	66.5	74.9	70.8	79.2	72.9
3	4/29/00	1	2.0	1.0	450	2	1.2	31.5	33.8	42.6	27.3
4	4/29/00	1	2.0	1.0	230	3	-5.1	14.7	12.5	30.8	13.2
5	4/29/00	1	2.0	1.0	850	4	19.2	41.0	44.1	48.9	38.3
6	5/03/00	1	2.0	0.2	300	5	13.0	34.5	42.8	43.4	33.4
7	5/05/00	1	2.0	0.2	170	6	18.6	31.8	38.9	43.2	33.1
8	5/06/00	1	2.0	0.2	450	7	26.3	44.4	50.0	51.9	43.2
9	5/09/00	1	2.0	0.2	350	8	58.0	22.4	27.2	28.6	34.1
10	5/11/00	2	4.0	0.4	350	0	23.5	54.2	58.5	62.3	49.6
11	5/12/00	2	4.0	1.0	350	1	63.5	75.6	76.2	79.4	73.7
12	6/06/00	2	4.0	1.0	200	4	-5.1	29.9	38.9	45.1	27.2
13	6/07/00	2	2.0	1.0	220	5	2.9	34.9	42.4	50.9	32.8
14	6/08/00	2	8.0	1.0	200	6	0.29	9.8	13.4	18.4	10.47
15	6/21/00	2	4.0	1.4	200	0	9.6	40.3	45.1	51.8	36.7
16	6/22/00	2	16.0	1.4	200	1	-5.6	5.5	6.3	11.5	4.4
17	6/22/00	2	8.0	1.4	200	2	-1.1	13.6	16.4	23.5	13.1
18	6/23/00	2	4.0	1.4	200	3	0.96	27.3	29.4	35.5	23.3

contact efficiency and performance was deteriorating, so testing was stopped after Test 5. An inspection of the module was unable to locate the exact source of the leak, but previous experience had shown the corners where the module sections were assembled to be suspect. A problem with the urethane material was assumed to be the culprit. Two modules received later were constructed similar to the first two, but an alternate potting material was used so that testing could continue while the urethane problems were investigated further. Tests with these modules were started with a lower oil pressure and more conservative flow rates (0.2 L/min) to prevent leakage failures. Removal efficiencies were lower during the next tests, most likely because of the lower driving forces from the reduction of oil pressure and flow. A number of modifications were made to the return piping on the apparatus to reduce back pressure in hopes of increasing oil flow without raising the static pressure. This was successful in bringing flow up to 0.4 L/min with a back pressure of about 5.0 psi. Results showed an obvious increase in removal efficiency, although still lower than the target of 80 percent. The two modules were then arranged in parallel on the oil side and in series on the air side to double the contact time without risking higher oil pressures. The efficiency again increased, but not as dramatically as had been achieved with higher oil flow rates, so the next step was to increase the oil flow and pressure. Again, plumbing modifications were made to reduce back pressure, and flow was increased to 1.0 L/min with an increase in pressure to 12.5 psi. Although removal efficiency increased, it quickly became apparent that both modules were again leaking oil. Based on these trials, AMT proposed a number of design modifications to be used in the pilot-scale version to prevent the leakage problems of the corners and joints.

4.1.2 Pilot-Scale Tests

Pilot-scale testing produced several tough challenges that reduced the number of successful tests. Initial runs were hampered by inconsistent spray gun paint application, although the apparatus was designed to maintain a constant trigger position. In addition, only the last five tests were run with both air-side analytical systems. Upon data review, the comparability of these two analyti-cal methods and its implications are important enough to focus primarily on these results, shown in Table 12. The overall removal rate is shown by averaging the GC/MS results for the eight listed compounds and by the average removal reported by the total hydrocarbon analyzer. For all five tests, both methods passed pre-and post-analysis calibration checks. However, agreement was achieved only for Tests 1 and 3, with 7.4 and 16.9 percent differences, respectively. Comparability for Test 5 was lower at 35.6 percent difference, and Tests 2 and 4 show gross differences. Similar trends were seen for the bench-scale module in that MEK shows much lower results compared to the other compounds, and removal generally improves with higher oil flow and lower air flow.

To understand the removal results requires a short review of the methods used. During bench-scale testing the air-side analytical method (GC/FID) agreed closely with the oil-side analysis method in

Table 12. Summary of Pilot-Scale VOC Tests

Test/VOC Load (ppm)	Air Flow Rate (ft^3/min)	Oil Flow Rate (L/min)	VOC Removal (%)									
			Individual Constituents								Average	
			MIBK	Xylene			2-Heptanone	MEK	*n*-Butyl Acetate	Ethyl-benzene	GC/MS	Total HC Analyzer
				para	*meta*	*ortho*						
1/300	200	4.6	49.5	55.2	53.0	33.5	59.9	33.9	49.8	55.7	48.8	45.3
2/260	100	3.85	69.9	73.9	73.9	50.5	77.4	63.2	71.6	73.9	69.3	0.0
3/310	100	1.8	38.6	50.4	47.2	45.2	54.1	35.0	46.3	48.3	45.6	54.0
4/225	100	6	78.6	81.7	81.5	73.8	84.2	75.2	81.3	81.3	79.7	20.0
5/260	140	4.4	26.0	40.8	37.6	36.5	45.2	17.6	33.4	38.1	34.4	24.0

total mass balance. This was largely due to using four pure compounds to create the pollutant stream, and each method could differentiate and quantify the known four compounds. The change to pilot-scale brought the use of real paint to simulate a paint-booth exhaust. It was known beforehand that even compounds listed on the MSDS, such as MEK and xylene, would be impure compounds that would have significant variations in constituents. For this reason, the air-side analysis was changed to a total hydrocarbon analyzer because it would be capable of analyzing all known and unknown VOCs. Because no better alternative existed, the oil-side analysis was unchanged and analyzed for only the same four constituents identified during the bench-scale testing. An additional analysis was added for the air side with the knowledge that the module could turn out to be selective in its removal rate; additional samples were taken parallel with the total hydrocarbon analyzer to be analyzed by EPA Method 25. These carbon tube samples were extracted and analyzed on a GC that is normally used for identifying unknown compounds in coatings formulations. A sample run identified eight compounds on the standard search list.

Pilot-scale test results were variable and, at times, difficult to understand. Initial test results using the total hydrocarbon analyzer showed inlet and outlet results varying from 20 to 65 percent removal. Oil analysis, however, almost never agreed with those removal rates, and during later tests, when charcoal tubes were analyzed by GC/MS, averaged removal rates based on the eight constituents were always reported higher than those with the other two methods. To understand this, it is important to remember that each method was different and comparability was not a given. The total hydrocarbon analyzer measures total carbon atoms, and the relationship between its readout in parts per million and the other methods requires the use of a multiplier to account for the more-complex molecular structure of organic compounds. Regardless, with any reasonable factor (e.g., 4.0 for typical paint compounds), the data from GC/MS barely exceed 1 percent of the reading produced by the total hydrocarbon analyzer. This implies that the eight compounds that were identified by GC/MS represented only 1 percent of the total constituent VOC content of the paint, and while the module was relatively efficient at removing some compounds, especially those identified by the GC/MS, it was unable to remove other compounds, especially after the oil had been used. The total hydrocarbon analyzer reported an overall VOC removal rate that was comparable to the rate reported by GC/MS at times and not comparable at other times.

More problematic was that the oil analysis data rarely reflected the air side removal. In some cases, the oil showed no removal, while the air side showed removal of 20 percent or more. One contributing factor is that the oil analytical procedure was developed during the bench-scale studies, and calibrations were based on removal of four, well characterized, pure compounds rather than the eight identified in the GC/MS samples, or the many unknown compounds contributing to the total hydrocarbon analyzer data. However, with even the four known compounds, the GC/MS data did not always agree with the oil data. A possible explanation is that much of the stripped VOCs did not

pass through the fiber boundary but, rather, was adsorbed and temporarily held both on the wetted outer surface of the fibers and by the static oil that had formed a puddle inside the apparatus during the tests. Contributing to this theory is a daily operational aspect. Each time a test was completed, the air fan was left running to prevent migration of the paint vapors to office areas adjoining the laboratory. During this time, the oil outside the fibers that had adsorbed VOCs was thus desorbed, and this cleaned oil was again the dominant remover during the next test.

To treat the needed 500 ft^3/mim, 20 modules were ordered with the latest in design specifications of the bench-scale module: 2.3 m^2 area and 3.5 × 10 × 1.5 inches (89 × 254 × 38 mm). Although scaling up by using many small modules was not an ideal approach, project time requirements for delivery required using existing production methods, and this was the largest size that could be made with existing production equipment. To reduce bypass around the side, a shelf area was added to overlap the fibers, and the silicone rubber bridge that became distorted on the first bench-scale version was dropped. One advantage of the small modules was that, to suit various test scenarios, they could be arranged in a range of patterns such as multiple banks of module for increased contact time or parallel arrangements for greater air flow rates. The rest of the apparatus (module mounting frames, ducting, transitions, and oil piping) was designed with this in mind, and to reduce assembly time, the transitions and mounting frames were constructed while the modules were in production.

After the 20 modules were delivered, a number of tests were done to determine their basic integrity. Although AMT tested the modules under pressure with air, no tests had been done with silicone oil. Therefore, each module was to be unpackaged, visually inspected, and then tested under 5 psi oil pressure. Based on visual inspection, several of the modules exhibited question-able potting material with bubbles and extrusions. The bubbles were due to the urethane curing at humidity that was not ideal. Two with obvious porosity problems were chosen for pressure testing, and each leaked almost immediately upon start up. This was seen as serious enough to warrant stopping further tests while AMT addressed the problem. After these were sent back, AMT determined that one was damaged in shipment and could be repaired. To conserve the short time remaining in the project, a decision was reached to test some of the remaining modules. The apparatus was easily able to test 10 modules arranged in two series-arranged banks. Therefore, they were assembled into a reduced-size, pilot-scale apparatus so testing could begin. This required a reduction in airflow from the planned 500 cfm. The maximum treated stream was 200 cfm.

Meanwhile, AMT was unable to locate the leak in the second returned module. The leak that had been seen during receiving tests was the result of a slow, but continuous, sweating of oil through the pores of the fibers. This suggested a difference between AMTs tests and the receiving tests; the receiving tests had used silicone oil with a viscosity similar to octanol, or about 5 cs, whereas AMT's tests were done with the more commonly available 50-cs oil. Further study revealed that the

thinner silicone oil was acting more solvent-like; it was seeping through the pores of the fibers, both wetting the outside of the fibers and accumulating, over time, in a puddle at the bottom of the module. Based on this information, AMT advised that further tests should be limited in pressure and oil flow rate.

After a number of tests with the 10-module arrangement, the apparatus was disassembled for a visual inspection, and it was apparent that wetting the fibers had created a problem that had previously gone unnoticed. The fibers were again distorted much like had occurred during the bench-scale testing. It was then determined that the distortion was not due just to swelling the silicone rubber bridge that had been deleted from the design but was also due to individual fibers swelling much as had occurred in the octanol compatibility tests. The thinner, 5.0 cs oil had acted on the fibers much like an aggressive solvent, and the stretching was creating voids and packed areas. Therefore, the modules had an unknown, but certainly not optimal, contact efficiency. At this time, AMT recommended that we use the remaining 10 modules in another test using the thicker, 50 cs oil. Their reasoning was that the thicker oil would be unlikely to seep through the fibers. After assembling the remaining 10 modules, a shakedown test was started. To attain the same flow rate that was used in previous tests required a much higher pressure (about 30 psig) setting, and one or more modules ruptured, causing a catastrophic loss of oil, and the testing was stopped. In retrospect, while thicker oil would be less likely to seep through the fiber, its viscosity requires much higher pressure for any given flow rate. To prevent failure of the urethane potting material would have required a much lower flow rate, and with lower flow rates, the driving forces would be reduced, so any advantages may have been lost. Contaminated stripper fluid from the pilot plant was transferred to the NCSU laboratory for bio-treatment.

4.2 Biological Treatment System

The experiments related to the biological treatment system can be organized into four major categories of suspended cell experiments performed in shake flasks, biofilm experiments performed in flat-sheet membrane units, biofilm experiments performed in hollow-fiber membrane units, and experiments involving hollow-fiber units in series with a stirred tank reactor. These categories represent qualitatively different objectives.

- Shake flask (suspended-cell) experiments determine organism and mixed-culture characteristics,
- Flat-sheet biofilm experiments determine the basic behavior of pure- and mixed-culture biofilms,
- Hollow-fiber-module experiments determine the robustness of the degradative activity and evaluate biofouling control schemes, and
- Experiments involving the hollow-fiber module operated in series with a suspended-cell

reactor demonstrate the capability to simultaneously degrade aliphatic and aromatic VOCs.

Characterization of the performance of the bacterial consortium on mixed VOCs is confounded by three facts: (1) growth and degradative behaviors of a mixed culture cannot be expected to be the sum of the behaviors for each organism in the culture grown separately; (2) immobilized-cell (biofilm) growth kinetics often deviate significantly from suspension-culture (shake-flask) growth kinetics; and (3) growth of a single organism on a mixture of compounds is not easily related to growth on the individual compounds.

The complex interactions between species and compounds must be identified and quantified before one can effectively design and operate a biotreatment module. To adequately describe the behavior of this system, a series of suspended-cell-growth studies and membrane-supported-biofilm-reactor experiments were completed. Complete data sets for each experiment can be found in Appendix B.

4.2.1 Suspended-Cell Experiments

A significant number of growth studies were performed during the course of this research, many in response to the degradative behavior exhibited by the mixed-biofilm reactor system. The first set of experiments to be described pertain to the need to identify degraders for compounds found in MilSpec paints; specifically *m*-xylene, *p*-xylene, ethylbenzene, butyl acetate, butanol, MEK and acetone.

4.2.1.1 Screening Studies

Original screening studies were performed to identify organisms capable of degrading *m*-xylene, and two organisms were ultimately established with those capabilities, respectively designated MX-1 and X1. Subsequent screening studies were undertaken to establish degradation of *p*-xylene, ethylbenzene, butanol, butyl acetate, and acetone.

4.2.1.2. Xylene Degraders

The first of these studies involved the screening of MX and X1 for growth on *p*-xylene and ethylbenzene. This was done to select one of the two different strains for further studies.

Methods: Cultures were grown under sterile conditions in 250-mL flasks incubated at 30 °C in a shaker (250 rpm). The flasks contained 50 mL of L-salts medium; individual VOCs were added as liquid in quantities of 5–7.5 µL. The flasks were covered with foil and sealed with Parafilm before incubation. Optical density of the culture at 600 nm was monitored for up to 72 hours to detect growth. The initial concentrations of *p*-xylene and ethylbenzene were 150 ppm and 100 ppm, respectively.

Results: Both organisms were able to grow on *p*-xylene, but only X1 grew on ethylbenzene. Based on these results, X-1 was chosen for the staged biotreatment experiment.

4.2.1.3 Aliphatic Degraders

Two organisms that had been isolated previously, designated M1 and AOC-1, were screened for growth on butanol, butyl acetate, MEK, and acetone. This was done to select the better aliphatic-compound degrader of the two strains for the staged biotreatment study.

Methods: Cultures were grown under sterile conditions in 250-mL flasks incubated at 30 °C in a shaker (250 rpm). The flasks contained 50 mL of L-salts medium; individual VOCs were added as liquid in quantities of 5–7.5 µL. The flasks were covered with foil and sealed with Parafilm before incubation. Optical density of the culture at 600 nm was monitored for up to 72 hours to detect growth. Initial concentrations of all substrates were 150 ppm.

Results:

Organism	MEK	Acetone	Butanol	Butyl Acetate
M1	+	+	+	+
AOC-1	(-)	+	+	+

M1 grew on all four substances. AOC-1 grew on acetone, butanol, and butyl acetate; but growth on MEK was very uncertain. Therefore M1 was chosen for the staged biotreatment experiment.

4.2.1.4 Growth Studies

Many growth studies were carried out in conjunction with screening studies to quantify growth rates and extents of VOC degradation. These growth studies involved the organisms MX, X1, and M1. Table 13 summarizes the experiments performed over the course of the project. Only the experiments that have not been described in previous reports or publications will be commented on directly; the results of all the experiments can be found in the appendices. Although each experiment involved specific organisms and substrates, a general methodology was employed for culture growth and characterization.

Culture growth: Growth flasks were prepared under sterile conditions in screw-top flasks. L-salts were added to the flask, and the headspace was filled with oxygen. The substrate was added, and inoculation was effected by adding a sufficient amount of an overnight culture to a total liquid volume of 150 mL. The flask was sealed with an open-top closure with a PTFE-coated septum, and a needle pierced through the septum connected to a Teflon valve. A control flask was prepared in a similar way but without inoculation. Liquid was withdrawn by use of a glass syringe for optical

Table 13. Suspension-Culture Experiments

Experiment No.	Organisms	Substrates	Rationale
GS1	X1	*m*-Xylene	Strain characterization
GS2	X1	Toluene	Substrate range
GS3	X1	*m*-Xylene, toluene	Metabolic regulation
GS4	M1	Toluene	Substrate range
GS5	M1	MEK, toluene	Metabolic regulation
GS6	M1	MEK, *m*-xylene	Metabolic regulation
GS7	M1	Toluene, *m*-xylene	Substrate range
GS8	M1	MEK, toluene, *m*-xylene	Metabolic regulation
GS9	M1, X1	MEK, toluene	Metabolic regulation
GS10	M1, X1	MEK, toluene, *m*-xylene	Organism interactions
GS11	MX	*p*-Xylene	Substrate range
GS12	X1	*p*-Xylene	Substrate range
GS13	X1	*m*-Xylene, ethylbenzene	Metabolic regulation
GS14	X1	*m*-Xylene, *p*-xylene	Metabolic regulation
GS15	M1	Butyl acetate	Substrate range
GS16	M1	MEK, butyl acetate	Metabolic regulation

density (OD) and VOC measurements. During the sampling, oxygen was added to the flasks to compensate for the volume withdrawn. The control flask was treated in the same way, but the samples for OD were discarded.

General analytical procedure: The sample withdrawn for VOC analysis (1 mL) was transferred into a 2-mL vial containing 1 drop of acetic acid to acidify the sample. Extraction of the VOCs was carried out by addition of pentane (0.1–0.2g) containing heptane as internal standard. The sample was shaken vigorously for 2 minutes and stored upside down at 5 °C. Analysis was performed with a Hewlett–Packard 5890 gas chromatograph (GC) equipped with a J&W Scientific capillary column (DB-624) and a FID detector. A 1-µL portion of the pentane phase was injected into the GC, and the response was compared to the response from standards prepared in pentane.

4.2.1.5 MX and X1 Growth on *p*-Xylene (GS 11, 12)

The objective of these experiments was to study the growth and degradation of *p*-xylene by the *m*-xylene-degraders in order to choose the best organism for xylene degradation in the staged biotreatment unit. The substrate (*p*-xylene) was added so that initial concentrations varied from 100–150 ppm.

Results:

Organism	Growth Rate (h^{-1})
MX	0.29
X1	0.49

The inoculum was grown on *m*-xylene, so not surprisingly both organisms exhibited a long lag phase (20–30 hours). The growth rates indicate that X1 degrades *p*-xylene more rapidly than does MX. Although suspension culture behavior is not completely indicative of the behavior of organisms when attached to a surface, X1 was selected for further evaluation.

4.2.1.6 Effect of Ethylbenzene on Growth of X1 on m-Xylene (GS13)

The objective of this experiment was to determine whether ethylbenzene has a positive or negative effect on the rate of degradation of *m*-xylene by X1. This would indicate whether the pathways involved in the degradation of these two compounds were synergistic, antagonistic, or non-interactive.

Methods: Growth flasks were prepared as described above. The initial concentration of *m*-xylene was 150 ppm in all flasks. Initial concentrations of ethylbenzene were varied: 0 ppm, 50 ppm, 100 ppm, and 150 ppm. The flasks were closed as described above. Optical densities were followed for 26 hours.

Results: Ethylbenzene appeared to have very little effect on the growth rate. It seems that the initial lag phase was shorter in the presence of ethylbenzene, indicating that the presence of ethylbenzene might facilitate *m*-xylene degradation. Another possibility is that ethylbenzene was degraded as well. However, no VOC analysis was undertaken.

The presence of ethylbenzene in high concentrations (150 ppm) did affect the apparent growth yield obtained after 26 hours. For an initial concentration of ethylbenzene of 150 ppm, the final optical density was 0.17 compared to 0.24–0.26 for cultures exposed to lower concentrations of ethylbenzene. The growth had reached a stationary growth phase in all the flasks, which was confirmed by a sample point after 32.5 hours. The lower OD level for the high concentration of ethylbenzene indicated that the growth of X1 on *m*-xylene was inhibited rather than ethylbenzene was degraded itself. For further study of the effect from ethylbenzene, VOC analysis should be done to determine if ethylbenzene is being degraded. The table below shows the growth rates calculated for each concentration of ethylbenzene, and the optical densities of each culture after 26 hours.

Concentration of Ethlybenzene (ppm)	Growth Rate (h^{-1})	Period for Exponential Growth (h)	OD after 26 hours
0	0.23	11 – 19	0.24
50	0.20	7 – 16.5	0.26
100	0.24	7 – 16.5	0.24
150	0.22	4 – 16.5	0.17

4.2.1.7 Growth of X1 on *m*-Xylene and *p*-Xylene (GS14)

The objective of this experiment was to study the growth and degradation of mixtures of *m*- and *p*-xylene by X1. Again, the concern was that there might be negative interactions between the two degradative pathways or intermediates generated therein.

Methods: Growth flasks were prepared as described above; *m*-Xylene and *p*-xylene were added to a concentration of 75 ppm each.

Analytical procedure: It was not possible to separate *m*-xylene from *p*-xylene, so a total concentration of the two xylenes was calculated.

Results: The growth curve indicated that the two substrates were degraded concurrently. The growth took place within 10 hours, and no lag phase was observed. After 9 hours, *m*-xylene and *p*-xylene could not be detected in the liquid. The growth rate obtained in this study is compared to growth rates determined in previous studies of X1 growing on *m*-xylene and *p*-xylene as single substrates. Results show that the growth rate obtained in the presence of both substrates is lower than the one obtained when only *m*-xylene is present, but higher compared to the growth rate obtained for *p*-xylene.

Substrate	Growth Rate (h^{-1})
m-Xylene	0.78
p-Xylene	0.49
m-Xylene + *p*-xylene	0.58

4.2.1.8 M1 Growth on Butyl Acetate and a 50:50 Mixture of Butyl Acetate and MEK (GS 15, 19)

The objective of these experiments was to study the effect of butyl acetate on the rate of MEK degradation and of growth of M1 on MEK.

Methods: For the study with butyl acetate, the concentration of substrate in the flask was 150 ppm, whereas concentrations of butyl acetate and MEK were 75 ppm each for the mixed-substrate study.

Results: The growth curve indicated that butyl acetate and MEK were degraded concurrently. An effect from the presence of MEK was seen on the growth rate for butyl acetate; the growth rate obtained for the mixture of butyl acetate and MEK was lower than that obtained for M1 growing on butyl acetate alone.

Substrate	Growth Rate (h^{-1})
MEK	0.5
Butyl Acetate	0.70
MEK + Butyl Acetate	0.57

4.2.2 Flat-Sheet Biofilm Experiments

Experiments were performed utilizing a small contactor using a flat, square section of porous polypropylene substrate. The basic configuration employed in these studies is shown in Figure 9.

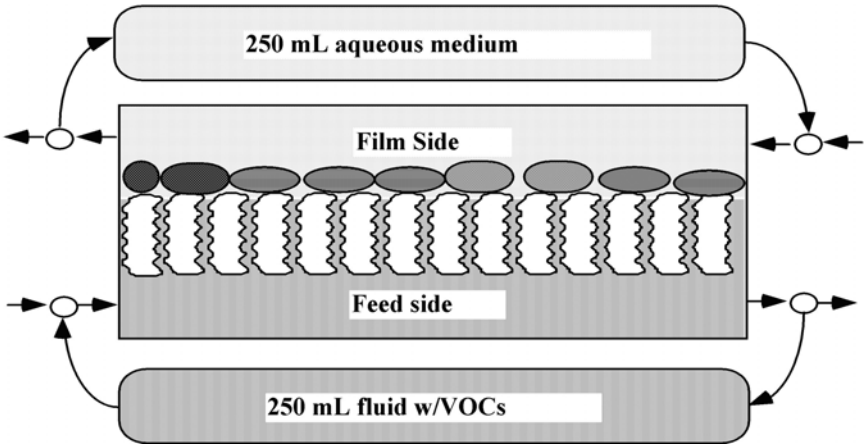

Figure 9. Flat-Sheet Contactor Schematic

The system was operated under countercurrent flow with a flow rate significantly smaller than the recycle flow rate, resulting in well mixed fluid in the reservoirs and on each side of the membrane within the contactor. This configuration was adopted because it allowed relatively rapid establishment of films and determination of degradative activity and because the film could be sampled directly for characterization (thickness, composition).

Initiation of all of these experiments involved aqueous phases on both sides of the membrane, with the substrate being provided through the membrane in all cases. Subsequent to establish-ment of a viable, active biofilm, the feed fluid either remained aqueous or was switched to an oleophilic fluid (octanol or silicon oil, for example).

Flat sheet biofilm experiments were conducted according to the matrix in Table 14.

Table 14. Flat-Sheet Biofilm Experiments

Experiment No.	Organism(s)	Substrate(s)	Comments
FS1	M1	MEK, toluene	aq/aq
FS2	M1	MEK	aq/octanol
FS3	M1, X1	MEK, toluene	aq/aq
FS4	M1, X1	MEK, toluene, *m*- xylene	aq/aq
FS5	M1, X1	MEK, toluene	aq/octanol
FS6	X1	*p*-Xylene	aq/aq
FS7	X1	*m*- Xylene	aq/aq
FS8	X1	*m*- Xylene, *p*-xylene	aq/aq
FS9	X1	*m*- Xylene, *p*-xylene	aq/silicone oil

General experimental procedures: During experiments to determine the degradative capacity of the biofilm developed on the membrane, a 1-L flask containing 800 mL of oxygenated L-salts (reservoir) replaced the chemostat (CSTR), and a 1-L flask with 800 mL feed solution replaced the feed bottle. Both flasks were stirred, and flow rates were as given above. For analyses of VOC concentration, 1.0-mL samples were withdrawn hourly. VOC concentrations in the reservoir and feed bottle were followed for at least 5 hours.

General analytical procedures: The liquid samples were transferred to a 2-mL vial containing 1 drop of acetic acid for preservation. VOC extraction was carried out by adding pentane (0.1– 0.2g) containing heptane as an internal standard. The sample was shaken vigorously for 2 minutes and stored upside down at 5 °C. Analysis was performed with a Hewlett–Packard 5890 GC equipped with a J&W Scientific capillary column (DB-624) and a FID. A 1-μL portion of the pentane phase was injected into the GC, and the response was compared to the response from standards prepared

in pentane. A total xylene concentration was calculated for experiments involving both *p*-xylene and *m*-xylene because it was not possible to separate the two xylenes in the GC analysis.

4.2.2.1 Growth of X1 on *m*-Xylene and *p*-Xylene (FS 6, 7, 8)

The objective of these experiments was to study the degradation capacity and biofilm characteristics of a xylene-degrading biofilm. Degradation of *m*-xylene and *p*-xylene supplied as single substrates and as part of a mixture were investigated.

Experimental configuration: Two flat-sheet contactors connected in series were run co-currently with aqueous solution on both side of the membrane. The biofilm side was connected to a CSTR and the opposite side (feed-side) was connected to a feed bottle saturated with the VOC. A slow airflow was passed through a pure solution of the VOC (*m*-xylene or *p*-xylene), and the exhaust air was fed to the bottom of the feed bottle, obtaining a saturated solution. The feed-bottle contained 5 liters of distilled water. Operational data were as follows:

Parameter	Value
Volume of CSTR	1-L vessel with 500 mL culture
Average flow of L-Salts to CSTR	30 mL/h
Ph in CSTR	7.0
Temperature in CSTR	30 °C
Flow on feed side	7.7 L/h
Flow on biofilm side	34 L/h

The CSTR was inoculated with X1. When exponential growth was obtained in the CSTR, the contactors were inoculated by passing the suspension over the membrane on the biofilm side.

Results: Experiments were carried out for two levels of *p*-xylene and *m*-xylene. The feed was prepared from the saturated solution, which made the concentration difficult to control. For the last two experiments reported below (A, B), the feed solution was made by adding the pure VOCs to distilled water that had been oxygenated for 10 minutes. An overview of the experiments is shown.

After the experiments with *p*-xylene, the biofilm was harvested, and the system was inoculated again. A very thin biofilm with black and gray spots was observed on the membranes. The second biofilm was grown for 38 days. After 38 days, the biofilm appeared yellow and was filling out the space between the support material and the membrane to the thickness allowed by the gasket.

Substrate	Level	Age of Biofilm (days)
p-Xylene	High	5
	Low	7
m-Xylene	High	5
	Low (150 ppm)	10[A]
p-Xylene + *m*-Xylene	100 ppm of each	25[B]

Results: All experiments exhibited very low VOC concentrations in the fil*m*-side reservoir. The concentrations were below 1 ppm except for the first experiment, for which a high concentration (26 ppm) was observed for the very first point and an increase from 0.1 ppm to 4 ppm was observed during the 10-hour run. Because of the insignificant concentrations in the film-side reservoir, the removal of VOC from the feed may be considered as the amount degraded in the biofilm.

For the young biofilms (5–7 days), the average removals of *p*-xylene and *m*-xylene from the feed bottle were in the range 4–11 ppm/h. For the 10-day-old biofilm, the average removal of *m*-xylene was 20 ppm/h. However, the removal appeared to take place only during the first 4–7 hours of exposure to the substrate. After 4 hours, the concentration in the feed bottle established a constant level and no further degradation was seen. This could be due to oxygen limitation in the system, as no oxygen was supplied during the experiment. For the 10-day-old biofilm, the feed solution was oxygenated prior to the experiment, which may explain the higher removal. This could also be due to growth of the biofilm and, hence, an increase in active biomass. For the same experiment, the reservoir was replaced by a new oxygenated reservoir after 21 hours. After the replacement, additional substrate removal was observed, which may confirm that the *m*-xylene degradation was oxygen-limited.

When *p*-xylene and *m*-xylene were supplied as a mixture, the biofilm was 25 days old, and an average removal of 60 ppm/h was observed for the first 2.5 hours. The feed solution was also oxygenated prior to this experiment, making higher removal possible. However, the removal obtained in this study (150 ppm) compared to the removal obtained in the study with the 10-day-old biofilm (80 ppm) should be equal if the amount of oxygen was the critical limitation, since the same amount of oxygen was supplied in the two experiments. The discrepancy between the two results may still be oxygen limitation, but a limitation inside the biofilm rather than in the aqueous phases.

4.2.2.2 Growth of X1 on *m*-Xylene and *p*-Xylene (FS 9)

The objective of these experiments was to determine the ability of the biofilm to extract substrate from an oleophilic feed fluid.

Experimental configuration: Two flat-sheet contactors were connected in series. After establishment of the biofilm (1–2 weeks), the activity of each contactor unit was determined separately. In each case, silicon oil was fed to the feed side, and L-salts medium was fed to the biofilm side. The oil and the L-salts were run counter-current in closed loops. The capacity of the contactor unit was determined by following the concentration of the substrate in both reservoirs after spiking the oil with VOC. After determination of the capacity, the biofilm was harvested, and samples for biofilm thickness (wet weight), cell count, and protein content were collected.

Results: Removal of *m*-xylene and *p*-xylene from the silicone oil was not detectable during the 25-hour- long experiment.

Contactor	Film Age (days)	Biofilm Thickness (μm)	Protein Content (μg/cm^2)	Cell Count (cells/cm^2)
1	12	14	4.7	24×10^6
2	19	95	—	86×10^6

4.2.3 Hollow-Fiber Membrane Experiments

A series of experiments using hollow-fiber modules was performed to establish the efficacy of the proposed biotreatment module for enhanced VOC removal from the octanol. The liquid/liquid stripping efficiency of MEK (octanol to water) was determined for the biotreatment module both with and without a biofilm present. Three aqueous (absorbent) flow rates were examined, with a constant 5000-ppm MEK concentration in octanol and an octanol flow rate of 290 mL/min. Samples were taken in duplicate. Results shown in Table 15 (comparing the 301-mL/min flow, abiotic vs. biofilm) indicate that the presence of a live biofilm enhanced MEK removal by approximately 43 percent.

Table 15. Biomembrane Mass Transfer

Experiment Type	Abiotic			Biofilm
Aqueous Phase	filtered tap water			L-salts[a]
$Q_{aqueous}$ (mL/min)	116	301	598	301
$Q_{octanol}$ (mL/min)	290			
MEK in Octanol (ppm)	5000			
Mass Transfer Rate (g/m^2h)	1.80	2.07	4.45	2.97

[a] pH-balanced trace-nutrient source for microbiological organisms

4.2.4 Staged Biotreatment of VOC Mixtures in Lab-Scale Reactor

A membrane bioreactor for treatment of a broad range of compounds found in paints for aircraft was set up. Different levels of water solubility among the compounds suggested a staged bioreactor comprising a membrane contactor (Liqui-Cel) and a chemostat (CSTR). VOCs were supplied to the Liqui-Cel in silicone oil. The Liqui-Cel served as the reactor for removal of compounds with low water solubility, whereas compounds with high water solubility are more likely to be removed in the CSTR. The objective was to study the performance of the staged bioreactor system and to study the degradative capacity for mixtures of VOCs with different water solubilities in the bioreactor system inoculated with two organisms. A limited number of VOCs were chosen, and the removal of these compounds was monitored. VOC-contaminated oil obtained during air treatment was treated as well.

Experimental configuration: A Celgard Liqui-Cel unit with polypropylene fibers was used as the membrane contactor. The volume of the shell side was 0.4 L and of the lumen side was 0.15 L. The oil passed through the lumen side at a flow rate of 54 mL/min. (3.2 L/h). A CSTR with a liquid volume of 4 L was connected to the shell side, and the bacterial suspension was passed through the shell side in a counter-current mode. The flow rate of the aqueous phase was 400 mL/min (24 L/h). Aerated L-salt medium was supplied to the CSTR at 100 mL/h. The temperature was set at 30 °C, and pH was adjusted to 7.0. The supply of L-salt medium to the CSTR was turned off during the experiment, and the outlet and the air vent from the reactor closed. Oil samples were withdrawn from the oil reservoir, and aqueous samples were taken at the inlet and outlet from the Liqui-Cel. M1 and X1 were cultivated in a 1-L chemostat, and when exponential growth was obtained, the Liqui-Cel was inoculated by passing the suspension through the shell side. The attached CSTR was inoculated with M1, and after reaching exponential growth, the reactor was supplied with L-salt medium containing MEK until a biofilm was established. The systems were combined, and oil containing both MEK and *m*-xylene served as the substrate source.

Analytical procedure: All oil samples and aqueous samples containing both MEK and butyl acetate or paint components were analyzed by ARCADIS. GC analysis was performed on the aqueous samples for determination of the aromatics, and high performance liquid chroma-tography (HPLC) analysis was done to determine aqueous MEK concentrations. Samples for aromatics were transferred to 2-mL vials containing 1 drop of acetic acid for preservation. Extraction of VOCs was carried out by addition of pentane (0.1– 0.2g) containing heptane as internal standard. The samples were shaken vigorously for 2 minutes and stored upside down at 5 °C. Analysis was performed with a Hewlett–Packard 5890 GC equipped with a J&W Scientific capillary column (DB-624) and a FID. A 1-µL sample of the pentane phase was injected into the GC, and the response was compared to the response from standards prepared in pentane. Samples for MEK were collected in 2-mL plastic vials and kept in the freezer until the analysis. HPLC analysis was performed by use of a Spectra Physics HPLC equipped with a Waters 990 Photodiode Array Detector and a reverse-phase Altima C-18 column. The mobile phase used was methanol and phosphate buffer (50 mM KH_2P_4) acidified with 0.1 percent trifluoroacetic acid. The thawed samples were centrifuged to spin down the cell mass. Sample volumes of 100 µL were analyzed.

Experimental procedure: The substrates were chosen to represent constituents in paint were *m*-xylene and *p*-xylene (aromatics), MEK (ketones), and butyl acetate (BA) (esters). Table 16 describes the substrate levels and combinations used in the experiments.

Table 16. Biotreatment of VOC Mixtures in a Lab Scale Reactor

Experiment No.	Substrates	Concentrations in Oil (ppm)	Volume Oil (mL)	Volume Aqueous Phase (mL)
SB1	MEK + *m*-xylene	500	1000	4000
SB2	MEK + *m*-xylene	1000	1000	4000
SB3	MEK + *m*-xylene	1500	1000	4000
SB4	MEK + *p*-xylene	500	1000	4000
SB5	MEK + *p*-xylene	1000	1000	4000
SB6	MEK, BA, *m*-xylene	500	1000	4000
SB7	Oil with MEK, BA, ethylbenzene, *m*-	Various	1800/2000	4000
SB8	Oil with paint	Various	1800/2000	4000

Results: Treatment of MEK and *m*-xylene in mixture was examined in seven experiments. The system was closed down after the first three experiments due to operational problems. The system was set up and inoculated again, and four more experiments were done with MEK and *m*-xylene.

In the first three experiments, a high removal of *m*-xylene from the oil was observed. In the aqueous phase, *m*-xylene was either not detectable or detectable only at low concen-trations. The waste outlet and the air vent from the CSTR were not closed during the first three experiments, which may have contributed to the high removal. Removal of *m*-xylene at rates up to 18 ppm/h was obtained during an 8–10 hour period in the next four experiments. Rapid transfer of MEK from the oil to the aqueous phase was observed in all the experiments. However, the removal of MEK was very low, and an accumulation of MEK in the aqueous phase was observed. After the experiments with MEK and *m*-xylene, *p*-xylene replaced *m*-xylene in the mixture. Removal of *p*-xylene was not detectable. Removal of MEK from the aqueous phase appeared to take place in the range of 5-14 ppm/h.

When mixtures of MEK, BA, *m*-xylene, and *p*-xylene were treated, MEK removal was observed as well. It was not possible to separate *m*-xylene from *p*-xylene in the GC analysis, so total xylene concentration was determined. The rate of removal of the xylenes was 36 ppm/h. BA appeared to be removed as well (standard curve for MEK was used for the GC-analysis).

Treatment of oil containing a mixture of BA, ethylbenzene, *m*-xylene, and *o*-xylene showed only insignificant removal of VOCs from the oil. When oil run in the air treatment system with paint was treated, only xylene removal was observed. MEK and BA appeared only in the oil run with paint for two hours and both compounds were removed immediately from the oil.

5.0 Conclusions

This study was performed to collect data on a novel hollow-fiber membrane-based technology to extract and process VOCs from a dilute stream produced by processes such as paint spray booths. The resultant reactions would form water and CO_2 as a final exhaust stream. This system was at least partly developed during the execution of this project, and the components tested were judged by their capability to produce a system that is economically competitive with such other technologies as thermal afterburners or adsorption systems (e.g., carbon filters). It is concluded that the process science is sound. Under tests/evaluations in which process economics were not considered, VOC removal rates (greater than 70 percent) of certain compounds were measured. Although many of the problems were technical in nature, many could likely be resolved through further research and resource allocations.

5.1 Separation System

No suitable separation module currently exists, and the project's development efforts failed to produce a suitable module to deliver a complete, cost-competitive system for VOC control. Membrane-contactor developers are currently devoting their time and resources to applications they deem more promising with brighter payoff potentials. Equipment size is a problem as well. Microfiber contactor modules are typically developed for small-scale processes, and a module suitable for extracting VOCs from a large paint booth would require manufacturing capabilities that are not currently available. A suitable module could be as much as 20 to 50 times the size of the largest module currently available for any process, and its production equipment would be required to outfit more than just paint booth processing equipment to meet the necessary economies of scale. In addition, radial modules are the most-commonly available, but the separation contactor for paint booth work needs to be a box-type cross-flow module to reduce the air-side pressure drop to reasonable levels.

A number of microporous fibers were tested for their potential to develop appropriate high-performance modules. In early testing, a number of modules with uncoated fibers were tested that produced reasonable results, but pressure balancing between the air side and transfer-fluid side was determined to be economically unfeasible, so modules with coated fibers were pursued as a solution. Pore size as well as coating thickness and consistency are the important parameters for producing the appropriate extraction performance in fibers. The coating must be inert to prevent reactions and such performance detriments as coating swelling or softening. The coating must adhere to the fiber walls. A plasma-polymerized silicone-rubber-coated fiber developed by AMT proved to have good adherence and inertness properties, and this fiber displayed good endurance under a wide range of pressures. The AMT fiber has a greater potential for module development than any other coated

fiber developed or tested in this project. Although testing showed this fiber leaked silicone oil, the coating thickness could have been adjusted to address this problem if more time had been available. Other adjustment are also available to address this problem including coating treatments, pore size, and post-treatment processing steps.

A successful module must be developed simultaneously with testing the intended transfer fluid to be certain of material and physical compatibility. Before modules are developed, potting and module-frame materials must be tested with the intended contact fluid using extended contact times and under the intended operating pressure. Seals such as O-rings or other gaskets must be able to withstand constant immersion in the intended transfer fluid. Octanol attacked many O-ring materials that were used on the Celgard modules during early testing, and the only O-ring found to withstand this fluid was cost prohibitive for production purposes. Subsequently, octanol was found to also swell the coated fibers that were used in the AMT cross-flow separation contactor. This swelling caused bunching and voids in the fiber bundle that resulted in air flow channeling and poor contact. A number of alternate fluids were considered before settling on a replacement for octanol. These alternatives included canola oil and mineral oils, both of which have too many impurities to allow accurate GC determination of extracted compounds, and silicone oil, which would be cost prohibitive in a full-scale facility and would have unknown effects on bugs over a long period. Silicone oil was chosen as an alternative to octanol but, because of time constraints, was not thoroughly tested for partitioning performance, and this may have played a big role in the disappointing removal efficiency test results. In addition, although materials compatibility testing with a higher-viscosity silicone oil produced acceptable results, performance results with a lower-viscosity oil, chosen for its similarity to octanol, resulted in unforeseen problems such as weeping, leaking, and stretched fibers. An optimized module must be closely matched in all characteristics to its extraction fluid. Based on the experience with this project, a fluid or fiber substitution will almost always require a complete return to the beginning of the development cycle.

The AMT cross-flow module has the necessary characteristics for acceptable air-side pressure-drop performance. However, distortion of the fibers caused by small leaks of the thin silicone oil produced uneven contact that counteracted any performance improvements. Data showed that performance from a given arrangement of modules is adversely affected by increased airside flow. Extraction performance drops progressively as the oil absorbs higher quantities of VOCs, but the results of testing may have showed the limited capacity of silicone oil compared to octanol. This conclusion seems particularly obvious when seeing that VOC absorbance dropped quickly during some runs, when the oil was still lightly loaded. On the other hand, increasing oilside flow and pressure enhances performance. This increased performance is, of course, limited by module integrity, and running at higher pressures caused failure of several modules.

5.2 Biotreatment System

5.2.1 Biodegradation Range and Extent

The screening studies, and subsequent growth studies, indicate that several organisms that were isolated are capable of degrading the model compounds tested (*m*-xylene, *p*-xylene, toluene, methyl ethyl ketone, butyl acetate). As one would expect, no single organism was capable of simultaneously degrading all of the compounds used during the project. Therefore, a consortium of organisms was used to effect degradation of VOC mixtures. The majority of the work performed focused on two organisms, designated M1 and X1. These organisms were isolated utilizing aliphatic and aromatic substrates, respectively.

The degree of degradation exhibited by the organisms used in the study was significant. Between the two organisms, all of the compounds could be reduced to levels below 250 ppb in an aqueous phase. These levels were exhibited in experiments GS2–GS10, GS14, FS3, and FS5–FS8. In every case, this VOC level represented greater than 99 percent reduction in the amount of compound present initially.

5.2.2 Problems Arising from Metabolic Regulation

The experimental results obtained indicate that concurrent degradation of aromatic and aliphatic VOCs in a single bioreactor is problematic. Cultures containing M1 and X1 (individually or in combination) exhibited roughly concurrent degradation of the aromatic compounds, followed by degradation of the aliphatics. Table 17 indicates those experiments where concurrent (or nearly so) degradation or aromatic–aliphatic sequential degradation was observed and identifies the compounds involved.

Table 17. Concurrent Degradation

Experiment No.	Organism(s)	Compounds
GS3	X1	Toluene, *m*-xylene
GS5	M1	Toluene, MEK
GS6	M1	*m*-Xylene, MEK
GS7	M1	Toluene, *m*-xylene
GS9	M1 AND X1	Toluene, MEK
GS10	M1 AND X1	Toluene, *m*-xylene, MEK
GS14	X1	*m*-Xylene, *p*-xylene

Ethylbenzene was found to have a predominantly, but not exclusively, inhibitory effect on culture

growth and biodegradative activity, as indicated directly by the results of experiment GS13 and as can be inferred from the results of experiments SB7 and SB8. The results from GS13 indicate that ethylbenzene stimulates growth to a small degree at aqueous phase levels below 100 ppm, but a level of 150 ppm prematurely terminates cell growth. The low rate of degradation of aromatic compounds exhibited in experiments SB7 and SB8 (ethylbenzene present) relative to results from experiments SB3, SB5, and SB6 (ethylbenzene absent) suggests that aqueous-phase ethylbenzene levels as low as 40 ppm might have an inhibitory effect on aromatic degradation in biofilm cultures. This is, however, a supposition; further testing is necessary before this can be reliably concluded. Fortunately, no such inhibition was noted for degradation of butyl acetate or MEK.

5.2.3 Treatment Strategy

Given the sequential nature that was observed for aromatic/aliphatic degradation, the strategy was adopted to circulate the aqueous phase of the biofilm reactor through a continuously stirred tank reactor containing primarily M1 (the aliphatic degrader). As indicated in experiments SB2 through SB6, this strategy is quite successful in concurrently reducing aliphatics (MEK and/or butyl acetate) and aromatic compounds (*m*- or *p*-xylene) in the oil phase. This behavior was indicated by staged biotreatment systems with fresh films (SB4, 6) and films regenerated following EDTA-induced sloughing (SB3, SB5).

5.2.4 Implementation

The flat-sheet and staged-bioreactor studies indicate that "bioextraction" of VOCs from the carrier fluid occurs at rates sufficient to maintain active cell growth and activity. These studies also indicate that the hollow-fiber membrane units available to this project had inadequate surface area to effectively treat the carrier fluid in anything approaching real time. The hollow-fiber membrane units do, however, offer effective contacting of the biofilm with the carrier fluid. It would appear that the next steps in evaluation of this configuration would involve (1) identifying an effective degrader of ethylbenzene and (2) designing a membrane contactor that would enable sampling of the biomass so that comparisons can be made between the flat-sheet results (where biomass can be sampled directly) and the hollow-fiber unit performance.

6.0 Recommendations

The technology developed as a result of this project must be technically and fiscally sound before a decision will be made for future full-scale implementation. Although the technology has been demonstrated to have technical promise or potential, no results have been produced that warrant further consideration and study until manufacturing techniques for membrane modules advance enough to allow the cost-effective fabrication of low-pressure-drop, high-efficiency, leak-free modules. The potential cost and environmental benefits of such a system do warrant consideration of further basic development projects aimed at improved fibers, coatings, stripping fluids, and module designs.

Future efforts should concentrate on fiber and module development. Many options are available for fiber materials and for coatings (see AMT response), and more are being developed each year, usually for some specific application that suddenly becomes financially promising. Module construction is also undergoing groundbreaking development in many other applications.

Paints are also being reformulated, and this will make specific module development more difficult, especially considering the difficulty experienced in identifying paint constituents. Future work should pay particular attention to the great difference between common paint constituents, such as industrial-grade xylenes and pure compounds, when performance testing. The use of a total hydrocarbon analyzer through each phase will more clearly establish whether performance goals are being achieved or if many compounds are escaping notice.

6.1 AMT Recommendations

Applied Membrane Technology, Inc.'s objective was to develop low-pressure-drop cross-flow hollow-fiber membrane modules for use in the MBT system intended for high volumetric flow rates containing low contaminant concentrations of fugitive target compounds. To provide suitable low-pressure-drop modules within the project time constraints, both module fabrication and membrane composition needed to be based as much as possible upon known parameters of module construction and chemical formulation. In other words, a thorough investigation of alternative materials of construction that might be more suitable was not feasible during AMT's period of involvement.

AMT's module design was based on a previous project for the US Navy for use in a low-pressure-drop seawater application. This design was adapted for the ARCADIS VOC air project with several minor alterations to make it more compatible for air-stripping applications. AMT successfully designed and built a winding fixture that could wind four cross-flow membrane modules at a time. (Scale-up to larger volumes would be straightforward based on this design). The modules produced

using this design yield a very low air side pressure drop as intended. The module housings were constructed from polycarbonate due to the need to rapidly tool fixture parts and module components. Other module housing materials suitable for long-term applica-tions could be utilized in the future.

The hollow-fiber membranes proved to be a more-problematic issue. Preliminary testing and evaluations of membrane fibers and prototype modules utilizing plasma-polymerized, silicone-coated, polypropylene fibers indicated adequate flux of VOCs and tolerance for contact with silicone oil up to 35 to 40 psi. AMT lab evaluations of octanol stripping agents ruled them out due to excessive swelling and distortion of polypropylene membrane substrates supplied by all vendors.

Membrane compositions for use with silicone-oil stripping agents could be made utilizing stronger polypropylene substrates produced by Celgard US or AKZO Membrana, although they will exhibit some degree of swelling depending on pressure, temperature, and the nature of the membrane top coating. AMT could place copolymer coatings, such as silicone/Teflon or silicone/propylene, onto these microporous substrates instead of the straight silicone membrane.

The latter copolymer compositions have shown higher resistance to oil permeation and swelling effects in other AMT lab projects and during evaluation of flat-film samples conducted by outside research groups. The ability to tailor the coatings' chemical composition offers potential avenues for future improvements. Other groups encountered similar problems of oil and solvent swelling/permeation during the successful development of solvent extraction from oil in the de-waxing process performed by petroleum companies. Mobil Oil and Texaco use several commercial units based on flat membranes. AMT can make hollow-fiber versions of similar copolymers, which may merit investigation for applications such as the MBT system. AMT would need to evaluate a series of potting compounds and determine appropriate potting techniques for assembling bundles of such coated fibers because adhesion becomes more difficult as the concentration of Teflon or polypropylene increases in the membrane coatings. It is a doable proposition, but the time constraints of this project would not have allowed for such trials.

In addition, AMT could evaluate both polymeric and ceramic non-propylene-based substrates. For example, new ceramic-based hollow fibers of dimensions comparable to conventional microporous membranes and coated with a silicone/PTFE copolymer membrane via plasma polymerization may offer the ideal membrane composition for membrane-mediated extraction of VOCs. The ceramic materials would tolerate broad temperature and pressure regimes and exhibit no swelling behavior, and the membrane coatings could be tailored to optimize VOC flux while restricting oil permeation. The objective of such an endeavor would be to raise the operating window of the cross flow module so that higher pressures (i.e., faster liquid sweep rates) could be utilized to enhance module VOC-stripping performance as well as to fix the hollow fibers in place for air flow distribution without

later shifting due to swelling, as observed in the current units.

In summary, the general design and method used to fabricate the cross-flow membrane modules was found to be suitable for producing the low-pressure-drop units. More adequate allocation of resources in terms of time and research expenditures directed at optimizing the hollow-fiber substrate/coating composite formulation may result in superior membrane performance, which, in turn, would provide a more-economic and commercially viable operating window for the MBT process.

Appendix A

Literature Search and Review

The success of the VOC treatment technology we are developing is dictated by the performance of the separation and biotreatment modules. Certain design and operational criteria are recognized as essential to the efficient and economical operation of each contactor. For the air/VOC separation module, these criteria include the following:

- High surface-area-to-volume ratio
- Membrane composition and configuration to maximize VOC transfer
- Membrane configuration to minimize leakage of transfer fluid into air stream
- Module design to minimize airside pressure drop
- Possibility for commercial availability of module

For the bioreactor module these criteria include the following:

- High surface-area-to-volume ratio
- Membrane configuration to minimize leakage of transfer fluid into aqueous stream
- Design and operation to minimize biofouling of the aqueous side
- Maximize degradative activity of biofilm
- Capability to rapidly degrade a wide variety of VOCs

In consideration of these issues, the following extensive literature search was undertaken to guide the subsequent development of the process.

AIR/VOC SEPARATION MODULE

Module Type

Although membrane-based gas separation was first commercialized in 1977 for the enrichment of oxygen from air, the predominant applications currently are for the production of high-purity (99.95%) and medium-purity (95–99.5%) nitrogen (Prasad, 1994), CO_2 removal from natural gas (McKee, 1991), and hydrogen purification for recycle (Shaver, 1991). All of these processes employ asymmetric or composite polymer membranes (Stern, 1994). These applications have come on the heels of 20 years of intensive research that saw the development of asymmetric membranes that exhibited high fluxes (Loeb, 1963), a method for the synthesis of robust hollow fibers (Vos, 1969), and a method for the casting of ultrathin, high- permeability, nonporous polymer films onto existing membranes (Ward, 1976) [subsequently improved upon and commercialized by Monsanto (Henis, 1981; Henis, 1980)]. Commercial membrane-based nitrogen production processes, for example, predominantly utilize hollow-fiber membrane configurations instead of plate-and-frame or spiral-wound. The rationale for this choice is clear when considering the relative membrane module areas. Koros and Fleming report that membrane module areas for the three configurations are: 100–150 ft^2/ft^3 for plate-and-frame modules, 200–250 ft^2/ft^3 for spiral-wound, and 2000– 4000 ft^2/ft^3 for hollow-fiber modules (Koros, 1993). The advantageous surface-to-volume ratio attained by hollow-fiber systems was a major factor in our selection of this configuration for our modules.

Membrane Composition

Membrane transport

To select among the plethora of materials available for membrane construction, it is important to first understand the molecular basis of flux through porous and nonporous polymeric materials. Because essentially all commercial gas-separation membrane systems utilize nonporous membranes, the

description of transport through strictly porous materials will be abbreviated. Flux is the rate of transport of a chemical species (also referred to as the penetrant) through a given membrane or pore-filling material. Flux is determined by the chemical potential gradient of the transported species across the membrane, the membrane thickness, and in the case of nonporous membranes, the solubility of the species in the membrane material. The mechanism of species flux through nonporous material has been generally described as solution–diffusion (Koros, 1989; Koros, 1991) and depends upon the solubility (or condensability) and the diffusivity of the species in the polymer.

The chemical potential gradient is represented by the partial pressures of the species on either side of the membrane for gas–gas separations or, in the case of a gas–liquid separation, the "effective" partial pressure of the species on the liquid side of the membrane. An intrinsic property of polymeric material relative to species transport is the permeability (P_A), which is "a parameter equal to the pressure-and-thickness-normalized flux" (Koros, 1993), as shown in Eq. 1:

$$P_A = (\text{flux of } A \text{ per unit area})/(\Delta p_A/d_m) \quad (1)$$

where Δp_A is the partial pressure gradient of species A across the membrane and d_m is the membrane thickness. Permeability is a direct measure of the ease of transport of the species through the membrane, and it can be written as the product of the solubility coefficient, S_A (a thermodynamic parameter) and the diffusion coefficient D_A (a kinetic parameter);

$$P_A = (S_A)\,(D_A) \quad (2)$$

These coefficients can themselves be complex functions of many variables, including identity and concentrations of current and past sorbed species as well as temperature (Koros, 1989; Koros, 1991). What is of importance to those seeking to separate two gas-phase species (A, B) is the separation factor, or selectivity, (α_{AB}), which is defined in terms of the mole fractions of the two species (y_A, y_B) upstream (subscript 1) and downstream (subscript 2) of the membrane.

$$\alpha_{AB} = \frac{y_{A2}/y_{B2}}{y_{A1}/y_{B1}} \quad (3)$$

The separation factor can also be written in terms of the permeabilities of the two penetrants and the relative partial pressure driving forces (Ashworth, 1992; Koros, 1993; Stern, 1994):

$$\alpha_{AB} = \frac{P_A}{P_B} \times \frac{\Delta p_A/p_{A1}}{\Delta p_B/p_{B1}} = \frac{D_A}{D_B} \times \frac{S_A}{S_B} \times \frac{\Delta p_A/p_{A1}}{\Delta p_B/p_{B1}} \quad (4)$$

Written in this manner, the separation factor can be seen to have contributions derived from penetrant solubility (S_A/S_B) and penetrant mobility (D_A/D_B). Selective solubility is the controlling factor in processes involving the separation of vapors from gases, such as VOC removal from air (Baker, 1987; Watson, 1990; Lund, 1996; Deng, 1998). The motion of polymer segments in the membrane controls mobility selectivity. As these segments move, free volume becomes available to the penetrant and it "hops" from one intersegmental free volume to another (Kumins, 1968; Frisch, 1983; Zielinski, 1992). The frequency of these movements is affected by membrane temperature (Kulkarni, 1983), by the size of the side chains along the polymer backbone, and by whether the polymer is glassy or rubbery (above or

below the glass transition temperature for that polymer). This theory has been used successfully to describe the permeability of organic vapors in several rubbery polymers (Fujita, 1968; Suwandi, 1973), most particularly silicone rubber (Sok, 1992) or poly(dimethylsiloxane) (PDMS).

Membrane experimental configurations

Use of membranes to separate VOCs from a contaminated stream has taken two primary forms: pervaporation and vapor-phase extraction. In pervaporation, a contaminated aqueous phase contacts the shell side of a microporous hollow fiber, which has been coated with a nonporous thin film, most often PDMS. A vacuum is drawn, or a carrier gas flows on the tube side of the membrane, and the VOCs permeate through and evaporate from the membrane. Vapor-phase extraction, on the other hand, generally involves a contaminated gas stream with a vacuum or extraction fluid on the other side of the membrane. The driving force in these cases is the same as described above, the chemical potential gradient caused by low downstream penetrant concentration.

Porous membranes

When a gas–vapor mixture is made to flow through a porous solid medium, the condensable species (vapors) have much higher transport rates than the noncondensable species (gases). This phenomenon is the result of several transport mechanisms, including adsorbed flow (Carman, 1952) and capillary condensation (Rhim, 1975, Lee, 1986; Qiu, 1991). For the condensable gas, capillary condensation can occur on the insides of the pores at a pressure much less than the ordinary condensation pressure (or at a concentration much less than normal). Once condensed, the transport of the condensate through small pores can be regarded as viscous flow, and this flow blocks the transport of the noncondensable gas through the pores. A mathematical treatment of these phenomena was presented by Qiu and Hwang (1991) and compared to experimental results using a porous glass membrane.

Nonporous membrane materials

A significant number of investigations have focused on the effect of polymer modifications on transport properties for both glassy and rubbery polymers. Two generalizations can be made regarding the results obtained:

1. Permeability and selectivity exhibit an inverse relationship.
2. Rubbery polymers exhibit high permeability and low selectivity; glassy polymers exhibit high selectivity.

Several exceptions to these "rules" do exist, and it is instructive to investigate more closely the literature regarding glassy and rubbery polymers separately.

Glassy Polymers

Generally, these polymers exhibit higher selectivity and lower permeability than rubbery polymers. However, PTMSP (poly [(1-trimethylsilyl)-1-propyne]), a polyacetylene which has a repeating structure of $[-(CH_3)C=C(Si[CH_3]_3)-]_x$, is a glassy polymer that has been found to have roughly ten-fold higher permeability than PDMS with only somewhat lower selectivity (Masuda, 1983; Takada, 1985; Masuda, 1988; Ichiraku, 1987). Prior to these results, PDMS was found to have the highest permeability of any nonporous polymer. The high permeability of PTMSP is attributed to the bulky side groups ($-Si[CH_3]_3$) which generate a large free-volume fraction (estimated to be 0.20–0.27) (Platé, 1991) for penetrant diffusion. Unfortunately, since glassy polymers are non-equilibrium materials, their excess free volume

tends to decrease over time and is highly dependent on the processing history of the polymer. As such, unmodified PTMSP is not suitable for long-term commercial applications.

Significant effort has also been put forth to investigate the substituted polyacetylenes, including analogs of PTMSP, to determine whether achieving even higher permeabilities with little loss of selectivity and with enhanced stability is possible. Early efforts, summarized by Odani and Masuda (Odani, 1992), indicate that polyacetylenes with bulky substituents tend to have the highest permeabilities and that the substitution of long *n*-alkyl groups for the silyl group, or long alkyl groups for a methyl group on the silyl group, greatly reduces the permeability of the polymer.

More-recent efforts by Nakagawa and co-workers have investigated the modification of PTMSP by bromination (Nagai, 1994) and by copolymerization (Nagai, 1997). Brominated PTMSP also exhibited a time-dependent decline in gas permeability for a number of gases (O_2, N_2, CO_2, C_3H_8). However, the decline was less pronounced than exhibited by PTMSP, and once it restabilized, consistent permeability was observed throughout a 175-day period (Nagai, 1994). Much greater success was achieved by copolymerization or blending of PTMSP with poly(1-phenylpropyne) (PPP), a glassy polymer with excellent stable gas permeability but lower permeability than PTMSP (Nagai, 1995). PPP concentrations up to 10% in either blended or copolymerized form caused less than an order-of-magnitude decrease in permeability and essentially complete stability over a 30-day period.

Work similar in breadth and focus has been underway for polyimides, poly(ether imides), polypyrrolones, poly(amide imides), polycarbonates, polysulfones, cellulose acetate and poly(phenylene oxide). While many of these studies show promise for development of high-performance vapor-separation materials, few are sufficiently advanced to warrant detailed consideration. Interested readers are directed to Stern (1994) for a review of early literature in these areas. We will deal directly with polysulfones with specific mention of poly(alkylsulfone) (PAS-16).

In general, polysulfones are glassy at room temperature and have the high penetrant size selectivity characteristic of glassy polymers. However, PAS-16 is a rubbery polysulfone copolymer of hexadecene and sulfur dioxide as shown in Figure 1. It exhibits some side chain crystallinity at room temperature; the degree of which is dependent upon the thermal processing of the polymer. This makes the permeability of PAS-16 history-dependent, which is atypical of rubbery polymers (Singh, 1997).

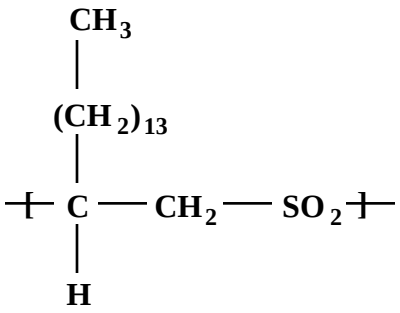

Figure A-1. PAS-16 Repeating Unit

Extensive characterization of PAS-16 for permanent gases (O_2, N_2, H_2 and CO_2) indicates that the PAS-16 behaves as a typical rubbery polymer. However, a comparison of permeabilities for PAS-16 and PDMS indicates that permeability in PAS-16 is roughly one order of magnitude lower than that in PDMS (Gray, 1976; Gray 1984; Singh, 1997), which makes it the next-most permeable-polymer given the high

permeability of PDMS. The permeability of PAS-16 to organic vapors is likewise high, though some crystallinity is manifested in these experiments, with permeability decreasing dramatically upon first exposure to toluene (induces local crystallization) and then remaining constant for a given penetrant (toluene, *n*-hexane, acetone and methanol) at different partial pressures (Singh, 1997). The relative permeability of the top two penetrants (toluene and *n*-hexane) is temperature dependent, with *n*-hexane permeability highest under 40 °C and toluene permeability highest at higher temperatures (Singh, 1997). This polymer behaves as do the rubbery and ultrahigh-free-volume glassy polymers (PTMSP, for example) regarding permeability dependence on penetrant solubility (Freeman, 1997), and as such, it deserves further investigation to establish its suitability for commercial application.

Rubbery Polymers

PDMS $(-(CH_3)_2SiO-)_x$ has incredibly high permeability to a wide variety of gases; more than an order of magnitude greater than the nearest polymer (with the exception of PTMSP, as previously described). The high permeability of this polymer is generally accompanied by low overall selectivity for low-molecular-weight gases. The high permeability of PDMS is attributed to the flexibility of the siloxane (-SiO-) linkages of this polymer. Research with this polymer has focused on modifications that exhibit higher selectivity without sacrificing permeability. Results analogous to those obtained for PTMSP were obtained:

1. Bulkier functional groups on the side chain (replacing a methyl group) decreased permeability by increasing chain stiffness (Stern, 1987; Lee, 1988). These substituents act by reducing the diffusivity of the penetrant in the polymer, not by reducing solubility.
2. An inverse relationship holds between permeability and selectivity.
3. Substituents that induce formation of crystalline domains greatly reduce permeability (Stern, 1987).
4. Specific interactions between the penetrant and the polymer that increase solubility dramatically increase the permeability of the polymer to that penetrant (Ashworth, 1991).

The overall selectivity of highly permeable silicone polymers is a function of the solubility selectivity (S_A/S_B), not the mobility selectivity (D_A/D_B) (Stern, 1987). Given this fact, and in light of item (4) above, a potentially effective method for increasing selectivity in silicone polymers, without impairing permeability, is to substitute functional groups that interact specifically with selected penetrants.

Membrane Configuration

Composites versus single-polymer (simple) membranes

The transport mechanisms of gases through composite membranes involve two major diffusional pathways, as shown in Figure A-2 (adapted from Kimmerle, 1991).

Path 1 runs through the nonporous top layer (thin film) polymer, which generally exhibits some selectivity, then into the pore space of the basement membrane. Path 2 runs through the thin film and then through the basement membrane polymer (substructure) itself before reaching a pore space. The basement membrane material is usually selected to provide structural support for the thin film and is of high porosity to minimize the contribution of basement membrane resistance to the overall resistance to transport of the penetrant. The key parameters determining the flux through composite membranes under a given driving force can be developed in the following manner.

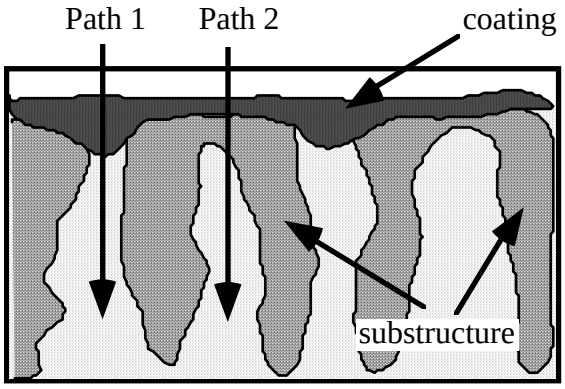

Figure A-2. Two Pathways for Transport Through a Composite Membrane

The volume flux of penetrant, *J*, can be related to membrane structure by substitution of the appropriate terms into the general relationship that flux is equal to the product of the driving force and area, divided by the resistance to transport. For path 1, this equation is (Pinnau, 1988):

$$J_i^{L,P} = \frac{\left(\Delta p_i \times A^P\right)}{\left(\frac{d^L}{P_i^L} + \frac{d^P}{P_i^P}\right)} \tag{5}$$

where P_i^x is the permeability of penetrant *i* in membrane component *x*, where $x = L$ denotes the top layer, $x = P$ denotes the pore and, in equation (6), $x = S$ denotes the membrane substructure material. A^P denotes the surface area of the pores and d^x denotes the thickness of the particular membrane component *x* (=*L*, *P*). For path 2, transport can be expressed in the following way (Henis, 1981):

$$J_i^{L,S} = \frac{\left(\Delta p_i \times A^S\right)}{\left(\frac{d^L}{P_i^L} + \frac{d^S}{P_i^S}\right)} \tag{6}$$

where A^S denotes the surface area of the substructure, which is equal to the total membrane surface area, A^M, minus the pore area, A^P. The porosity of the membrane ε can be expressed as

$$\varepsilon = \frac{A^P}{A^M} \tag{7}$$

The total flux of penetrant *i* through the membrane is given by

$$J_i^M = J_i^{L,S} + J_i^{L,P} \tag{8}$$

An expression for the total volume flux (per unit area), $J_{i,A}$, can be expressed by combining equations (5-8) to give:

$$J_{i,A}^M = \left\{ \varepsilon \left(\frac{d^L}{P_i^L} + \frac{d^P}{P_i^P} \right)^{-1} + (1-\varepsilon) \left(\frac{d^L}{P_i^L} + \frac{d^S}{P_i^S} \right)^{-1} \right\} \Delta p_i \tag{9}$$

There are three scenarios to be considered using this equation relative to what controls the performance of the composite membrane: (1) to*p*-layer controlled, (2) support-structure controlled, and (3) mixed-flux control. Kimmerle concludes the following regarding membrane configuration:

> If the transport properties of a membrane are determined by the selective top layer it can be optimized in terms of its flux and selectivity by preparing a support structure which has the highest possible porosity and permeability in the pore structure. The permeability of the selectivity top layer should furthermore be as high and its thickness as low as possible. (Kimmerle, 1991)

This conclusion is endorsed by a large number of practitioners in the field (Koros, 1993; Parthasarathy, 1994; Stern, 1994; Prasad, 1994; Nagai, 1997; Zhu, 1983; Blume, 1990; Bessarabov, 1996; Das, 1998; Poddar, 1996b; Cha, 1996) who have evaluated single polymer and composite membranes for gas separation and VOC removal from liquid and air streams.

In a recent review of commercial air separation processes, Prasad and co-authors list the development of ultrathin barrier layers as one of the key technical innovations in the commercial development of membranes in air separation. "The discovery by Loeb and Sourirajan (Loeb, 1963) of integrally skinned, high-flux asymmetric membranes was essential in transforming membranes to a technology of significant commercial interest" (Prasad, 1994). Ashworth provides an excellent illustration of the direct benefit of composite membranes using the separation of H_2 from CO as the goal and polysulfone and silicone rubber as the membrane materials under consideration (Ashworth, 1992). The following data are taken from his paper.

Table A-1. Effect of Membrane Composition on Permeability and Selectivity

Polymer	Permeability (cm^3(STP)-cm/cm^2-sec-cmHg)		$\alpha_{H2/CO}$
	H_2	CO	
Silicone rubber (SR)	5.2×10^{-8}	2.5×10^{-8}	2.1
Polysulfone (PS)	1.2×10^{-9}	3.0×10^{-11}	40
SR/PS (99:1)[a]	3.65×10^{-8}	2.68×10^{-9}	13.6
SR/PS (91:9)[a]	1.08×10^{-8}	3.29×10^{-10}	32.8

[a] The ratio denotes the relative thicknesses of the two polymers in a bilayer composite.

Obviously, the productivity of the composite membrane is nearly an order of magnitude higher than that achieved by the pure polysulfone membrane (approximately 80% selectivity, ninefold increase in H_2 permeability). Experiments involving the separation of dichloroethane, chlorobenzene and chloroform from water across polyvinyl acetate, PTFE, or polysulfone membranes (simple or composite) also support such a conclusion. In all cases, the separation factor was at least an order of magnitude higher for the

composite membranes than the equivalent simple membrane (Zhu, 1983). In addition, the composite membranes exhibited greater structural stability (Zhu, 1983).

Blume (1990) compared the permeability and separation factor for trichloroethane, ethyl acetate, acetone and ethanol in a pervaporation through PDMS and PDMS/polyolefin composite membranes. As expected, the PDMS membrane exhibited permeabilities that were an order of magnitude greater than those achieved by the PDMS/polyolefin composite, but the separation factors of the composite were an order of magnitude greater than that of the PDMS membrane so that the flux of a penetrant through the membranes was equivalent, and the concentration of penetrant in the downstream gas was much higher for the composite membrane (Blume, 1990).

Film composition

Baker and co-workers at Membrane Technology & Research Inc. (1987) investigated eight membrane materials for their permeabilities to acetone, toluene, octane, trichloroethane and nitrogen. Each membrane was a flat sheet, cast to a thickness of 25–50 μm, and evaluated at 40 °C. Figure A-3 is taken from Baker (1987) and presents the relationship between toluene permeability and selectivity when toluene was removed from a nitrogen gas stream by pervaporation. Note that the permeability of PDMS (silicone rubber) is nearly matched by that of chloroprene (Neoprene™), which exhibits a higher selectivity than PDMS. Figure A-4, which presents equivalent data for acetone, indicates that silicone rubber is not uniformly the best rubberized membrane for organic compound permeability (Baker, 1987).

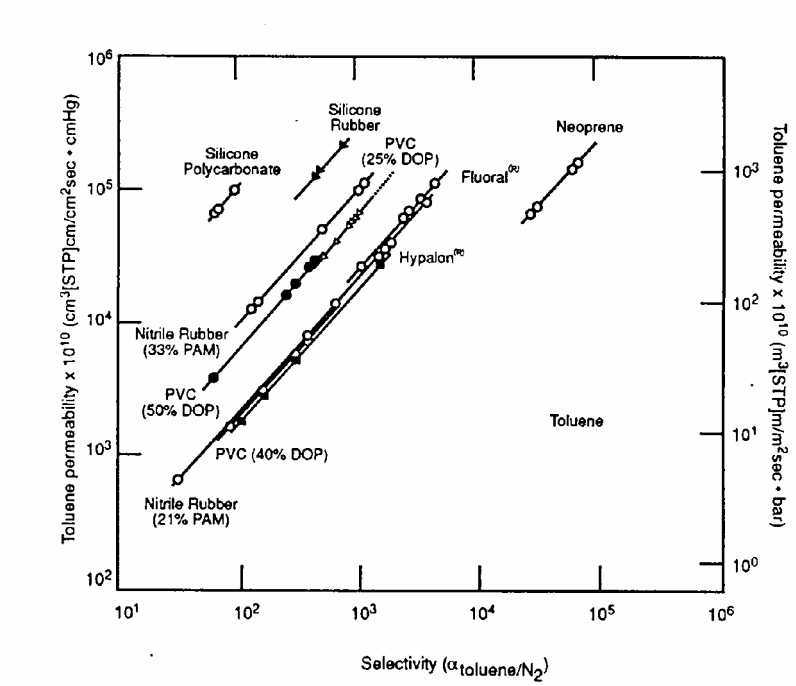

Figure A-3. Toluene Permeability vs. Selectivity For Toluene Over Nitrogen

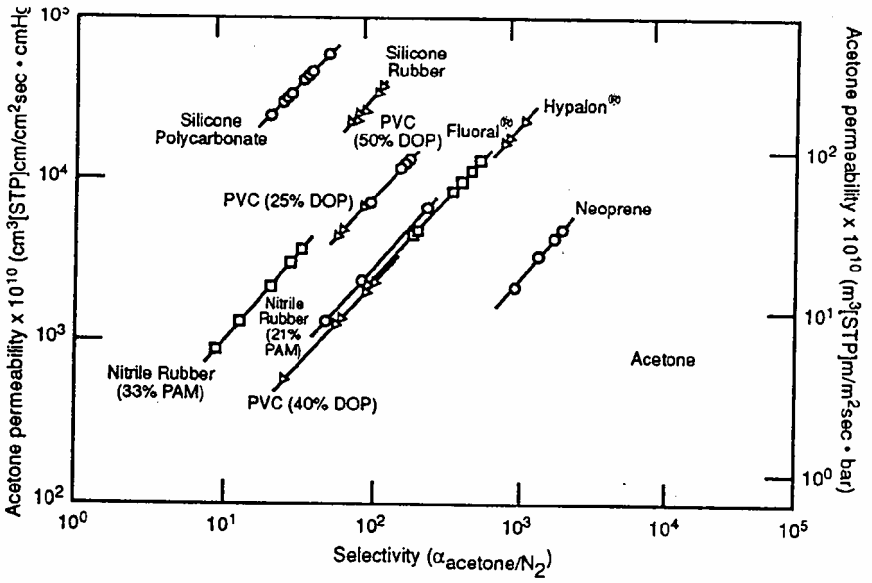

Figure A-4. Acetone Permeability Vs. Selectivity For Acetone Over Nitrogen

Inner versus outer films

The question of placement of the thin film in a composite membrane relative to the liquid and gas phases is an important one. If the film is on the same side of the membrane as the liquid, then the pores will be gas-filled, and vice versa. Gas-phase diffusivities are several orders of magnitude larger than liquid-phase diffusivities (Semmens, 1989). This is significant because the resistances-in-series model has been found to be applicable to composite membrane transport. If one considers the composite membrane and the affiliated resistance, shown in Figure A-5, one finds four potential resistances, through fluid boundary layers, R_{f1} and R_{f2}, through the film, R_F, and through the porous membrane, R_{PM}. Total resistance to transport, R_T, is equal to:

$$R_T = R_{f1} + R_F + R_{PM} + R_{f2} \qquad (10)$$

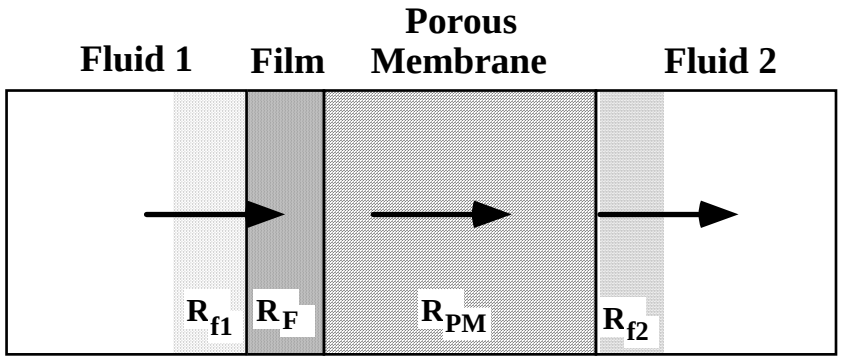

Figure A-5. Transport of Penetrant Through Different Resistances of a Composite Membrane

Studies of the transport of organics through uncoated pervaporation membranes indicate that the liquid-side boundary-layer mass transfer resistance is a significant fraction of the total mass transfer resistance (Raghunath, 1992). In some cases where nonporous films coat the fiber, the film resistance dominates so that all other resistances can be neglected, as was the case reported for transport of methylene chloride across a PDMS/polyethylene composite and absorption into either silicone oil 200 fluid or Paratherm NF mineral oil (Poddar, 1996a). However, using the same experimental system, the film resistance represented only 64% of the total resistance to transport of acetone (Poddar, 1996a). In that case, the porous membrane and liquid boundary layer were found to contribute significantly to the overall resistance. The resistance could have been lowered had the pores been filled with gas (Das, 1998; Semmens, 1989) instead of oil, a point made clearly by Semmens et al. (1989). In a study of pervaporation of several organic compounds (CCl_4, C_2Cl_4, C_2HCl_3, $CHCl_3$, $C_2H_3Cl_3$) in a vapor phase across microporous polypropylene fibers without a coating film, Semmens found that the gas-filled membrane pores offered negligible resistance to transfer (Semmens, 1989).

Cha et al. (1997) also studied vapor-phase pervaporation (gas/vapor mixture on one side on the membrane, vacuum on the other) where the feed side was varied from the film side to the non-film side of a PDMS-coated polypropylene hollow fiber. Surprisingly, the fastest permeation rates were achieved with the gas/vapor mixture exposed to the non-skin side of the composite membrane (tube side in this case). This was attributed to condensation of the vapors within the pores and decreased pressure drop within the pores (Cha, 1997).

Sirkar and co-workers (Das, 1998) studied trichloroethylene (TCE) removal from water utilizing hydrophobic, microporous, polypropylene, hollow fibers (Celgard™ X-10) with a plasma-polymerized silicone coating on the fiber outside (shell side) in pervaporation studies. The aqueous stream was fed through the fiber (tube side) instead of the traditional shell-side contacting. TCE removal was found to be significantly lower when the feed was on the shell side compared to tube-side feed. The most plausible explanation proffered involved bypassing of the fluid flow on the shell side given the tight packing of the fibers and the relatively low fluid velocity. Such shell-side bypassing has been observed with similar modules used for liquid–liquid extraction (Tompkins, 1993).

VOC Transport

Solubility

Preferential solubility of different penetrants in the membrane determines the permeability and selectivity of the membrane. High penetrant–membrane affinity leads to high permeation rates. Several investigators have evaluated the effect of membrane composition on separation and permeation performance. It has generally been established that penetrants with solubility parameters close to that of the membrane material sorb to the polymer and permeate more rapidly than those penetrants with solubility parameters significantly different from the membrane (Zhu, 1983). Table A-2 contains solubility parameters (δ) for several common polymers and organic compounds. The solubility parameter, δ, is defined in Eq. (11):

$$\delta = \left(\frac{\Delta U^V}{V^L} \right)^{.5} \tag{11}$$

Where ΔU^V is the energy of complete vaporization of the liquid, and V^L is the liquid molar volume. Table A-3 indicates the separation factors (α) achieved for different penetrant/membrane pervaporation systems.

Table A-2. Solubility Parameters (Zhu, 1983)

Compound	δ (cal/cm^3)$^{.5}$
Chloroform (CF)	9.3
chlorobenzene (CB)	9.5
1,2 dichloroethane (DCE)	9.8
water	23.4

Compound	δ (cal/cm^3)$^{.5}$
PTFE	6.2
polyvinyl acetate (PVAc)	9.3
polysulfone (PSF)	10.2
cellulose acetate (CA)	11.5

Table A-3. Separation Factors for Membrane/Penetrant Pervaporation Systems (Zhu, 1983)

Polymer	α CF	CB	DCE
PTFE	5–19	7–16	2– 6
PVAc	50–75	46–55	45– 60
PSF	3–10	1–8	5– 7
CA	1	N/A	N/A

Watson and Payne (1990) evaluated the separation factor and permeability of silicone rubber membranes (0.2 mm thickness) for *n*-alcohols (C_1–C_{10}) and a variety of other organic compounds in dilute aqueous solutions using pervaporation. The separation factor (α) was shown to rise monotonically with alcohol chain length (Watson, 1990), as shown in Table A-4. Included in Table A-4 are diffusion coefficients, *D*, measured at 80+ 3 °C in a 0.8 mm thick silicone rubber membrane.

Table A-4. Separation Factor Dependence on Chain Length for *n*-Alcohols

n-Alcohol	Feed concentration (%v)	α	*D* (x10^{-10}m^2-sec^{-1})
Methanol	1.0	9	10.0
Ethanol	1.0	17	7.1
Propanol	1.0	67	6.2
Butanol	1.0	74	5.5
Hexanol	0.5	1050	4.2
Octanol	0.05	3100	3.9
Decanol	0.005	5000	2.5

For pervaporation, since the downstream pressure of the penetrant is essentially zero, Eq. (4) reduces to $\alpha_{AB} = \frac{D_A}{D_B} \times \frac{S_A}{S_B}$. The increase in separation factor exhibited by the *n*-alcohols in the face of declining diffusivities, shown in Table 4, indicates that the increase in separation factor measured through the silicone rubber membrane is driven by the selectivity factor, $\frac{S_A}{S_B}$, not the diffusivity factor, $\frac{D_A}{D_B}$. The results of further investigations are presented in Table A-5. The solubility factor (*A*) in Table 5 is based on the Scatchard–Hildebrand activity–solubility equation (Hildebrand, 1970), which allows the development of a relationship for the partition coefficient, *P*, of component *i*, between an aqueous solution (*w*) and a membrane (*m*), as defined in Eq. (12):

$$P = C_i^m / C_i^w = const \times e^{\left\{\left(\frac{\bar{V}_i}{RT}\right) A\right\}} \tag{12}$$

$$A = \left[(\delta_w - \delta_i)^2 - (\delta_m - \delta_i)^2\right] \tag{13}$$

As the solubility factor *A*, defined in Eq. (13), increases, the partitioning of component *i* into the membrane also increases.

Table A-5. Separation and Solubility Factors for a PDMS Membrane Pervaporation System

Compound	Feed concentration (%v)	α separation factor	*A* (cal/cm^3) solubility factor
Methanol	1.0	9	-2.3
Ethanol	1.0	17	5.0
Phenol	1.16[a]	97	24
Acetone	1.0	170	35
Octanol	0.05	3100	64
Nitrobenzene	0.1	4200	62
Chloroform	0.01	15,000	50
Benzene	0.1	20,000	69
Toluene	0.01	36,000	81
Ethylbenzene	0.01	43,000	97

[a] Percent mass

The data presented in Tables A-4 and A-5 indicate that, for poly(dimethylsiloxane) (PDMS), solubility selectivity is the controlling factor in determining permeability, a conclusion which is in agreement with other findings (Bell, 1988).

Operating Conditions

Leemann (Leemann, 1996) investigated the temperature and concentration dependence of the permeability of pure PDMS hollow fibers (OD approximately 1.0 mm, ID approximately 0.85 mm, length = 250 mm) operated as pervaporation membranes. The permeabilities for toluene, *p*-xylene, ethyl acetate, MEK, acetone and ethanol vapors decrease with increasing temperature, exhibiting Arrhenius dependence on temperature (Leemann, 1996). This is due to the strongly exothermic nature of absorption of organic vapors into PDMS (Leemann, 1996). Similar temperature dependence was noted for pervaporation of carbon dioxide and methane through polypropylene and PDMS membranes coated with fluoropolymer films (Oh, 1996), acetone and ethanol permeation through microporous glass (Qiu, 1991), and acetone pervaporation through silicone rubber (Deng, 1998)

Penetrant concentration, as indicated by the partial pressure of the penetrant in the vapor phase, has a greater effect upon permeability through PDMS at lower temperatures (below 50 °C). At low feed-gas temperatures, permeability increases with penetrant partial pressure, presumably due to increasing diffusivity due to polymer swelling (Leemann, 1996). This was noted specifically for PDMS–polypropylene composite membranes with permeation of toluene, methanol, acetone and methylene chloride (Cha, 1997). However, studies of gas–liquid pervaporation systems indicate that as organic concentration increases in the aqueous feed phase, the separation factor falls dramatically for silicone rubber membranes (Seok, 1987; Ishihara, 1986; Leeper, 1987). The separation factor has also been found to decrease with increasing aqueous phase concentration of the solute until a limiting value is reached for a wide variety of organic compounds (Zhu, 1983; Watson, 1990, Seok, 1987).

The picture is rendered more complex when multiple organic vapors are considered. As different penetrants exhibit different permeation rates, the more slowly permeating compound will build up on the upstream membrane surface (Feng, 1992; Haraya, 1987; Psaume, 1988) diluting the faster penetrant at the membrane surface and resulting in lower permeation rates for the faster penetrant. A parametric study was undertaken to investigate the significance of this phenomenon, termed concentration polarization (Feng, 1992). It was determined that (1) concentration polarization is significant for highly permeable and selective membranes, (2) separation is effective for low vapor content, and (3) for highly selective membranes, variable permselectivity has little effect on permeant concentration but greatly influences permeant flux (Feng, 1992).

However, Ji et al. (1994) found no decrease in membrane permeability for multiple VOCs in the liquid phase (toluene, trichloroethane, methylene chloride) through PDMS; instead, they found that for dilute liquid mixtures, downstream VOC dilution occurred, increasing permeability of all VOCs by increasing the driving force (Ji, 1994b). Similar results are reported for polyurethane and polyether–*block*–polyamides (Ji, 1994a).

Pressure also plays a role in permeability though the picture is not quite clear. Nagai (Nagai, 1994) investigated the permeation properties of brominated PTMSP (Br-PTMSP) and untreated PTMSP above and below the glass-transition temperature. In both regions, for both polymers, permeability decreased with increasing upstream pressure for propane and carbon dioxide. Conversely, Strathmann reports increased permeability through PDMS as upstream pressure increases for octane, toluene, trichloromethane and acetone, up to 10–15 cmHg (Strathmann, 1986).

Membrane-Mediated Absorption

Kamalesh Sirkar's research group has investigated membrane-mediated absorption for VOC removal from gas streams (Poddar, 1996b; Poddar, 1996a, Poddar, 1997). Hollow fibers constructed of microporous,

hydrophobic Celgard™ X-10 polypropylene were used throughout. On the fibers of some of these modules, an ultrathin (approximately 1μm), plasma-polymerized, nonporous, PDMS coating was placed on the shell side of the fibers (Advanced Membrane Technologies, Inc, Minnetonka, Minn.). A VOC–N_2 gas mixture was pumped through the tube side of the fibers, and an extracting liquid was pumped countercurrently in the shell space. Three absorbents were used; silicone oils 50-cs, 200 (Dow Corning, Midland, Mich.) and a mineral-oil-based fluid, Paratherm NF (Paratherm Corp., Conshohocken, Pa.). The VOC–N_2 mixtures were supplied as standard cylinders (Matheson, E. Rutherford, N.J.) containing relatively high VOC concentrations (993 ppmv acetone, 999 ppmv dichloromethane, 514 ppmv methanol, 236 ppmv toluene). At gas residence times between 1 and 1.5 seconds in uncoated fibers, dichloromethane and toluene exit gas concentrations were lowered to 1–2 ppmv using fresh silicone oil flowing at approximately 5% of the gas flow rate (Poddar, 1996a). Similar performance was achieved using Paratherm NF with toluene, but the silicone oil performance was significantly superior for gas residence times between 0.2 and 0.5 seconds.

Using coated fibers, residence times between 5 and 7 seconds are required to reduce dichloromethane to similar concentrations in the exit gas with fresh silicone oil. However, the difference between Paratherm™ NF and silicone oil is negligible to gas residence times down to a single second. A mixed VOC–N_2 stream was evaluated, with the results summarized in Table A-6. What is obvious is that longer residence times are required for high removal percentage as VOC concentration decreases.

Table A-6 Absorption Data for VOC–N_2 Gas Mixture

VOC feed concentration ppmv		Removal % at given gas contact times	
		17 seconds	5 seconds
Acetone	226	93.8	61.5
Methylene chloride	201	95.5	91.0
Toluene	204	100.0	100.0
Methanol	163	52.7	21.5
Total	794	87.4	70.6

This absorption system was also operated in an absorbent recycle mode with an uncoated hollow-fiber module used to remove VOC from the gas stream (Poddar, 1996b). After extracting VOC from the air, the absorbent flows through the coated, hollow-fiber module membrane operated as a pervaporator. The absorbent then flows into a storage vessel before recirculation through the extracting module. The VOC–N_2 mixtures were supplied in standard cylinders (Matheson, E. Rutherford, N.J.) containing relatively high VOC concentrations (993 ppmv acetone, 999 ppmv dichloromethane, 514 ppmv methanol, 236 ppmv toluene). At gas residence times of 1–1.5 seconds in silicone oil flowing at approximately 5% of the gas flow rate through the extraction module, the dichloromethane exit gas concentration was approximately 50 ppmv and the toluene exit gas concentration was about 25 ppmv (Poddar, 1996b). Comparison of these numbers to the 1–2 ppmv achieved with fresh absorbant indicates that residence times greatly in excess of 1 minute will be required for removal percentages near 90%.

For a given VOC and process condition, silicone oil provided higher removal efficiency than Paratherm™. However, silicone oil exhibits deterioration over an 18 month period causing leakage of the

oil into the gas stream. For that reason, Paratherm™ is the preferred oil for these applications (Poddar, 1996a).

BIOTREATMENT MODULE

Biofouling, in the form of a biofilm colonizing a solid surface, has been a significant problem for many important industrial and medical systems, including water supplies, heat-transfer units, ship hulls, and implanted medical prostheses. To suppress the formation or growth of biofilms in these instances, application of biocides has been the dominant mode of operation. The following review will instead focus on efforts involving reduction of biofouling in biotreatment systems, where the emphasis is on maintenance of an active film, and avoidance of excess biofilm thickness.

Membrane Biofouling

Biological systems for the treatment of contaminated water or gas streams generally involve columns packed with solids operated either as a static or a fluidized bed. The biomass in these systems is generally in the form of a biofilm attached to a solid surface. Excess biomass concentration in the bed retards mass transfer (oxygen, inorganic ions, carbon and energy sources), blocks liquid and gas flow, and generally leads to a loss in reactor productivity. To maintain the reactor activity, two general approaches to prevention of biomass clogging have been evaluated; cleaning and metabolic strategies to suppress biomass growth rate.

Cleaning

Cleaning strategies involve the application of high shear forces or a cleaning treatment to remove a substantial fraction of the biofilm material. These approaches act by disrupting some aspect of the biofilm structure. Characklis (Characklis, 1981) was among the first to characterize the shear stresses (normal and parallel to the surface) that contributed to erosion of biofilms. Rittmann (Rittmann, 1980) developed a series of equations describing the friction factor and resulting shear stresses generated by liquid flow through a packed bed. These equations were modified, using data generated by Characklis, to calculate biofilm loss rates as a function of biofilm thickness, biofilm density, and the shear stress (Rittmann, 1982).

Stress is applied to solid packing to remove unwanted biomass in several different ways. Wubker (Wubker, 1997) used a screw stirrer to periodically mix the polyamide-bead packing within a trickle-bed reactor and found that the amount of biomass removed was directly related to the magnitude of the applied shear stress (stirrer rotation rate) and the total stress applied (stirring time). Daily stirring was sufficient to maintain maximal toluene degradation in this reactor. Taylor et al. (Taylor, 1996) determined that weekly removal, washing, and reinoculation of packing material maximized the productivity of an ethanol fermentation process. Smith et al. (Smith, 1996) determined that the efficient operation of a highly VOC-loaded biofilter could be extended indefinitely if a backwash system that expanded the bed by roughly 40% was used twice weekly. The expansion of the bed led to vigorous mixing of the beads, shearing film from the bead surface. Backwashing, however, is necessarily limited to those biofilters containing packing that can be fluidized.

Weber and Hartmans (Weber, 1996) reported chemical washing of a biotrickling filter. Every two weeks a 0.1*M* NaOH solution was flushed through the system for 3 hours. Curiously, the toluene removal rate of the bed after the washing was 50% higher than a similar bed that was unwashed. Loss of activity was observed immediately following washing, but recovered to pre-wash levels within 24 hours (Weber, 1996). This approach has significant advantages relative to fluidization, because of its applicability to

beds that are difficult to fluidize and that utilize fluid flow rates much lower than required for fluidization (Cox, 1998).

Biofilm structure can also be disrupted ionically. The extracellular polysaccharide that forms the bulk of the biofilm is crosslinked by divalent cations (primarily Ca^{2+}, to a lesser extent Mg^{2+}). Release of biofil*m*-bound calcium could lead to biofilm dissolution or detachment from the surface. Gross biofilm detachment was observed by Turakhia (Turakhia, 1983) following exposure of a biofilm to a pulse of a calcium chelating agent, (ethylene glycol)bis(2-aminoethyl ether) (EGTA).

Metabolic strategies

All metabolic strategies are predicated on discovering a nutrient limitation that has a minimal negative effect on biodegradative activity but causes a significant growth rate decrease by increasing the maintenance energy requirement. For example, Schonduve (Schonduve, 1996) determined that while using nitrate as a nitrogen source rather than ammonium caused a noticeable decrease in mixed culture biomass formation rate, the degradation rate was more severely depressed. Smith (Smith, 1996) did find that for a toluene-degrading mixed culture, the use of nitrate in place of ammonium led to a 50% decrease in biomass yield without affecting degradation rates at all.

Addition of 0.4*M* NaCl led to a 32% greater decrease in biomass formation rate than degradation rate (Schonduve, 1996). Similar results were reported for 30g/L NaCl (Strachan, 1996). Potassium and phosphate limitation were each shown to increase the specific butanol degradation rate of a mixed culture while decreasing the biomass yield by as much as a factor of five (Wubker, 1996), and potassium was shown to increase the specific toluene degradation rate while decreasing the biomass yield (Wubker, 1997).

References

Ashworth, A. J., B.J. Brisdon, R. England, B.S.R. Reddy and I. Zafar (1991). “The permeability of polyorganosiloxanes containing ester functionalities.” *J. Membrane Sci*. 56: 217.

Ashworth, A. J. (1992). “Relation between gas permselectivity and permeability in a bilayer composite membrane.” *J. Membrane Sci*. 71: 169–173.

Baker, R. W., N. Yoshioka, J.M. Mohr and A.J. Kahn (1987). “Separation of organic vapors from air.” *J. Membrane Sci*. 31: 259.

Bell, C. M., F.J. Gerner, and H. Strathmann (1988). “Selection of polymers for pervaporation membranes.” *J. Membrane Sci*. 36: 315.

Bessarabov, D. G., E.P. Jacobs, R.D. Sanderson and I.N. Beckman (1996). “Use of nonporous polymeric flat-sheet gas-separation membranes in a membrane–liquid contactor: experimental studies.” *J. Membrane Sci*. 113: 275–284.

Blume, I., J.G. Wijmans, and R.W. Baker (1990). “The separation of dissolved organics from water by pervaporation.” *J. Membrane Sci*. 49: 253-286.

Carman, P. C. (1952). “Diffusion and flow of gases and vapors through micropores.” *Proc. Roy. Soc. Ser.* 211A: 526.

Cha, J. S., R. Li and K.K. Sirkar (1996). “Removal of water vapor and VOCs from nitrogen in a hydrophilic hollow-fiber gel membrane permeator.” *J. Membrane Sci*. 119: 139.

Cha, J. S., V. Malik, D. Bhaumik, R. Li and K.K. Sirkar (1997). “Removal of VOCs from waste gas streams by permeation in a hollow fiber permeator.” *J. Membrane Sci*. 128: 195.

Characklis, W. G. (1981). "Fouling biofilm development - A process analysis." *Biotechnol. Bioeng*. 23: 1923.

Cox, H. H. J., and M.A. Deshusses (1998). “Biological waste air treatment in biotrickling filters.” *Current Opinion in Biotechnology* 9: 256.

Das, A., I. Abou–Nemeh, S. Chandra and K.K. Sirkar (1998). “Membrane-moderated stripping process for removing VOCs from water in a composite hollow fiber module.” *J. Membrane Sci*. 148: 257.

Deng, S., A. Tremblay and T. Matsuura (1998). “Preparation of hollow fibers for the removal of volatile organic compounds from air.” *J. Appl. Polym. Sci*. 69: 371–379.

Feng, X., and R.Y.M. Huang (1992). “Organic vapor/gas mixture separation by membrane—a parametric study.” *Separation Sci. Tech.* 27(15): 2109.

Freeman, B. D., and I. Pinnau (1997). “Separation of gases using solubility-selective polymers.” *Trends in Polymer Sci.* 5: 167.

Frisch, H. L., and S.A. Stern (1983). “Diffusion of small molecules in polymers.” *CRC Crit. Rev. Solid State Material Sci.* 11: 123.

Fujita, H. (1968). Organic vapors above the glass transition temperature. *Diffusion in Polymers*. New York, Academic Press. 75.

Gray, D. N. (1976). “Olefin/sulfur dioxide copolymers.” *Polymer News* 3: 141.

Gray, D. N. (1984). Polymeric membranes for artificial lungs. *Polymeric materials and artificial organs*. American Chemical Society. 151.

Haraya, H., T, Hakuta, H. Yoshitome, and S. Kimura (1987). *Sep. Sci. Technol*. 22: 1425.

Henis, J. M. S., and M.K. Tripodi (1980). “Multicomponent membranes for gas separation.” *US Patent* 4,230,463:

Henis, J. M. S., and M.K. Tripodi (1981). “Composite hollow fiber membranes for gas separation: The resistance model approach.” *J. Membrane Sci*. 8: 233.

Hildebrand, J. H., J.M. Prausnitz, and R.L. Scott (1970). *Regular and Related Solutions*. New York, Van Nostrand Reinhold Co.

Ichiraku, Y., S.A. Stern and T. Nakagawa (1987). “An investigation of the high gas permeability of poly(1-trimethylsilyl-1-propyne).” *J. Membrane Sci*. 34: 5.

Ishihara, K., Y. Nagesse, and K. Matsui (1986). “Pervaporation of alcohol water mixtures through PTMSP.” *Makromol. Chem. Rapid Commun*. 7: 43.

Ji, W., S.K. Sikdar, and S.–T. Hwang (1994a). “Modeling of multicomponent pervaporation for removal of volatile organic compounds from water.” *J. Membrane Sci*. 93: 1.

Ji, W., A. Hilaly, S.K. Sikdar, and S.–T. Hwang (1994b). “Optimization of multicomponent pervaporation for removal of volatile organic compounds from water.” *J. Membrane Sci*. 97: 109.

Kimmerle, K., T. Hofmann and H. Strathmann (1991). “Analysis of gas permeation through composite membranes.” *J. Membrane Sci.* 61: 1–17.

Koros, W. J., and M.W. Hellums (1989). Transport Properties. *Encyclopedia of Polymer Science*. New York, Wiley–Interscience Publishers. 724.

Koros, W. J., M.R. Coleman and D.R.B. Walker (1991). “Controlled permeability polymer membranes.” *Annual Review of Materials Science* 22: 47–90.

Koros, W. J., and G.K. Fleming (1993). “Membrane-based gas separation.” *J. Membrane Sci.* 83: 1–80.

Kulkarni, S. S., and S.A. Stern (1983). “The diffusion of CO_2, CH_4, C_2H_4, and C_3H_8 in polyethylene at elevated temperatures.” *J. Polym. Sci., Polym. Phys. Ed*. 21: 441.

Kumins, C. A. and T. K. Kwei (1968). Free volume and other theories. *Diffusion in Polymers*. New York, Academic Press. 107–140.

Lee, C.–L., H.L. Chapman, M.E. Cifuentes, K.M. Lee, L.D. Merril, K.L. Ulman and K. Venkataraman (1988). “Effects of polymer structure on the gas permeability of silicone membranes.” *J. Membrane Sci.* 38: 55.

Lee, K.–H., and S.–T. Hwang (1986). “The transport of condensable vapors through a microporous Vycor glass membrane.” *J. Colloid Interface Sci.* 110: 544.

Leemann, M., G. Eigenberger, and H. Strathmann (1996). “Vapour permeation for the recovery of organic solvents from waste air streams: separation capacities and process optimization.” *J. Membrane Sci.* 113: 313.

Leeper, S. A. (1987). Membrane separations in the production of alcohol fuels by fermentation. *Membrane separations in biotechnology*. New York, N.Y., Marcel Dekker. 161.

Loeb, S., and S. Sourirajan (1963). “Sea water demineralization by means of an osmotic membrane.” *ACS Symp. Ser.* 38: 117.

Lund, L. W., W.J. Federspiel and B.G. Hattler (1996). “Gas permeability of hollow fiber membranes in a gas–iquid system.” *J. Membrane Sci.* 117: 207–219.

Masuda, T., E. Isobe and T. Higashimura (1983). “Poly 1-(trimethylsilyl)-1-propyne: a new high polymer synthesized with transition-metal catalysts and characterized by extremely high gas permeability.” *J. Am. Chem. Soc.* 105: 7473.

Masuda, T., Y. Iguchi, B.–Z. Tang and T. Higashimura (1988). “Diffusion and solutions of gases in substituted polyacetylene membranes.” *Polymer* 29: 2041.

McKee, R. L., M.K. Changela and G.J. Reading (1991). “Carbon dioxide removal: Membrane plus amine.” *Hydrocarbon Processing* 70(4): 63–71.

Nagai, K., A. Higuchi and T. Nakagawa (1994). “Gas permeation and sorption in brominated poly(1-trimethylsilyl-1-propyne) membrane.” *J. Appl. Polym. Sci.* 54: 1353.

Nagai, K., A. Higuchi and T. Nakagawa (1995). "CAS Permeability and stability of poly(1-trimethylsilyl-1-propyne-*co*-1-phenyl-1-propyne) membranes." *J. Polym. Sci., Part B: Polym. Phys.* 33: 289.

Nagai, K., M. Mori, T. Watanabe and T. Nakagawa (1997). "Gas permeation proerties of blend and copolymer membranes composed of 1-trimethylsilyl-1-propyne and 1-phenyl-1-propyne structures." *J. Polym. Sci. Part B:Polym. Phys.* 35: 119.

Odani, H., and T. Masuda (1992). Design of polymer membranes for gas separation. *Polymers for Gas Separation*. New York, VCH. 107.

Oh, S.-J., and W.P. Zurawsky (1996). "Gas permeation through poly(dimethylsiloxane) -plasma polymer composite membranes." *J. Membrane Sci.* 120: 89.

Parthasarathy, A., C.J. Brumlik, C.R. Martin, and G.E. Collins (1994). "Interfacial polymerization of thin polymer films onto the surface of a microporous hollow-fiber membrane." *J. Membrane Sci.* 94: 249–254.

Pinnau, I., H.J. Wijmans, I. Blume, T. Kuroda and K.V. Peinemann (1988). "Gas permeation through composite membranes." *J. Membrane Sci.* 37: 81.

Platé, N. A., A.K. Bokarev, N.E. Kaliuzhnyi, E.G. Litvinova, V.S. Khotimski, V.V. Volkov and Y.P. Yampol'skii (1991). "Gas and vapor permeation and sorption in poly(trimethylsilyl-propyne)." *J. Membrane Sci.* 60: 13.

Poddar, T. K., S. Majumdar, and K.K. Sirkar (1996a). "Membrane-based absorption of VOCs from a gas stream." *AIChE Journal* 42(11): 3267.

Poddar, T. K., S. Majumdar and K.K. Sirkar (1996b). "Removal of VOCs from air by membrane-based absorption and stripping." *J. Membrane Sci.* 120: 221.

Prasad, R., F. Notaro, and D.R. Thompson (1994). "Evolution of membranes in commercial air separation." *J. Membrane Sci.* 94: 225–248.

Psaume, R., P. Aptel, Y. Aurelle, J.C. Mora, and J.L. Bersillon (1988). "Pervaporation: importance of concentration polarization in the extraction of trace organics from water." *J. Membrane Sci.* 36: 373.

Qiu, M. M., and S.–T. Hwang (1991). "Continuous vapor–gas separation with a porous membrane permeation system." *J. Membrane Sci.* 59: 53–72.

Raghunath, B., and S.–T. Hwang (1992). "Effect of boundary layer mass transfer resistance in the pervaporation of dilute organics." *J. Membrane Sci.* 65: 147.

Rhim, H., and S.–T. Hwang (1975). "Transport of capillary condensate." *J. Colloid Interface Sci.* 52: 174.

Rittmann, B. E., and P.L. McCarty (1980). "Model of steady-state-biofilm kinetics." *Biotechnol. Bioeng.* 22: 2343.

Rittmann, B. E. (1982). “The effect of shear stress on biofilm loss rate.” *Biotechnol. Bioeng.* 24: 501.

Schonduve, P., M. Sara, and A. Friedl (1996). “Influence of physiologically relevant parameters on biomass formation in a trickle-bed bioreactor used for waste gas cleaning.” *Appl. Microbiol. Biotechnol.* 45: 286.

Semmens, M. J., R. Qin, and A. Zander (1989). “Using a microporous hollow-fiber membrane to separate VOCs from water.” *Journal AWWA* : 162.

Seok, D. R., S.G. Kang, and S-T. Hwang (1987). “Use of pervaporation for separating azeotropic mixtures using two different hollow fiber membranes.” *J. Membrane Sci.* 33: 71.

Shaver, K. G., G.L. Poffenbarger and D.R. Grotewald (1991). “Membranes recover hydrogen.” *Hydrocarbon Processing* 70(4): 77–82.

Singh, A. (1997). "Gas and vapor sorption and permeation properties of high free volume glassy polymers." Ph.D. thesis, North Carolina State University.

Smith, F. L., G.A. Sorial, M.T. Suidan, A.W. Breen, and P. Biswas (1996). “Development of two control strategies for extended, stable operation of highly efficient biofilters with high toluene loadings.” *Environ. Sci. Technol.* 30: 1744.

Sok, R. M., and H.J.C. Berendsen (1992). “Molecular dynamics simulation of the transport of small molecules across a polymer membrane.” *Polym. Prepr. Am. Chem. Soc., Div. Polym. Chem.* 33: 641.

Stern, S. A., V.M. Shah and B.J. Hardy (1987). “Structure/permeability relationships in silicone polymers.” *J. Polym. Sci. Part B:Polym. Phys.* 25: 1263.

Stern, S. A. (1994). “Polymers for gas separations: the next decade.” *J. Membrane Sci.* 94: 1–65.

Strachan, L. F., L.M. Freitas dos Santos, D.J. Leak, and A.G. Livingston (1996). “Minimisation of biomass in an extractive membrane bioreactor.” *Wat. Sci. Tech. 34*: 273.

Strathmann, H., C.M. Bell, and K. Kimmerle (1986). “Development of synthetic membranes for gas and vapor separation.” *Pure & Appl. Chem.* 58: 1663.

Suwandi, M. S., and S.A. Stern (1973). “Transport of heavy organic vapors through silicone rubber.” *J. Polym. Sci., Polym. Phys. Ed.* 11: 663.

Takada, K., H. Matsuya, T. Masuda and T. Higashimura (1985). “Gas permeability of polyacetylenes carrying substituents.” *J. Appl. Polym. Sci.* 30: 1605.

Taylor, F., M.J. Kurantz, N. Goldberg, and J.C. Craig, Jr. (1996). “Control of packed column fouling in the continuous fermentation and stripping of ethanol.” *Biotechnol. Bioeng.* 51(1): 33.

Tompkins, C. J., A.S. Michaels, and S.W. Peretti (1993). “Removal of *p*-nitrophenol from aqueous solution by membrane–membrane solvent extraction.” *J. Membrane Sci.* 75: 277.

Turakhia, M. H., K.E. Cooksey, and W.G. Characklis (1983). "Influence of a calcium-specific chelant on biofilm removal." *Appl. Environ. Microbiol.* 46: 1236.

Vos, K. D., and F.O. Burris (1969). “Drying of cellulose acetate reverse osmosis membranes.” *Ind. Eng. Chem., Proc. Res. Dev.* 8: 84.

Ward, W. J., W.R. Browall and M. Salemme (1976). “Ultrathin silicone/polycarbonate membranes for gas separation processes.” *J. Membrane Sci.* 1: 99.

Watson, J. M., and P.A. Payne (1990). “A study of organic compound pervaporation through silicone rubber.” *J. Membrane Sci.* 49: 171–205.

Weber, F. J., and S. Hartmans (1996). “Prevention of clogging in a biological trickle-bed reactor removing toluene from contaminated air.” *Biotechnol. Bioeng.* 50(1): 91.

Wubker, S.–M., and C.G. Friedrich (1996). “Reduction of biomass in a bioscrubber for waste gas treatment by limited supply of phosphate and potassium ions.” *App. Microbiol. Biotechnol.* 46: 475.

Wubker, S.-M., A. Laurenzis, U. Werner, and C. Friedrich (1997). “Controlled biomass formation and kinetics of toluene degradation in a bioscrubber and in a reactor with a periodically moved trickle-bed.” *Biotechnol. Bioeng.* 55(4): 686.

Zhu, C. L., C.–W. Yuang, J.R. Fried and D.B. Greenberg (1983). “Pervaporation membranes—A novel separation technique for trace organics.” *Environ. Prog.* 2(2): 132.

Zielinski, J. M., and J.L. Duda (1992). “Predicting polymer/solvent diffusion coefficients using free-volume theory.” *AIChE J.* 38: 405.

APPENDIX B

BENCH-SCALE DATA

Table B-1. AMT Module, Test 1, 0.5 ft^3/min Air, 1.0 L/min Oil, 500 ppm VOCs

042700												
Test 1												
Test Date	4/27/00											
Initial Settings:		magnehelic (1) ~1.0"H2O;positive flow measurement 50 cc/min;heater set ~280C										
		magnehelic(2) >1.0"H2O;syringe flow 2.0ml/hr;										
run#	MEK Front Detector	MEK Rear Detector	% Difference	n-Butyl Acetate Front Detector	n-Butyl Acetate Rear Detector	% Difference	Ethyl Benzene Front Detector	Ethyl Benzene Rear Detector	% Difference	o-Xylene Front Detector	o-Xylene Rear Detector	% Difference
1	150.315	130.062	13.47371	89.126	67.699	24.041245	35.881	26.768	25.39784	214.818	155.381	27.66854
2	153.145	138.194	9.762643	91.612	70.278	23.287342	36.914	27.742	24.84694	221.479	161.184	27.2238
3	143.296	137.945	3.734228	87.884	72.005	18.068135	35.411	28.437	19.69445	213.098	165.741	22.22311
4	148.908	136.583	8.276923	88.65	72.437	18.288776	35.749	28.79	19.46628	214.407	168.397	21.45919
5	145.134	137.084	5.546598	87.979	73.853	16.056104	35.439	29.334	17.22678	213.086	172.465	19.0632
6	142.971	132.215	7.523204	86.233	73.949	14.245127	34.667	29.51	14.87582	208.276	174.276	16.32449
7	145.94	138.263	5.260381	88.783	75.424	15.046799	35.689	30.021	15.88164	214.788	177.675	17.2789
8	143.996	135.188	6.116837	87.305	75.6	13.407021	35.105	30.177	14.03789	210.832	178.909	15.14144
9	146.268	135.548	7.329012	88.615	75.617	14.667946	35.605	30.226	15.10743	213.969	179.796	15.97101
10	134.227	129.722	3.356255	83.79	75.48	9.9176513	33.638	30.224	10.14924	202.525	180.798	10.72806
11	136.837	123.254	9.926409	82.883	73.603	11.196506	33.3	29.676	10.88288	200.097	178.365	10.86073
12	150.697	102.9	31.71729	90.417	46.423	48.656779	36.409	19.275	47.05979	218.704	115.088	47.37728
13	175.156	110.369	36.98817	103.662	44.659	56.918639	41.771	18.712	55.20337	250.329	108.054	56.8352
14	191.428	123.568	35.44936	112.785	47.188	58.161103	45.351	19.796	56.34936	271.844	112.28	58.6969
15	166.186	126.673	23.77637	102.004	48.609	52.345986	40.935	20.412	50.13558	246.625	113.708	53.89437
16	136.714	112.95	17.38227	87.39	45.901	47.475684	34.99	19.489	44.30123	211.471	109.703	48.12386
17	130.304	108.047	17.08083	81.858	44.409	45.748736	32.796	18.732	42.88328	197.83	103.539	47.66264
18	142.684	105.631	25.96857	85.938	42.426	50.631851	34.525	18.088	47.60898	207.39	100.128	51.71995
19	162.393	121.14	25.40319	96.488	45.4	52.947517	38.805	19.129	50.70481	232.733	104.992	54.88736
20	148.302	119.684	19.29711	90.879	45.541	49.888313	36.466	19.156	47.46888	219.457	105.588	51.8867
21	146.432	117.69	19.62822	89.249	44.893	49.699156	35.766	18.913	47.12017	215.25	103.787	51.78304
22	135.969	118.304	12.99193	85.13	46.149	45.789968	34.134	19.293	43.47864	205.983	106.105	48.48847
23	142.63	116.638	18.22338	86.986	44.625	48.698641	34.868	18.843	45.95905	209.62	102.297	51.19884
24	154.354	126.517	18.03452	93.55	47.05	49.70604	37.513	19.692	47.5062	225.313	106.584	52.69514
25	142.248	122.586	13.82234	88.443	47.209	46.622118	35.447	19.741	44.3084	213.457	107.435	49.66902
26	139.154	118.97	14.50479	85.307	46.315	45.707855	34.188	19.384	43.30174	205.426	105.148	48.81466
27	138.814	122.3	11.89649	86.002	47.694	44.54315	34.458	19.876	42.31818	207.62	107.965	47.99875
28	131.055	117.642	10.23463	81.987	47.276	42.3372	32.867	19.863	39.56552	198.192	107.077	45.9731
29	151.703	125.706	17.13677	90.754	47.488	47.673932	36.491	19.678	46.07437	218.836	106.18	51.47965
30	137.319	123.105	10.35108	85.575	48.112	43.777973	34.342	20.001	41.75936	207.071	108.561	47.57305
31	142.491	122.195	14.24371	86.57	47.598	45.017905	34.767	19.812	43.01493	209.006	106.946	48.83113
32	141.586	126.176	10.88384	87.118	49.108	43.630478	34.911	20.349	41.71178	210.171	109.923	47.6983
33	135.562	121.383	10.45942	83.925	47.712	43.14924	33.653	19.849	41.01863	202.695	106.913	47.25425
34	152.744	126.865	16.94273	90.981	48.734	46.43497	36.537	20.208	44.69168	219.093	108.378	50.53334
35	148.702	132.139	11.13838	91.053	50.868	44.133636	36.501	21.014	42.42897	219.446	112.885	48.5591

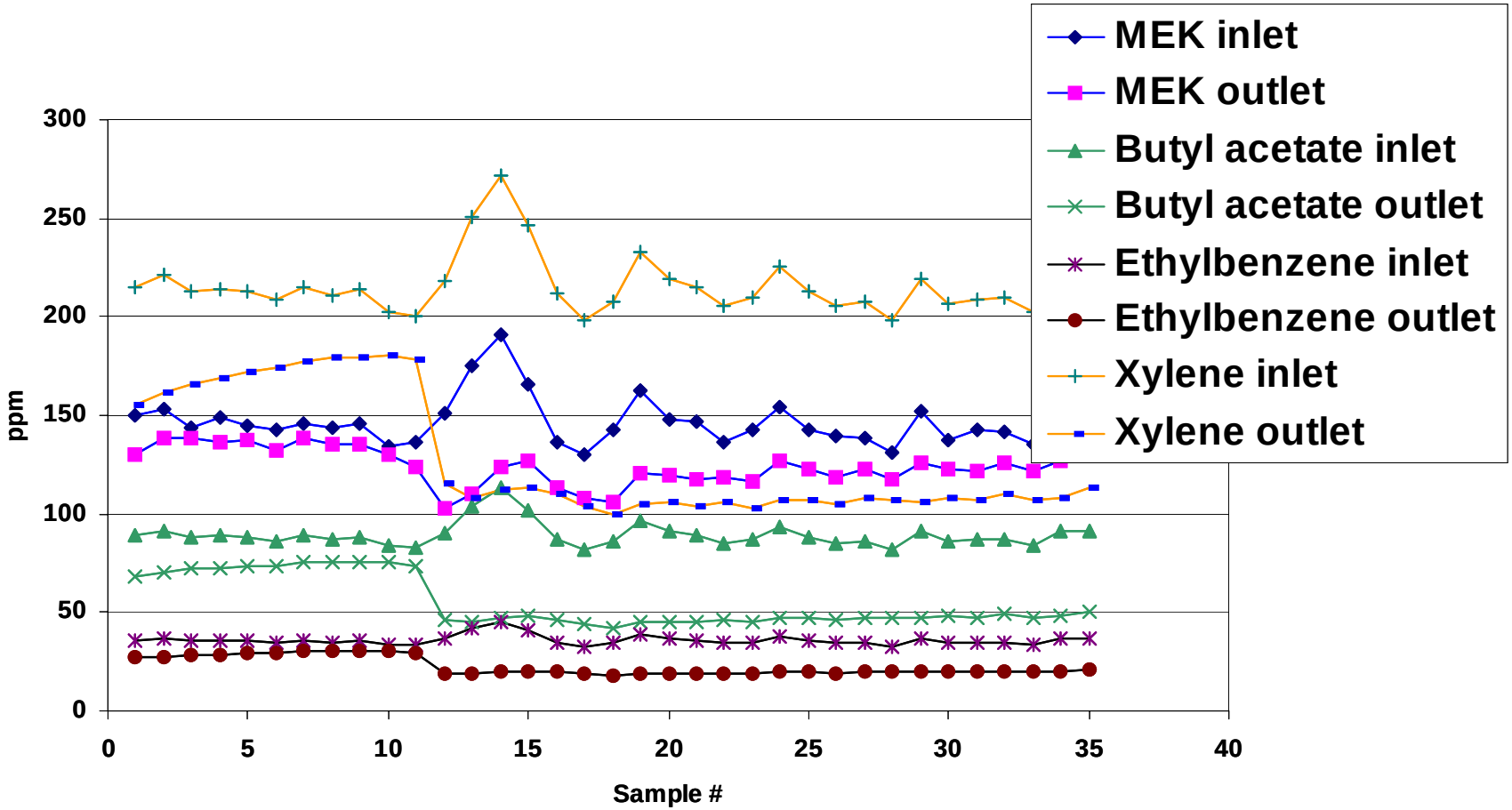

Figure B-1: AMT Module, Test 1, 0.5 ft^3/min Air, 1.0 L/min Oil, 500 ppm VOCs

Table B-2. AMT Module, Test 2, 0.5 ft^3/min Air, 1.0 L/min Oil, 2100 ppm VOCs

Test 2												
Run Date:	4/27/00											
sequence	042700a											
Initial settings:		syringe pump set at 2.0 ml/hr;0.5cfm;temp controller										
		290C;magnehilic (1) rding 1"H20;magnehelic (2) rding >1"H20;										
Gen notes	did not experience any software errors during sampling											
	should have adjusted syringe sampling rate to a lower setting (1/4 of what it was set) as a result our numbers are											
	much higher than we expected.											
run#	MEK Front Detector	MEK Rear Detector	% Difference	n-Butyl Acetate Front Detector	n-Butyl Acetate Rear Detector	% Difference	Ethyl Benzene Front Detector	Ethyl Benzene Rear Detector	% Difference	o-Xylene Front Detector	o-Xylene Rear Detector	% Difference
1	681.961	377.218	44.68628	410.593	101.304	75.327392	171.399	38.443	77.57105	1043.313	204.793	80.3709
2	702.241	330.247	52.97241	432.769	87.043	79.88696	179.723	34.172	80.9863	1091.209	184.561	83.08656
3	625.748	361.555	42.22035	384.748	97.123	74.756724	160.54	37.504	76.63884	980.284	203.155	79.2759
4	675.842	350.573	48.12796	389.346	96.337	75.256713	162.387	37.329	77.01232	979.173	203.841	79.18233
5	709.953	334.148	52.93379	436.724	84.916	80.556141	181.329	33.055	81.7707	1101.906	176.789	83.95607
6	511.676	389.961	23.78751	339.472	107.931	68.206214	142.086	41.344	70.90213	879.358	224.101	74.51539
7	609.509	312.931	48.65851	343.157	94.794	72.37591	143.154	87.598	38.80856	859.247	207.1	75.8975
8	890.686	295.112	66.86689	483.275	76.617	84.146294	198.553	71.71	63.8837	1173.823	159.938	86.37461
9	693.19	379.609	45.23738	475.43	76.729	83.861136	197.178	28.914	85.33609	1221.902	144.917	88.14005
10	657.94	385.654	41.38462	381.081	105.657	72.274398	158.654	96.372	39.2565	959.683	221.517	76.91769
11	697.476	363.508	47.88236	447.328	88.42	80.233743	177.678	33.267	81.2768	1077.098	176.13	83.64773
12	698.65	380.423	45.54884	442.492	97.394	77.989659	175.995	37.457	78.71701	1065.251	193.751	81.8117
13	632.709	394.233	37.69126	407.762	104.566	74.35612	162.248	40.501	75.0376	984.326	210.261	78.63909
14	574.213	376.799	34.37993	365.677	105.395	71.178116	145.245	40.817	71.89783	881.118	216.217	75.46106
15	672.908	360.621	46.40857	416.343	93.11	77.636228	165.348	36.054	78.19508	997.284	187.441	81.20485
16	568.607	400.99	29.47853	370.812	107.192	71.092629	147.615	40.731	72.40728	897.819	211.567	76.43545
17	578.692	360.337	37.73251	363.342	100.622	72.306532	144.152	38.977	72.96118	870.6	205.926	76.34666
18	687.882	358.966	47.81576	424.38	90.92	78.575805	168.437	35.188	79.1091	1013.724	181.146	82.13064
19	642.209	403.282	37.20393	407.004	102.042	74.928502	161.922	38.609	76.1558	982.041	197.743	79.86408
20	674.566	386.024	42.77447	421.249	98.041	76.726117	167.319	37.702	77.46699	1009.392	193.824	80.79795
21	637.705	397.736	37.6301	408.842	100.912	75.317604	162.608	38.527	76.30682	986.365	197.63	79.96381
22	617.514	384.006	37.8142	389.518	102.316	73.732664	154.649	39.22	74.63934	935.273	203.762	78.21363
23	708	375.488	46.96497	436.517	94.715	78.302105	173.044	36.539	78.88456	1041.451	186.716	82.07155
24	541.946	444.311	18.01563	368.106	112.969	69.310742	146.544	42.327	71.11652	896.285	215.611	75.94392
25	398.468	361.162	9.362358	272.646	111.063	59.264761	108.163	100.795	6.811941	661.669	230.568	65.15357
26	411.618	320.555	22.12318	266.533	101.209	62.027591	105.593	39.148	62.92557	640.938	210.336	67.1831
27	571.609	314.159	45.03953	346.246	86.748	74.946137	136.853	34.036	75.12952	820.518	175.728	78.58329
28	748.405	347.828	53.52409	452.524	83.199	81.614456	178.974	32.136	82.04432	1070.831	158.686	85.18104

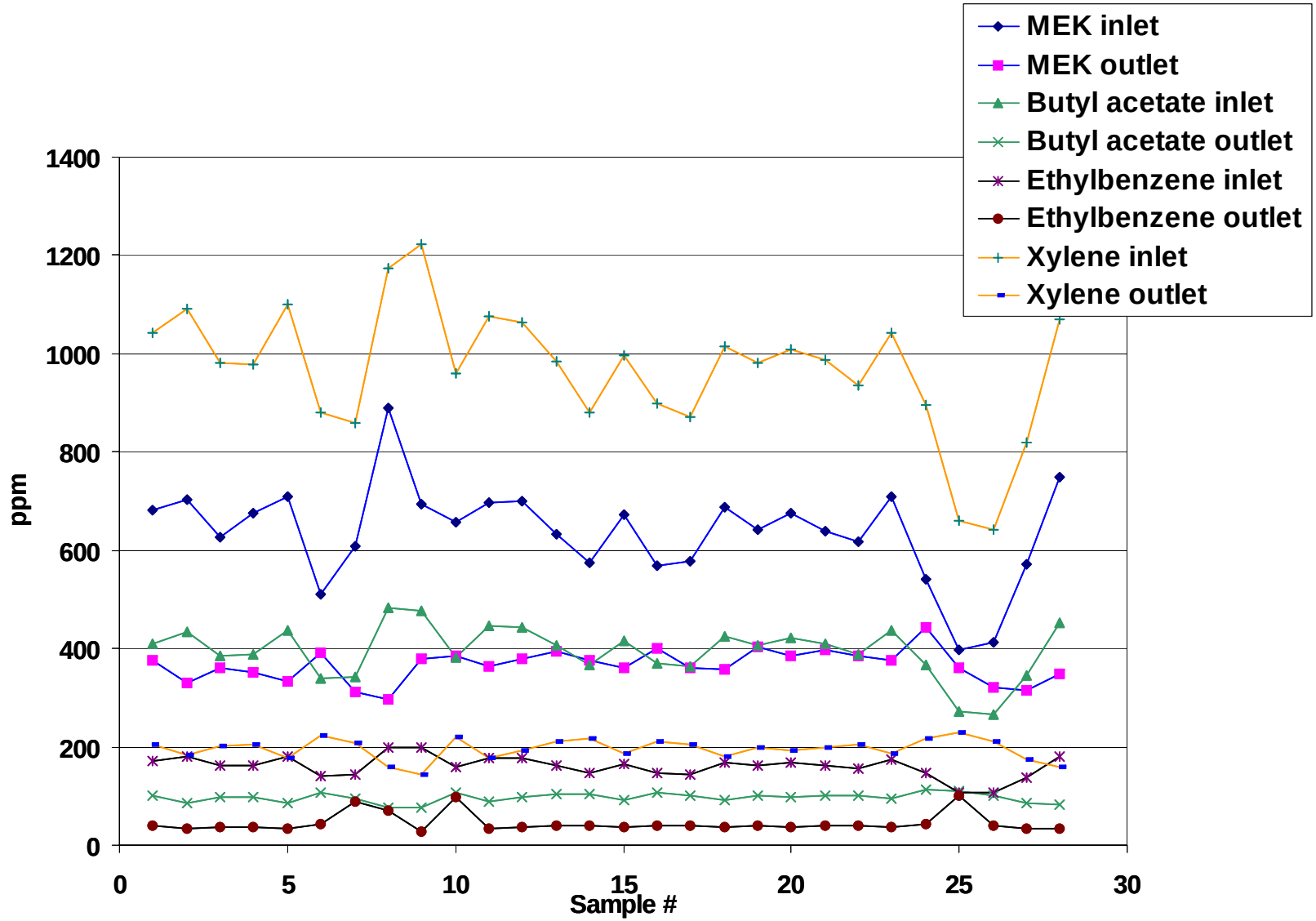

Figure B-2. AMT Module, AMT Module, Test 2, 0.5 ft^3/min Air, 1.0 L/min Oil, 2100 ppm VOCs

Table B-3. AMT Module, Test 3, 2.0 ft^3/min Air, 1.0 L/min Oil, 450 ppm VOCs

Test 3												
Initial settings:		positive flow measured 52cc/min;magnehelic (2) rds >1.0"H20;magnehelic (1) ~1.0"H20;oil flow rate set at 110- rotameter										
		at 110 on rotameter;										
Sequence:	042900&o42900a&042900b											
Test Date:	4/28/00											
run#	MEK Front Detector	MEK Rear Detector	% Difference	n-Butyl Acetate Front Detector	n-Butyl Acetate Rear Detector	% Difference	Ethyl Benzene Front Detector	Ethyl Benzene Rear Detector	% Difference	o-Xylene Front Detector	o-Xylene Rear Detector	% Difference
1	3.757	32.314	-760.101	5.623	13.999	-148.95963	2.166	5.653	-160.988	14.411	26.11	-81.181
2	3.543	35.619	-905.334	5.246	13.385	-155.14678	2.028	6.132	-202.367	13.751	22.453	-63.2827
3	3.66	45.528	-1143.93	5.003	12.948	-158.80472	1.889	6.048	-220.169	12.645	21.451	-69.6402
4	3.177	44.738	-1308.18	4.618	12.862	-178.51884	1.741	6.088	-249.684	11.704	20.808	-77.7854
5	34.575	47.879	-38.4787	17.828	13.928	21.875701	7.569	6.53	13.72704	44.581	22.939	48.54534
6	4.057	49.392	-1117.45	5.933	14.864	-150.53093	2.194	6.917	-215.269	14.575	25.115	-72.3156
7	2.992	45.53	-1421.72	4.213	13.394	-217.92072	1.555	6.443	-314.341	10.518	21.304	-102.548
8	2.816	45.604	-1519.46	3.782	13.097	-246.29825	1.42	6.416	-351.831	9.803	20.616	-110.303
9	2.7	45.733	-1593.81	3.549	13.069	-268.24458	1.332	6.45	-384.234	9.237	20.344	-120.245
10	97.198	130.086	-33.8361	57.138	39.764	30.407085	23.454	15.821	32.54456	141.676	73.321	48.24741
11	159.303	145.773	8.493249	92.56	50.205	45.759507	37.459	19.681	47.45989	224.81	98.965	55.97838
12	13.58	69.131	-409.065	16.095	26.546	-64.933209	6.243	11.42	-82.9249	40.095	51.837	-29.2854
13	3.745	49.379	-1218.53	6.07	17.445	-187.39703	2.27	8.237	-262.863	15.338	30.816	-100.913
14	4.136	46.849	-1032.71	5.201	15.396	-196.02	1.937	7.487	-286.526	12.81	26.018	-103.107
15	124.961	125.973	-0.80985	71.011	41.594	41.425976	28.929	16.656	42.42456	173.228	79.313	54.21468
16	134.06	136.895	-2.11472	79.728	49.515	37.895093	32.236	19.527	39.42487	194.064	98.636	49.17347
17	133.615	137.501	-2.90836	80.918	51.76	36.03401	32.621	20.401	37.46053	196.848	104.484	46.92148
18	129.124	135.529	-4.96035	79.073	51.745	34.560469	31.829	20.437	35.79126	192.195	104.869	45.43615
19	138.012	140.345	-1.69043	83.759	53.479	36.151339	33.672	21.087	37.37527	203.042	108.343	46.6401
20	139.722	143.644	-2.807	86.295	54.88	36.404195	34.664	21.544	37.84907	209.467	110.974	47.02077
21	132.683	136.536	-2.90391	81.828	53.903	34.12646	32.852	21.27	35.25508	198.336	110.077	44.49974
22	126.854	121.63	4.11812	78.614	54.163	31.102603	31.518	19.206	39.06339	190.18	105.393	44.5825
23	123.283	118.879	3.572269	76.064	55.693	26.781395	30.486	21.182	30.51893	183.871	109.765	40.30326
24	129.445	123.384	4.682298	79.119	56.29	28.854005	31.762	20.995	33.899	191.522	109.63	42.75853
25	131.092	137.907	-5.19864	81.34	56.003	31.149496	32.582	21.206	34.91498	196.867	114.541	41.81808
26	124.473	121.593	2.313755	77.96	55.433	28.895587	31.21	21.175	32.15316	188.668	112.209	40.52569
27	126.922	123.426	2.754448	79.046	54.31	31.293171	31.65	21.477	32.14218	191.087	111.667	41.56222
28	128.208	131.99	-2.94989	79.707	55.551	30.305996	31.894	21.663	32.07813	192.484	113.859	40.84755
29	121.068	122.157	-0.89949	76.174	55.032	27.754877	30.475	21.553	29.27646	184.333	112.633	38.897
30	128.288	123.072	4.065852	79.282	55.14	30.450796	31.783	21.369	32.76594	191.833	112.526	41.34169
31	136.72	138.287	-1.14614	84.999	57.159	32.753327	34.055	22.414	34.18294	205.927	116.906	43.2294
32	138.344	135.802	1.837449	84.908	56.432	33.537476	34.025	22.063	35.1565	205.265	115.167	43.8935
33	143.485	138.543	3.444262	88.735	58.214	34.395673	35.513	22.648	36.22617	214.446	118.697	44.64947
34	132.866	131.286	1.189168	83.492	58.042	30.481962	33.38	22.535	32.48951	201.816	118.431	41.31734
35	140.485	140.769	-0.20216	86.925	58.208	33.036526	34.778	22.853	34.28892	210.01	119.085	43.29556
36	138.949	139.632	-0.49155	86.766	58.337	32.765138	34.715	22.639	34.78612	209.783	118.869	43.33716
37	139.296	130.346	6.425167	86.57	58.524	32.396904	34.62	22.284	35.63258	209.087	118.265	43.43742
38	142.173	130.54	8.182285	88.287	58.595	33.631225	35.291	22.583	36.00918	213.183	119.004	44.17754
39	129.481	129.824	-0.2649	81.965	58.018	29.216129	32.783	22.75	30.60428	198.621	118.828	40.1735
40	135.624	136.905	-0.94452	84.695	58.382	31.06795	33.869	22.86	32.50465	204.659	119.293	41.71133
41	129.345	130.313	-0.74839	80.506	56.508	29.808958	32.206	22	31.68975	194.441	115.524	40.5866
42	135.328	130.21	3.781922	84.266	57.367	31.921534	33.707	22.494	33.26609	203.681	116.686	42.7114
43	134.72	136.918	-1.63153	84.271	58.252	30.87539	33.678	22.784	32.34753	203.618	118.717	41.69622
44	130.53	126.024	3.45208	81.976	57.017	30.446716	32.733	22.25	32.02578	197.842	116.275	41.22835
45	134.244	131.213	2.257829	84.873	58.852	30.658749	33.906	22.755	32.88798	205.262	119.129	41.96247
46	131.524	127.052	3.40014	82.77	58.041	29.876767	33.072	22.435	32.16316	199.922	117.865	41.04451
47	137.039	127.922	6.652851	84.483	58.02	31.323462	33.773	22.48	33.43795	203.613	117.589	42.24878

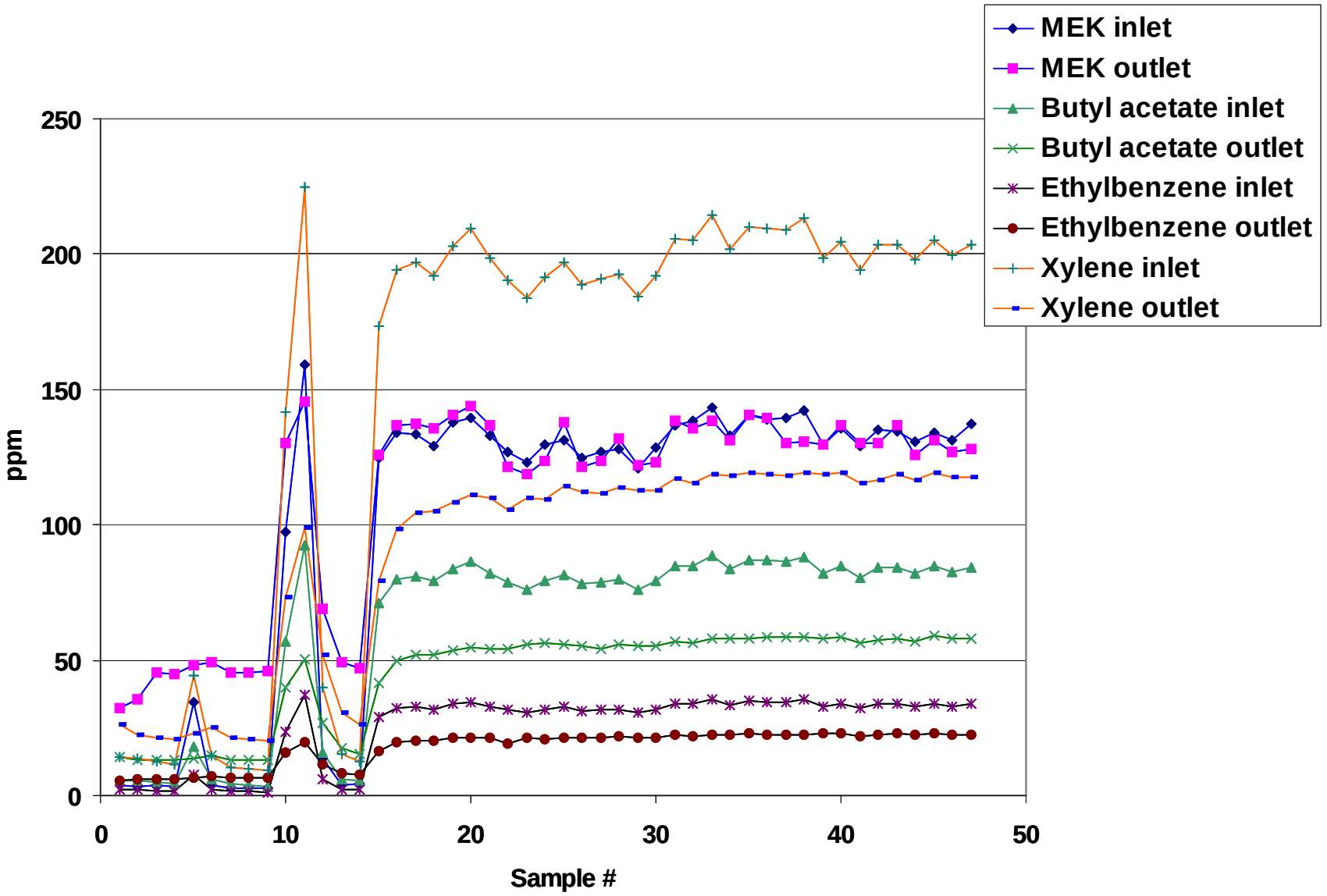

Figure B-3. AMT Module, AMT Module, Test 2, 0.5 ft^3/min Air, 1.0 L/min Oil, 2100 ppm VOCs

Table B-4. AMT Module, Test 4, 2.0 ft^3/min Air, 1.0 L/min Oil, 230 ppm VOCs

Test 4												
Initial settings:		syringe flow set 1.0ml/hr;0.5cfm air;magnehelic (1) ~0.9"H2O;magnehelic (2) >1.0"H20										
run date:	4/28/00											
sequence used :		042900c&d										
Gen notes:		software error ocurred which automatically aborted sequence-immediately started new sequence (042900d)										
run#	MEK Front Detector	MEK Rear Detector	% Difference	n-Butyl Acetate Front Detector	n-Butyl Acetate Rear Detector	% Difference	Ethyl Benzene Front Detector	Ethyl Benzene Rear Detector	% Difference	o-Xylene Front Detector	o-Xylene Rear Detector	% Difference
1	66.225	69.884	-5.5251	41.646	35.677	14.332709	16.685	14.063	15.71471	100.718	69.825	30.67277
2	67.129	68.288	-1.72653	41.59	35.282	15.167107	16.635	14.728	11.46378	100.227	68.875	31.28099
3	69.965	74.479	-6.4518	43.662	36.869	15.558151	17.462	14.659	16.052	105.388	70.835	32.78647
4	68.354	70.326	-2.88498	42.871	35.988	16.055142	17.174	14.212	17.247	103.737	70.683	31.86327
5	65.418	68.88	-5.29212	41.149	36.592	11.074388	16.448	14.414	12.36625	99.33	70.073	29.45434
6	66.901	68.833	-2.88785	41.762	36.329	13.009434	16.704	14.322	14.26006	100.765	69.763	30.76664
7	71.567	73.801	-3.12155	44.6	36.662	17.798206	17.843	15.303	14.23527	107.638	71.795	33.29958
8	70.914	81.521	-14.9576	44.329	37.108	16.289562	17.715	15.4	13.06802	106.949	72.361	32.34065
9	70.793	75.56	-6.73372	44.699	37.48	16.150249	17.858	15.489	13.26576	107.988	73.32	32.10357
10	70.109	71.897	-2.55031	44.093	37.875	14.102012	17.625	14.655	16.85106	106.424	72.307	32.05762
11	68.472	70.538	-3.01729	43.257	36.489	15.646023	17.284	15.197	12.07475	104.508	71.546	31.54017
12	70.272	71.531	-1.79161	43.801	37.9	13.472295	17.516	14.57	16.81891	105.694	72.318	31.57795
13	71.815	71.163	0.907888	44.497	36.734	17.44612	17.807	15.324	13.94395	107.229	72.501	32.38676
14	69.01	70.579	-2.27358	43.289	36.424	15.858532	17.313	14.305	17.37423	104.441	71.315	31.71743
15	68.487	68.816	-0.48038	42.955	36.117	15.918985	17.152	14.861	13.35704	103.49	71.055	31.34119
16	71.998	80.286	-11.5114	44.673	36.783	17.661675	17.865	15.266	14.548	107.7	72.162	32.99721
17	70.486	79.729	-13.1132	44.147	36.861	16.503953	17.624	15.315	13.10145	106.403	72.38	31.9756
18	70.25	75.262	-7.13452	44.188	37.388	15.388793	17.648	15.527	12.01836	106.658	73.016	31.54194
19	71.417	74.997	-5.01281	44.507	37.234	16.34125	17.788	15.546	12.604	107.173	73.028	31.8597
20	69.171	73.45	-6.18612	43.449	36.796	15.312205	17.346	15.351	11.50121	104.73	72.042	31.21169
21	67.824	73.352	-8.15051	42.251	37.244	11.850607	16.864	15.678	7.032732	101.631	71.788	29.36407
22	69.692	70.423	-1.0489	43.512	36.775	15.483085	17.381	14.538	16.35694	104.838	72.291	31.04504
23	68.943	69.619	-0.98052	43.464	37.076	14.697221	17.35	15.291	11.86744	104.828	72.508	30.83146
24	67.639	70.38	-4.0524	42.634	36.358	14.720645	17.022	15.05	11.58501	102.772	71.556	30.37403
25	69.136	70.085	-1.37266	43.088	36.516	15.252506	17.198	14.955	13.04221	103.662	71.583	30.94577
26	67.33	69.073	-2.58874	42.146	36.556	13.263418	16.815	15.252	9.295272	101.488	71.92	29.13448
27	65.916	69.09	-4.81522	41.603	36.284	12.785136	16.577	15.183	8.409242	100.193	71.602	28.53593
28	63.953	69.793	-9.13171	40.672	36.04	11.38867	16.214	15.148	6.574565	98.055	71.224	27.36321
29	64.112	74.936	-16.883	40.498	35.877	11.41044	16.154	15.032	6.945648	97.579	70.799	27.44443
30	63.302	68.238	-7.79754	40.176	35.89	10.668061	16.002	15.075	5.793026	96.655	71.13	26.40836
31	69.961	71.137	-1.68094	43.185	36.552	15.3595	17.259	15.33	11.17678	103.894	72.258	30.45027
32	69.135	71.957	-4.08187	43.293	36.947	14.658259	17.267	15.463	10.44767	104.213	73.006	29.9454

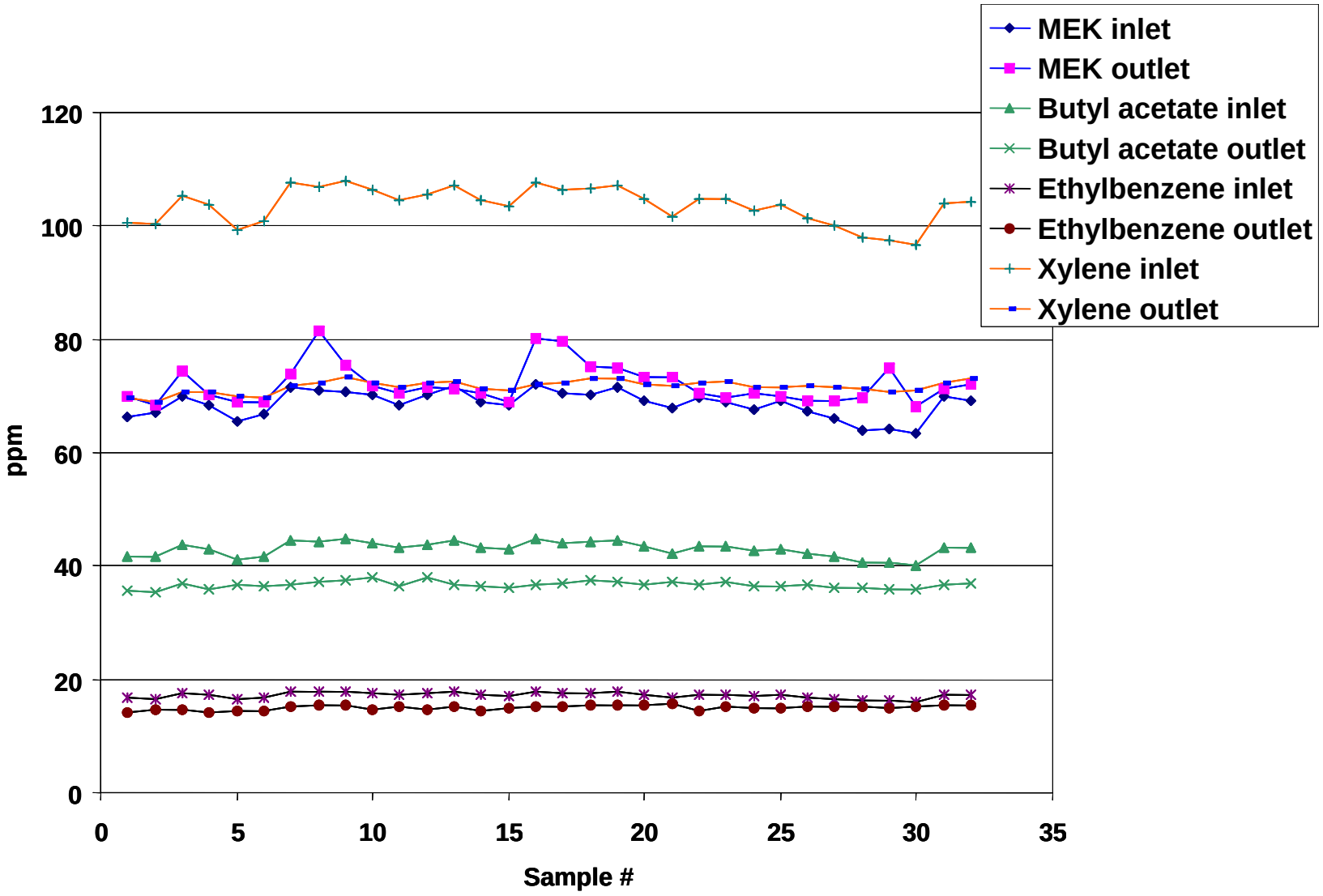

Figure B-4. AMT Module, Test 4, 2.0 ft^3/min Air, 1.0 L/min Oil, 230 ppm VOCs

Table B-5. AMT Module, Test 5, 2.0 ft^3/min Air, 1.0 L/min Oil, 850 ppm VOCs

Test 5												
run date:	4/28/00											
sequence used :		0429e&f										
Initial settings:		syringe pump set at 3.5ml/hr;positive net sample flow 50cc/min;magnehelic (1) ~0.9"H2O										
		magnehelic (2) >1.0"H2O										
run#	MEK Front Detector	MEK Rear Detector	% Difference	n-Butyl Acetate Front Detector	n-Butyl Acetate Rear Detector	% Difference	Ethyl Benzene Front Detector	Ethyl Benzene Rear Detector	% Difference	o-Xylene Front Detector	o-Xylene Rear Detector	% Difference
1	258.118	196.099	24.02738	158.541	77.836	50.904813	63.119	29.327	53.53697	381.073	156.69	58.88189
2	235.798	189.425	19.66641	146.143	85.804	41.287643	58.13	32.671	43.79666	351.1	177.338	49.49074
3	246.903	201.885	18.23307	153.555	89.928	41.435968	61.018	34.127	44.0706	368.879	186.289	49.49862
4	255.548	208.471	18.42198	159.528	94.122	40.999699	63.397	34.963	44.8507	383.122	193.603	49.46701
5	238.781	193.458	18.98099	148.642	89.258	39.951023	59.05	33.327	43.56139	356.841	186.187	47.82354
6	226.632	181.656	19.84539	140.802	87.869	37.593926	55.888	32.773	41.3595	337.046	184.331	45.30984
7	228.48	189.155	17.21157	144.341	89.08	38.285033	57.273	33.677	41.19917	346.809	188.48	45.65308
8	252.031	202.259	19.74836	155.649	91.968	40.913209	61.791	34.945	43.44646	372.998	191.591	48.63485
9	254.606	194.285	23.6919	157.526	90.335	42.653911	62.493	34.263	45.17306	376.575	189.25	49.74441
10	230.948	203.771	11.76758	148.972	95.288	36.036302	59.075	35.309	40.23022	358.591	197.982	44.78891
11	12.208	51.564	-322.379	24.672	44.703	-81.189202	9.251	18.621	-101.286	60.193	100.169	-66.413
12	5.66	32.563	-475.318	11.193	28.586	-155.39176	4.175	12.375	-196.407	27.278	57.266	-109.935

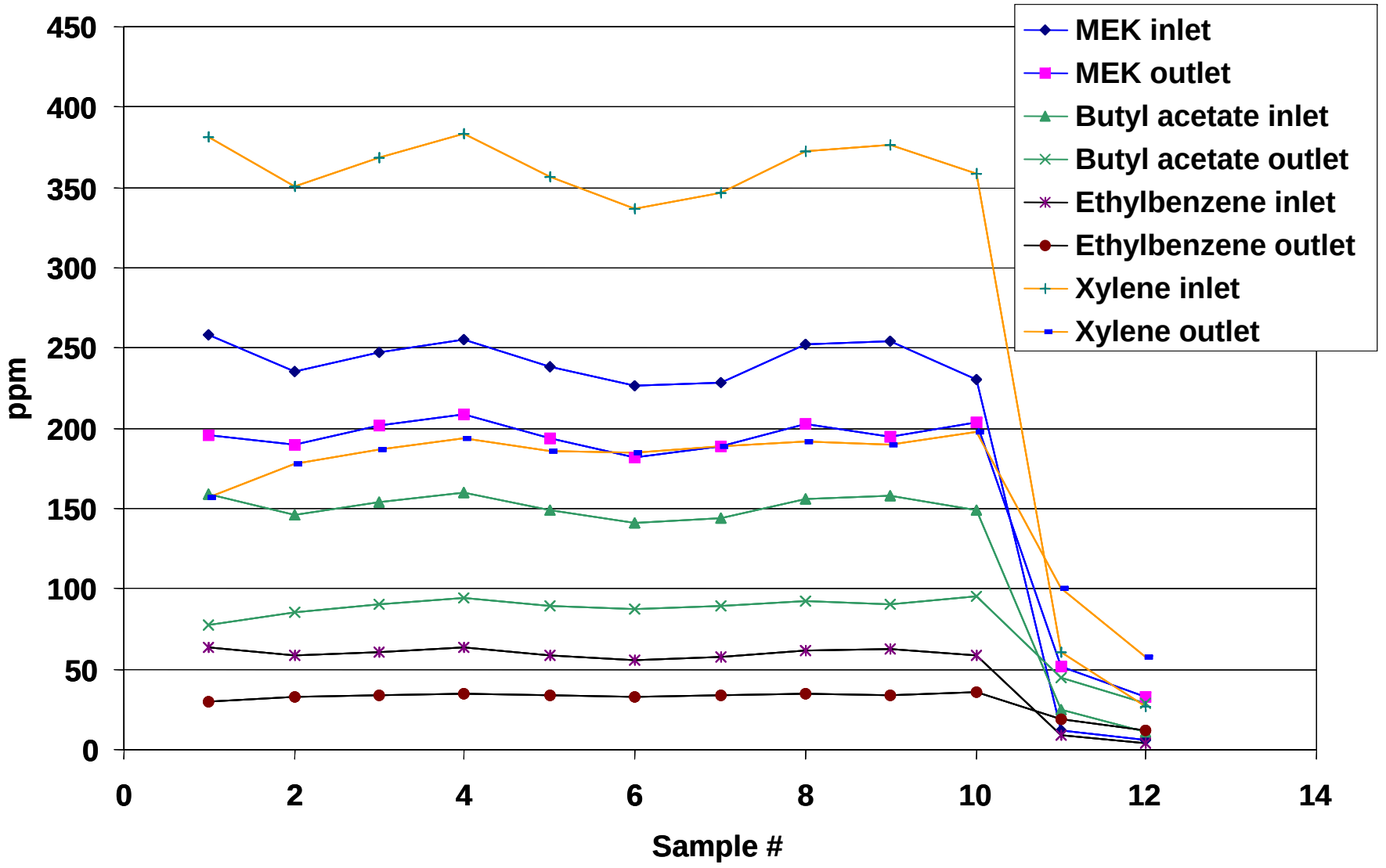

Figure B-5. AMT Module, Test 5, 2.0 ft^3/min Air, 1.0 L/min Oil, 850 ppm VOCs

Table B-6. AMT Module, Test 6, 2.0 ft^3/min Air, 0.2 L/min Oil, 300 ppm VOCs

Test 6												
Sequence	050300b											
date run:	5/3/00											
Initial settings:		syringe pump set 2/0ml/hr;air flow set at 337 ft/min;heater set at 290C;magnehelic (1) rds 0.9"H2O										
		magnehelic (2) rds > 1.0"H2O;net positive sample flow ~55cc/min;										
run#	MEK Front Detector	MEK Rear Detector	% Difference	n-Butyl Acetate Front Detector	n-Butyl Acetate Rear Detector	% Difference	Ethyl Benzene Front Detector	Ethyl Benzene Rear Detector	% Difference	o-Xylene Front Detector	o-Xylene Rear Detector	% Difference
17	9.983	7.921	20.65511	4.477	3.3	26.289926	1.736	1.304	24.88479	12.306	6.016	51.11328
18	98.127	86.06	12.29733	56.009	28.649	48.849292	20.831	8.704	58.21612	146.81	53.936	63.26136
19	96.557	88.905	7.924853	56.99	39.845	30.084225	20.984	12.217	41.77945	148.628	77.471	47.8759
20	96.712	91.91	4.965258	58.05	46.756	19.455642	21.305	14.633	31.31659	151.185	94.923	37.21401
21	94.921	88.473	6.793017	57.282	49.092	14.297685	21.016	15.666	25.45679	149.178	104.412	30.00845
22	88.494	91.3	-3.17084	53.439	52.224	2.2736204	19.572	16.862	13.84631	138.721	114.357	17.56331
23	98.396	89.574	8.965812	59.087	52.521	11.112427	21.609	17.13	20.72747	153.301	118.46	22.72718
24	91.496	88.104	3.707266	56.02	53.019	5.3570154	20.502	17.46	14.83758	145.623	122.318	16.00365
25	92.385	86.708	6.144937	56.568	52.421	7.3309999	20.7	17.376	16.05797	147.037	123.229	16.19184
26	96.107	78.114	18.72184	58.774	39.726	32.408888	21.464	12.957	39.63381	152.668	93.853	38.52477
27	98.44	80.872	17.8464	60.149	37.114	38.296564	21.933	12.006	45.26057	156.212	86.639	44.53755
28	92.791	78.503	15.39805	57.039	36.182	36.566209	20.854	11.639	44.18817	148.273	83.477	43.70047
29	93.765	78.983	15.76494	57.162	36.952	35.355656	20.893	11.813	43.45953	148.29	83.943	43.39268
30	90.232	77.21	14.43169	55.614	35.496	36.174345	20.289	11.361	44.00414	144.548	80.838	44.07532
31	89.777	77.286	13.91336	55.336	35.193	36.401258	20.196	11.238	44.35532	143.835	79.718	44.57677
32	90.082	78.004	13.40778	55.626	35.188	36.741811	20.301	11.243	44.61849	144.686	79.281	45.20479
33	94.605	81.424	13.93267	57.847	35.956	37.84293	21.105	11.398	45.99384	150.067	80.328	46.47191
34	87.307	76.669	12.18459	53.961	35.305	34.573118	19.686	11.257	42.81723	140.232	79.39	43.38667
35	86.451	77.371	10.50306	53.993	35.339	34.548923	19.721	11.256	42.92379	140.587	79.196	43.66762
36	84.87	74.861	11.79333	52.134	34.241	34.321172	19.006	10.928	42.50237	135.44	76.866	43.24719
37	89.215	78.06	12.5035	54.666	35.26	35.499213	19.956	11.189	43.93165	141.953	78.574	44.64788
38	86.825	75.605	12.92255	53.442	35.103	34.315707	19.506	11.138	42.89962	139.053	78.342	43.66033
39	88.171	76.857	12.83188	54.145	35.505	34.426078	19.762	11.265	42.99666	140.659	78.934	43.88272
40	88.651	77.577	12.49168	54.609	35.486	35.018037	19.918	11.24	43.56863	142.028	78.699	44.5891
41	89.224	78.399	12.13239	54.853	36.225	33.959856	20.007	11.458	42.73004	142.466	80.319	43.62234
42	89.563	76.426	14.66789	54.52	35.674	34.567131	19.917	11.308	43.22438	141.61	79.273	44.0202
43	89.622	79.966	10.77414	55.498	36.71	33.853472	20.214	11.578	42.72287	144.27	81.1	43.78596
44	90.273	78.773	12.73914	55.418	36.57	34.01061	20.22	11.557	42.84372	144.069	80.863	43.87203
45	86.586	77.493	10.5017	53.212	36.622	31.177178	19.415	11.578	40.3657	138.399	81.12	41.38686
46	87.998	78.186	11.15025	54.076	36.515	32.474665	19.733	11.549	41.47367	140.653	80.883	42.49465
47	86.636	80.28	7.336442	53.638	38.088	28.990641	19.559	12.058	38.35063	139.645	83.487	40.21483

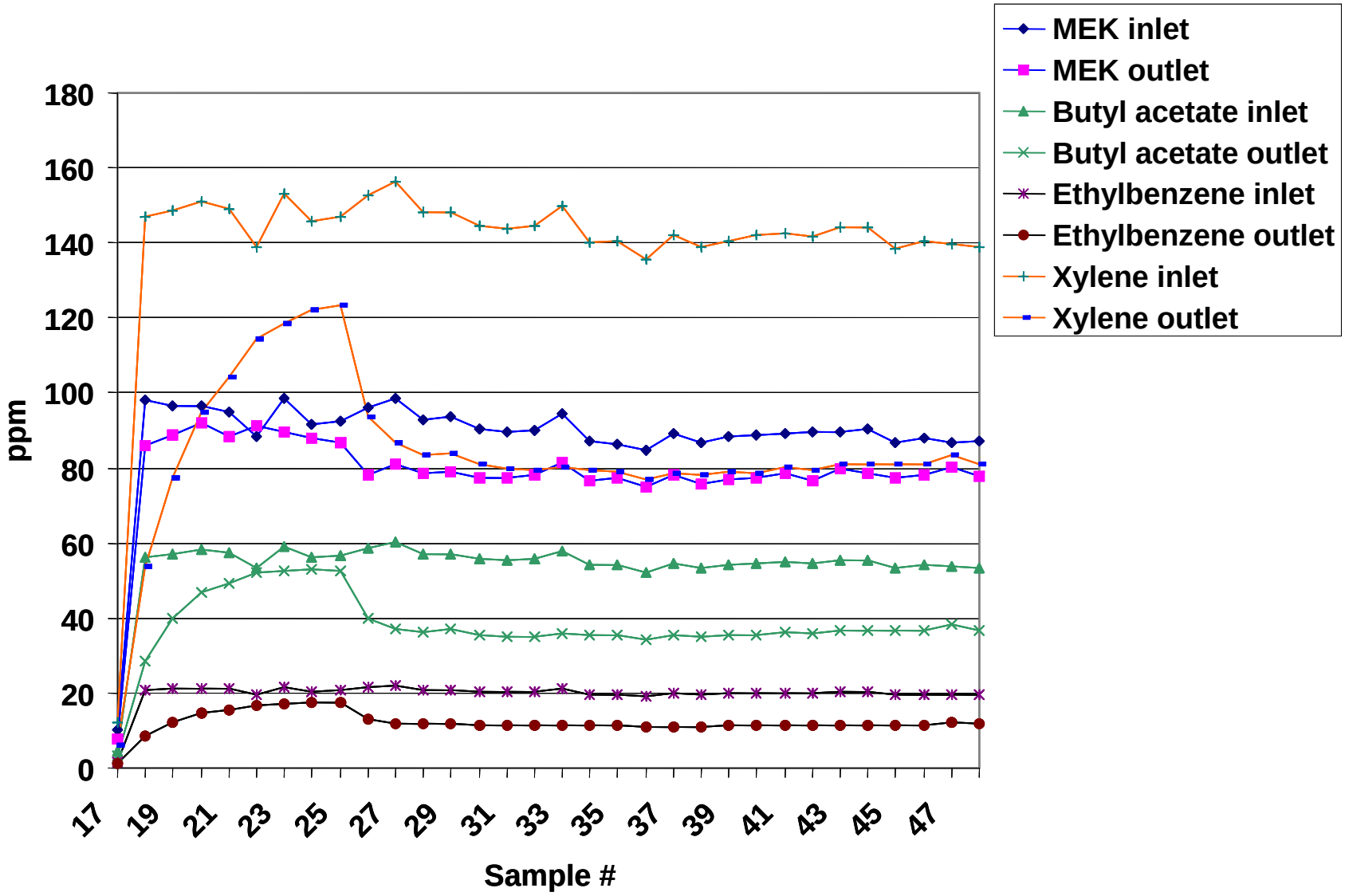

Figure B-6. AMT Module, Test 6, 2.0 ft^3/min Air, 0.2 L/min Oil, 300 ppm VOCs

Table B-7. AMT Module, Test 7, 2.0 ft^3/min Air, 0.2 L/min Oil, 170 ppm VOCs

Test 7												
Run Date:	5/5/00											
run start	3:15											
Initial settings:		did not verify net positive sample flow; syringe pump set at 1.0 ml/hr;air flow set 341;temp at syringe tip										
		tip 290C;magnehilic (1) rding 1"H20;magnehelic (2) rding >1"H20;										
run#	MEK Front Detector	MEK Rear Detector	% Difference	n-Butyl Acetate Front Detector	n-Butyl Acetate Rear Detector	% Difference	Ethyl Benzene Front Detector	Ethyl Benzene Rear Detector	% Difference	o-Xylene Front Detector	o-Xylene Rear Detector	% Difference
1	52.52	44.503	15.26466	32.4	21.152	34.716049	12.922	7.42	42.57855	75.912	39.721	47.67494
2	52.909	42.708	19.28027	32.664	20.832	36.223365	13.003	7.447	42.7286	76.467	40.253	47.35899
3	53.834	42.879	20.34959	32.943	20.949	36.408342	13.098	7.5	42.73935	76.985	40.597	47.26635
4	51.304	41.942	18.24809	31.672	20.838	34.20687	12.609	7.472	40.74074	74.112	40.63	45.17757
5	50.703	41.517	18.11727	31.255	20.622	34.020157	12.421	7.392	40.48788	73.018	40.323	44.77663
6	53.456	43.012	19.53756	32.986	21.207	35.709089	13.087	7.579	42.08757	77.029	41.336	46.33709
7	51.818	42.066	18.81972	32.131	21.101	34.328219	12.758	7.548	40.83712	74.988	41.317	44.90185
8	50.982	42.066	17.48853	31.461	21.101	32.929659	12.489	7.548	39.56282	73.376	41.317	43.6914
9	52.202	42.377	18.82112	32.312	21.073	34.782743	12.83	7.533	41.28605	75.46	41.359	45.19083
10	51.247	41.892	18.25473	31.908	21.22	33.496302	12.679	7.584	40.18456	74.688	41.68	44.19452
11	49.504	40.98	17.21881	30.735	20.982	31.732552	12.187	7.507	38.40158	71.726	41.232	42.51457
12	50.484	41.414	17.96609	31.355	21.246	12.392	12.392	7.61	38.58941	73.15	41.445	43.34245
13	53.219	42.519	20.1056	32.835	21.444	34.69164	12.963	7.635	41.1016	76.394	41.679	45.44205
14	53.579	43.632	18.56511	33.458	21.995	34.260864	13.2	7.817	40.7803	77.824	42.75	45.06836
15	52.533	42.575	18.9557	32.739	21.835	33.305843	12.906	7.776	39.74895	76.015	42.59	43.97158
16	49.32	40.465	17.95418	30.865	21.274	31.074032	12.165	7.601	37.51747	71.653	41.73	41.76099
17	48.944	40.199	17.86736	30.531	21.118	30.830959	12.034	7.557	37.20293	70.93	41.447	41.56633
18	50.794	41.991	17.33079	31.844	21.654	31.999749	12.554	7.726	38.45786	74.035	42.278	42.89458
19	53.114	42.093	20.74971	32.886	21.612	34.282065	12.956	7.712	40.47546	76.326	42.271	44.61782
20	51.362	41.356	19.48133	31.936	21.628	32.277054	12.577	7.719	38.62606	74.111	42.356	42.84789
21	51.299	41.39	19.31617	31.961	21.67	32.198617	12.58	7.741	38.46582	74.097	42.453	42.70618
22	52.05	41.923	19.45629	32.359	21.907	32.300133	12.739	7.819	38.62156	75.021	42.912	42.80002
23	53.31	42.394	20.47646	33.134	22.036	33.494296	13.031	7.852	39.74369	76.848	43.087	43.93218
24	49.831	41.357	17.00548	31.461	22.026	29.989511	12.386	7.879	36.38786	73.16	43.343	40.75588
25	49.312	40.455	17.96115	30.895	21.712	29.723256	12.167	7.777	36.0812	71.786	42.635	40.6082
26	51.265	41.201	19.63133	31.85	21.962	31.045526	12.542	7.845	37.45017	73.887	42.97	41.84363
27	51.59	41.243	20.05621	32.134	22.039	31.415323	12.64	7.865	37.7769	74.542	43.026	42.27952
28	51.296	41.914	18.28993	32.351	22.142	31.556984	12.714	7.905	37.82445	75.038	43.362	42.21328
29	50.909	41.575	18.33468	31.871	22.272	30.118289	12.508	7.958	36.37672	73.864	43.712	40.82097
30	51.634	41.934	18.78607	32.429	22.536	30.506645	12.755	8.046	36.91886	75.285	44.319	41.1317
31	50.322	40.311	19.89388	31.369	22.096	29.561032	12.347	7.917	35.87916	72.779	43.592	40.1036
32	47.509	39.588	16.67263	29.892	21.869	26.839957	11.755	7.853	33.19439	69.332	43.217	37.66659
33	46.676	38.418	17.69218	29.42	21.454	27.076818	11.553	7.713	33.23812	68.225	42.399	37.85416

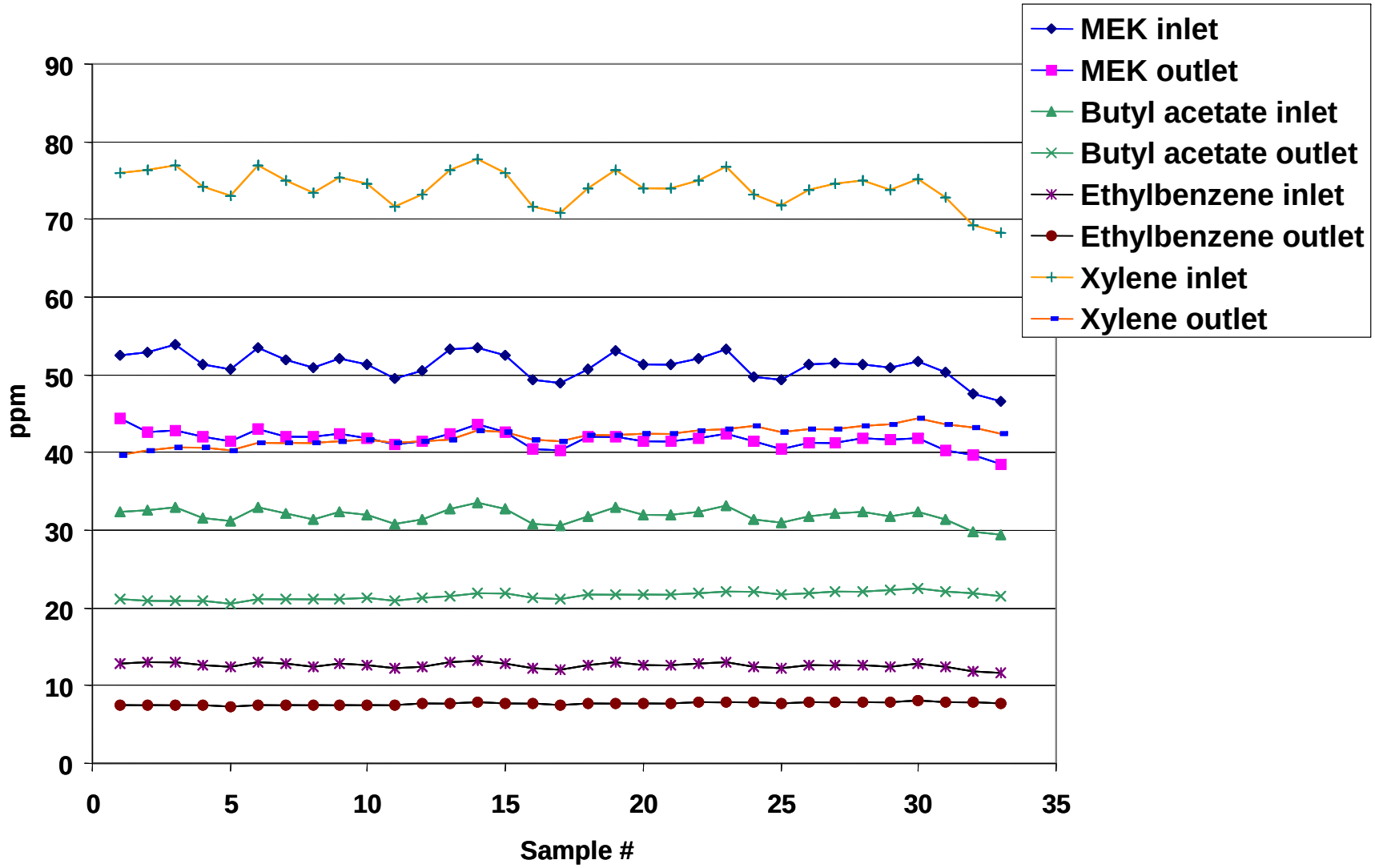

Figure B-7. AMT Module, Test 7, 2.0 ft^3/min Air, 0.2 L/min Oil, 170 ppm VOCs

Table B-8. AMT Module, Test 7, 2.0 ft^3/min Air, 0.22 L/min Oil, 170 ppm VOCs

Test 8												
Initial settings:		syringe pump 3.5ml/hr;silicon oil pressure 5.1psi;oil temp 71;air flow reading 344; temp at syringe tip ~290C										
		magnehelic 1(rding at sample port 1) ~1.0"H2O;mag. 2 (rding taken near vac. Pump) >1.0"H2O										
		net positive flow verified at 50cc/min										
start/stop time		7:00am-9:45am										
run date:		5/6/00										
Run sequence:		050600, 050600a, 050600b										
run#	MEK Front Detector	MEK Rear Detector	% Difference	n-Butyl Acetate Front Detector	n-Butyl Acetate Rear Detector	% Difference	Ethyl Benzene Front Detector	Ethyl Benzene Rear Detector	% Difference	o-Xylene Front Detector	o-Xylene Rear Detector	% Difference
1	4.552	3.65	19.81547	3.503	3.662	-4.5389666	1.393	1.906	-36.827	8.524	9.151	-7.3557
2	3.289	2.658	19.18516	2.646	3.125	-18.102797	1.046	1.652	-57.935	6.465	8.053	-24.563
3	3.157	6.072	-92.3345	2.545	5.339	-109.78389	0.963	2.293	-138.11	6.079	10.402	-71.1137
4	3.524	6.179	-75.3405	2.519	6.002	-138.26915	1.006	2.44	-142.545	6.483	11.006	-69.7671
5	2.51	5.428	-116.255	1.968	6.017	-205.74187	0.742	2.443	-229.245	4.902	10.983	-124.051
6	2.962	5.456	-84.1999	2.018	5.977	-196.18434	0.774	2.422	-212.92	5.113	10.915	-113.475
7	1.649	5.365	-225.349	1.465	5.93	-304.77816	0.472	2.405	-409.534	3.42	10.808	-216.023
8	1.137	4.698	-313.193	1.499	6.073	-305.13676	0.49	2.449	-399.796	3.592	11.098	-208.964
9	0.834	4.179	-401.079	1.135	5.722	-404.14097	0.375	2.34	-524	2.78	10.47	-276.619
10	137.872	65.605	52.41601	69.982	15.888	77.297019	28.084	5.681	79.7714	163.814	29.695	81.87273
11	151.286	102.345	32.34999	89.985	42.128	53.183308	34.858	14.152	59.401	207.138	78.021	62.33381
12	142.512	98.408	30.94757	85.919	44.01	48.777337	33.181	15.136	54.38353	197.311	84.547	57.15039
13	139.46	101.085	27.51685	85.927	45.668	46.852561	33.137	15.72	52.56058	197.591	88.826	55.04552
14	138.875	101.811	26.68875	86.336	46.47	46.175408	33.274	16.052	51.75813	198.545	91.292	54.01949
15	145.758	104.656	28.1988	89.561	47.204	47.294023	34.503	16.323	52.69107	205.751	93.335	54.63692
16	142.474	104.737	26.48694	88.78	47.981	45.95517	34.195	16.804	50.85831	204.471	97.677	52.22941
17	152.286	109.495	28.0991	94.257	49.884	47.07661	36.24	17.443	51.8681	216.196	100.626	53.45612
18	159.376	111.562	30.00075	98.568	50.774	48.488353	37.933	17.637	53.50486	226.656	102.83	54.63169
19	155.164	112.545	27.46707	97.672	51.512	47.260218	37.54	18.121	51.72882	225.039	104.066	53.75646
20	146.13	108.617	25.67098	92.16	50.841	44.833984	35.406	17.617	50.2429	212.006	103.52	51.17119
21	148.17	108	27.11075	93.482	51.22	45.208703	35.859	17.822	50.29979	214.562	104.314	51.38282
22	145.813	110.063	24.5177	92.387	51.622	44.124173	35.485	17.833	49.74496	212.703	104.645	50.80229
23	145.6	110.408	24.17033	92.216	52.007	43.603062	35.394	18.109	48.83596	212.24	105.455	50.31332
24	148.854	111.876	24.84179	94.211	53.133	43.602127	36.144	18.231	49.56009	216.427	105.709	51.1572
25	156.511	115.287	26.33936	97.995	53.933	44.963519	37.605	18.519	50.75389	225.161	106.749	52.58992
26	154.064	114.648	25.58417	96.341	54.222	43.718666	37	18.615	49.68919	221.235	107.161	51.56237
27	155.588	114.328	26.51875	96.976	54.369	43.935613	37.234	18.669	49.86034	222.84	107.549	51.73712
28	154.746	114.354	26.10213	97.155	54.495	43.909217	37.269	18.738	49.72229	223.296	107.871	51.69148
29	151.776	111.986	26.21627	95.588	54.214	43.283676	36.662	18.635	49.1708	219.433	107.392	51.05932
30	148.536	110.742	25.44434	93.973	54.513	41.990785	36.032	18.732	48.01288	215.84	108.106	49.91383
31	149.849	114.368	23.67784	94.943	55.38	41.670265	36.44	19.006	47.84303	218.428	109.504	49.86723
32	150.134	115.314	23.19261	95.226	55.63	41.581081	36.54	19.092	47.75041	218.946	109.932	49.79036
33	145.804	110.928	23.91978	92.654	54.986	40.654478	35.541	18.932	46.73194	213.008	109.302	48.68643
34	146.056	109.193	25.23895	91.772	54.055	41.098592	35.202	18.62	47.10528	210.566	107.482	48.95567
35	145.557	109.421	24.82601	91.851	54.346	40.832435	35.19	18.692	46.88264	210.736	107.935	48.78189
36	149.602	112.035	25.1113	93.961	54.919	41.551282	36.033	18.849	47.68962	215.74	108.557	49.68156
37	148.367	111.632	24.75955	93.637	55.22	41.027585	35.912	18.98	47.14859	215.021	109.227	49.20171
38	143.993	108.654	24.54217	90.839	55.134	39.305805	34.817	19.056	45.26812	208.587	109.495	47.50632

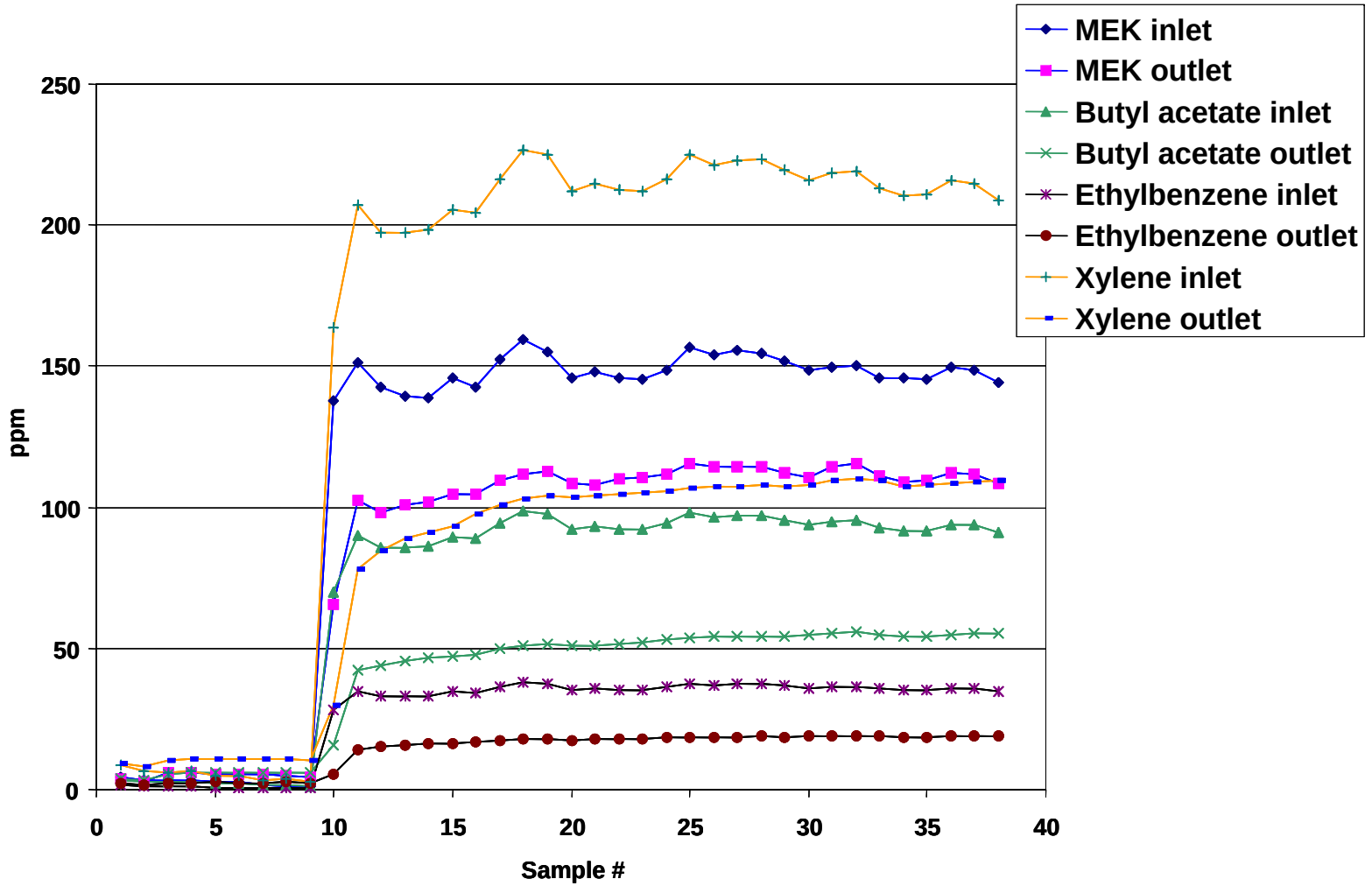

Figure B-8. AMT Module, Test 7, 2.0 ft^3/min Air, 0.22 L/min Oil, 170 ppm VOCs

Table B-9. AMT Module, Test 9, 2.0 ft^3/min Air, 0.2 L/min Oil, 350 ppm VOCs

Test 9												
36655												
Initial conditions:		magnehelic (1) ~0.9"H2O;magnehelic (2) >1"H2O;ran at 200ppm&4cfm = 4ml/hr and 680;oil pressure 5psi;										
		oil temp 78;temp controller setting 290C;sample flow through rotameter 53;										
Observations:		VOC removal was low during this test run. Recommend changing oil and running at a higher VOC conc-										
		centration.										
run#	MEK Front Detector	MEK Rear Detector	% Difference	n-Butyl Acetate Front Detector	n-Butyl Acetate Rear Detector	% Difference	Ethyl Benzene Front Detector	Ethyl Benzene Rear Detector	% Difference	o-Xylene Front Detector	o-Xylene Rear Detector	% Difference
1	0.631	7.321	-1060.22	1.025	10.458	-920.29268	0.316	4.126	-1205.7	2.324	20.191	-768.804
2	0.592	7.327	-1137.67	1.041	10.621	-920.26897	0.311	4.159	-1237.3	2.366	20.18	-752.916
3	0.603	7.17	-1089.05	0.992	10.579	-966.43145	0.294	4.123	-1302.38	2.266	20.134	-788.526
4	0.668	7.031	-952.545	1.185	10.447	-781.60338	0.316	4.083	-1192.09	2.24	19.882	-787.589
5	0.603	6.673	-1006.63	1.042	10.268	-885.41267	0.291	4.025	-1283.16	2.163	19.668	-809.293
6	0.692	6.472	-835.26	0.269	10.166	-3679.1822	0.308	3.995	-1197.08	2.115	19.552	-824.444
7	0.559	6.213	-1011.45	0.99	10.065	-916.66667	0.237	3.935	-1560.34	1.954	19.434	-894.575
8	0.716	5.919	-726.676	1.323	9.928	-650.41572	0.319	3.949	-1137.93	2.117	19.36	-814.502
9	0.72	5.888	-717.778	1.334	9.82	-636.13193	0.294	3.884	-1221.09	2.013	19.127	-850.174
10	0.655	5.662	-764.427	1.084	9.733	-797.87823	0.225	3.859	-1615.11	1.875	19.018	-914.293
11	0.703	5.484	-680.085	1.282	9.617	-650.15601	0.288	3.829	-1229.51	1.923	18.919	-883.827
12	0.382	5.294	-1285.86	1.062	9.441	-788.98305	0.265	3.772	-1323.4	1.913	18.69	-876.999
13	0.636	5.006	-687.107	1.164	9.269	-696.30584	0.292	3.714	-1171.92	1.944	18.44	-848.56
14	0.599	4.828	-706.01	1	9.107	-810.7	0.227	3.674	-1518.5	1.852	18.179	-881.587
15	4.975	9.396	-88.8643	2.71	10.911	-302.61993	1.009	4.316	-327.75	6.049	21.923	-262.424
16	79.607	68.491	13.9636	47.051	31.646	32.741068	18.528	11.399	38.4769	109.293	62.138	43.14549
17	91.54	75.87	17.1182	55.828	39.67	28.942466	21.604	14.238	34.09554	128.364	79.611	37.98027
18	85.396	76.173	10.80027	56.145	41.499	26.086027	21.691	14.988	30.90222	129.922	84.97	34.59922
19	5.554	9.845	-77.2596	6.997	18.707	-167.35744	2.426	7.365	-203.586	15.225	42.504	-179.172
20	3.666	7.675	-109.356	4.297	13.198	-207.14452	1.482	5.336	-260.054	9.175	30.346	-230.747
21	81.17	53.965	33.51608	43.521	22.564	48.153765	17.341	8.406	51.52529	101.028	45.66	54.80461
22	6.463	13.55	-109.655	10.362	21.204	-104.63231	3.631	7.974	-119.609	22.634	45.981	-103.15
23	3.16	6.587	-108.449	3.979	12.834	-222.54335	1.356	5.103	-276.327	8.94	28.567	-219.541
24	2.22	6.21	-179.73	2.988	11.303	-278.27979	0.952	4.57	-380.042	6.383	25.19	-294.642
25	1.888	4.967	-163.083	2.657	10.478	-294.35454	0.805	4.2	-421.739	5.304	22.886	-331.486
26	88.969	72.766	18.21196	52.085	33.297	36.071806	20.459	11.95	41.5905	120.944	66.25	45.22258
27	92.782	78.099	15.82527	56.78	40.623	28.455442	22.058	14.535	34.10554	130.801	82.121	37.21684
28	94.794	73.99	21.94654	58.039	41.684	28.179328	22.596	15.03	33.4838	134.027	86.213	35.6749
29	87.924	72.883	17.10682	55.353	42.146	23.859592	21.43	15.392	28.17545	127.459	89.125	30.07555
30	84.366	73.662	12.68758	53.926	42.669	20.874903	20.805	15.571	25.15741	124.02	90.522	27.01016
31	88.22	76.025	13.8234	56.077	43.14	23.070064	21.649	15.707	27.447	128.937	91.34	29.1592
32	91.059	74.687	17.97955	57.131	43.414	24.009732	22.08	15.832	28.2971	131.048	92.286	29.57848
33	88.697	75.567	14.80321	56.414	43.272	23.295636	21.764	15.808	27.36629	129.557	92.133	28.88613
34	88.202	74.665	15.34772	56.561	43.155	23.701844	21.804	15.772	27.66465	130.092	92.042	29.24853
35	86.866	71.566	17.61334	55.012	42.789	22.218789	21.217	15.661	26.18655	126.134	91.581	27.39388
36	85.83	72.856	15.11593	54.92	43.329	21.105244	21.183	15.855	25.15224	126.024	92.687	26.4529
37	91.721	78.726	14.16797	58.651	45.509	22.40712	22.643	16.523	27.02822	134.872	96.507	28.44549
38	95.437	81.768	14.32254	61.606	46.901	23.869428	23.708	16.987	28.34908	141.706	99.275	29.94298
39	96.661	80.491	16.72857	61.82	46.699	24.459722	23.804	16.925	28.8985	141.991	99.107	30.20191
40	93.705	80.413	14.18494	60.159	46.691	22.38734	23.174	16.958	26.82316	138.243	99.444	28.0658
41	95.434	80.002	16.17034	61.035	46.468	23.866634	23.506	16.888	28.15451	140.175	98.926	29.42679
42	96.435	77.94	19.17872	61.348	45.941	25.114103	23.626	16.737	29.15855	140.753	98.062	30.33044
43	92.36	78.248	15.27934	59.478	46.378	22.02495	22.921	16.909	26.22922	136.655	99.143	27.45015
44	91.043	79.597	12.57208	59.2	47.009	20.592905	22.815	17.129	24.9222	136.329	100.414	26.34436
45	93.232	79.387	14.85005	59.922	46.539	22.334034	23.115	16.991	26.49362	137.928	99.601	27.78769
46	94.528	79.312	16.09682	60.129	46.689	22.351943	23.192	17.039	26.5307	138.103	99.949	27.62721
47	94.751	78.851	16.78083	60.285	46.571	22.748611	23.254	16.981	26.976	138.341	99.592	28.00977
48	91.775	77.304	15.76791	59.015	45.955	22.129967	22.793	16.79	26.33703	135.783	98.465	27.48356
49	89.062	74.638	16.19546	57.12	45.269	20.747549	22.028	16.578	24.74124	131.207	97.432	25.74177
50	87.042	75.892	12.80991	56.641	45.856	19.040977	21.846	16.781	23.18502	130.375	98.558	24.40422
51	90.907	78.336	13.82842	58.8	46.44	21.020408	22.663	16.967	25.13348	135.307	99.552	26.42509
52	91.285	77.471	15.13283	58.703	46.252	21.21016	22.595	16.917	25.12945	134.867	99.344	26.33928
53	89.465	76.244	14.77785	57.455	45.528	20.758855	22.179	16.679	24.79823	132.123	97.891	25.90919
54	89.725	75.301	16.07579	57.322	45.067	21.379226	22.133	16.506	25.42358	131.794	96.898	26.47768
55	91.056	73.616	19.15305	57.913	45.056	22.200542	22.36	16.515	26.14043	133.052	97.044	27.0631
56	85.559	72.865	14.83655	55.092	45.063	18.204095	21.262	16.535	22.23215	126.521	97.199	23.1756
57	86.82	74.576	14.10274	56.109	45.279	19.301716	21.651	16.604	23.3107	129.041	97.579	24.3814
58	95.245	78.84	17.224	60.555	45.877	24.239121	23.367	16.77	28.23212	139.344	98.307	29.45014
59	93.165	79.109	15.08721	59.54	46.774	21.441048	22.981	17.105	25.56895	136.827	100.303	26.69356
60	93.709	78.902	15.80104	59.971	46.791	21.977289	23.114	17.112	25.96695	137.831	100.201	27.30155

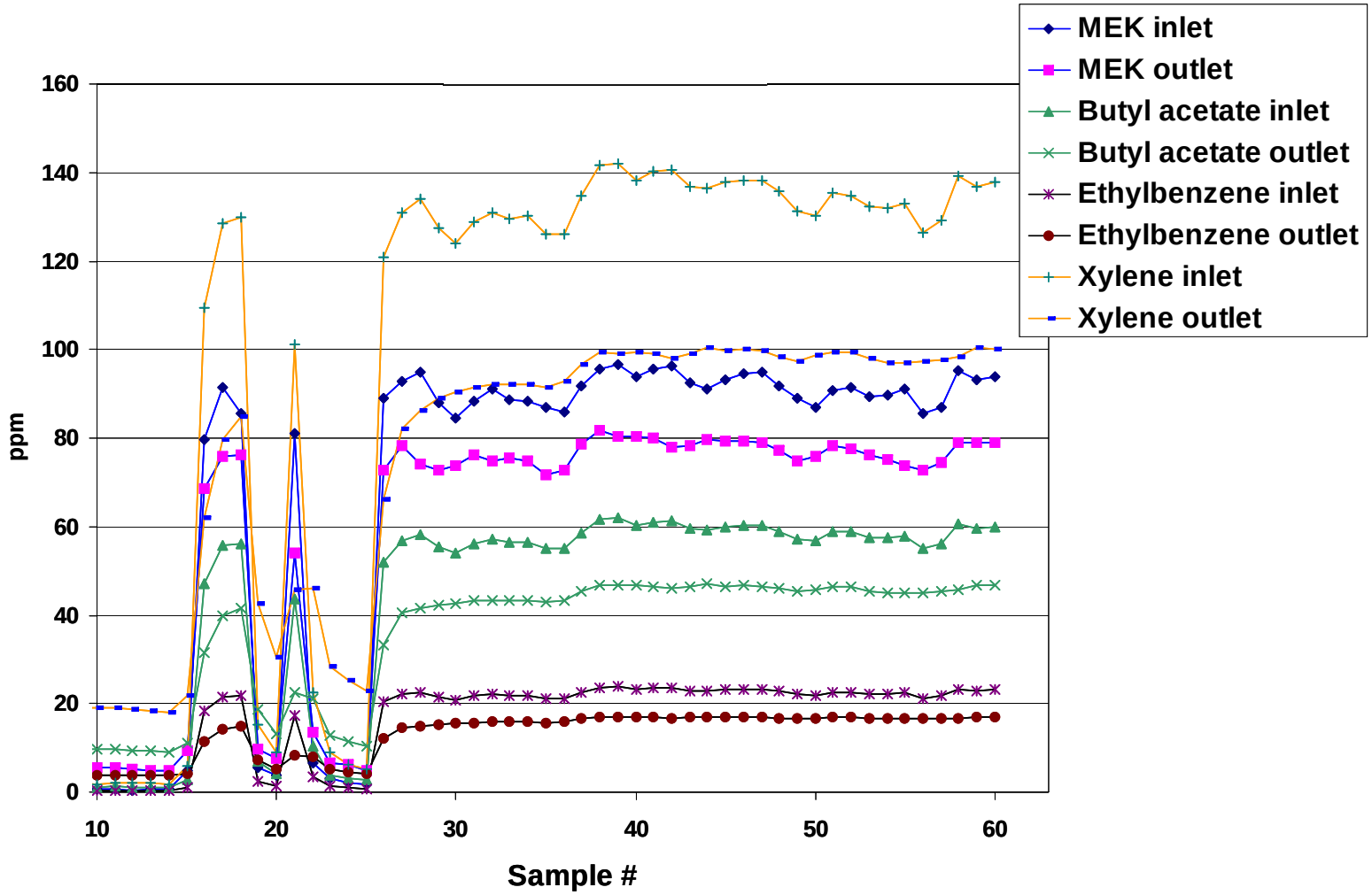

Figure B-9. AMT Module, Test 9, 2.0 ft^3/min Air, 0.2 L/min Oil, 350 ppm VOCs

Table B-10. Two Parallel AMT Modules, Test 10, 4.0 ft^3/min Air, 0.4 L/min Oil, 350 ppm VOCs

Test 10												
Run date 5/11/00												
sequence used:		051100a										
Initial parameters:		mag. (1) ~0.9"H2O;mag (2) >1.0"H2O;oil temp 74C;air temp74C;temp controller set 290C;air velocity 639;										
		oil pressure ~5.1psi;excess sample flow set ~55 (dual rotameter);syringe set 4ml/hr										
run#	MEK Front Detector	MEK Rear Detector	% Difference	n-Butyl Acetate Front Detector	n-Butyl Acetate Rear Detector	% Difference	Ethyl Benzene Front Detector	Ethyl Benzene Rear Detector	% Difference	o-Xylene Front Detector	o-Xylene Rear Detector	% Difference
1	1.196	0.841	29.68227	2.549	1.724	32.365634	0.396	0.942	-137.879	1.839	3.353	-82.3274
2	0.518	1.072	-106.95	2.053	1.969	4.0915733	0.224	1.007	-349.554	1.647	3.357	-103.825
3	1.18	2.452	-107.797	2.13	2.233	-4.8356808	0.224	1.063	-374.554	1.623	3.347	-106.223
4	1.079	0.868	19.55514	2.492	1.565	37.199037	0.305	0.845	-177.049	1.681	3.205	-90.6603
5	1.062	0.837	21.18644	2.294	1.48	35.483871	0.277	0.84	-203.249	1.675	3.144	-87.7015
6	0.992	0.763	23.08468	2.114	1.474	30.274361	0.227	0.812	-257.709	1.551	3.074	-98.1947
7	0.726	0.859	-18.3196	1.745	1.731	0.8022923	0.189	0.918	-385.714	1.461	3.086	-111.225
8	1.006	0.594	40.95427	2.26	1.748	22.654867	0.284	0.918	-223.239	1.61	3.053	-89.6273
9	0.46	0.846	-83.913	1.715	1.793	-4.548105	0.178	0.954	-435.955	1.444	3.09	-113.989
10	0.957	0.733	23.40648	2.135	1.414	33.770492	0.252	0.829	-228.968	1.499	2.991	-99.533
11	2.289	2.32	-1.3543	2.736	2.212	19.152047	0.429	1.253	-192.075	3.16	4.016	-27.0886
12	1.239	1.178	4.923325	2.234	1.941	13.115488	0.273	1.085	-297.436	1.75	3.492	-99.5429
13	3.925	4.432	-12.9172	3.703	2.714	26.708075	0.846	1.401	-65.6028	5.412	4.878	9.866962
14	95.553	56.539	40.8297	56.971	11.345	80.08636	21.585	3.968	81.61686	127.561	18.208	85.72604
15	101.631	67.474	33.60884	64.59	19.195	70.281777	24.366	6.355	73.91858	145.574	31.711	78.21658
16	103.881	70.809	31.83643	67.57	22.666	66.455528	25.427	7.604	70.09478	152.193	39.211	74.236
17	108.447	74.369	31.42364	71.053	24.641	65.320254	26.704	8.383	68.6077	160.135	43.862	72.60936
18	106.268	74.521	29.87447	69.664	25.774	63.002412	26.165	8.831	66.24881	156.784	47.01	70.01607
19	107.389	74.361	30.75548	70.392	26.385	62.517047	26.474	9.016	65.94395	158.739	48.825	69.24196
20	108.873	76.766	29.49032	72.267	27.376	62.118256	27.16	9.337	65.62224	163.193	51.107	68.68309
21	109.67	76.9	29.88055	72.683	27.897	61.61826	27.27	9.515	65.10818	163.499	52.194	68.07687
22	108.389	80.158	26.046	72.683	28.979	60.129604	27.23	9.912	63.59897	163.409	54.163	66.85433
23	111.554	82.145	26.36302	74.933	29.759	60.285855	28.122	10.071	64.18818	168.989	55.401	67.21621
24	110.226	80.289	27.15965	73.647	30.18	59.020734	27.639	10.259	62.88216	165.939	56.627	65.87481
25	109.571	80.121	26.87755	72.776	30.6	57.953171	27.335	10.411	61.9133	164.004	57.554	64.90695
26	109.47	81.358	25.6801	72.566	30.965	57.328501	27.231	10.531	61.32716	163.649	58.135	64.4758
27	109.668	81.099	26.05044	72.899	31.426	56.891041	27.37	10.674	61.0011	164.194	58.859	64.15277
28	101.128	83.763	17.17131	69.849	32.046	54.121033	26.184	10.93	58.25695	158.458	59.934	62.17673
29	100.226	80.463	19.71844	68.236	32.201	52.809367	25.629	10.959	57.23985	154.617	60.554	60.83613
30	102.113	79.441	22.20285	68.725	32.231	53.101491	25.803	10.999	57.37317	155.173	60.783	60.82888
31	103.253	80.731	21.81244	69.402	32.598	53.030172	26.013	11.107	57.30212	156.484	61.279	60.84009
32	103.484	81.486	21.25739	69.592	33.015	52.559202	26.129	11.194	57.15871	156.888	61.819	60.59673
33	103.967	81.257	21.84347	69.918	33.221	52.485769	26.212	11.279	56.97009	157.562	62.223	60.50888
34	100.367	79.535	20.75583	67.711	33.498	50.527979	25.446	11.386	55.25426	152.755	62.634	58.99709
35	101.594	79.006	22.2336	67.97	33.574	50.604679	25.498	11.458	55.06314	152.957	63.063	58.77077
36	104.337	83.383	20.083	70.162	34.422	50.939255	26.334	11.66	55.72264	158.286	64.097	59.50558
37	106.155	83.507	21.33484	71.522	34.988	51.080786	26.835	11.834	55.90088	160.994	64.973	59.6426
38	101.175	80.757	20.18087	68.224	34.93	48.801008	25.589	11.894	53.51909	153.78	65.34	57.51073
39	104.382	82.376	21.08218	69.773	35.147	49.626646	26.198	11.959	54.35148	157.353	65.529	58.35542
40	105.964	81.905	22.70488	70.128	35.778	48.981862	26.322	12.15	53.84089	157.875	66.315	57.99525
41	102.268	82.505	19.32472	69.134	36.021	47.896838	25.932	12.252	52.75335	156.088	66.913	57.13123
42	101.934	82.631	18.93676	68.362	36.519	46.579971	25.618	12.397	51.60824	154.439	67.87	56.05385
43	103.229	82.532	20.0496	68.693	36.679	46.604458	25.738	12.48	51.51138	154.992	68.379	55.88224
44	101.861	83.264	18.25723	68.689	37.183	45.867606	25.766	12.65	50.90429	154.876	69.333	55.23322
45	106.432	84.464	20.64041	70.928	37.233	47.505921	26.635	12.658	52.47607	159.897	69.338	56.63583
46	104.331	84.73	18.78732	70.381	37.744	46.37189	26.414	12.836	51.40456	158.894	70.027	55.92848
47	103.369	82.745	19.95182	69.099	38.102	44.858826	25.927	12.997	49.87079	155.831	70.891	54.50777
48	101.328	85.423	15.69655	68.983	38.605	44.036937	25.856	13.162	49.09499	156.188	71.748	54.06305

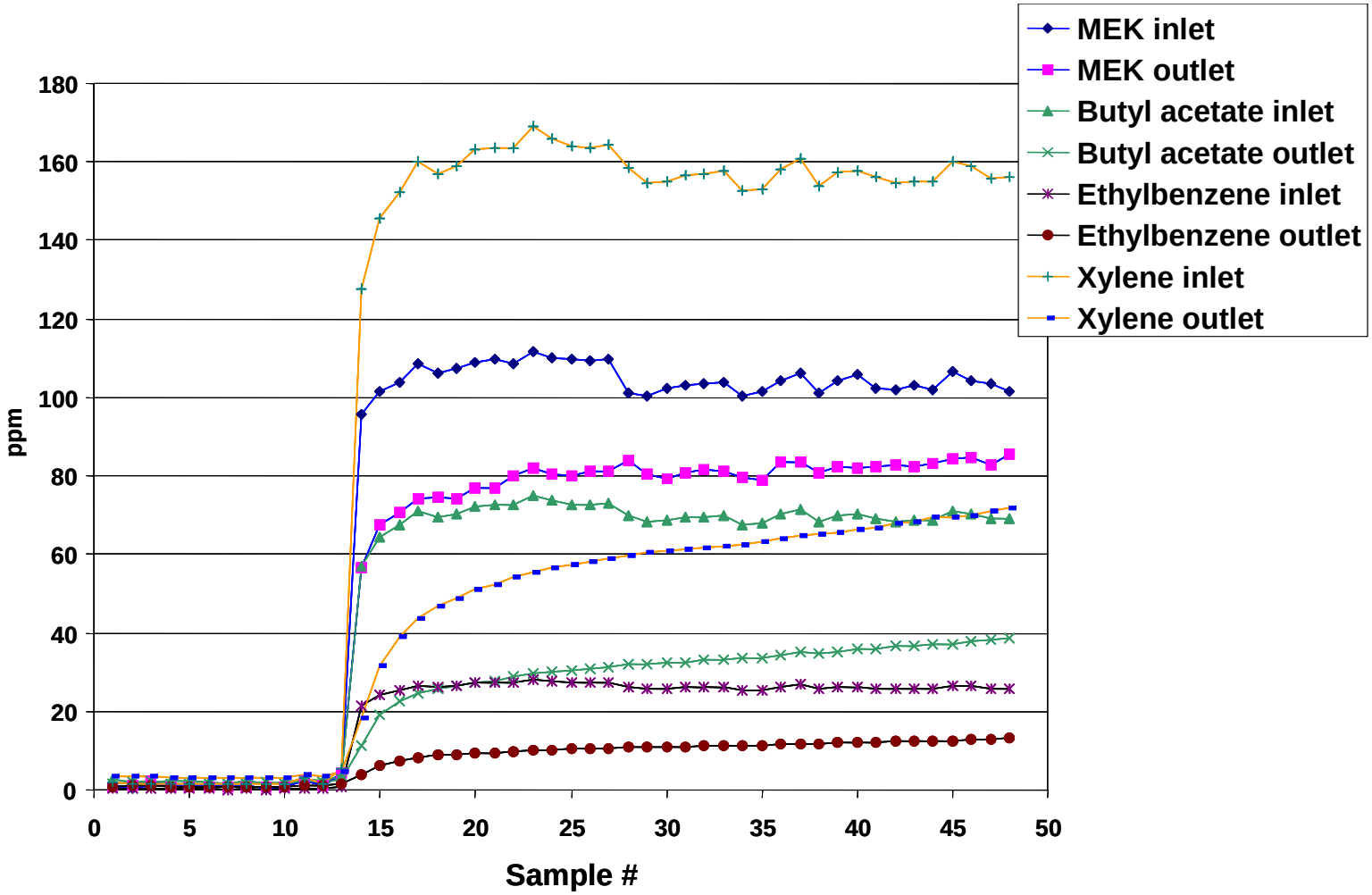

Figure B-10. Two Parallel AMT Modules, Test 10, 4.0 ft^3/min Air, 0.4 L/min Oil, 350 ppm VOCs

Table B-11. Two Parallel AMT Modules, Test 11, 4.0 ft^3/min Air, 1.0 L/min Oil, 350 ppm VOCs

Test 11												
Run date 5/12/00												
Initial parameters:		temp controller set 290C;air velocity ~ 4cfm;mag (1) ~0.9"H2O;mag (2) >1.0 "H2O										
		oil flow 1L/min;excess sample flow set ~55 (dual rotameter);syringe set 4ml/hr										
run#	MEK Front Detector	MEK Rear Detector	% Difference	n-Butyl Acetate Front Detector	n-Butyl Acetate Rear Detector	% Difference	Ethyl Benzene Front Detector	Ethyl Benzene Rear Detector	% Difference	o-Xylene Front Detector	o-Xylene Rear Detector	% Difference
1	0.167	0	100	0.6	0	100	0.0804	0	100	0.633	0	100
2	0.185	0.0944	48.97297	0.623	1.609	-158.26645	0.0779	0.902	-1057.89	0.637	3.743	-487.598
3	0.161	0	100	0.541	1.505	-178.18854	0.0821	0.838	-920.706	0.638	0.434	31.97492
4	0.175	0.708	-304.571	0.581	1.807	-211.01549	0.0783	1.022	-1205.24	0.594	3.915	-559.091
5	0.165	0	100	0.603	1.693	-180.76285	0.0758	1.063	-1302.37	0.59	3.975	-573.729
6	0.141	0.117	17.02128	0.589	1.755	-197.96265	0.0707	0.943	-1233.8	0.574	3.531	-515.157
7	0.164	0	100	0.565	1.287	-127.78761	0.0743	0.798	-974.024	0.568	3.459	-508.979
8	0.166	0	100	0.527	1.332	-152.75142	0.0681	0.778	-1042.44	0.576	3.328	-477.778
9	0.17	0	100	0.541	1.231	-127.54159	0.0657	0.753	-1046.12	0.56	3.375	-502.679
10	0.167	0	100	0.551	1.365	-147.7314	0.0693	0.822	-1086.15	0.566	3.473	-513.604
11	0.138	0	100	0.593	1.522	-156.66105	0.0672	0.908	-1251.19	0.572	3.533	-517.657
12	0.438	0.336	23.28767	0.746	1.696	-127.34584	0.102	0.984	-864.706	0.596	3.714	-523.154
13	2.651	1.749	34.0249	2.063	2.051	0.5816772	0.421	1.135	-169.596	3.456	4.706	-36.169
14	91.613	28.112	69.3144	56.414	8.005	85.81026	19.254	2.735	85.79516	129.88	14.008	89.21466
15	98.666	31.338	68.2383	62.718	10.845	82.708313	21.261	3.605	83.04407	144.055	19.688	86.333
16	99.243	32.387	67.36596	63.42	11.947	81.162094	21.449	4.03	81.21125	145.064	22.469	84.51097
17	100.032	30.637	69.3728	64.249	11.61	81.92968	21.706	3.974	81.6917	146.984	22.642	84.5956
18	94.5	29.651	68.62328	60.395	12.265	79.692027	20.353	4.131	79.70324	137.525	24.148	82.44101
19	90.672	33.68	62.85513	59.439	13.621	77.084069	20.017	4.561	77.21437	135.864	26.633	80.39731
20	96.57	35.03	63.72579	63.161	13.945	77.921502	21.264	4.663	78.07092	144.393	27.308	81.08773
21	99.858	35.457	64.49258	64.854	14.348	77.876461	21.827	4.77	78.14633	148.138	27.837	81.20874
22	98.082	32.521	66.84305	63.905	13.233	79.2927	21.485	4.428	79.39027	145.832	25.713	82.36807
23	98.47	34.158	65.31126	63.999	13.686	78.615291	21.586	4.515	79.08367	146.387	26.379	81.97996
24	101.48	33.959	66.53626	64.88	14.239	78.053329	21.836	4.758	78.21029	147.465	27.904	81.07754
25	85.385	30.279	64.53827	56.963	13.195	76.835841	19.152	4.413	76.95802	130.192	25.873	80.12704
26	91.338	33.577	63.23874	60.568	14.286	76.413288	20.385	4.739	76.75251	138.598	27.571	80.10722
27	93.357	31.704	66.04004	61.75	14.047	77.251822	20.781	4.634	77.70078	141.376	27.457	80.57874
28	100.211	37.655	62.42428	66.06	15.774	76.121708	22.253	5.16	76.81212	151.244	30.325	79.94962
29	102.656	39.426	61.59406	67.151	16.39	75.592322	22.601	5.347	76.34175	153.35	31.62	79.3805
30	103.548	36.538	64.71395	67.276	15.683	76.688567	22.657	5.104	77.47275	153.487	30.468	80.14946
31	89.665	32.365	63.90453	58.708	14.843	74.717245	19.708	4.918	75.04567	133.521	28.991	78.28731
32	87.894	33.585	61.7892	58.912	15.131	74.315929	19.798	4.972	74.88635	134.829	29.466	78.14565
33	94.948	35.449	62.66483	62.748	15.893	74.671703	21.113	5.226	75.24748	143.379	30.457	78.7577
34	100.195	38.518	61.55696	65.998	16.743	74.631049	22.194	5.461	75.39425	150.839	32.06	78.74555
35	99.847	37.44	62.50263	65.791	16.398	75.075618	22.113	5.299	76.03672	150.372	31.394	79.12244
36	98.724	35.81	63.72716	65.309	16.438	74.830422	21.986	5.332	75.7482	149.493	31.627	78.84383
37	103.372	36.414	64.77383	66.509	16.883	74.615466	22.371	5.536	75.25368	150.98	32.694	78.34548
38	89.169	35.871	59.77189	59.61	16.98	71.514847	20.037	5.524	72.431	136.233	32.705	75.99333
39	94.252	37.411	60.30747	62.548	17.222	72.465946	21.039	5.595	73.40653	143.013	32.766	77.0888
40	96.381	35.333	63.34028	63.457	16.468	74.048568	21.337	5.39	74.73872	144.757	31.599	78.171
41	98.367	37.034	62.3512	64.804	16.801	74.074131	21.788	5.527	74.63283	148.01	32.43	78.08932
42	101.793	38.27	62.40409	66.393	17.483	73.667405	22.322	5.7	74.46465	151.408	33.421	77.92653
43	102.717	34.905	66.01828	66.874	17.203	74.275503	22.488	5.643	74.90662	152.081	33.305	78.10049
44	94.515	40.619	57.02375	62.536	19.612	68.638864	21.007	6.327	69.88147	142.765	37.854	73.4851
45	94.499	41.676	55.89795	63.291	19.767	68.768071	21.263	6.387	69.96191	144.796	37.778	73.9095
46	98.897	41.753	57.78133	65.393	19.723	69.839279	22.001	6.359	71.09677	149.575	37.681	74.80796
47	97.976	37.6	61.62325	64.447	17.891	72.239204	21.652	5.824	73.10179	147.029	34.187	76.74812
48	97.06	36.067	62.84051	64.099	17.405	72.84669	21.539	5.631	73.85673	146.46	33.412	77.18695
49	99.215	34.905	64.81883	65.123	17.112	73.723569	21.893	5.58	74.5124	148.642	32.978	77.81381
50	99.981	39.438	60.55451	64.974	19.932	69.323114	21.82	6.451	70.43538	147.667	38.622	73.84521

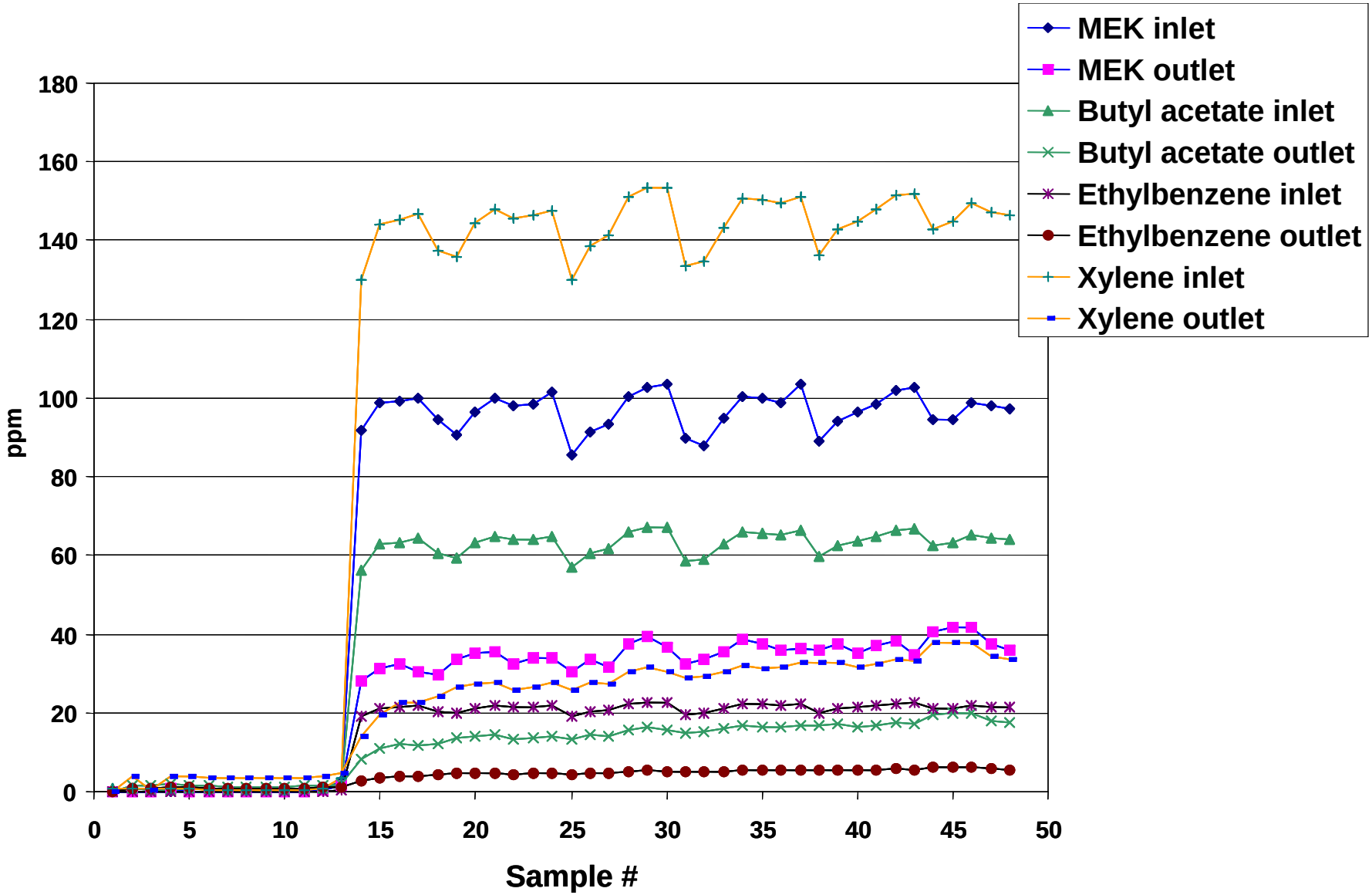

Figure B-11. Two Parallel AMT Modules, Test 11, 4.0 ft^3/min Air, 1.0 L/min Oil, 350 ppm VOCs

Table B-12. Two Parallel AMT Modules, Test 14, 4.0 ft^3/min Air, 1.0 L/min Oil, 350 ppm VOCs

Test 14												
Run date 6/06/00												
Initial parameters:		syringe set 4.0ml/hr;air 4cfm (1380-1390);sample flow rate 55cc's;injection temp 290C;										
		oil pressure set at 25psi(11.2 at the module);										
run#	MEK Front Detector	MEK Rear Detector	% Difference	n-Butyl Acetate Front Detector	n-Butyl Acetate Rear Detector	% Difference	Ethyl Benzene Front Detector	Ethyl Benzene Rear Detector	% Difference	o-Xylene Front Detector	o-Xylene Rear Detector	% Difference
1	105.47	96.546	8.461174	46.818	22.832	51.232432	12.325	5.277	57.18458	39.746	15.632	60.67026
2	105.427	100.266	4.89533	47.38	24.09	49.155762	12.481	5.569	55.38018	40.365	16.462	59.21714
3	105.966	100.33	5.318687	47.578	24.867	47.734247	12.519	5.74	54.14969	40.482	16.911	58.22588
4	115.016	105.482	8.289281	51.301	25.81	49.68909	13.508	6.022	55.41901	43.632	17.982	58.78713
5	300.907	184.784	38.59099	129.936	25.698	80.222571	34.11	5.521	83.81413	109.754	15.308	86.05244
6	249.146	195.881	21.37903	115.282	29.271	74.609219	30.238	6.112	79.78702	98.35	16.631	83.08998
7	106.579	108.212	-1.5322	50.156	30.601	38.988356	13.117	6.932	47.15255	42.555	20.095	52.77876
8	106.103	108.816	-2.55695	49	29.572	39.64898	12.852	6.749	47.48677	41.613	19.784	52.45716
9	110.194	111.831	-1.48556	50.329	30.206	39.982912	13.215	6.837	48.26334	42.797	19.884	53.5388
10	108.751	111.051	-2.11492	49.584	30.4	38.6899	13.017	6.877	47.16909	42.149	20.03	52.47811
11	109.137	110.57	-1.31303	49.243	30.717	37.621591	12.923	6.944	46.26635	41.748	20.117	51.81326
12	107.887	110.557	-2.47481	49.189	30.786	37.412836	12.916	6.963	46.09012	41.788	20.216	51.62248
13	109.278	111.426	-1.96563	49.377	30.869	37.483039	12.961	7.003	45.96868	41.859	20.387	51.29602
14	108.253	110.739	-2.29647	48.737	31.175	36.034225	12.785	7.074	44.66953	41.28	20.63	50.02422
15	106.088	111.303	-4.91573	48.138	31.451	34.664922	12.645	7.178	43.23448	40.934	20.991	48.71989
16	106.963	113.362	-5.98244	48.702	32.115	34.05815	12.802	7.316	42.85268	41.441	21.317	48.5606
17	110.332	115.603	-4.7774	50.225	32.712	34.869089	13.185	7.449	43.50398	42.718	21.651	49.31645
18	111.105	114.675	-3.21318	50.136	33.131	33.917744	13.155	7.535	42.7214	42.517	21.893	48.50766
19	109.971	114.096	-3.75099	49.862	33.618	32.577915	13.085	7.635	41.65075	42.346	22.144	47.70699
20	107.338	112.593	-4.89575	48.896	33.756	30.963678	12.812	7.691	39.97034	41.449	22.328	46.13139
21	106.586	111.945	-5.02786	48.382	33.901	29.930553	12.699	7.73	39.12907	41.107	22.463	45.35481
22	105.332	112.315	-6.62951	47.729	34.403	27.920132	12.524	7.853	37.29639	40.555	22.821	43.72827
23	106.985	115.814	-8.25256	49.054	35.02	28.609288	12.869	8.005	37.79625	41.731	23.249	44.28842
24	109.767	116.539	-6.16943	49.76	35.309	29.041399	13.051	8.074	38.13501	42.206	23.442	44.45813
25	110.551	115.57	-4.53999	50.304	35.538	29.353531	13.187	8.145	38.23463	42.707	23.715	44.47046
26	109.347	115.847	-5.94438	49.865	35.873	28.059761	13.061	8.216	37.09517	42.297	23.873	43.55864
27	110.497	116.581	-5.50603	50.167	36.183	27.874898	13.159	8.289	37.00889	42.607	24.07	43.50694
28	117.356	119.363	-1.71018	52.779	36.61	30.635291	13.856	8.352	39.72286	44.783	24.181	46.00406
29	115.04	120.343	-4.6097	52.095	37.604	27.816489	13.65	8.552	37.34799	44.101	24.683	44.03075
30	107.769	117.988	-9.48232	49.645	38.11	23.234968	12.967	8.71	32.82949	42.035	25.161	40.14274
31	111.199	118.72	-6.76355	50.758	38.282	24.579377	13.283	8.749	34.13386	42.998	25.304	41.15075
32	110.964	117.973	-6.31646	50.516	38.262	24.257661	13.216	8.762	33.70157	42.791	25.386	40.67444
33	108.632	116.986	-7.69018	49.734	38.276	23.038565	13.024	8.782	32.57064	42.224	25.465	39.6907
34	106.497	113.877	-6.92977	48.584	38.201	21.371233	12.734	8.798	30.90938	41.206	25.558	37.97505
35	105.282	112.155	-6.52818	47.979	38.387	19.99208	12.564	8.855	29.52085	40.633	25.724	36.69185
36	102.929	111.133	-7.97054	47.052	38.27	18.664456	12.304	8.879	27.83648	39.825	25.9	34.96547
37	100.181	109.982	-9.78329	46.052	38.283	16.87006	12.023	8.893	26.03344	38.935	25.963	33.31707
38	103.344	113.257	-9.59224	47.655	38.827	18.524814	12.447	9.007	27.63718	40.304	26.223	34.93698

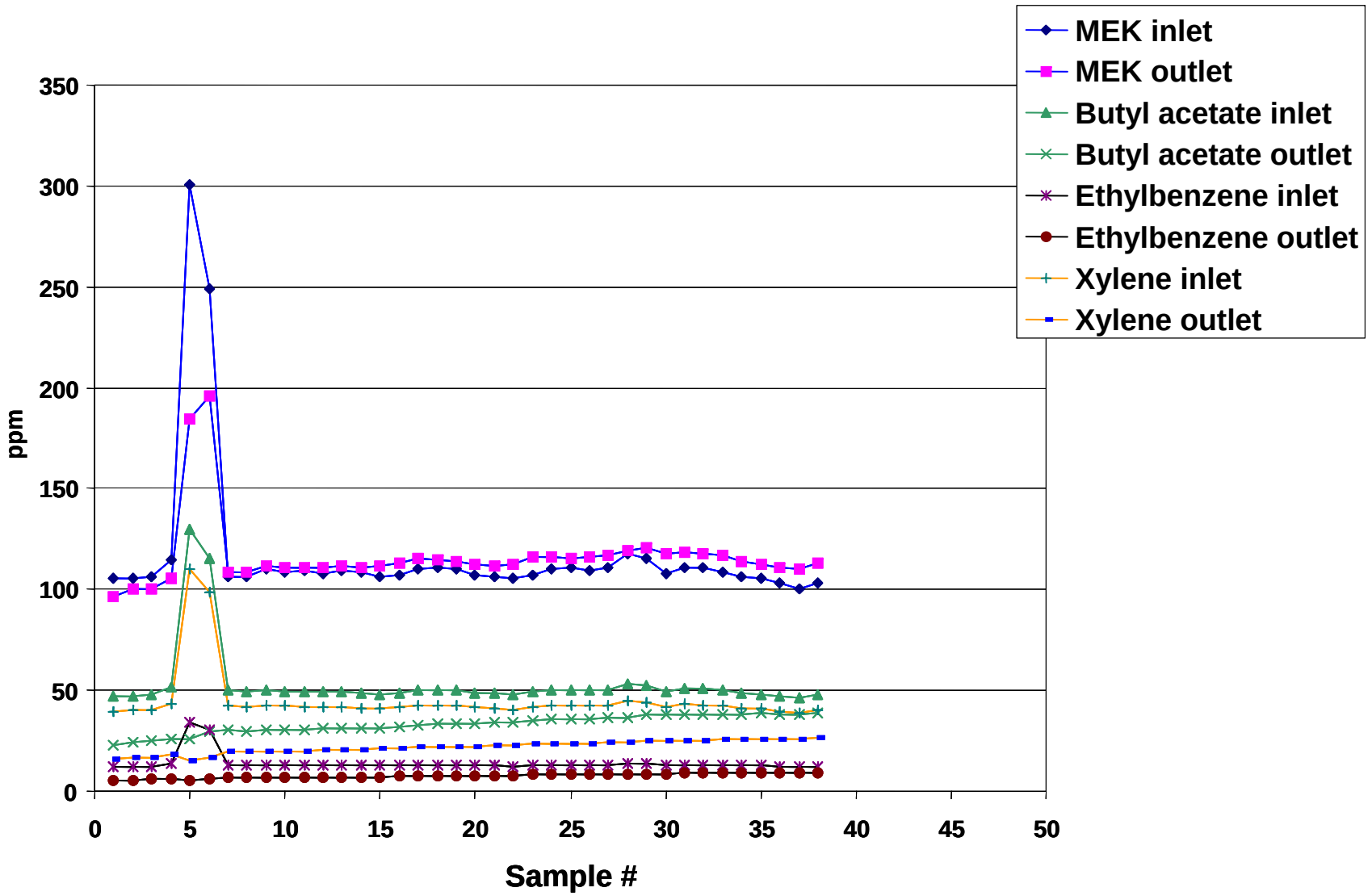

Figure B-12. Two Parallel AMT Modules, Test 14, 4.0 ft^3/min Air, 1.0 L/min Oil, 350 ppm VOCs

Table B-13. Two Parallel AMT Modules, Test 15, 2.0 ft^3/min Air, 1.0 L/min Oil, 220 ppm VOCs

Test 15												
Run date 6/07/00												
Initial parameters:	sample flow rate 55cc's;syringe set 2.0 ml/hr;air velocity ~2.0cfm (~500);											
run#	MEK Front Detector	MEK Rear Detector	% Difference	n-Butyl Acetate Front Detector	n-Butyl Acetate Rear Detector	% Difference	Ethyl Benzene Front Detector	Ethyl Benzene Rear Detector	% Difference	o-Xylene Front Detector	o-Xylene Rear Detector	% Difference
1	6.728	9.096	-35.1962	2.91	1.099	62.233677	0.81	0.277	65.80247	3.051	0.605	80.17044
2	13.384	34.031	-154.266	5.574	10.914	-95.801938	1.54	2.23	-44.8052	5.282	5.125	2.972359
3	11.191	34.246	-206.014	5.035	13.751	-173.10824	1.353	3.169	-134.22	4.752	7.707	-62.1843
4	7.336	31.168	-324.864	3.705	15.283	-312.49663	0.973	3.57	-266.906	3.612	8.931	-147.259
5	6.317	29.131	-361.152	3.055	16.239	-431.55483	0.82	3.802	-363.659	3.089	9.616	-211.298
6	0	16.805	#DIV/0!	0.916	16.066	-1653.9301	0.195	3.85	-1874.36	0.932	9.94	-966.524
7	0	4.907	#DIV/0!	0	13.229	#DIV/0!	0.0984	3.43	-3385.77	0.446	9.209	-1964.8
8	0	1.544	#DIV/0!	0	10.756	#DIV/0!	0.0786	3.002	-3719.34	0.341	8.363	-2352.49
9	0	8.601	#DIV/0!	0	9.206	#DIV/0!	0.065	2.672	-4010.77	0.28	7.599	-2613.93
10	0	14.966	#DIV/0!	0	12.432	#DIV/0!	0.0883	3.174	-3494.56	0.371	8.572	-2210.51
11	41.27	35.461	14.0756	15.282	14.993	1.8911137	4.183	3.613	13.62658	13.417	9.544	28.86636
12	48.805	52.175	-6.90503	21.061	18.214	13.517877	5.565	4.236	23.8814	18.133	11.143	38.5485
13	38.646	48.678	-25.9587	17.554	19.345	-10.202803	4.607	4.519	1.910137	15.096	11.964	20.74722
14	123.869	62.397	49.62662	46.728	20.095	56.995806	12.385	4.675	62.25273	39.116	12.51	68.0182
15	129.843	105.223	18.96136	55.723	24.799	55.495935	14.551	5.548	61.87204	46.852	14.712	68.59899
16	117.593	103.599	11.90037	51.623	27.364	46.99262	13.426	6.13	54.34232	43.32	16.406	62.12835
17	119.69	100.921	15.68134	52.435	28.592	45.471536	13.631	6.434	52.79877	43.908	17.402	60.36713
18	115.268	103.62	10.10515	51.258	29.534	42.381677	13.294	6.671	49.81947	42.938	18.15	57.72975
19	121.178	109.174	9.906089	54.391	30.17	44.531264	14.115	6.817	51.70386	45.654	18.601	59.25658
20	113.387	106.705	5.893092	51.57	30.96	39.965096	13.367	6.991	47.69956	43.248	19.128	55.77137
21	117.521	109.113	7.154466	52.625	31.509	40.125416	13.648	7.215	47.13511	44.043	19.772	55.10751
22	112.831	107.851	4.413681	51.287	31.716	38.159768	13.281	7.181	45.93028	43.031	19.778	54.03779
23	115.453	106.038	8.154834	51.497	31.819	38.211935	13.344	7.236	45.77338	43.059	19.988	53.57997
24	112.24	106.683	4.950998	51.037	32.071	37.161275	13.208	7.299	44.73804	42.711	20.212	52.6773
25	107.861	105.151	2.512493	48.986	32.237	34.191402	12.669	7.346	42.01594	40.973	20.338	50.36243
26	111.484	109.778	1.530264	51.237	32.908	35.772977	13.248	7.559	42.94233	42.946	20.893	51.35053
27	105.621	107.633	-1.90492	48.806	33.159	32.059583	12.616	7.656	39.31516	40.958	21.184	48.27872
28	112.309	110.408	1.692652	51.428	33.397	35.060667	13.3	7.691	42.17293	43.153	21.276	50.69636
29	113.297	108.437	4.28961	51.381	33.549	34.705436	13.292	7.762	41.60397	43.009	21.472	50.07557
30	108.576	101.77	6.26842	47.691	32.715	31.402151	12.379	7.623	38.4199	39.878	21.117	47.04599
31	107.545	107.399	0.135757	48.785	33.54	31.249359	12.662	7.758	38.73006	40.833	21.5	47.34651
32	111.265	109.18	1.873905	50.511	33.99	32.707727	13.069	7.853	39.91124	42.305	21.754	48.57818
33	111.241	112.387	-1.0302	51.243	34.594	32.490291	13.246	7.979	39.76295	42.977	22.084	48.61438
34	105.404	110.399	-4.73891	49.118	34.774	29.203143	12.697	8.042	36.6622	41.257	22.291	45.97038
35	113.319	111.859	1.288398	51.465	34.855	32.274361	13.318	8.069	39.41282	43.094	22.449	47.9069
36												
37	112.005	118.259	-5.58368	51.19	34.465	32.672397	13.215	7.875	40.40863	42.856	22.11	48.40862
38	110.054	116.358	-5.7281	50.602	35.111	30.613414	13.066	8.042	38.45094	42.371	22.664	46.51059
39	107.841	108.451	-0.56565	49.64	35.183	29.123691	12.822	8.032	37.35767	41.566	22.582	45.67194
40	118.185	113.142	4.267039	53.58	35.505	33.734602	13.856	8.11	41.4694	44.817	22.755	49.22686
41	109.017	116.007	-6.41184	50.772	37.108	26.912471	13.1	8.527	34.9084	42.541	23.552	44.63694
42	111.357	112.726	-1.22938	51.069	37.043	27.464803	13.197	8.525	35.40199	42.744	23.6	44.78757
43	112.028	113.582	-1.38715	51.283	37.274	27.317045	13.245	8.61	34.99434	42.887	23.836	44.42139
44	109.266	111.869	-2.38226	50.268	37.304	25.789767	12.977	8.611	33.64414	42.027	23.891	43.15321
45	110.727	115.051	-3.9051	51.107	38.477	24.712857	13.198	9.082	31.18654	42.734	24.068	43.67951

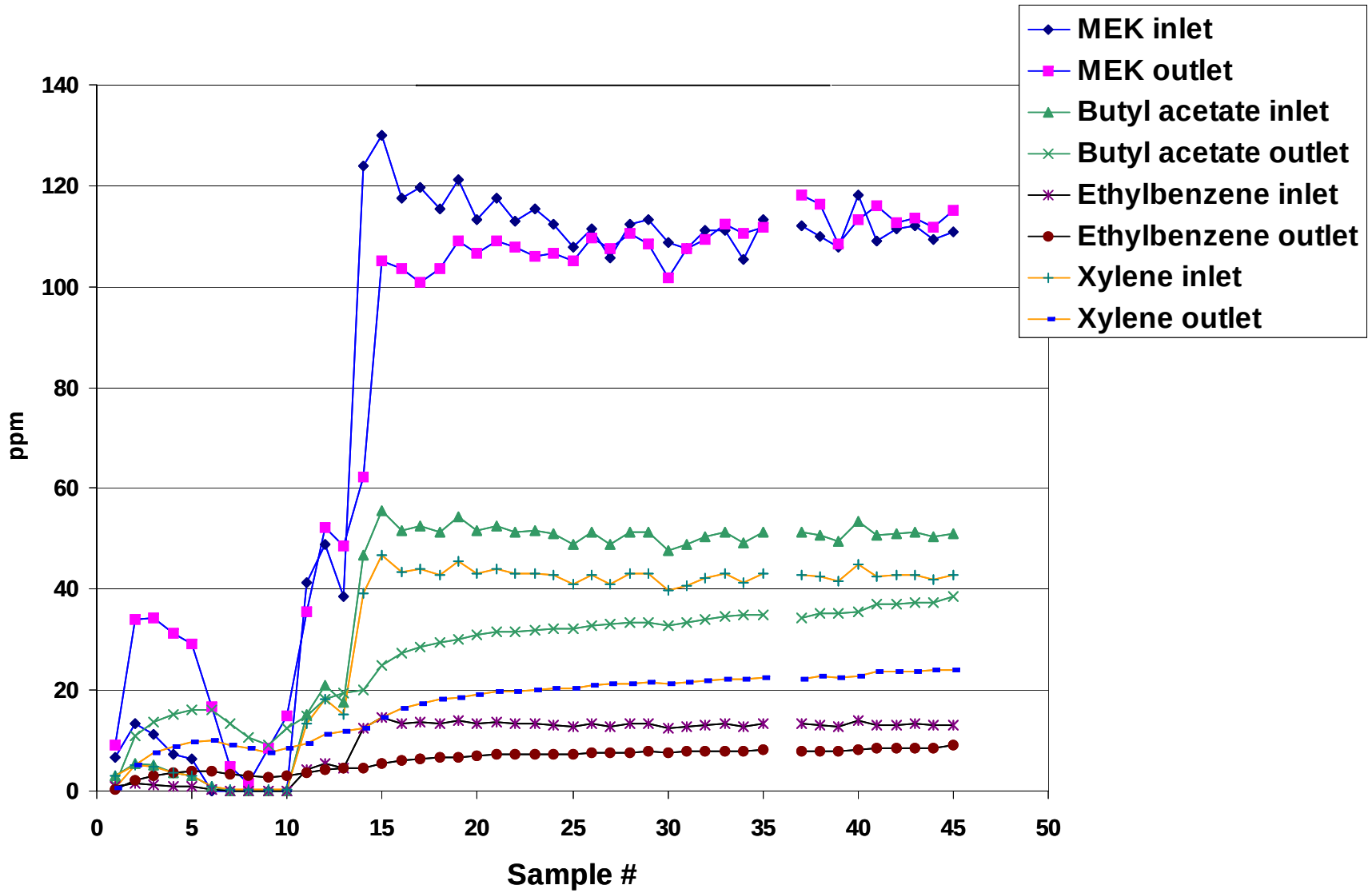

Figure B-13. Two Parallel AMT Modules, Test 15, 2.0 ft^3/min Air, 1.0 L/min Oil, 220 ppm VOCs

Table B-14. Two Parallel AMT Modules, Test 16, 8.0 ft^3/min Air, 1.0 L/min Oil, 200 ppm VOCs

Test 16												
Run date 6/08/00												
Initial parameters:		sample flow rate ~50 cc's;mag(1) 1.75"H20;mag(2) >1.0"H20;air velocity ~8.0cfm										
		oil pressure 11.5psi (on module);syringe flow 8.0ml/hr;**oil sampling time 120 min.**										
run#	MEK Front Detector	MEK Rear Detector	% Difference	n-Butyl Acetate Front Detector	n-Butyl Acetate Rear Detector	% Difference	Ethyl Benzene Front Detector	Ethyl Benzene Rear Detector	% Difference	o-Xylene Front Detector	o-Xylene Rear Detector	% Difference
1	4.372	10.217	-133.692	1.726	9.928	-475.20278	0.528	2.653	-402.462	2.07	7.494	-262.029
2	5.958	12.334	-107.016	2.579	10.821	-319.58123	0.734	2.869	-290.872	2.744	8.208	-199.125
3	104.996	98.911	5.795459	44.006	30.255	31.248012	11.614	7.203	37.98002	37.457	20.648	44.87546
4	106.824	99.866	6.513518	45.573	35.676	21.716806	11.917	8.605	27.79223	38.428	25.219	34.37337
5	102.041	101.48	0.549779	45.093	37.504	16.829663	11.758	9.114	22.48682	38.144	27.003	29.20774
6	104.018	101.963	1.97562	45.89	38.17	16.822837	11.933	9.321	21.88888	38.668	27.871	27.92231
7	104.187	97.588	6.333804	45.683	38.365	16.019088	11.879	9.439	20.54045	38.365	28.465	25.80477
8	99.362	101.927	-2.58147	44.865	39.336	12.323638	11.636	9.63	17.2396	37.807	29.057	23.14386
9	104.011	102.392	1.556566	46.309	39.604	14.478827	12.017	9.705	19.23941	38.902	29.294	24.69796
10	105.478	101.654	3.625401	47.044	40.09	14.781906	12.198	9.823	19.4704	39.539	29.691	24.90705
11	100.835	103.876	-3.01582	45.543	41.013	9.9466438	11.799	10.053	14.79786	38.31	30.37	20.72566
12	104.359	104.31	0.046953	46.963	41.309	12.039265	12.174	10.117	16.89667	39.52	30.574	22.63664
13	103.067	101.524	1.497084	46.281	40.838	11.760766	12	10.02	16.5	38.903	30.36	21.95975
14	100.093	102.068	-1.97316	45.314	41.307	8.8427418	11.723	10.145	13.46072	38.045	30.803	19.03535
15	101.703	103.98	-2.23887	46.066	41.339	10.261364	11.932	10.137	15.04358	38.765	30.824	20.48497
16	103.974	103.048	0.890607	46.511	41.046	11.749909	12.043	10.112	16.03421	38.974	30.808	20.95243
17	98.924	101.736	-2.84259	44.83	41.295	7.8853446	11.602	10.184	12.22203	37.675	31.076	17.51559
18	7.051	21.364	-202.992	7.433	25.178	-238.73268	1.842	6.744	-266.124	6.596	21.383	-224.181
19	8.567	17.154	-100.233	5.703	18.361	-221.95336	1.49	4.986	-234.631	5.245	16.016	-205.357
20	96.129	81.157	15.5749	39.473	25.829	34.565399	10.348	6.415	38.00734	33.104	19.249	41.85295
21	98.473	92.166	6.404801	42.91	35.465	17.350268	11.144	8.685	22.06569	35.981	26.169	27.26995
22	98.099	100.21	-2.15191	44.061	39.362	10.66476	11.414	9.66	15.36709	37.063	29.144	21.36632
23	5.387	22.932	-325.691	7.155	25.476	-256.0587	1.759	6.666	-278.965	6.363	21.135	-232.155
24	12.629	19.566	-54.9291	6.981	18.011	-158.00029	1.824	4.818	-164.145	6.28	15.482	-146.529
25	0	10.76	#DIV/0!	2.155	15.932	-639.30394	0.531	4.37	-722.976	2.345	13.937	-494.328
26	109.227	115.757	-5.97838	50.742	38.5	24.125971	13.298	9.269	30.29779	42.884	27.663	35.49342
27	2.216	13.342	-502.076	2.244	19.724	-778.96613	0.808	5.326	-559.158	3.204	16.67	-420.287
28	94.879	83.61	11.87723	39.239	27.744	29.294834	10.301	7.092	31.15232	33.137	21.277	35.79081
29	96.357	97.082	-0.75241	42.824	37.272	12.964693	11.104	9.082	18.20965	36.067	27.213	24.54876
30	101.499	99.005	2.457167	45.101	39.286	12.893284	11.678	9.658	17.29748	37.871	29.137	23.0625
31	102.192	97.82	4.278221	45.622	39.871	12.60576	11.804	9.853	16.5283	38.298	29.973	21.73743
32	99.815	100.198	-0.38371	44.847	40.987	8.6070417	11.595	10.14	12.54851	37.596	30.948	17.68273
33	101.665	101.546	0.117051	45.979	41.262	10.259031	11.881	10.208	14.08131	38.619	31.248	19.08646
34	105.134	103.295	1.749196	47.261	41.584	12.012018	12.218	10.296	15.73089	39.639	31.624	20.21999
35	103.982	101.145	2.728357	46.413	42.068	9.3616013	11.99	10.431	13.0025	38.852	32.138	17.28096
36	98.23	102.659	-4.50881	44.96	41.87	6.8727758	11.618	10.426	10.25994	37.782	31.127	17.61421
37	103.712	102.89	0.792579	46.627	41.674	10.622601	12.05	10.375	13.90041	39.078	32.001	18.10993
38	103.382	100.801	2.496566	46.56	41.532	10.798969	12.034	10.365	13.86904	39.071	32.014	18.06199
39	99.235	101.77	-2.55454	45.08	42.219	6.3464951	11.654	10.517	9.756307	37.847	32.487	14.16228
40	100.449	104.481	-4.01398	45.973	42.472	7.6153394	11.864	10.576	10.85637	38.64	32.648	15.50725

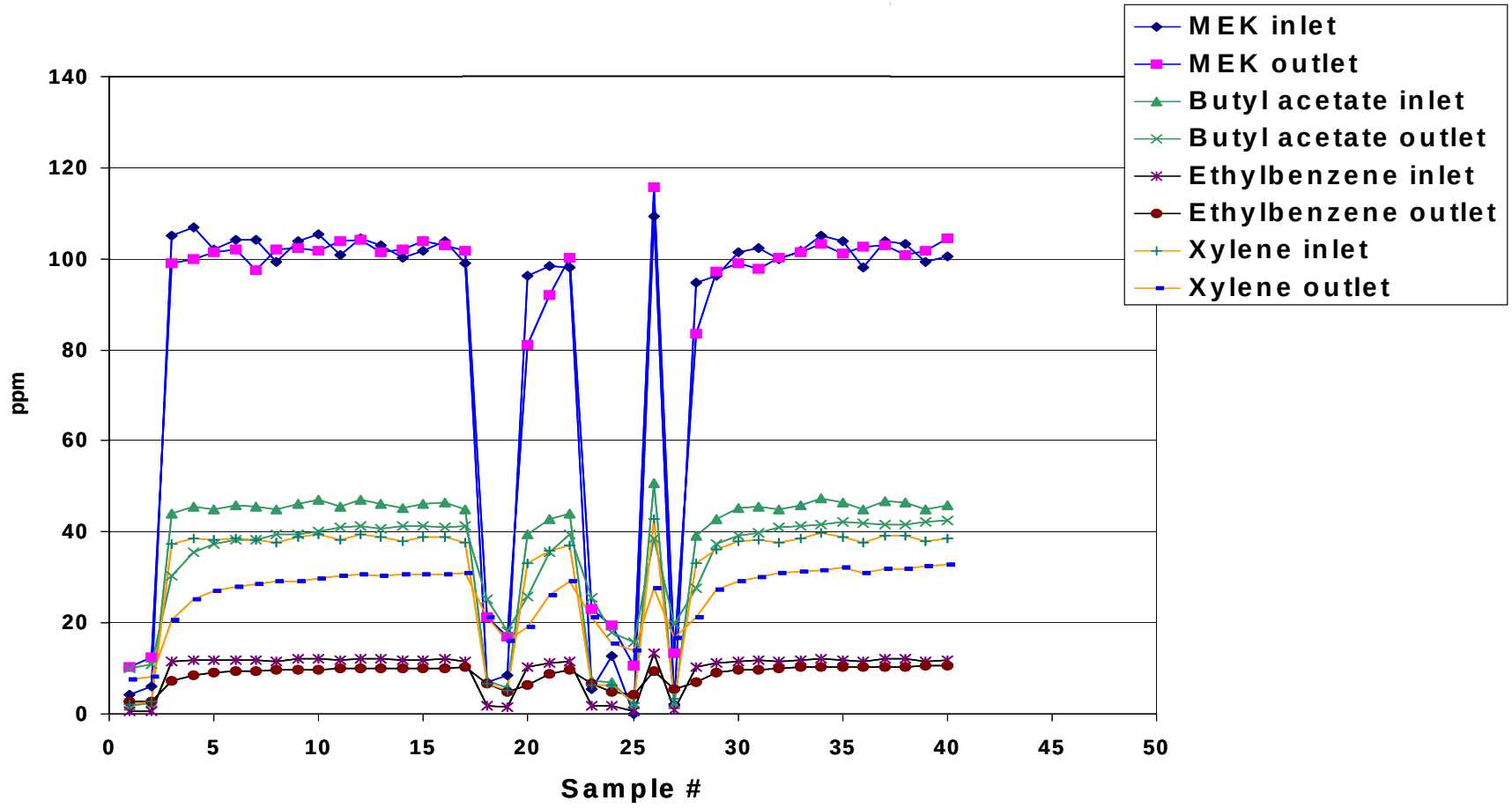

Figure B-14. Two Parallel AMT Modules, Test 16, 8.0 ft^3/min Air, 1.0 L/min Oil, 200 ppm VOCs

Table B-15. Two Parallel AMT Modules, Test 18, 4.0 ft^3/min Air, 1.0 L/min Oil, 200 ppm VOCs

Test 18												
Run date 6/21/00												
Initial parameters:		sample flow rate ~55 cc's;air velocity ~1.38 (4cfm)										
		oil pressure 11.0psi (on module);syringe flow 4.0ml/hr;used "new" silicon oil for this run.										
run#	MEK Front Detector	MEK Rear Detector	% Difference	n-Butyl Acetate Front Detector	n-Butyl Acetate Rear Detector	% Difference	Ethyl Benzene Front Detector	Ethyl Benzene Rear Detector	% Difference	o-Xylene Front Detector	o-Xylene Rear Detector	% Difference
1	88.002	74.253	15.62351	38.384	18.968	50.583576	9.834	4.455	54.69799	31.919	12.864	59.69799
2	98.329	78.066	20.60735	41.959	19.522	53.473629	10.748	4.561	57.5642	34.748	13.265	61.82514
3	100.382	82.108	18.20446	44.044	20.361	53.771229	11.273	4.753	57.83731	36.618	13.864	62.13884
4	104.511	90.61	13.30099	45.41	27.819	38.738163	11.636	5.045	56.64318	37.795	14.488	61.66689
5	106.649	89.638	15.95045	47.186	25.384	46.204383	12.07	5.244	56.55344	39.268	15.223	61.23307
6	93.856	83.16	11.39618	41.742	22.67	45.690192	10.67	5.246	50.83411	34.727	15.434	55.5562
7	95.895	81.769	14.7307	42.483	22.552	46.915237	10.872	5.265	51.57285	35.322	15.583	55.88302
8	109.373	85.859	21.49891	47.383	23.043	51.368634	12.146	5.514	54.60234	39.32	15.846	59.6999
9	95.189	89.645	5.824202	43.777	24.283	44.530233	11.148	5.756	48.36742	36.518	16.6	54.54297
10	95.905	86.355	9.957771	43.286	24.361	43.720834	11.056	5.78	47.72069	36.053	16.711	53.64879
11	97.77	89.541	8.416692	44.145	24.738	43.961944	11.278	5.861	48.03157	36.775	16.953	53.90075
12	102.199	90.91	11.0461	45.585	25.125	44.883185	11.679	5.938	49.15661	37.989	17.167	54.8106
13	98.691	85.092	13.77937	43.932	24.762	43.635619	11.237	5.854	47.90424	36.552	17.085	53.25837
14	94.481	86.745	8.18789	42.561	25.279	40.605249	10.874	6.005	44.77653	35.454	17.391	50.94771
15	96.441	87.659	9.106086	43.501	25.728	40.856532	11.128	6.076	45.39899	36.279	17.62	51.43196
16	95.747	88.644	7.418509	43.024	25.962	39.656936	11.002	6.166	43.95564	35.864	17.847	50.23701
17	96.454	89.096	7.628507	43.224	26.093	39.633074	11.039	6.209	43.75396	35.987	17.884	50.30428
18	99.554	90.258	9.337646	44.212	26.628	39.772008	11.301	6.343	43.87222	36.746	18.086	50.78104
19	103.593	90.436	12.70067	45.5	27.284	40.035165	11.638	6.501	44.13989	37.815	18.397	51.34999
20	99.296	92.753	6.589389	44.934	28.513	36.54471	11.467	6.755	41.09183	37.416	18.997	49.2276
21	121.198	108.551	10.43499	54.427	30.621	43.739321	13.906	7.224	48.0512	45.317	19.986	55.89735
22	100.809	106.562	-5.70683	48.806	31.229	36.014015	12.414	7.398	40.40599	40.971	20.654	49.58873
23	99.665	94.027	5.656951	45.047	30.085	33.214199	11.516	7.155	37.86905	37.52	20.078	46.48721
24	103.82	91.322	12.03814	45.887	29.442	35.838037	11.736	7.073	39.73245	38.08	19.913	47.70746
25	95.252	90.674	4.806198	43.298	29.788	31.202365	11.042	7.122	35.50082	36.048	20.062	44.34643
26	92.419	89.217	3.464656	42.174	29.426	30.227154	10.742	7.051	34.36045	35.119	20.056	42.89131
27	96.198	91.047	5.354581	43.616	29.987	31.247707	11.129	7.189	35.403	36.265	20.41	43.71984
28	99.273	93.876	5.436524	44.692	30.2	32.426385	11.413	7.201	36.90528	37.176	20.539	44.75199
29	96.808	90.61	6.402363	43.864	30.157	31.24886	11.192	7.213	35.55218	36.515	20.538	43.75462
30	93.933	90.179	3.996466	42.589	30.32	28.807908	10.86	7.296	32.81768	35.441	20.732	41.50278
31	96.878	92.791	4.218708	43.709	30.782	29.575145	11.149	7.352	34.05687	36.376	20.975	42.33835

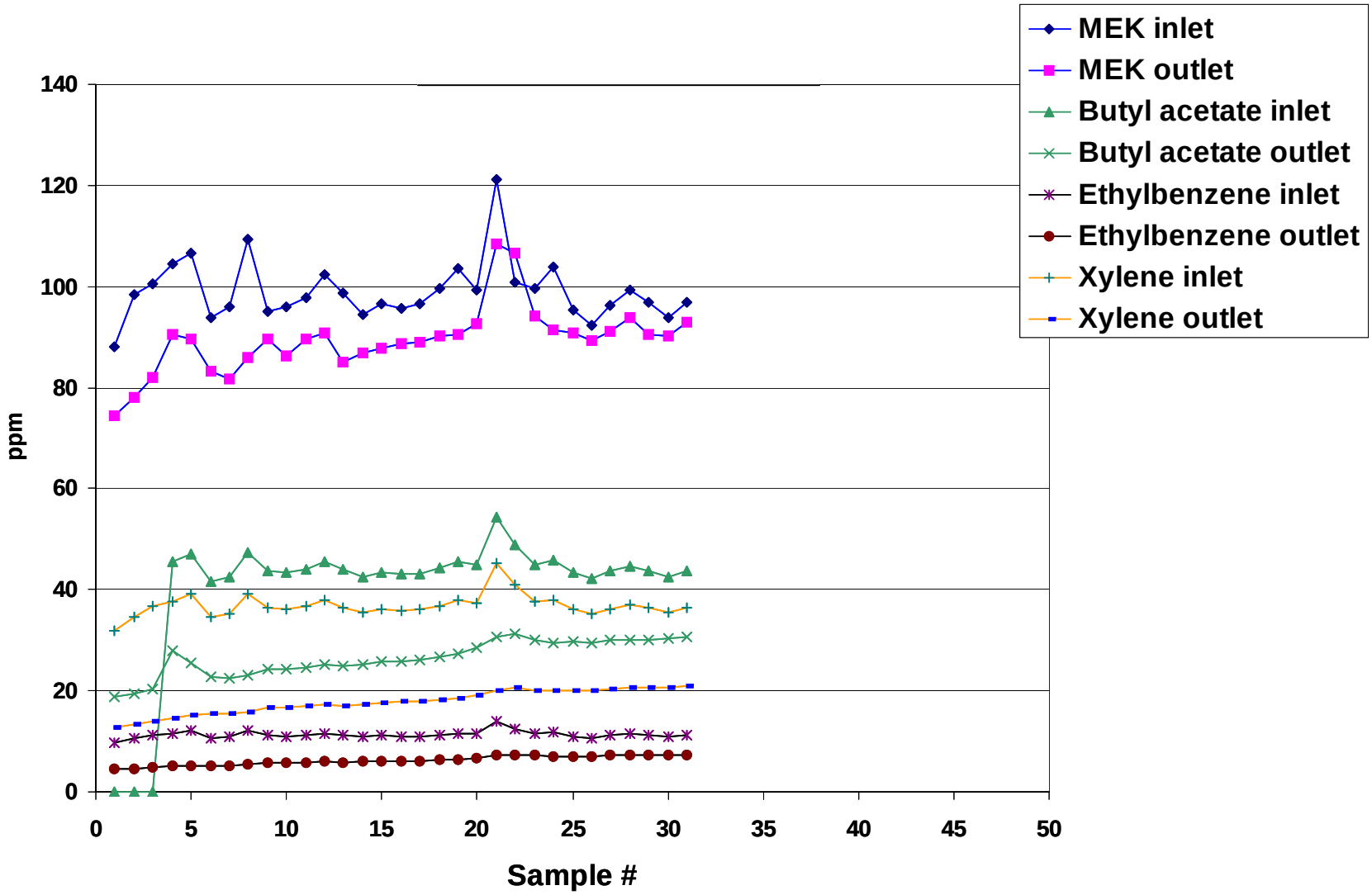

Figure B-15. Two Parallel AMT Modules, Test 18, 4.0 ft^3/min Air, 1.0 L/min Oil, 200 ppm VOCs

Table B-16. Two Parallel AMT Modules, Test 19, 8.0 ft^3/min Air, 1.0 L/min Oil, 200 ppm VOCs

Test 19												
Run date 6/22/00												
Initial parameters:		sample flow rate ~55 cc's;air velocity ~4.75 (8cfm);syringe flow rate 8.0ml/hr										
		oil pressure 11.3psi (on module);Mag(1) ~1.85"H2O;Mag(2)>1.0"H2O										
run#	MEK Front Detector	MEK Rear Detector	% Difference	n-Butyl Acetate Front Detector	n-Butyl Acetate Rear Detector	% Difference	Ethyl Benzene Front Detector	Ethyl Benzene Rear Detector	% Difference	o-Xylene Front Detector	o-Xylene Rear Detector	% Difference
1	87.752	6.59	92.4902	31.154	7.001	77.527765	8.579	1.989	76.81548	27.151	5.785	78.69323
2	98.834	89.061	9.888298	40.464	24.203	40.186338	10.638	5.768	45.77928	34.408	16.5	52.04604
3	94.184	92.763	1.508749	40.316	30.443	24.489037	10.516	7.336	30.23963	34.138	21.497	37.02912
4	101.746	102.712	-0.94942	44.876	33.737	24.821731	11.678	8.146	30.2449	38.068	24.035	36.86298
5	102.679	98.565	4.006662	44.031	36.08	18.057732	11.453	8.75	23.6008	37.066	25.96	29.96277
6	98.251	100.299	-2.08446	43.699	35.594	18.547335	11.362	8.622	24.11547	36.917	25.749	30.25165
7	100.983	97.21	3.736272	45.28	35.73	21.090989	11.758	8.676	26.21194	38.308	26.28	31.39814
8	95.234	99.253	-4.22013	42.497	36.26	14.67633	11.01	8.804	20.03633	35.869	26.615	25.79944
9	99.428	101.955	-2.54154	44.533	37.29	16.264343	11.54	9.427	18.31023	37.649	28.113	25.32869
10	105.346	98.155	6.826078	46.343	37.472	19.14205	12.032	9.491	21.11868	39.005	28.291	27.46827
11	91.263	97.288	-6.6018	41.543	37.211	10.42775	10.741	9.445	12.06592	35.139	28.239	19.6363
12	101.782	103.667	-1.852	45.488	38.602	15.138058	11.786	9.742	17.34261	38.402	29.115	24.18364
13	105.578	98.95	6.277823	46.032	38.622	16.097497	11.934	9.748	18.31741	38.619	29.365	23.9623
14	98.515	106.406	-8.00995	45.073	40.197	10.818006	11.674	10.124	13.27737	38.195	30.192	20.953
15	101.406	103.804	-2.36475	45.902	39.628	13.66825	11.885	10.014	15.74253	38.814	30.052	22.57433
16	97.151	101.602	-4.58153	43.782	39.84	9.0037002	11.234	10.087	10.21008	36.951	30.225	18.20248
17	100.032	103.511	-3.47789	45.353	40.499	10.70271	11.755	10.269	12.64143	38.385	30.568	20.36473
18	103.783	98.832	4.770531	46.622	40.179	13.819656	12.087	10.2	15.61181	39.422	30.52	22.5813
19	96.901	102.216	-5.48498	43.784	40.842	6.7193495	11.326	10.372	8.423097	36.968	30.918	16.36551
20	102.452	105.128	-2.61195	45.858	41.313	9.9110297	11.877	10.466	11.8801	38.689	31.231	19.2768
21	103.431	99.416	3.881815	46.118	40.477	12.231667	11.956	10.13	15.27267	38.819	30.296	21.95574
22	95.778	102.6	-7.12272	43.899	41.546	5.360031	11.346	10.498	7.474	37.128	31.203	15.95831
23	102.836	105.654	-2.74029	46.293	41.998	9.2778606	11.984	10.61	11.46529	39.066	31.583	19.15476
24	104.194	100.933	3.129739	45.502	42.163	7.338139	11.777	10.701	9.136452	38.208	31.96	16.3526
25	102.005	107.975	-5.85265	46.444	43.198	6.9890621	12.035	10.97	8.84919	39.317	32.688	16.86039
26	104.829	106.848	-1.92599	47.359	42.427	10.414071	12.268	10.8	11.96609	39.961	32.479	18.72326
27	94.909	105.07	-10.706	44.112	43.054	2.3984403	11.405	10.979	3.735204	37.366	32.862	12.05374
28	101.171	106.11	-4.88183	45.978	43.358	5.6983775	11.898	11.063	7.017986	38.83	32.914	15.23564
29	103.834	101.307	2.433692	46.772	42.906	8.265629	12.101	10.977	9.288489	39.426	32.77	16.88226

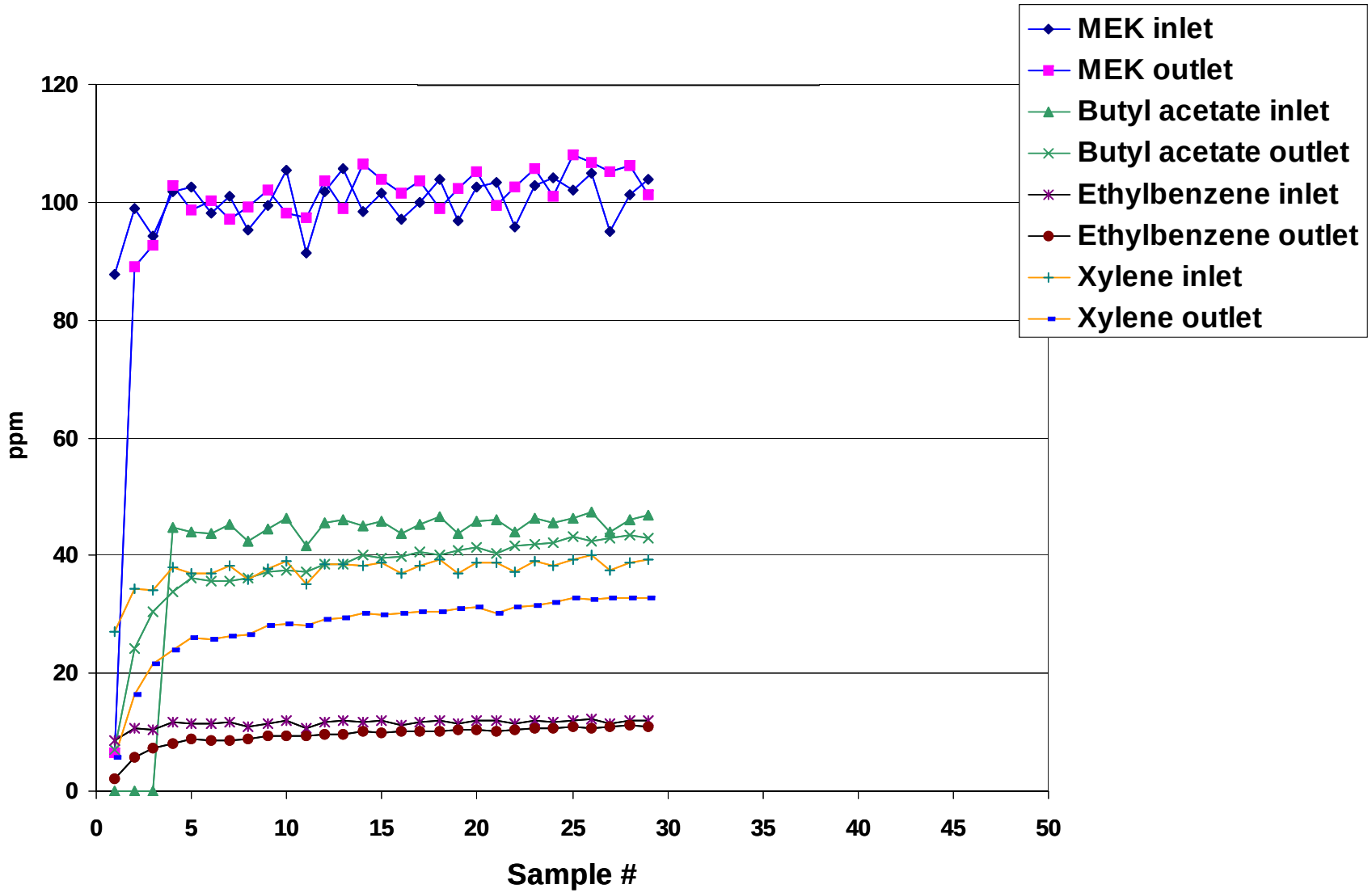

Figure B-16. Two Parallel AMT Modules, Test 19, 8.0 ft^3/min Air, 1.0 L/min Oil, 200 ppm VOCs

Table B-17. Two Parallel AMT Modules, Test 20, 16.0 ft^3/min Air, 1.0 L/min Oil, 200 ppm VOCs

Test 20												
Run date 6/22/00												
sequence used 062200c												
Initial parameters:		air velocity 16ml/hr (1657 volts);syringe flow rate 16ml/hr;										
		sample flow set at 55 cc's;Mag(1) >4.0"H2O;Mag(2) >1.0"H2O;										
		oil pressure at module 11.0psi;system oil pressure ~ 25psi										
run#	MEK Front Detector	MEK Rear Detector	% Difference	n-Butyl Acetate Front Detector	n-Butyl Acetate Rear Detector	% Difference	Ethyl Benzene Front Detector	Ethyl Benzene Rear Detector	% Difference	o-Xylene Front Detector	o-Xylene Rear Detector	% Difference
1	0	1.251	#DIV/0!	0	3.419	#DIV/0!	0.101	1.258	-1145.54	0.481	4.407	-816.216
2	94.2	81.32	13.67304	39.143	14.503	62.948675	10.293	3.84	62.69309	32.703	11.25	65.59949
3	100.263	89.618	10.61708	42.406	30.555	27.946517	11.213	7.81	30.3487	36.398	23.817	34.56509
4	91.144	91.918	-0.84921	41.958	31.763	24.298108	10.98	8.116	26.08379	36.301	25.025	31.06251
5	96.268	90.056	6.452819	41.758	34.67	16.973993	10.798	8.911	17.47546	35.262	27.848	21.02547
6	96.069	94.893	1.22412	40.141	35.055	12.670337	10.33	8.992	12.95257	32.369	28.529	11.8632
7	94.809	93.514	1.365904	47.131	35.078	25.573402	12.374	8.96	27.59011	42.379	27.875	34.2245
8	81.154	93.845	-15.6382	40.825	37.375	8.4507042	10.572	9.596	9.231933	35.465	30.663	13.54011
9	100.559	94.362	6.162551	45.199	36.741	18.712803	11.553	9.404	18.60123	37.544	29.446	21.56936
10	97.699	99.159	-1.49439	43.812	39.689	9.4106637	11.39	10.139	10.98332	36.518	32.113	12.06254
11	92.448	94.316	-2.0206	38.252	38.589	-0.8809997	9.812	9.889	-0.78475	31.751	31.437	0.988945
12	95.587	99.716	-4.31963	40.184	39.453	1.819132	10.321	10.02	2.916384	33.734	30.904	8.389162
13	94.787	99.908	-5.40264	45.001	38.815	13.746361	11.755	9.912	15.67843	38.955	30.993	20.43897
14	94.682	103.119	-8.91088	41.141	39.233	4.6377093	10.576	10.016	5.295008	34.067	30.938	9.184842
15	92.419	99.139	-7.27123	43.623	39.988	8.3327602	11.274	10.172	9.774703	37.746	31.606	16.26662
16	100.865	97.135	3.698012	44.62	41.154	7.7678171	11.565	10.576	8.551665	38.54	33.61	12.7919
17	10.036	101.095	-907.324	18.313	40.565	-121.50931	4.627	10.363	-123.968	17.997	32.654	-81.4414
18	98.049	121.585	-24.0043	43.085	25.919	39.842172	11.195	6.657	40.53595	36.368	21.015	42.21568
19	88.711	99.752	-12.446	41.696	39.287	5.7775326	10.794	10.059	6.809339	35.962	31.734	11.75685
20	97.192	94.77	2.491975	43.112	40.141	6.8913528	11.261	10.294	8.587159	37.576	32.267	14.1287
21	97.516	98.534	-1.04393	45.042	39.707	11.844501	11.743	10.198	13.15677	37.722	32.228	14.56445
22	96.367	101.079	-4.88964	43.825	41.436	5.4512265	11.329	10.595	6.478948	37.147	33.287	10.39115
23	91.51	96.989	-5.98732	43.62	41.484	4.8968363	11.354	10.651	6.191651	37.398	33.537	10.32408
24	98.372	94.135	4.30712	43.934	41.01	6.6554377	11.457	10.533	8.064938	37.653	33.054	12.21417
25	97.53	100.278	-2.81759	43.962	41.724	5.0907602	11.375	10.726	5.705495	37.483	33.679	10.1486
26	94.823	98.003	-3.35362	41.885	40.956	2.2179778	10.786	10.543	2.25292	35.583	33.41	6.106849
27	88.641	98.97	-11.6526	42.744	41.12	3.7993637	11.111	10.572	4.851049	36.678	33.233	9.392551
28	97.423	94.395	3.108096	42.332	41.217	2.6339412	10.943	10.626	2.896829	35.988	33.395	7.20518
29	97.894	99.854	-2.00217	44.702	41.551	7.0489016	11.617	10.703	7.86778	38.239	33.6	12.13159
30	96.574	100.745	-4.31897	43.35	42.547	1.8523645	11.155	10.968	1.676378	36.603	34.233	6.474879
31	90.151	97.876	-8.56896	42.7	42.216	1.1334895	11.069	10.893	1.590026	36.659	34.253	6.56319
32	99.42	97.606	1.824583	43.292	42.314	2.2590779	11.199	10.93	2.402	36.307	34.202	5.79778

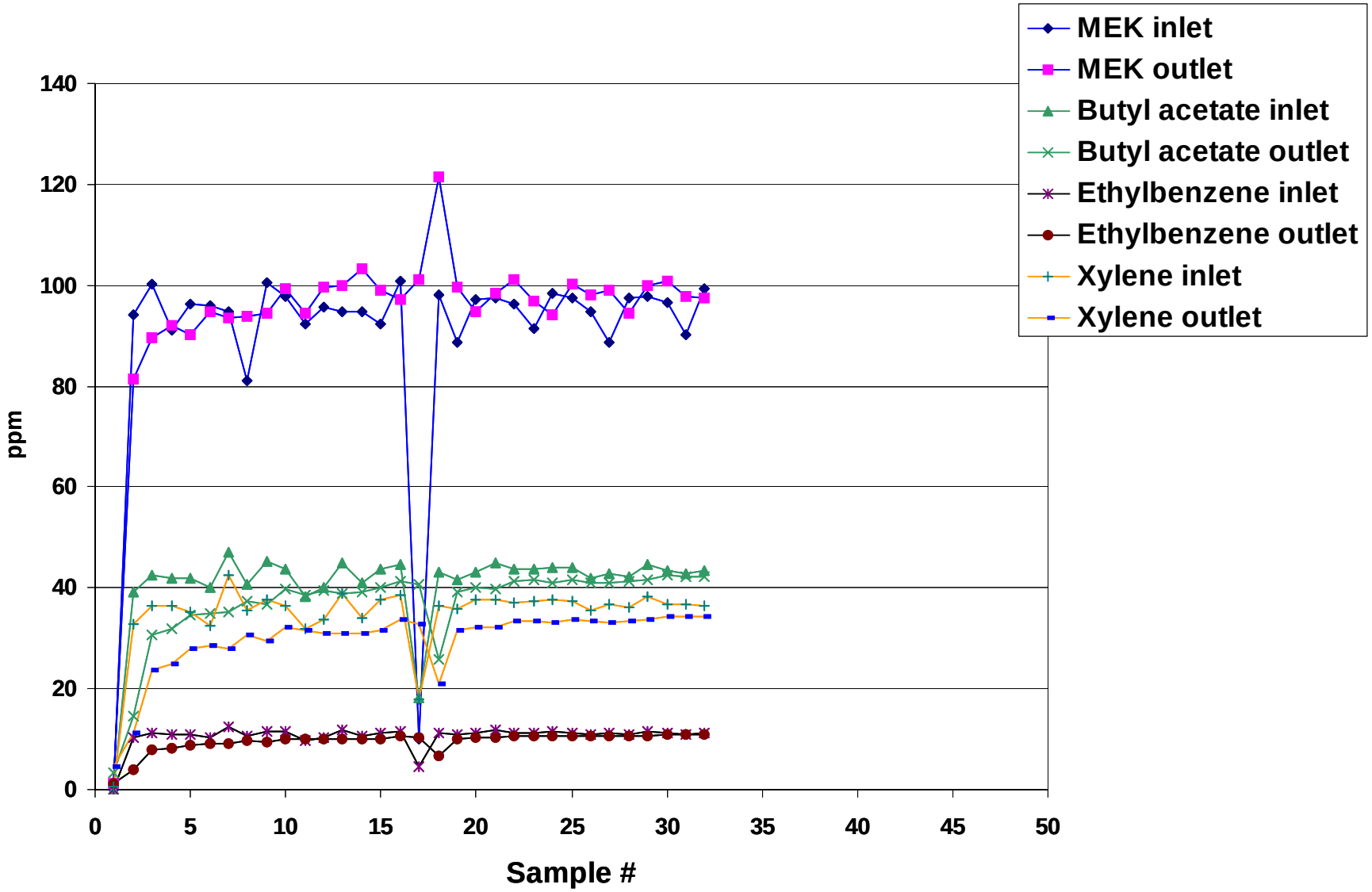

Figure B-17. Two Parallel AMT Modules, Test 20, 16.0 ft^3/min Air, 1.0 L/min Oil, 200 ppm VOCs

Table B-18. Two Parallel AMT Modules, Test 21, 4.0 ft^3/min Air, Maximum Oil Flow, 450 ppm VOCs

Test 21												
Run date 6/23/00												
Initial parameters:		sample flow rate 54cc's;syringe set 4.0 ml/hr;air velocity 4.0cfm (~680 shortridge);										
		oil flow set to max out on rotameter (147-150);Mag(1) 0.4"H2O;Mag(2) >1.0"H2O										
run#	MEK Front Detector	MEK Rear Detector	% Difference	n-Butyl Acetate Front Detector	n-Butyl Acetate Rear Detector	% Difference	Ethyl Benzene Front Detector	Ethyl Benzene Rear Detector	% Difference	o-Xylene Front Detector	o-Xylene Rear Detector	% Difference
1	0	13.367	#DIV/0!	0	21.175	#DIV/0!	0.333	6.36	-1809.91	1.528	19.716	-1190.31
2	64.951	15.655	75.89721	11.895	22.193	-86.574191	3.618	6.654	-83.9138	9.712	19.985	-105.776
3	192.374	134.858	29.89801	79.345	34.685	56.28584	20.934	8.844	57.75294	67.651	26.281	61.15209
4	177.908	141.566	20.42741	76.279	41.891	45.081871	19.989	10.427	47.83631	64.908	30.654	52.77316
5	159.284	142.272	10.68029	70.565	44.332	37.175654	18.434	11.141	39.56276	60.145	33.167	44.85493
6	147.608	141.718	3.990299	66.181	46.17	30.236775	17.267	11.632	32.63451	56.442	34.974	38.03551
7	187.124	158.048	15.53836	80.764	48.066	40.48586	21.135	12.12	42.65436	68.647	36.466	46.87896
8	209.879	173.806	17.18752	90.432	49.976	44.736377	23.642	12.519	47.04763	76.835	37.552	51.12644
9	157.312	156.131	0.750737	73.476	51.195	30.324187	19.149	12.823	33.03567	62.953	38.763	38.42549
10	154.252	160.913	-4.31826	70.418	52.651	25.230765	18.325	13.544	26.09004	60.038	40.342	32.80589
11	147.451	158.278	-7.34278	68.075	52.786	22.459053	17.727	13.511	23.78293	58.125	40.832	29.7514
12	199.244	173.059	13.14218	87.198	53.199	38.990573	22.792	13.6	40.32994	74.163	40.954	44.77839
13	193.64	179.061	7.52892	85.101	55.542	34.734022	22.199	14.115	36.41605	72.226	42.251	41.50168
14	204.175	177.21	13.20681	88.932	56.089	36.930464	23.224	14.227	38.7401	75.477	42.707	43.4172
15	212.275	180.12	15.1478	91.825	57.228	37.677103	23.96	14.492	39.51586	77.672	43.388	44.13946
16	185.903	191.249	-2.87569	84.123	59.379	29.414072	21.907	14.942	31.79349	71.636	44.495	37.88738
17	208.892	202.261	3.174368	93.692	60.509	35.417111	24.436	15.197	37.80897	79.82	45.195	43.37885
18	202.821	202.734	0.042895	91.208	61.411	32.669283	23.79	15.391	35.30475	77.665	45.757	41.08414
19	165.335	179.37	-8.48883	75.77	60.947	19.563152	19.706	15.405	21.82584	64.54	46.197	28.42113
20	161.36	164.754	-2.10337	72.637	59.238	18.446522	18.905	15.114	20.0529	61.758	45.66	26.06626
21	158.441	165.971	-4.75256	71.346	59.358	16.802624	18.571	15.107	18.65274	60.615	45.696	24.61272
22	183.288	190.975	-4.19395	81.923	61.373	25.084531	21.351	15.666	26.62639	69.698	46.06	33.91489
23	169.199	182.179	-7.67144	77.232	62.189	19.477678	20.102	15.788	21.46055	65.799	46.553	29.24968
24	169.133	177.753	-5.09658	75.214	61.979	17.596458	19.595	15.808	19.32636	63.869	46.603	27.03346
25	191.006	180.675	5.408731	82.829	61.938	25.221843	21.629	15.818	26.86671	70.218	46.627	33.5968
26	177.96	180.756	-1.57114	79.051	62.759	20.60948	20.584	15.921	22.65352	67.088	47.466	29.24815
27	161.095	185.522	-15.1631	74.957	63.982	14.641728	19.489	16.138	17.19431	63.996	48.022	24.96094
28	154.299	174.384	-13.0169	71.385	64.022	10.314492	18.556	16.285	12.23863	60.84	48.448	20.36818
29	230.611	218.196	5.383525	101.209	65.114	35.663824	26.446	16.386	38.03978	86.068	48.372	43.79793
30	216.034	199.39	7.704343	94.797	66.031	30.344842	24.742	16.589	32.95207	80.415	49.264	38.7378
31	217.209	204.263	5.960158	95.316	67.522	29.159847	24.836	16.913	31.90127	80.771	49.928	38.18573
32	152.515	185.308	-21.5015	72.493	68.527	5.470873	18.81	17.336	7.836257	61.914	50.919	17.7585

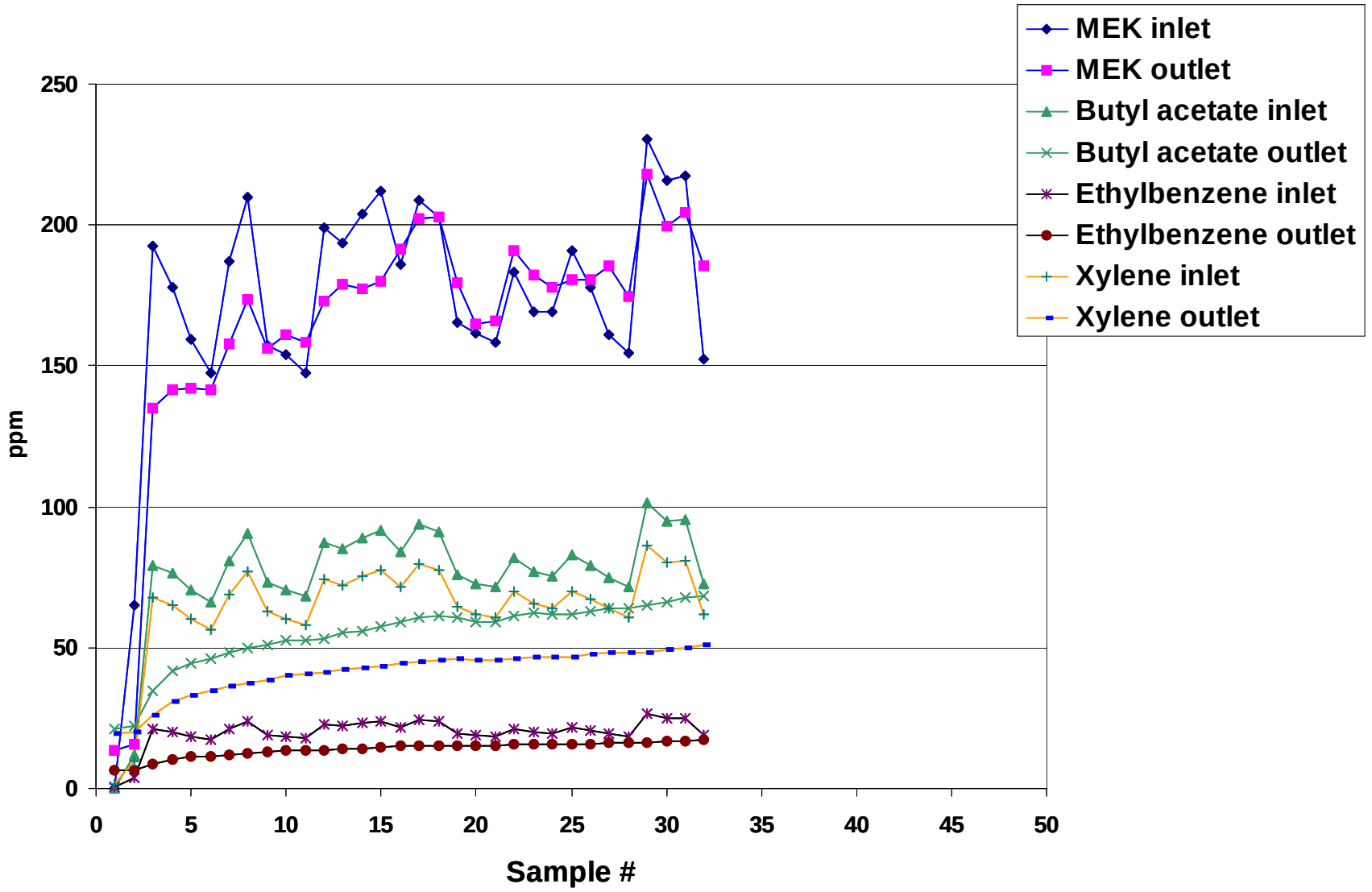

Figure B-18. Two Parallel AMT Modules, Test 21, 4.0 ft^3/min Air, Maximum Oil Flow, 450 ppm VOCs

Flat Sheet Biofilm Experiments

Table B-19. FS1: Degradation of MEK and Toluene by an M1 Biofilm: Aq/Aq Operation

Time	MEK Concentration - ppm (v)			Toluene Concentration - ppm (v)				
Days	Feed In	Feed Out	Film Out	Feed In	Feed Out	Film Out	MEK Feed	Toluene Feed
2	23.19	9.26	3.05				25	0
9	41.56	18.97	3.96				50	0
10	43.16	18.79	3.56				50	0
18	45.03	19.96	3.47				50	0
21	44.41	30.79	2.44				50	0
28	16.15	8.29	1.58	7.71	3.23	0	25	25
29	22.13	18.08	1.6	7.98	6.13	0	25	25
30	18.08	11.35	1.6	6.49	3.94	0	25	25

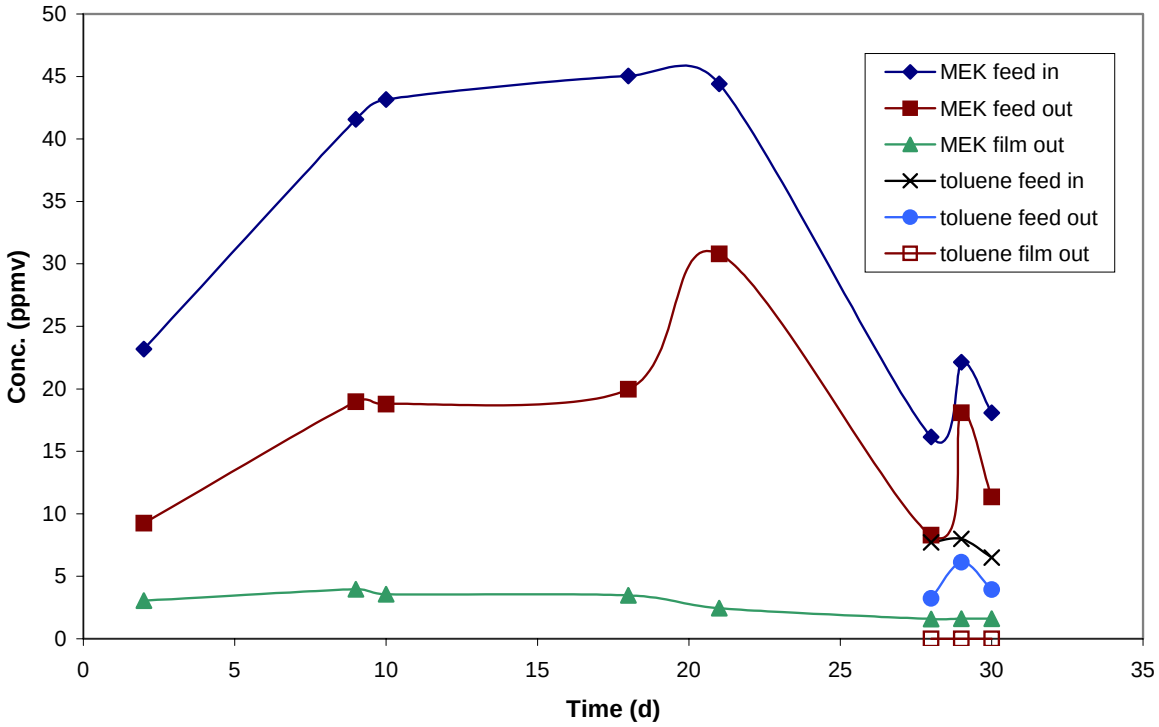

Figure B-19. FS1: Degradation of MEK and Toluene by an M1 Biofilm: Aq/Aq Operation

Table B-20. FS2: Degradation of MEK by an M1 Biofilm: Aq/Octanol Operation

Time	MEK concentration - ppm (v)		
minutes	Aq	Octanol	Concentrations represent
0	0	59.7	reservoir values
15	3	65.4	
40	3.25	61.3	
65	3.42	59.7	
90	3.61	59.1	
122	4.03	58.64	
152	4.18	54.02	
185	4.17	53.4	
245	5.36	51.7	
305	5.95	52	
365	6.36	50	
430	7.69	46.9	
495	8.69	44	

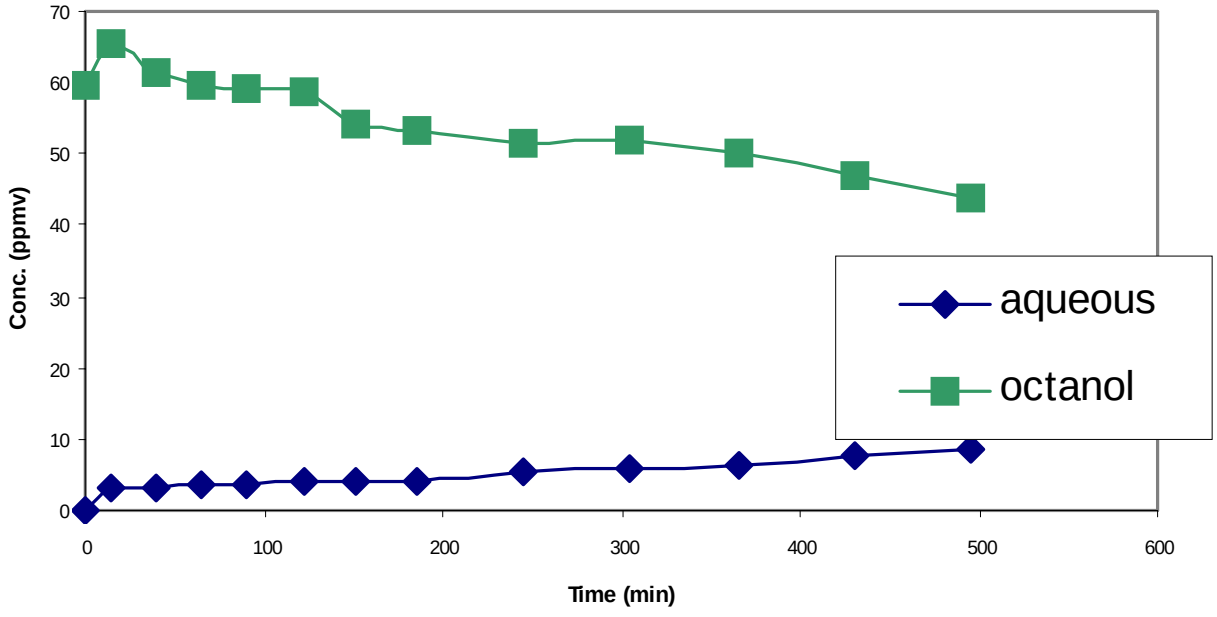

Figure B-20. FS2: Degradation of MEK by an M1 Biofilm: Aq/Octanol Operation

Table B-21. FS3: Degradation of Toluene and MEK by an M1/X1 Biofilm: Aq/Aq Operation

Time	Concentrations - ppm (v)			
hours	MEK feed	MEK film	Toluene feed	Toluene film
0	50	0	50	0
2	45.6	5.5	9.2	0.08
3	29.7	6.6	3.4	0.06
4	25.1	7.9	1.1	0.06
6	25.9	6.9	0.18	0.05
8	27.3	10.7	0.09	0.05

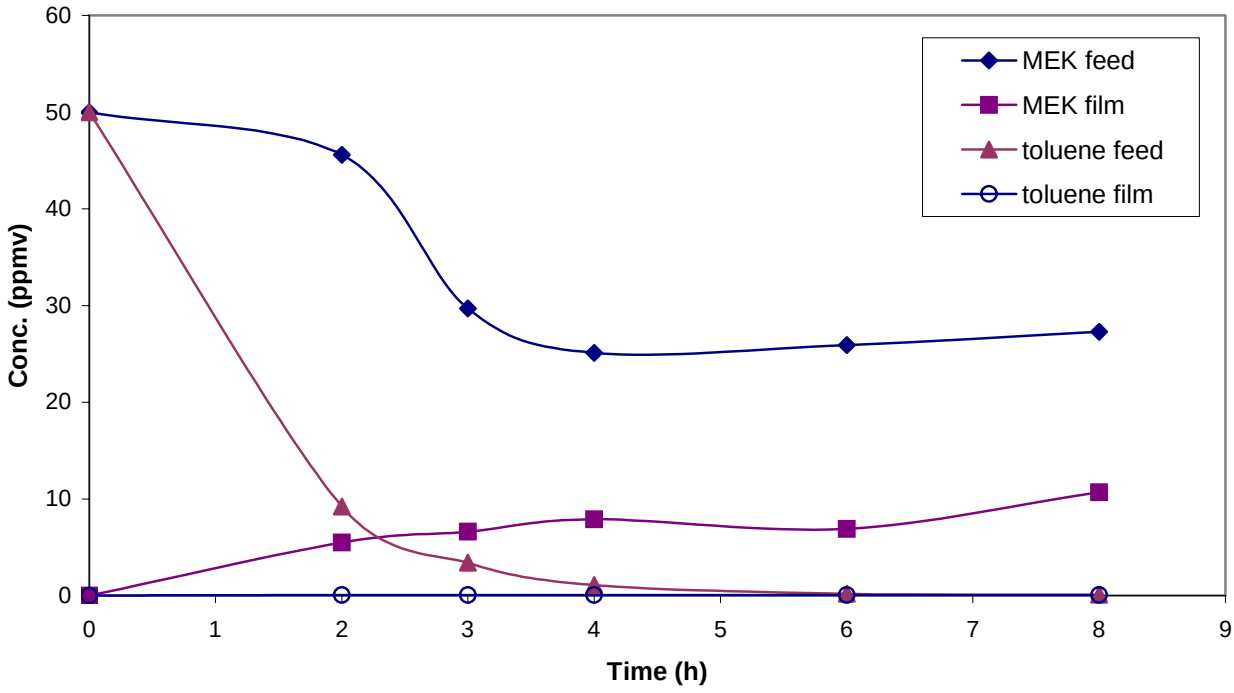

Figure B-21. FS3: Degradation of Toluene and MEK by an M1/X1 Biofilm: Aq/Aq Operation

Table B-22. FS4: Degradation of *M*-Xylene, Toluene, and MEK by an M1/X1 Biofilm: Aq/Aq Operation

Time Hours	Concentrations - ppm (v)					
	MEK Feed In	MEK Feed Out	Tol Feed In	Tol Feed Out	Xyl Feed In	Xyl Feed Out
20	27.8	24.1	26.3	20	20.6	14.9
24	27.9	25.4	35.2	15.3	27.4	11.6
47	24.9	26.1	21.2	19.4	16.7	14.9
50	28.4	23.4	17.4	13.5	17.4	13.5
67	26	22.2	19.5	15.1	15.2	11.5
71	33	34.9	20.8	14.9	16.6	11.6

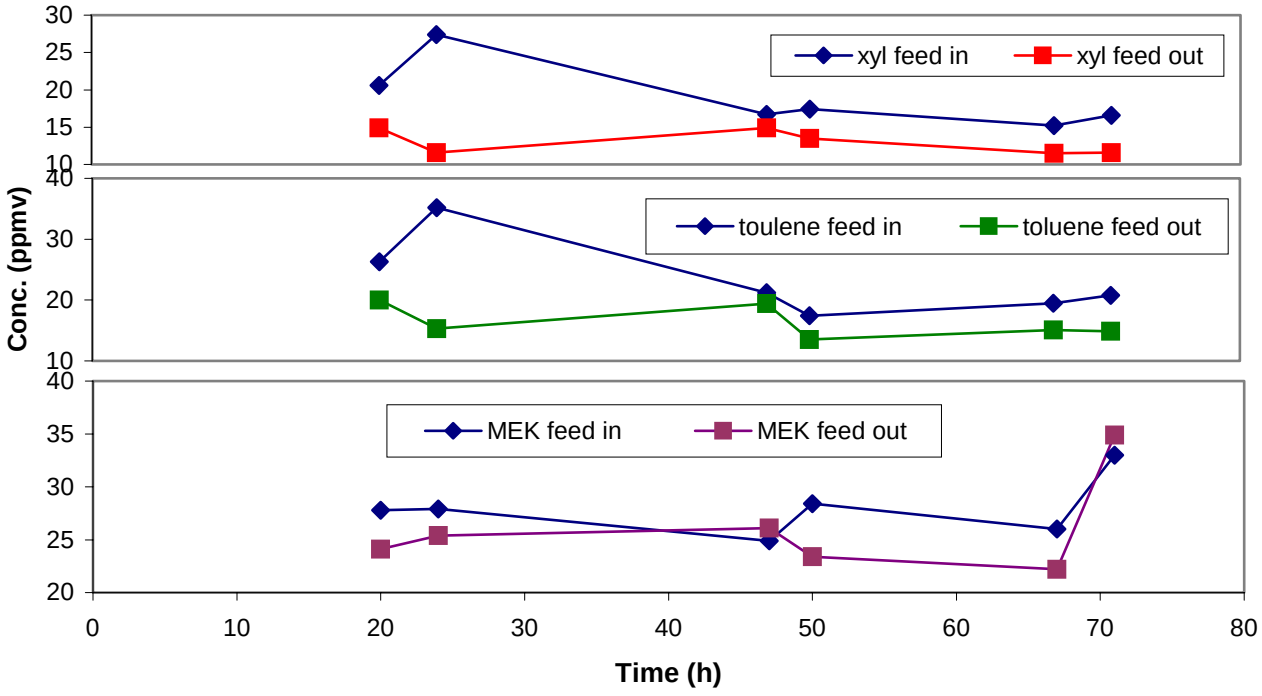

Figure B-22. FS4: Degradation of *M*-Xylene, Toluene, and MEK by an M1/X1 Biofilm: Aq/Aq Operation

Table B-23. FS5: Degradation of Toluene and MEK by an M1/X1 Biofilm: Aq/Octanol Operation

Time	Concentrations - ppm (v)			
Hours	MEK Feed	MEK Film	Toluene Feed	Toluene Film
1	21.5	3.3	5.1	0
2	24.4	3.4	2	0
3	27.4	2.9	0	0
4	24.9	3	0	0
5	25.5	3.2	0	0
6	24.4	3.2	0	0

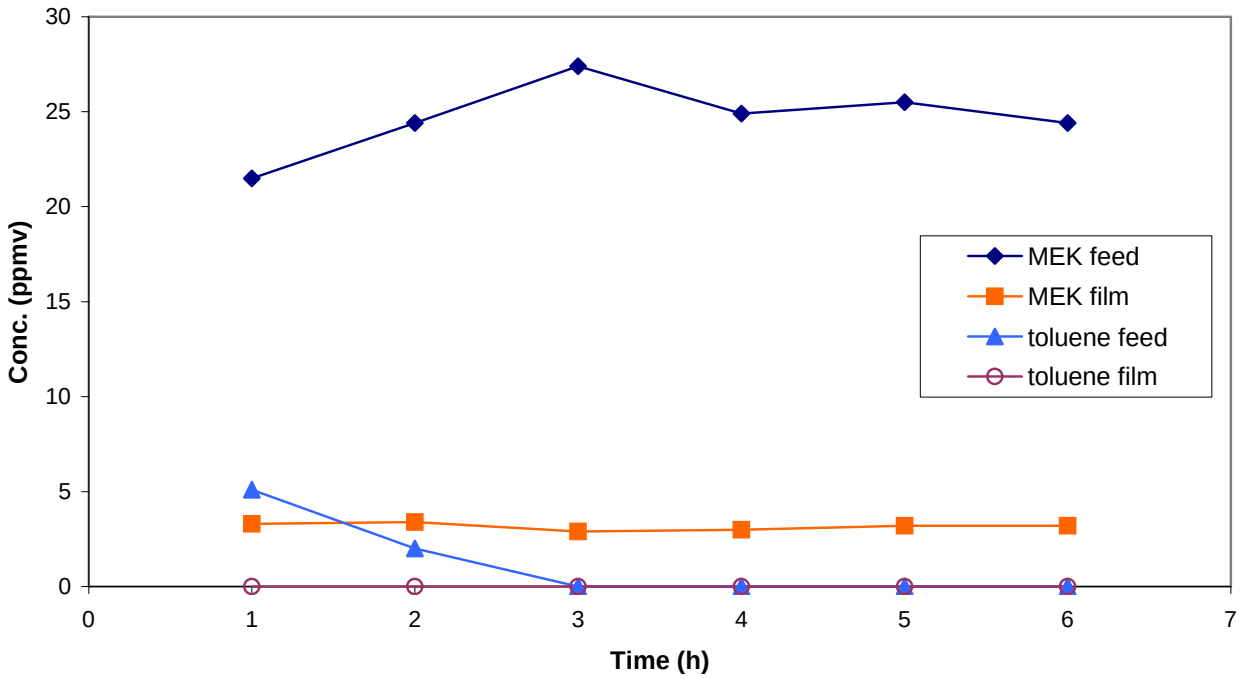

Figure B-23. FS5: Degradation of Toluene and MEK by an M1/X1 Biofilm: Aq/Octanol Operation

Table B-24. FS6: Degradation of *p*-xylene by an X1 Biofilm: Aq/Aq Operation

Time	*p*-xylene conc. - ppm (w)	
hours	Feed	Film
0	80	25.7
1	52	0.3
2	53	0.1
3.33	40	0.2
4.5	41.5	0.1
5.5	40.4	0.8
6.5	41.8	1.8
7.5	41.2	3
9.5	34.5	4
10	43.5	3.7

Time	*p*-xylene conc. - ppm (w)	
hours	Feed	Film
0	34.2	0
1	53.6	0
2	50.4	0.1
3	51	0
4	41.6	0.2
5.08	45	0
6	33.3	0.3
7	30.4	0.3

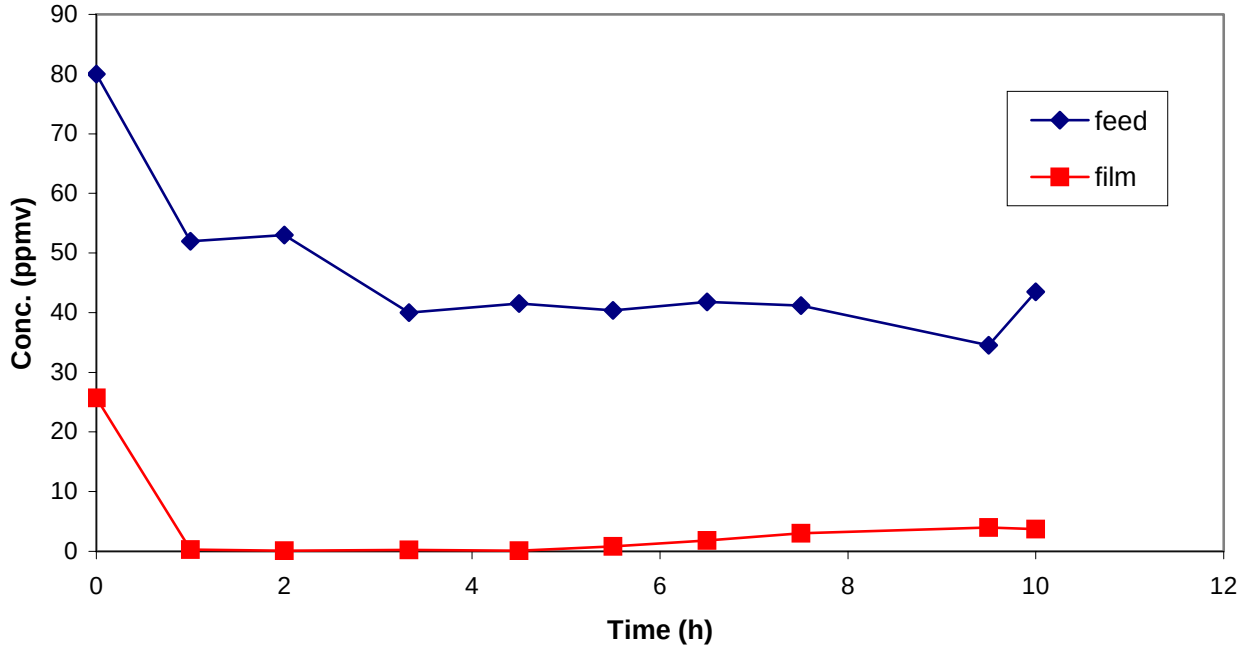

Figure B-24. FS6: Degradation of *p*-xylene by an X1 Biofilm: Aq/Aq Operation

Table B-25. FS7: Degradation of *m*-xylene by an X1 Biofilm: Aq/Aq Operation

Hours	Feed	Film	Hours	Feed	Film	Hours	Feed	Film
0	60.2	0.2	0	141	0.1	21.3	62.3	0.2
1	64.9	0	1.4	78.9	0	23.1	37.5	0
2	51.8	0	2.1	79.7	0	24.1	47.4	0
3.25	48	0.2	3.1	70.1	0	25.4	41.2	0
4	34.4	0.2	4.1	53.2	1.1	26.1	42.5	0
5	46	0	5.1	61	0	27.1	45.6	0
6	35.6	0.2	6.1	62.7	0.8	28.7	44.4	0
						29.4	40	0.2
						30.1	40.2	0

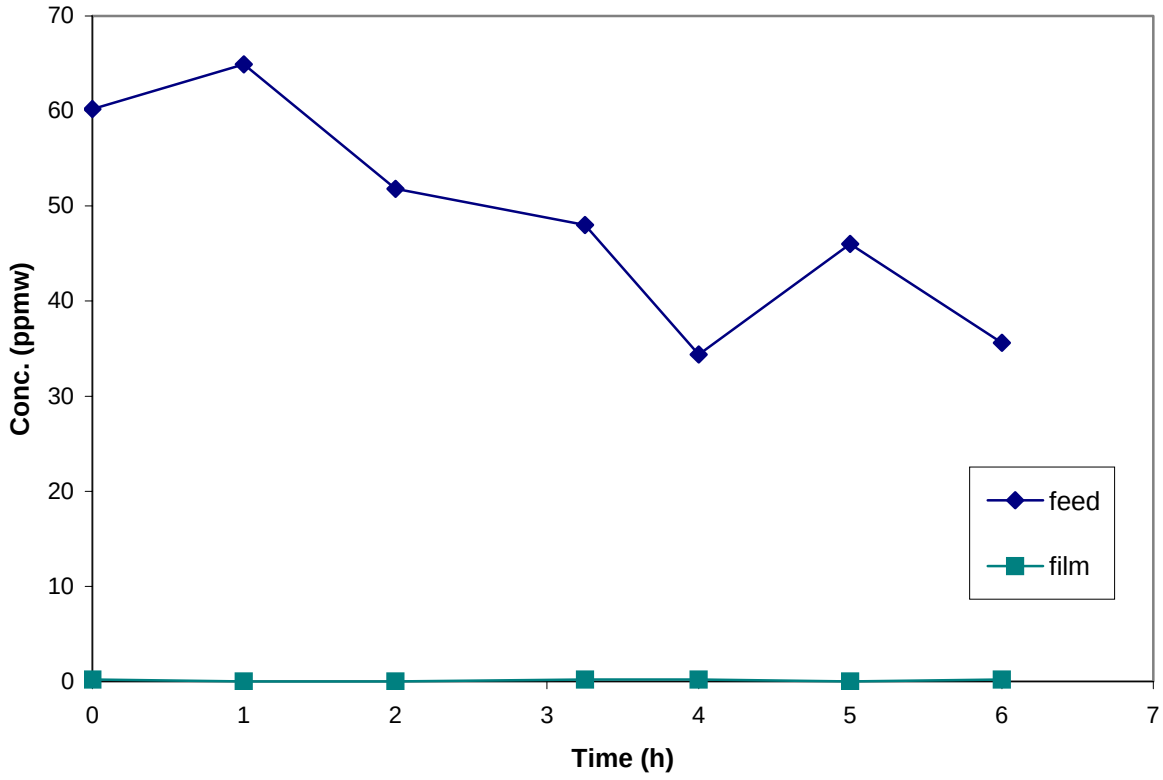

Figure B-25. FS7: Degradation of *m*-xylene by an X1 Biofilm: Aq/Aq Operation

Table B-26. FS8: Degradation of *m*-xylene and *p*-xylene by an X1 Biofilm: Aq/Aq Operation

initial concentration is 100 ppm each
concentration reported is total xylenes

Time	xylene conc. - ppm (w)	
hours	Feed	Film
0	203.2	0
1	78.7	0.2
2.5	42.7	0
3.7	49.7	0.2
4.5	50.2	0.2
20.5	35	0.1
21.5	22.5	0
22.5	23.6	0
23.5	25.5	0
24.6	23.3	0
25.6	24.3	0
27.5	22.3	0

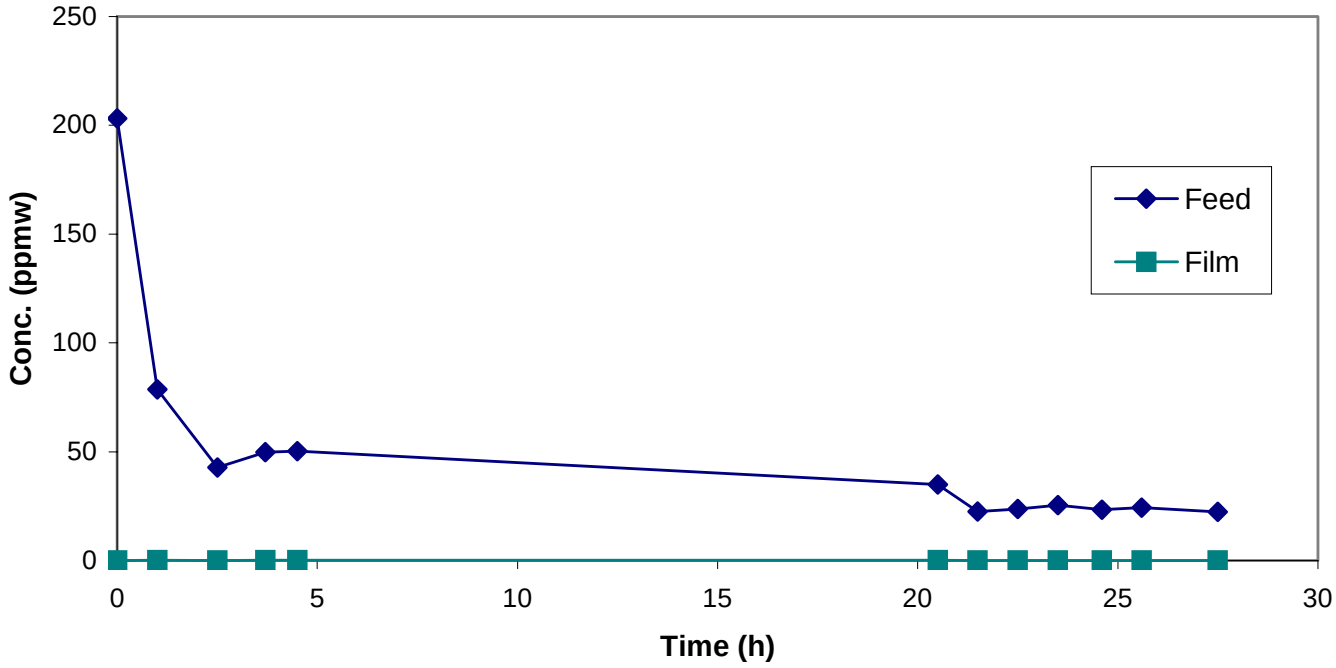

Figure B-26. FS8: Degradation of *m*-xylene and *p*-xylene by an X1 Biofilm: Aq/Aq Operation

Growth Study Experiments

Table B-27. GS1: Growth of X1 on *m*-xylene

Initial conc. of *m*-xylene: 250 ppm (v)

Time hours	OD600 250-I	OD600 250-II	Time hours	OD600 250-III	OD600 250-IV
0	0.006	0.011	0	0	0
2	0.005	0.008	4	0	0
3.5	0.016	0.016	5.33	0.002	0
4.67	0.036	0.039	6	0.002	0
5.5	0.062	0.062	6.5	0.002	0.002
6	0.074	0.08	7	0.007	0.007
7	0.127	0.156	8	0.016	0.01
7.75	0.201	0.235	9	0.034	0.025
8	0.228	0.262	10	0.062	0.046
8.25	0.266	0.297	11	0.115	0.081
8.5	0.283	0.333	11.5	0.16	0.109
8.75	0.32	0.354	12	0.212	0.15
9	0.351	0.378	12.5	0.258	0.19
9.25	0.367	0.399	13.08	0.323	0.259
9.5	0.388	0.405	13.5	0.361	0.295
9.75	0.397	0.408			
10	0.398	0.416			

Initial conc. of *m*-xylene: 100 ppm (v)

Time hours	OD600 100-I	OD600 100-II	Time hours	OD600 100-III	OD600 100-IV
0	0	0	0	0	0
3	0	0	4	0	0
6	0.011	0.041	5.33	0.002	0.003
7	0.04	0.101	6	0.007	0.007
7.25	0.052	0.125	7	0.013	0.015
7.5	0.06	0.13	8	0.032	0.036
7.75	0.073	0.152	9	0.068	0.069
8	0.083	0.178	10	0.131	0.124
8.25	0.104	0.21	10.25	0.161	0.146
8.5	0.124	0.22	10.5	0.19	0.176
8.83	0.149	0.223	10.75	0.223	0.203
9	0.174	0.225	11	0.247	0.21
9.33	0.2		11.25	0.25	0.219
9.5	0.203		11.5	0.25	0.219

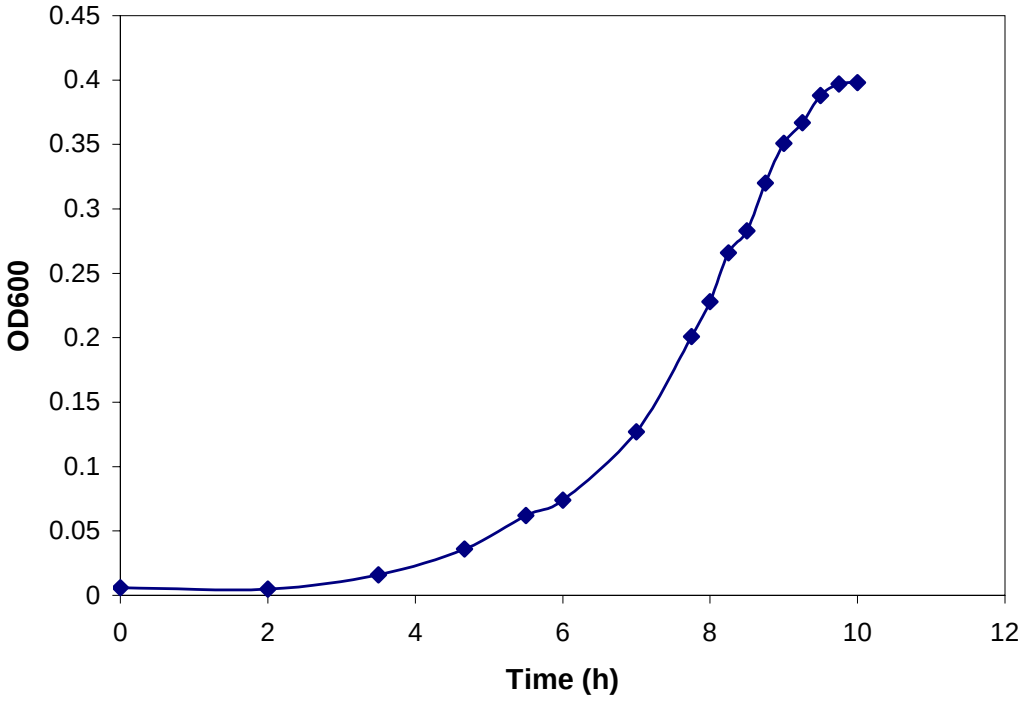

Figure B-27. GS1: Growth of X1 on *m*-xylene

Table B-28. GS2: X1 on Toluene

Time hours	OD600	tol ppm
0	0	80.8
10	0.007	
11.5	0.012	
12.5	0.016	
13.5	0.022	60.6
14.5	0.034	48.6
15.5	0.053	
16.5	0.063	39.8
17.5	0.111	
18.5	0.127	17.4
19.5	0.209	
20.5	0.225	0
21.5	0.222	

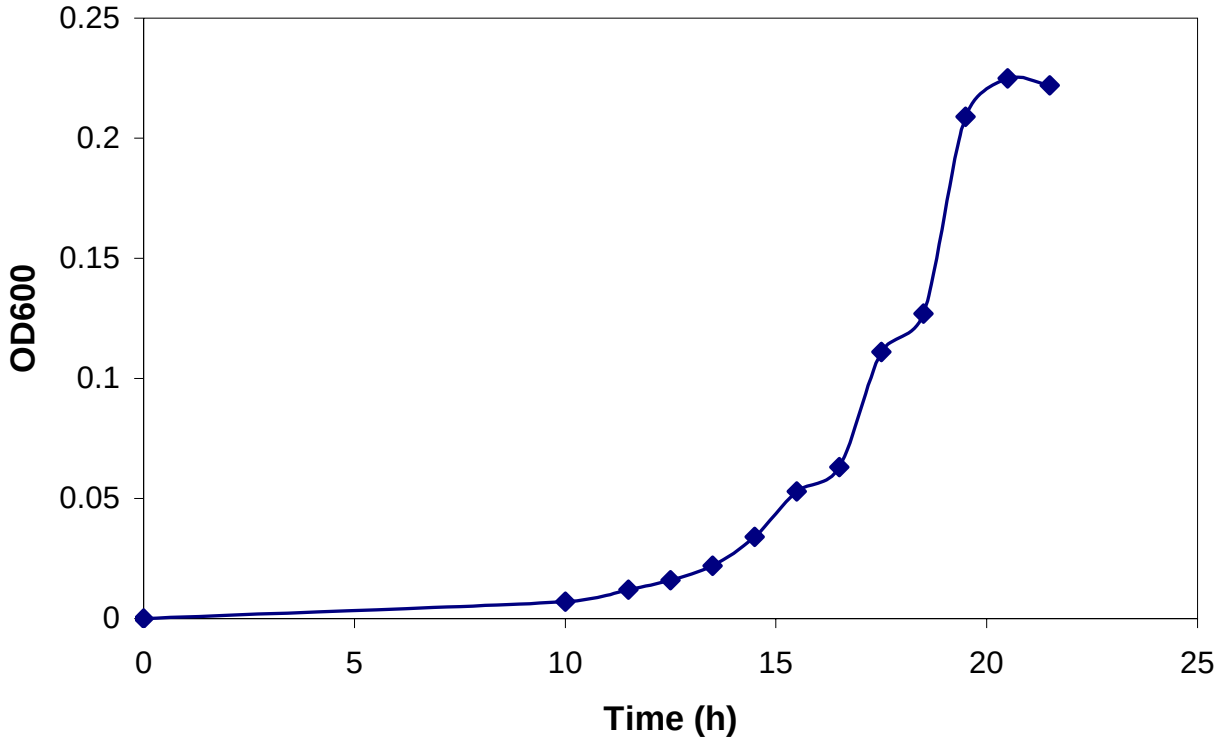

Figure B-28. GS2: X1 on Toluene

Table B-29. GS3: X1 on Toluene and *m*-xylene

Time hours	OD600	tol ppm (w)	*m*-xyl ppm (w)
0	0.001	44.7	44.7
2	0.001		
4	0.009		
5	0.009	45.6	45.1
6	0.018		
6.5	0.032	57.6	57.6
7.5	0.059	36.6	38.5
8.75	0.128	11.7	16.7
9.5	0.234		9.3
10.67	0.28	0.15	0.14
11.75	0.267	0.15	0.12
12.75	0.267	0.02	

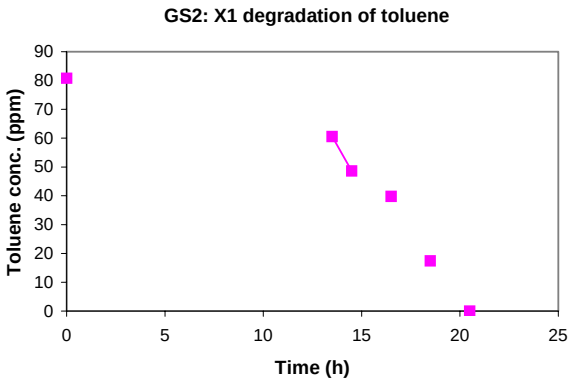

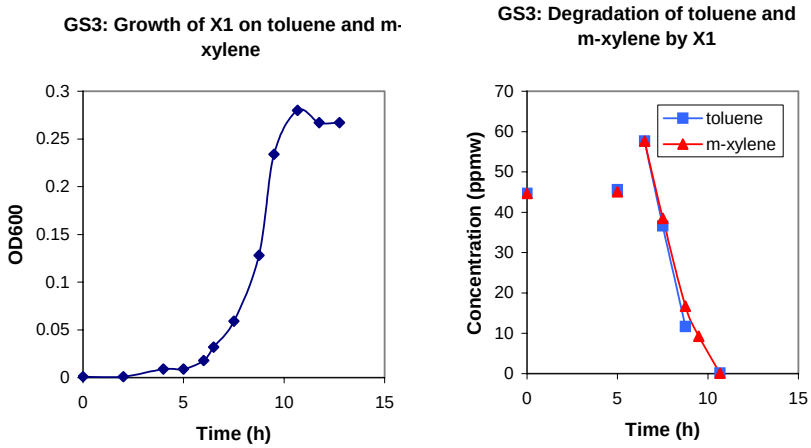

Figure B-29. GS3: X1 on Toluene and *m*-xylene

Table B-30. GS4: M1 on Toluene

Time hours	OD600
0	0
12.5	0.002
14	0.003
15.5	0.003
17.5	0.005
19	0.008
20.5	0.01
24	0.031
25	0.038
26	0.046
27	0.071
28	0.078
29	0.088
30	0.113
30.5	0.118
31	0.13
31.42	0.139
40	0.3

Time hours	OD600	tol ppm (w)
0	0.001	77.6
21.5	0.023	
24	0.043	70.2
25	0.048	
26.5	0.063	61.8
27.5	0.069	
30	0.106	39
31	0.133	
32	0.17	16.9
33.42	0.227	
34	0.238	0
35	0.232	
35.5	0.229	

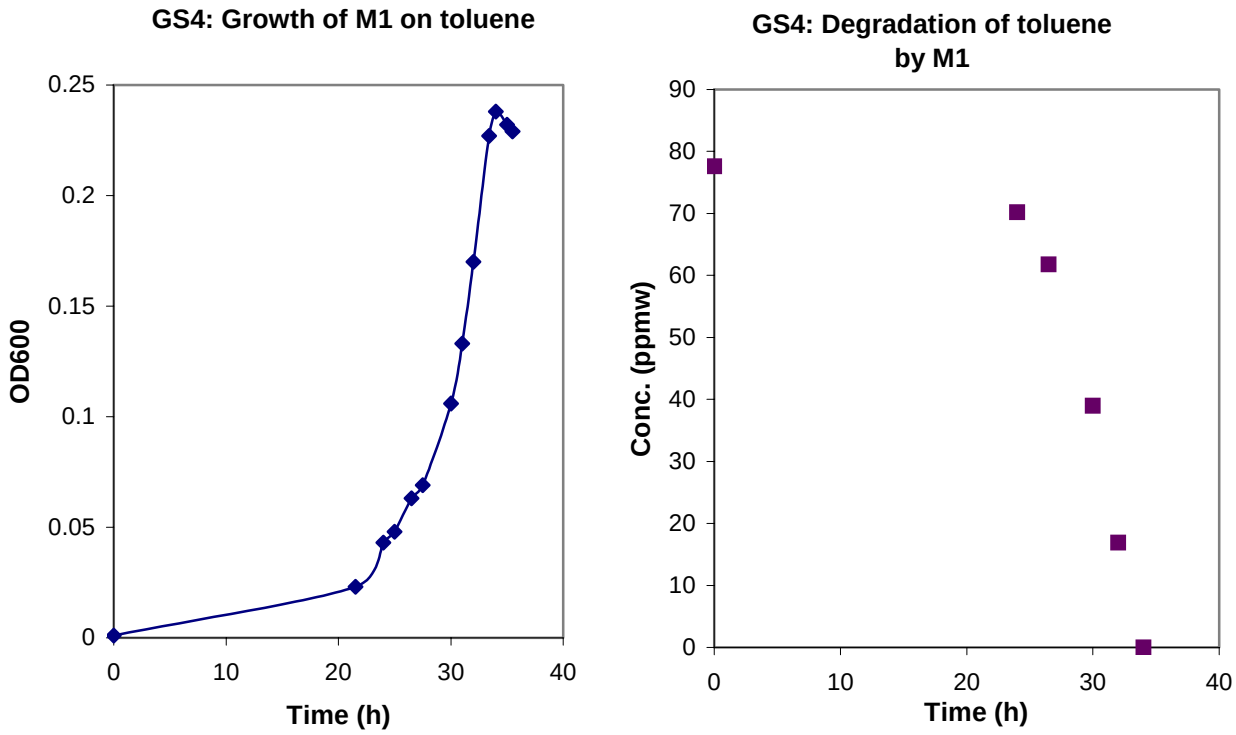

Figure B-30. GS4: M1 on Toluene

Table B-31. GS5: M1 on MEK and Toluene

Time hours	OD600	tol ppm (w)	MEK ppm (w)
0	0	24.9	46.3
8.25	0.012		
9.25	0.013	24.7	42.9
10.25	0.015		
11.25	0.021		
12.25	0.025	18.6	34.6
13.25	0.03		
14.25	0.033	12.8	27
15.25	0.046		
16.25	0.063	7.27	11.9
17.25	0.085		
18.25	0.141	0.155	6.4
19.25	0.167		
20.25	0.171	0	6.6
21.25	0.171		
22.25	0.165		

Time hours	OD600	tol ppm (w)	MEK ppm (w)
0	0	17.01	179.4
8	0.002	13.2	195.2
10.5	0.002		
12.5	0.005	9.6	175.7
13.5	0.008		
14.75	0.013	7.2	186.6
15.75	0.018		
16.75	0.024	2.3	171
17.75	0.034		
18.75	0.046	0.1	159
19.75	0.07		
20.75	0.079	0	124.7
21.75	0.096		
22.75	0.099	0.2	101
23.75	0.134		
24.75	0.174	0.1	43.4
25.75	0.189		
26.75	0.248	0	0

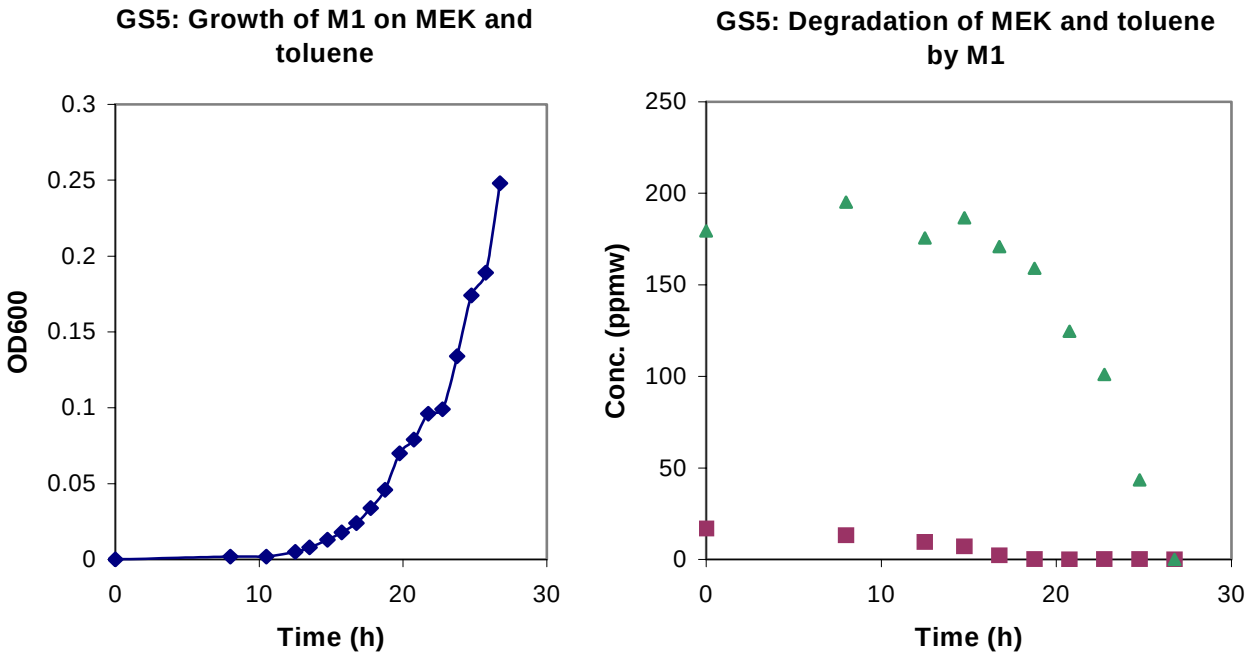

Figure B-31. GS5: M1 on MEK and Toluene

Table B-32. GS6: M1 on *m*-xylene and MEK

Time hours	OD600	*m*-xyl ppm (w)	MEK ppm (w)
0	0.001	33.8	68.1
9	0.056	3.7	68.7
9.75	0.082		
10.5	0.089	0	70.1
11.25	0.093		
12.25	0.094		
13.25	0.102		
14	0.108		30
14.75	0.125		
15.5	0.133		3.93
16.25	0.145		
17	0.15		2.89
17.75	0.154		
18.75	0.148		2.58
20.75			1.99

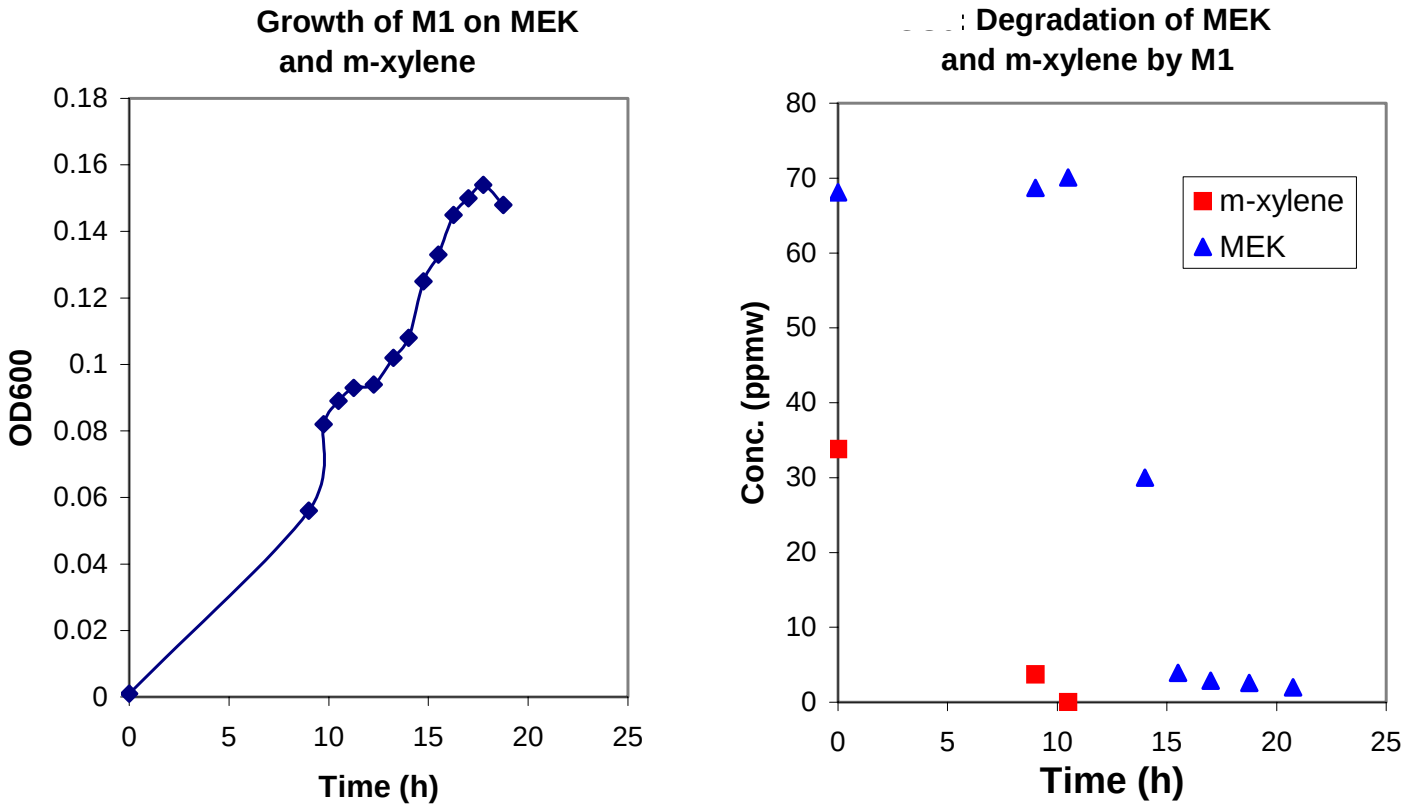

Figure B-32. GS6: M1 on *m*-xylene and MEK

Table B-33. GS7: M1 on Toluene and *m*-xylene

Time hours	OD600	tol ppm (w)	*m*-xyl ppm (w)
0	0		
8.75	0.005	32.6	35.2
9.75	0.008		
10.5	0.011	32.4	31.3
11.25	0.015		
12	0.024	28.8	23.1
12.75	0.032		
13.5	0.044	28.4	14.5
14.25	0.065		
15	0.089	27.4	0
15.75	0.109		
16.5	0.12	19.2	0
17.5	0.125		
18.5	0.132	0.4	0
20	0.154		
21	0.151	0	0

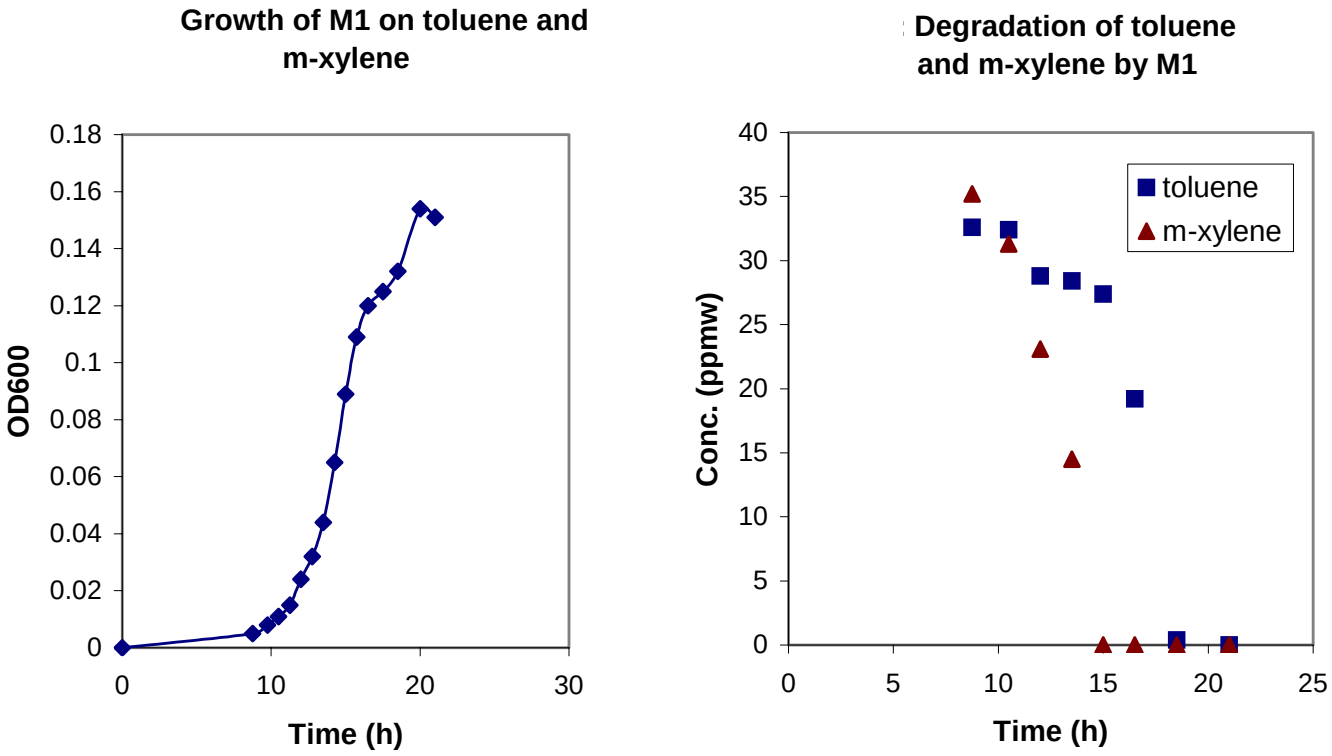

Figure B-33. GS7: M1 on Toluene and *m*-xylene

Table B-34. GS8: M1 on Toluene, *m*-xylene and MEK

Time hours	OD600	*m*-xyl ppm (w)	tol ppm (w)	MEK ppm (w)
0.25	0	24.5	20.8	19.9
8.33	0.023	27.8	19.2	7.3
9.33	0.038			
10	0.051	30.4	14.8	1
11	0.068			
11.75	0.071	26.7		
12.75	0.076			
13.5	0.076	31.7	3.6	0
14.5	0.076			
15.5	0.079			
16	0.082	17.1	0.1	
17	0.097			
18	0.125	19.9	0	
19	0.129			
20	0.128	15		
21	0.135			
22	0.146			
23	0.155			
24	0.159			
25	0.163			
26	0.163			

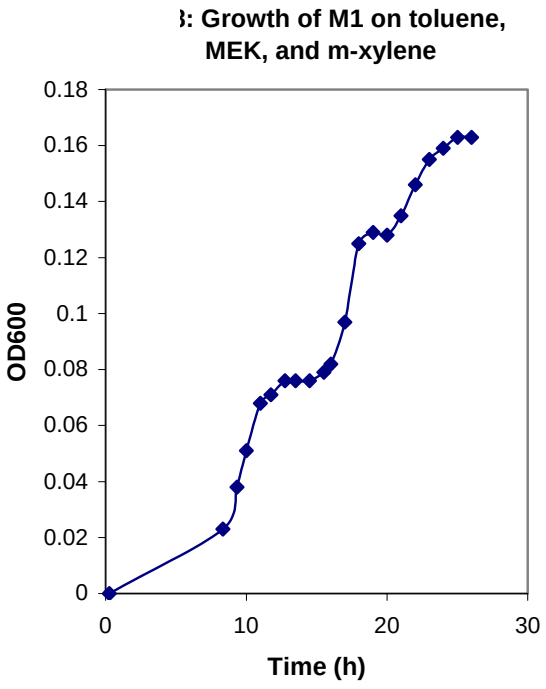

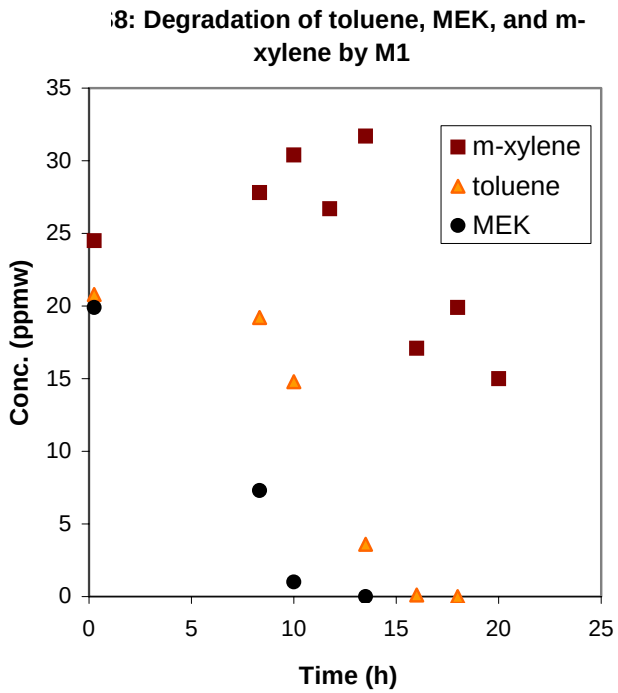

Table B-34. GS8: M1 on Toluene, *m*-xylene and MEK

Table B-35. GS9: M1 and X1 on MEK and Toluene

Time hours	OD600	MEK ppm (v)	tol ppm (w)
0	0.001	49.4	41.7
3	0.004	53.2	33.7
4	0.007		
5	0.01	59.4	32.2
6	0.014		
7.5	0.026		11.9
8.5	0.039		
9.5	0.055		8.8
10.5	0.054		
11.5	0.101	58.3	0
12.5	0.103		
13.5	0.1	58.5	0
14.5	0.101		
15	0.1		

Time hours	OD600	MEK ppm (v)	tol ppm (w)
0	0.005		19.4
10	0.068	44.7	0
11	0.073		
12	0.078	39.7	
13	0.089		
14	0.097	28.5	
15	0.104		
16	0.113		
17	0.118	10.1	
18	0.121		
19	0.121	7.3	
22	0.122	7.2	
24.67	0.125		
26.67	0.12		

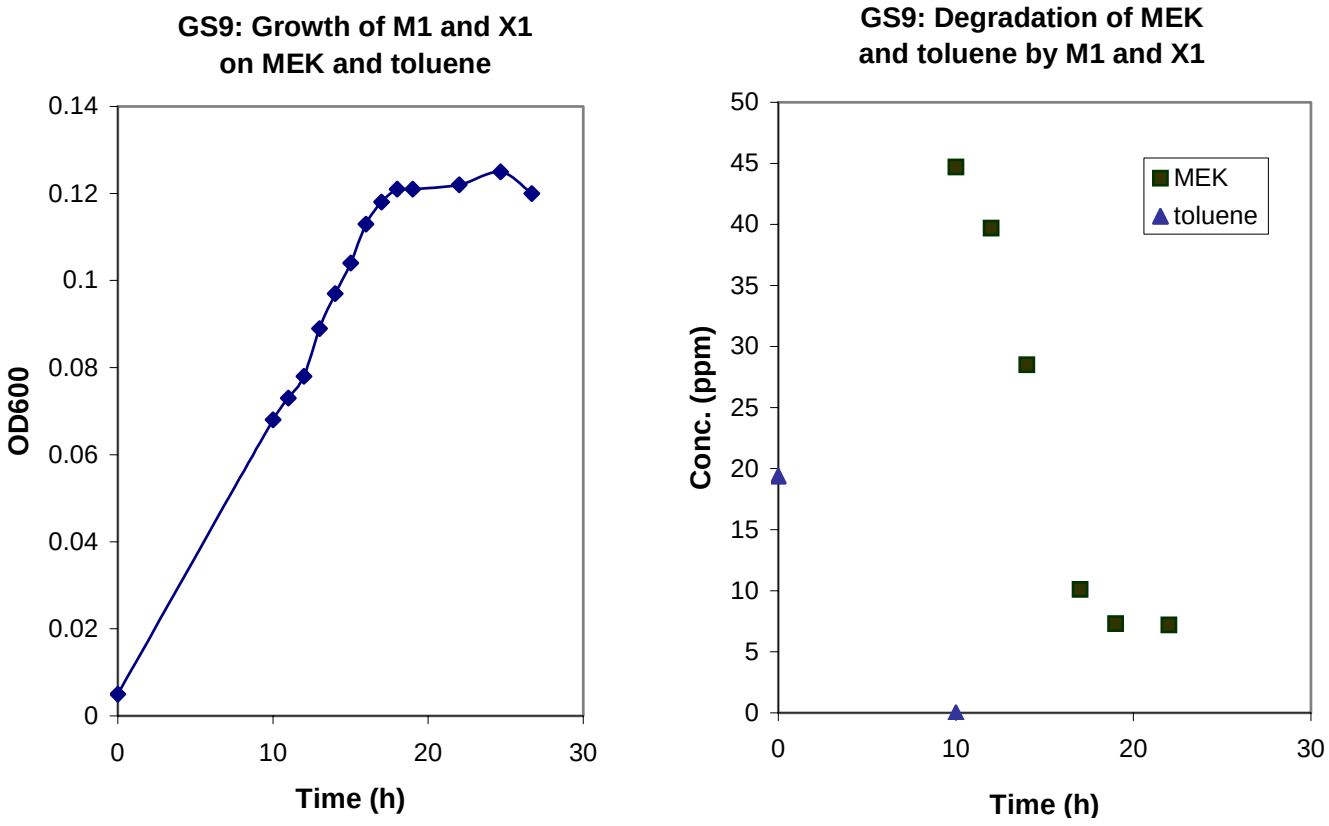

Figure B-35. GS9: M1 and X1 on MEK and Toluene

Table B-36. GS10: M1 and X1 on MEK, Toluene and *m*-xylene

Time hours	OD600	MEK ppm (w)	tol ppm (w)	*m*-xyl ppm (w)
0.42	0.001	26.5	18.6	14
3	0.001			
4.5	0.004			
5.5	0.006	27.7	16.6	10.7
6.5	0.013			
7.5	0.023		13.2	7.1
8.58	0.044			
9.5	0.056		2.7	0.1
10.5	0.088			
11.5	0.089		0	0
12.5	0.095			
13.5	0.092	32.1		
14.5	0.095			
15.5	0.102	19.1		
16.5	0.11			
17.5	0.119	7.5		
18.5	0.118			
19.5	0.123	6.6		
20.5	0.121			
26.17	0.135	5.5		

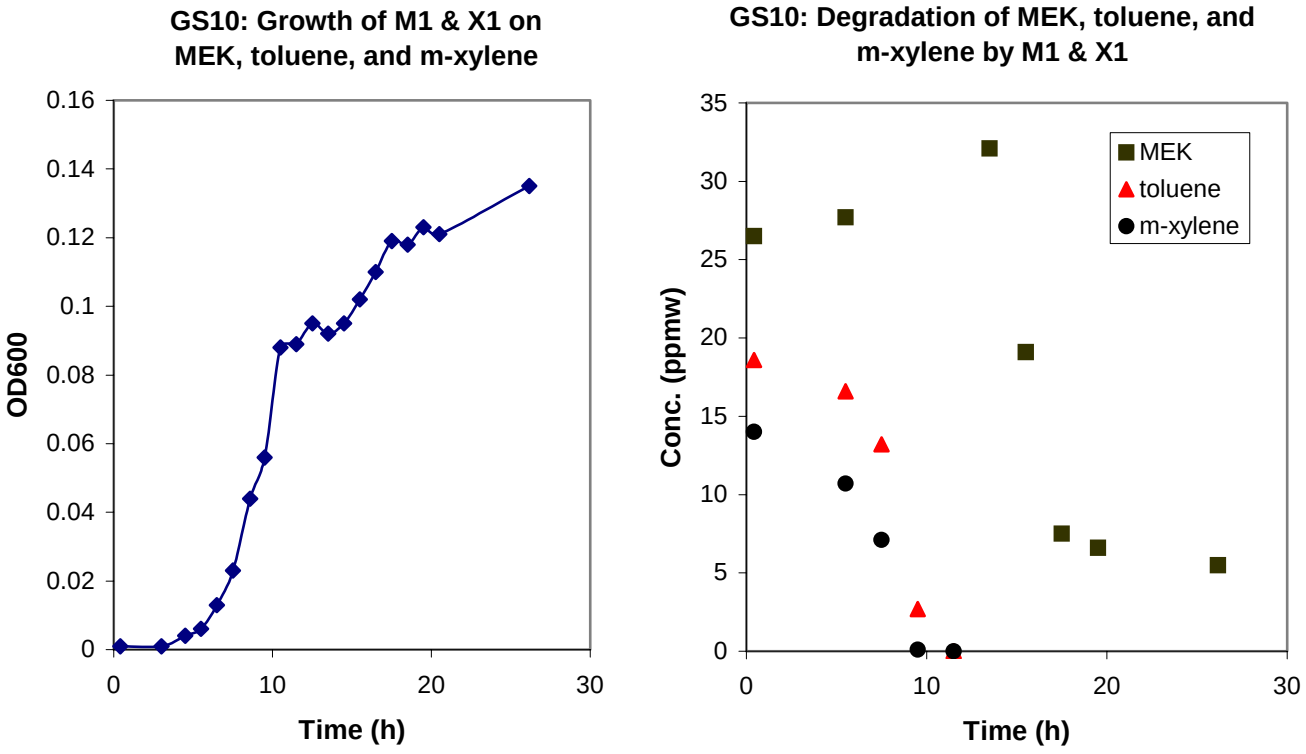

Figure B-36. GS10: M1 and X1 on MEK, Toluene and *m*-xylene

Table B-37. GS11: MX on *p*-xylene

Time hours	OD600
0	0
7.1	0.002
22.4	0.011
23.6	0.012
25.2	0.02
26.2	0.024
27.2	0.05
28.3	0.052
29.1	0.062
30.2	0.069
31.1	0.094
31.6	0.101
46.2	0.128

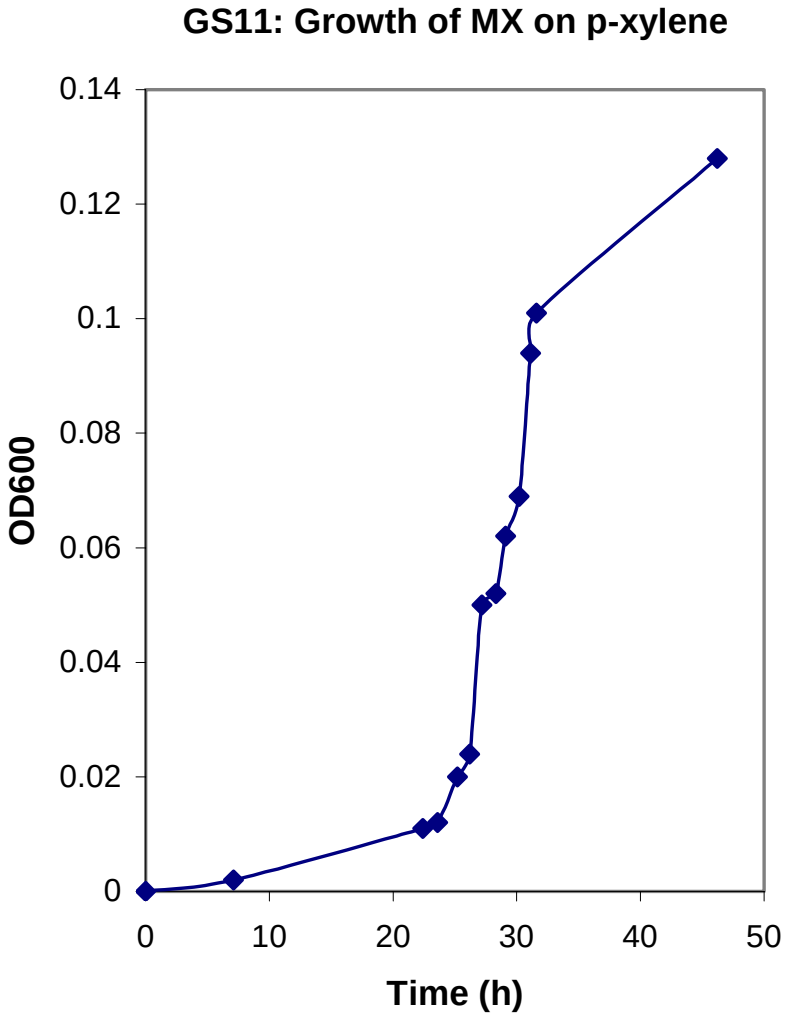

Figure B-37. GS11: MX on *p*-xylene

Table B-38. GS12: M1 on *p*-xylene

Time hours	OD600	Time hours	OD600	*p*-xyl ppm(w)	Time hours	OD600	*p*-xyl ppm(w)
0	0	0	0	57.8	0	0	122.9
22.3	0.082	10.8	0.064	32	9.4	0.007	113.4
23.5	0.105	12.2	0.091	20.1	33.4	0.008	61.5
25.2	0.129	12.8	0.114		35.4	0.021	
26.3	0.136	13.5	0.13	4.8	36.4	0.03	35.3
27.2	0.157	14.2	0.141	0	37.4	0.054	18
28.2	0.151	14.8	0.152		38.4	0.098	9
28.9	0.145	15.5	0.155		39.4	0.114	0
		16.6	0.159		40.4	0.148	
		18.4	0.161		41.4	0.161	
		21	0.175		42.4	0.177	
					43.9	0.182	
					44.6	0.18	
					45.1	0.182	

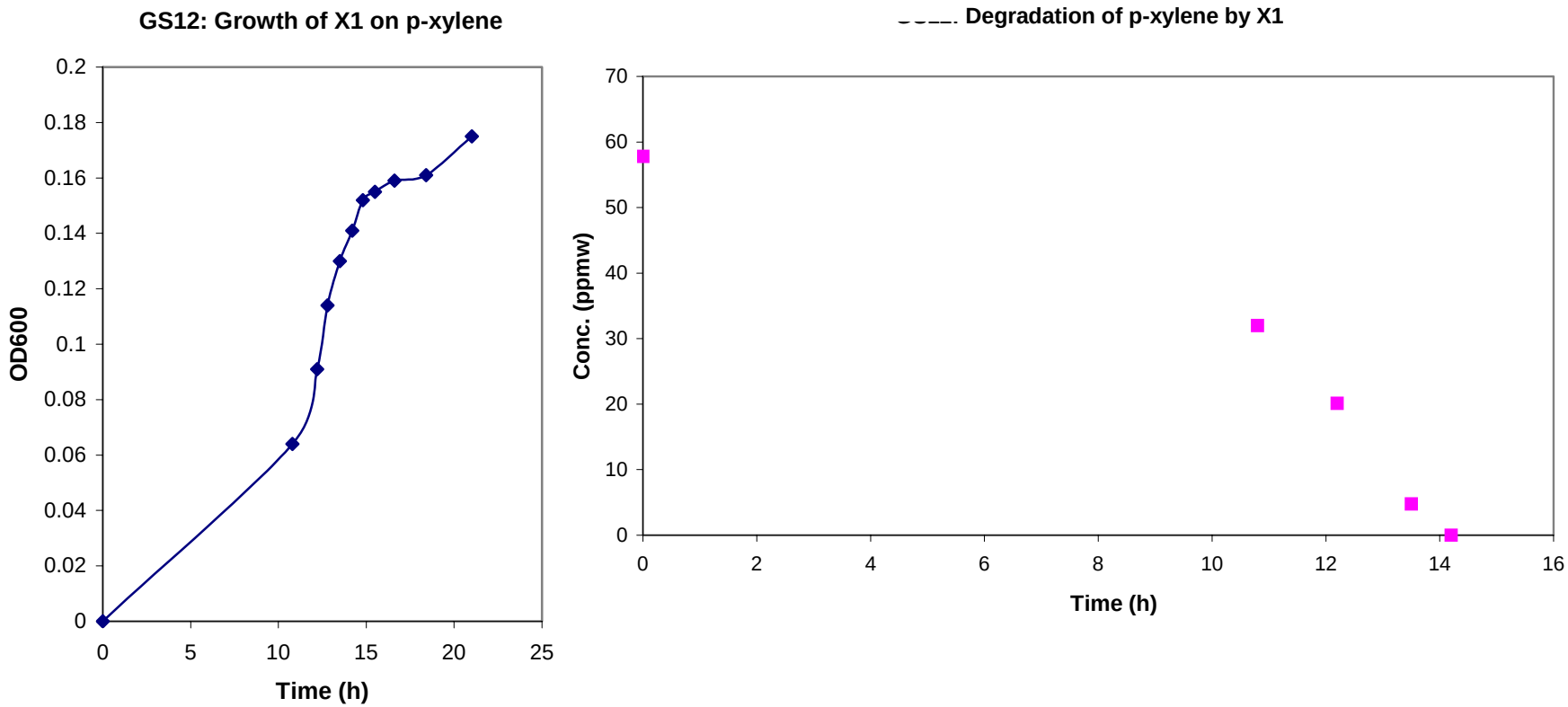

Figure B-38. GS12: M1 on *p*-xylene

Table B-39. GS13: X1 on 150 ppm *m*-xylene with Ethyl Benzene

	Ethyl benzene added at concentrations of 0, 50, 100 and 150 ppm			
Time hours	OD600 0 ppm	OD600 50 ppm	OD600 100 ppm	OD600 150 ppm
0	0.005	0.004	0.004	0.006
4	0.014	0.021	0.018	0.011
7	0.028	0.02	0.019	0.024
9	0.033	0.028	0.028	0.029
11	0.033	0.036	0.044	0.043
13	0.053	0.057	0.069	0.068
14	0.058	0.064	0.092	0.076
15	0.068	0.087	0.119	0.117
15.5	0.071	0.093	0.134	0.14
16	0.087	0.105	0.154	0.162
16.5	0.102	0.142	0.19	0.181
17	0.124	0.153	0.176	0.172
17.5	0.124	0.161	0.166	0.162
18	0.165	0.172	0.178	0.173
18.5	0.184	0.177	0.16	0.163
19	0.21	0.167	0.167	0.158
19.5	0.218	0.199	0.179	0.158
20	0.197	0.21	0.184	0.16
21	0.317	0.224	0.207	0.174
22	0.198	0.238	0.215	0.164
23	0.224	0.249	0.229	0.171
24	0.258	0.267	0.227	0.171
25	0.243	0.252	0.238	0.166
26	0.243	0.264	0.238	0.171
32.5	0.228	0.282	0.241	0.186

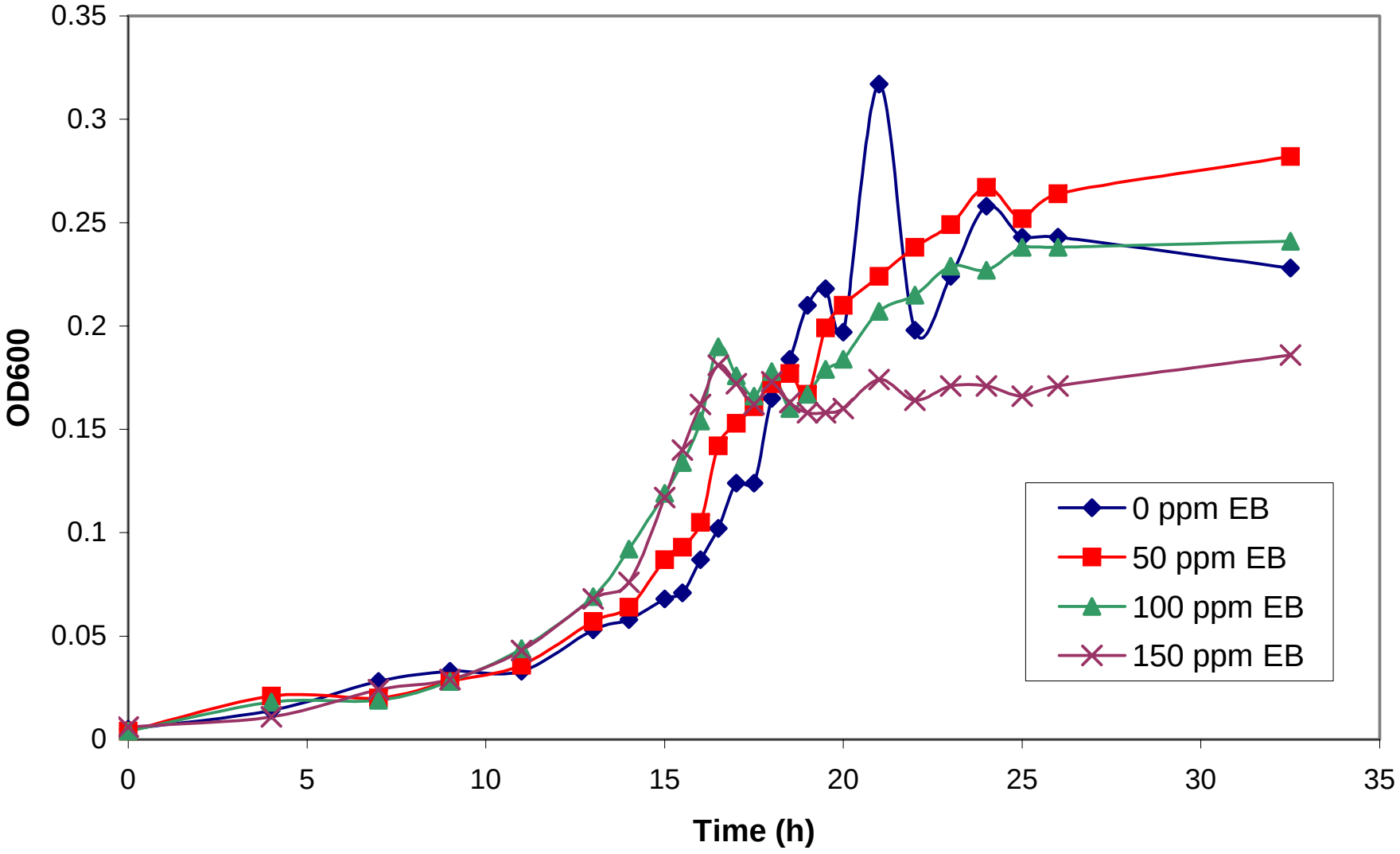

Figure B-39. GS13: X1 on 150 ppm *m*-xylene with Ethyl Benzene

Table B-40. GS14: X1 on a 50:50 Mixture of *m*- and *p*-xylene

Time hours	150 ppm total concentration OD600	Xylenes ppm(w)
0	0.001	61.5
1	0.007	105.9
2	0.013	112.1
3	0.025	104.9
3.5	0.035	94.3
4	0.04	96.1
5	0.083	75.5
6	0.14	51.4
6.5	0.176	25.8
7	0.228	4.6
7.5	0.251	0.1
8	0.257	0.2
8.5	0.268	0.4
9	0.251	0
10	0.228	

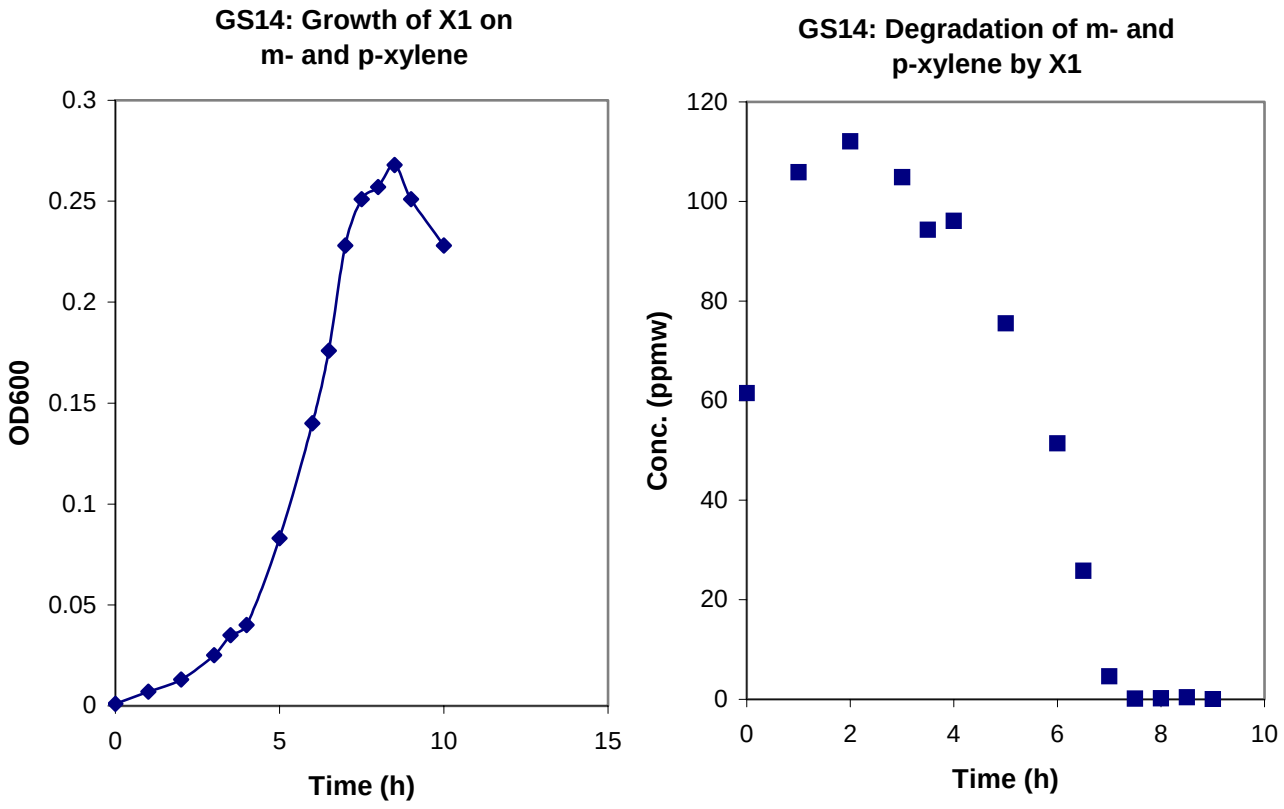

Figure B-40. GS14: X1 on a 50:50 Mixture of *m*- and *p*-xylene

Table B-41. GS15/16: M1 on Butyl Acetate (150 ppm) or a Mixture of MEK and Butyl Acetate (75 ppm each)

Time hours	OD600 BA	OD600 BA & MEK
0.25	0.006	0.011
1.3	0.018	0.019
2.25	0.028	0.023
3	0.048	0.05
3.7	0.072	0.077
4.3	0.088	0.09
5	0.094	0.102
5.7	0.116	0.151
6.15	0.129	0.19
6.8	0.141	0.212
7.25	0.156	0.236
8.25	0.197	0.276
9.25	0.217	0.206
10.25	0.219	0.239
11.25	0.265	0.209
12.25	0.28	0.199
13	0.266	0.205

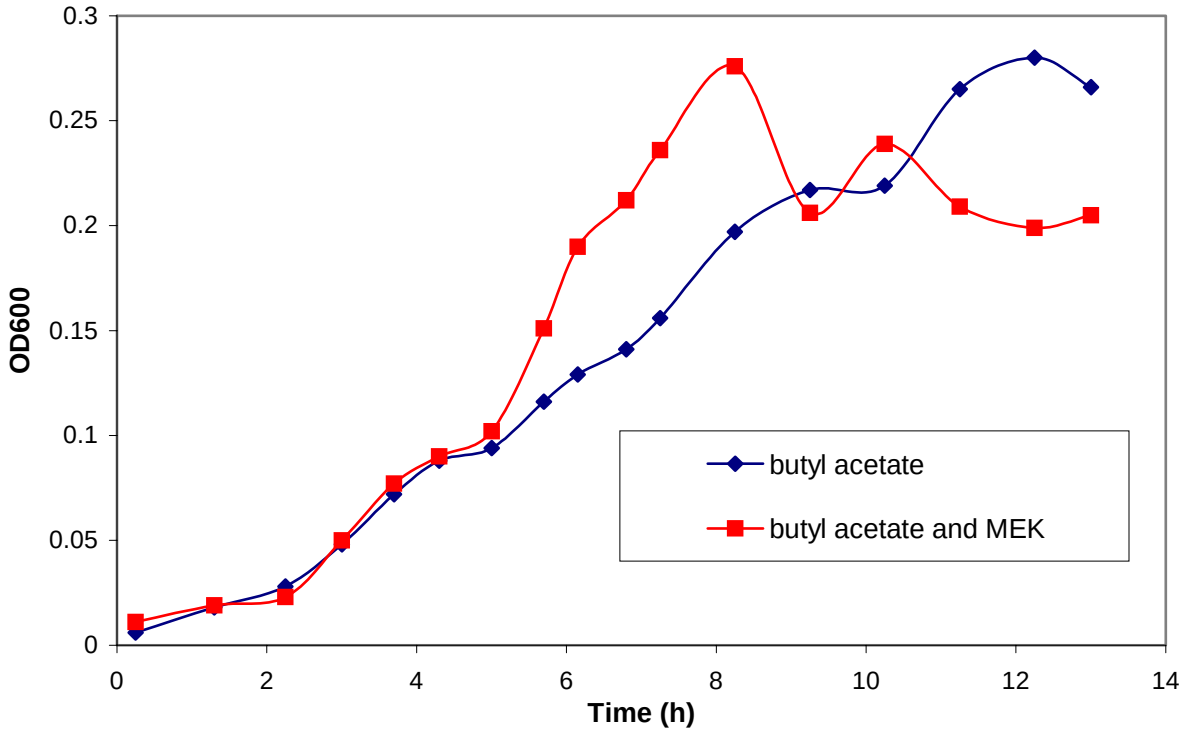

Figure B-41. GS15/16: M1 on Butyl Acetate

Staged Bioreactor Experiments

Table B-42. SB1: Degradation of MEK in a Staged Bioreactor - 500 ppm Case

Time hours	Oil *m*-xyl ppm	Oil MEK ppm	C MEK ppm in	Aq MEK ppm out
0	458.7	*		
1	402.0	0		
2	375.4	0		
3	332.7	0		
4	288.2	0		
5	259.3	0		
6	215.5	0	9.1	1.6
7	172.3	0		2.8
8	121.6	0	9.1	4.3

Time hour	Oil *m*-xyl ppm	Oil MEK ppm	Aq MEK ppm in	Aq MEK ppm out
0	449.8	413.6	350.6	426.1
1.17	496.0	365.5	460.5	443.6
2.17	463.9	336.1	467.3	446.9
3.25	439.4	351.1	473.6	445.0
4.33	446.1	351.9	463.1	431.8
5.42	409.2	317.4	455.3	417.6
10.25	378.8	288.6	376.1	353.5
11.42	373.4	270.8	352.0	359.0

Time hour	Oil *m*-xyl ppm	Oil MEK ppm	Aq MEK ppm in	Aq MEK ppm out	Aq *m*-xyl ppm in	Aq *m*-xyl ppm out
0	1109.7	356.0	166.3	177.8	0.00	0.00
1	1055.7	166.1	215.4	198.9	0.00	0.15
2	1094.5	158.4	222.3	207.3	0.00	0.00
3	1088.5	139.2	213.0	197.3	0.00	0.00
4	1047.3	160.0	216.7	175.7	0.00	0.52
5	1075.3	158.7	221.8	192.4	0.00	0.00
6	1051.4	164.4	158.2	191.2	0.53	0.00
7.5	1045.3	147.4	165.3	190.1	0.66	0.65

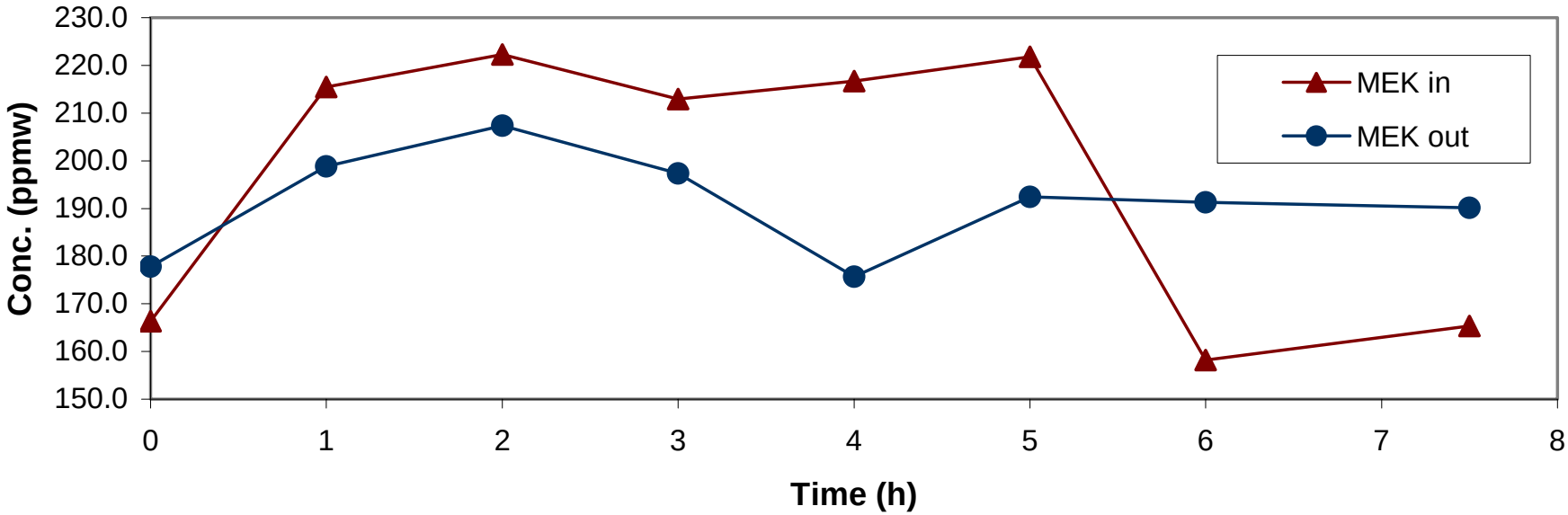

Figure B-42. SB1: Degradation of MEK in a Staged Bioreactor - 500 ppm Case

Table B-43. SB2: Degradation of MEK and *m*-xylene in a Staged Bioreactor - 1000 ppm Case

Time hours	Oil *m*-xyl ppm	Oil MEK ppm	Aq MEK ppm in	Aq MEK ppm out
0	731.4	260.3	140.6	
1.17	634.0	*	129.0	113.1
2.08	577.1	*	133.3	198.8
3.08	545.7	*	173.3	178.0
4.08	469.9	0	162.5	162.8
5.08	405.2	0	106.6	121.2
6.08	406.6	0	76.6	84.4
7.08	431.0	0	80.6	87.7

Time hours	Oil *m*-xyl ppm	Oil MEK ppm	Aq MEK ppm in	Aq MEK ppm out	Aq *m*-xyl ppm in	Aq *m*-xyl ppm out
0	854.8	541.1	157.1	210.5	0	0.36
1	829.6	240.0	249.5	243.5	0	0.35
2	784.6	203.4	270.9	249.5	0	0.48
3	777.9	209.2	259.9	237.3	0	0
4	778.4	198.4	254.2	237.2	0.08	0.46
5	792.0	209.3	257.6	237.6	0.13	0.46
6	710.9	164.1	258.3	256.5	0.24	0.43
7	703.7	186.0	267.6	261.0	0.52	0.56
8	700.3	183.5	257.6	260.7	0.62	0.62

m-xylene not detected in aqueous phase
*Matrix interference/acetic acid

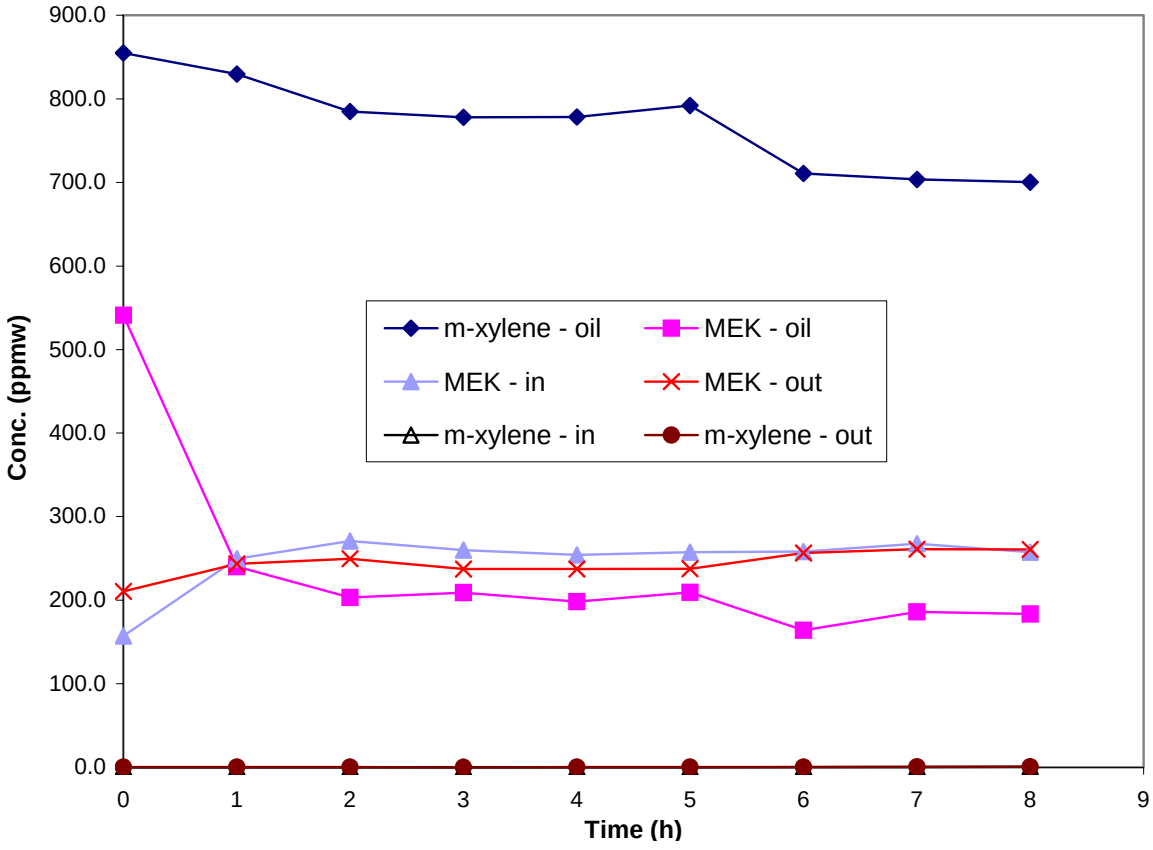

Figure B-43. SB2: Degradation of MEK and *m*-xylene in a Staged Bioreactor - 1000 ppm Case

Table B-44. SB3: Degradation of MEK and *m*-xylene in a Staged Bioreactor- 1500 ppm Case

Time hours	Oil *m*-xyl ppm	Oil MEK ppm	Aq MEK ppm in	Aq MEK ppm out	Aq *m*-xyl ppm in	Aq *m*-xyl ppm out
0	1646.6	801.8	129.1	327.8	0.08	0.69
1	1574.2	261.4	351.8	354.7	0.24	0.59
1.83	1538.1	253.3			0.07	0.00
2.83	1573.9	234.6	354.8	351.7	0.00	0.37
3.83	1497.5	268.2			0.00	0.19
4.83	1300.9	237.2	312.3	296.0	0.00	0.19
5.83	1275.7	98.1			0.00	0.23
6.83	1191.5	128.1	286.4	287.7	0.00	0.27
7.83	1110.4	112.3			0.00	0.29
8.83	1208.9	220.0	253.6	258.8	0.00	0.39

Time hours	Oil *m*-xyl ppm	Oil MEK ppm	Aq MEK ppm in	Aq MEK ppm out	Aq *m*-xyl ppm in	Aq *m*-xyl ppm out
0	1166.0	408.9	163.9	252.3	0.00	0.00
1	1085.1	175.7	312.4	329.8	0.00	0.25
2	1073.2	179.4	331.6	270.1	0.00	0.00
3	1071.0	156.7	333.4	259.8	0.00	0.54
4	1060.1	167.5	301.3	299.8	0.00	0.51
5	1030.5	164.9	296.2	311.4	0.35	0.91
6	993.4	152.2	294.0	302.7	0.39	0.49
7	1065.4	148.3	288.8	273.0	1.05	1.02

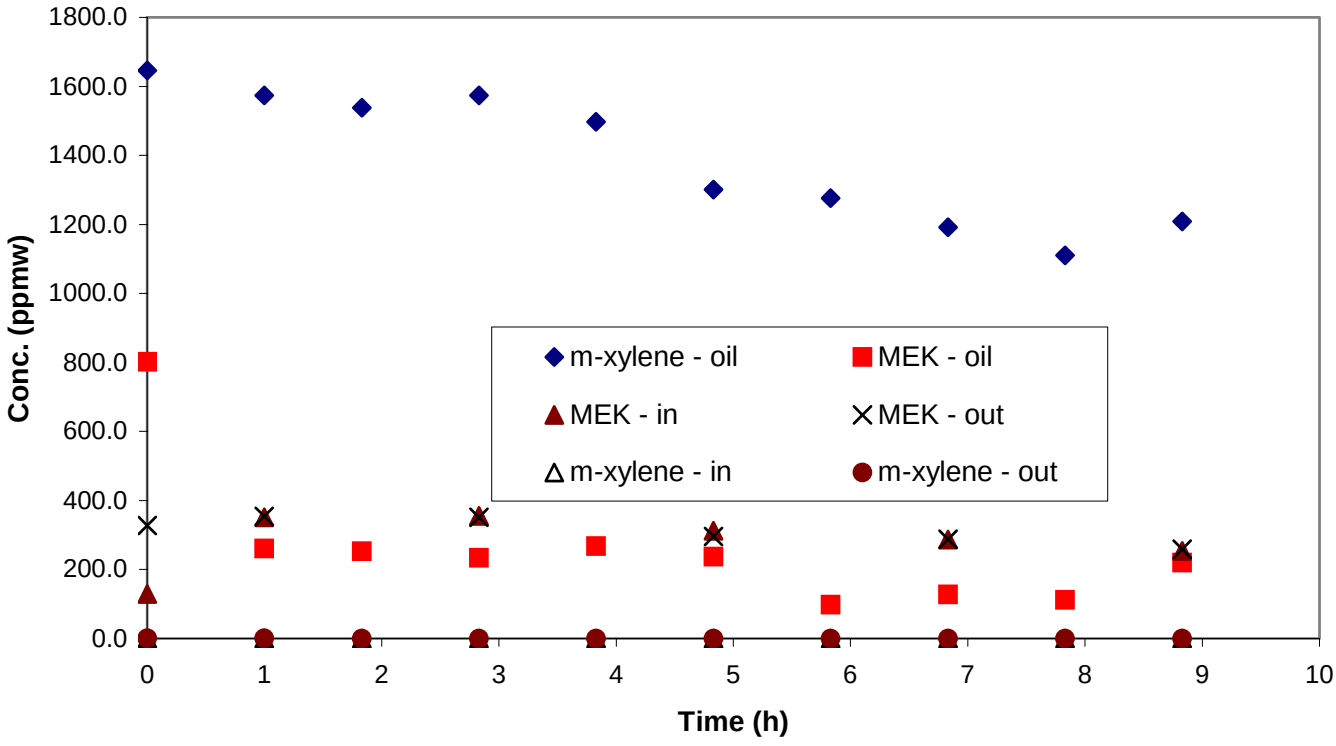

Figure B-44. SB3: Degradation of MEK and *m*-xylene in a Staged Bioreactor- 1500 ppm Case

Table B-45. SB4: Degradation of MEK and *p*-xylene in a Staged Bioreactor - 500 ppm Case

Time hours	Oil *p*-xyl ppm	Oil MEK ppm	Aq MEK ppm in	Aq MEK ppm out	Aq *p*-xyl ppm in	Aq *p*-xyl ppm out
0	554.5	301.5	43.0	75.20	0.00	0.00
1	540.4	100.6	83.6	73.74	0.19	0.00
2	538.3	127.0	95.7	92.21	0.20	0.00
3	533.1	95.5	88.2	88.30	0.32	0.00
4	551.5	91.7	83.4	70.67	0.48	0.10
5	538.5	57.2	80.0	80.03	0.10	
6	549.7	51.1	76.6	74.49	0.49	0.45
7.75	534.7	0.0	67.4	63.99	0.44	0.40

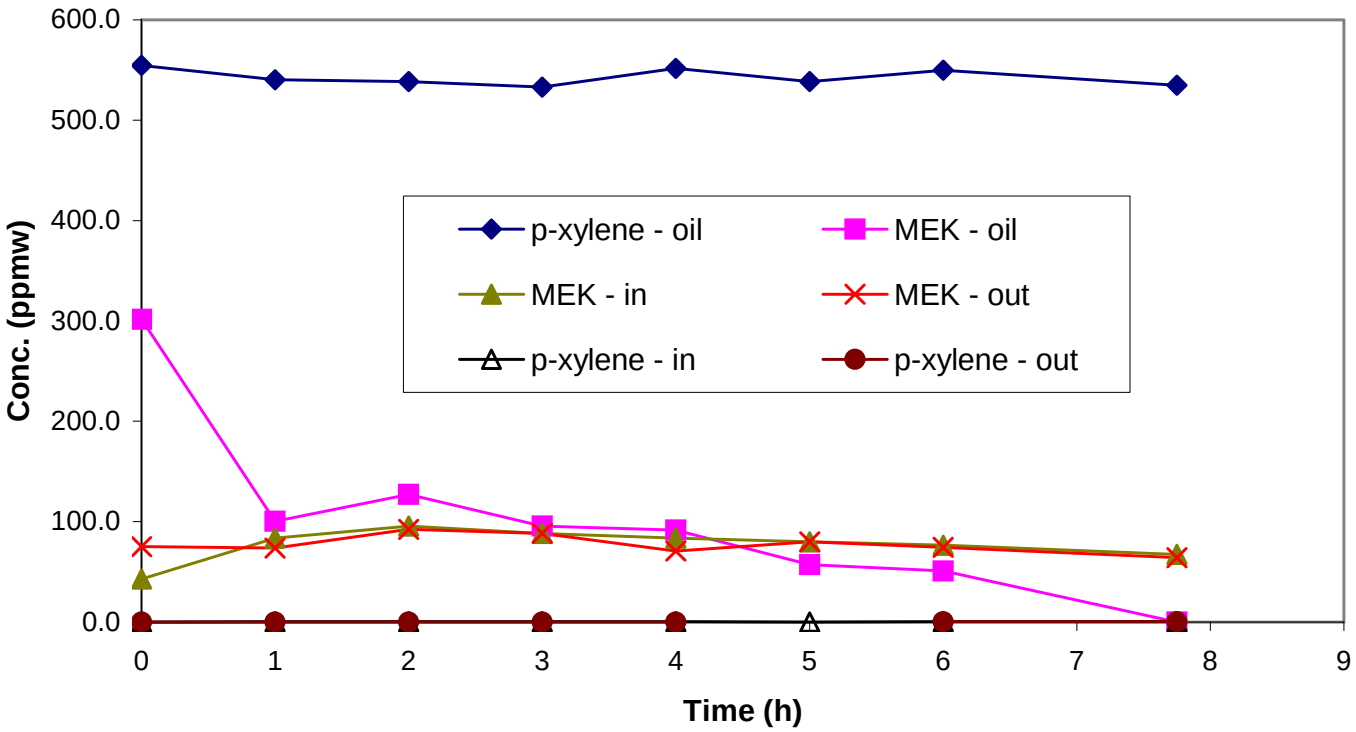

Figure B-45. SB4: Degradation of MEK and *p*-xylene in a Staged Bioreactor - 500 ppm Case

Table B-46. SB5: Degradation of MEK and *p*-xylene in a Staged Bioreactor - 1000 ppm Case

Time hours	Oil *p*-xyl ppm	Oil MEK ppm	Aq MEK ppm in	Aq MEK ppm out	Aq *p*-xyl ppm in	Aq *p*-xyl ppm out
0	1212.6	605.2	29.30	88.54	0	0.13
1	1152.3	172.3	140.20	160.66	0	0.39
2	1174.8	143.3	132.15	147.19	0	0.00
3	1121.6	127.7	136.72	126.19	0.15	0.08
4	1125.2	78.8	116.76	130.93	0.69	0.46
5	1118.5	110.2	94.68	86.99	0.81	
6	1141.7	162.9	96.00	96.74	0.95	0.69

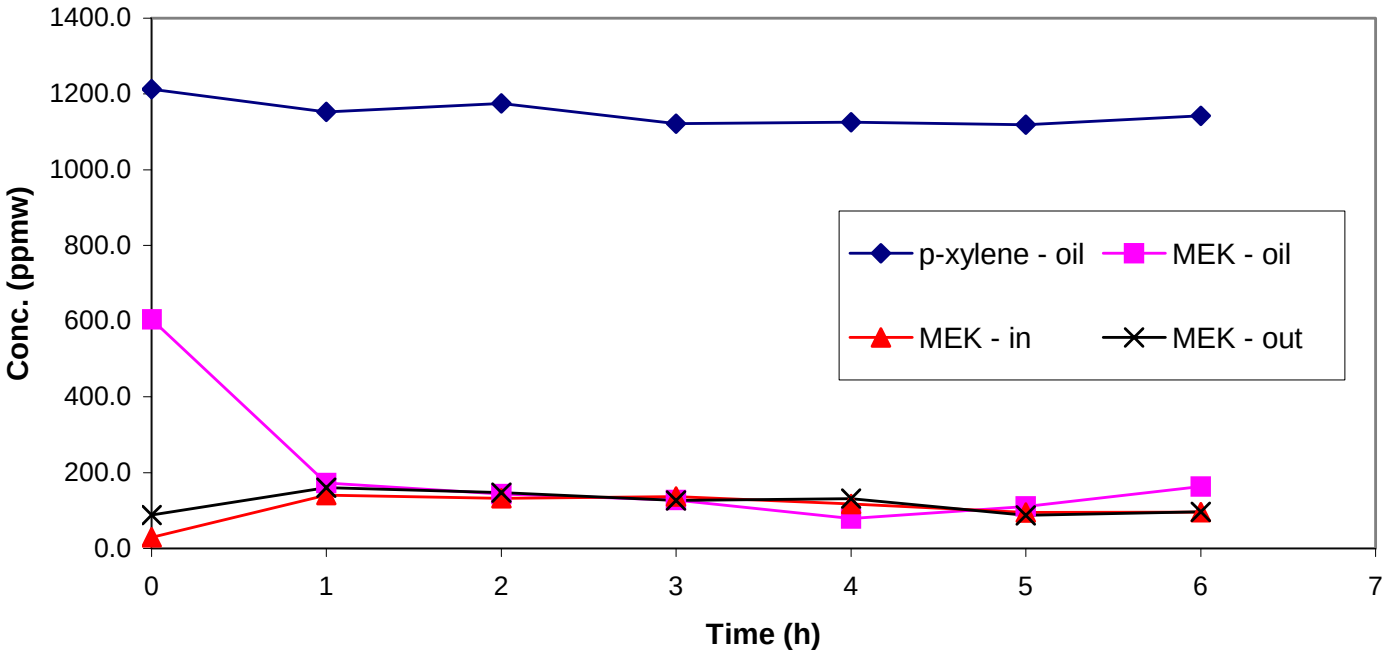

Figure B-46. SB5: Degradation of MEK and *p*-xylene in a Staged Bioreactor - 1000 ppm Case

Table B-47. SB6: Degradation of *m*-xylene, *p*-xylene, Butyl Acetate and MEK in a Staged Bioreactor

Time hour	Oil xyl ppm	Oil MEK ppm	Oil BA ppm	Aq xyl ppm in	Aq xyl ppm out	Aq MEK ppm in	Aq MEK ppm out	Aq BA ppm in	Aq BA ppm out
0	1832.8	349.3	301.1	0	0	21.99	50.6	0.45	1.52
1	1761.7	135.9	0.0	0	0	62.17	66.4	0.88	1.11
2	1783.3	0.0	0.0	0.89	0.11	62.85	61.58	0.93	0.94
3				0.98	0.76	58.67	58.38	0.81	0.6
4	1717.1	0.0	0.0	1.08	0.56	51.99	58.04	0.62	0.47
5	1632.2	0.0	0.0	1.43	0.26	52.51	51.54	0.47	0.43
6	1714.3	0.0	0.0	1.51	1.58	48.91	50.76	0.22	0.16
7	1630.1	0.0	0.0	1.5	0.98	50.43	48.06	0.07	0
8	1440.9	0.0	0.0						
24				0	0	3.67	2.77	0	0

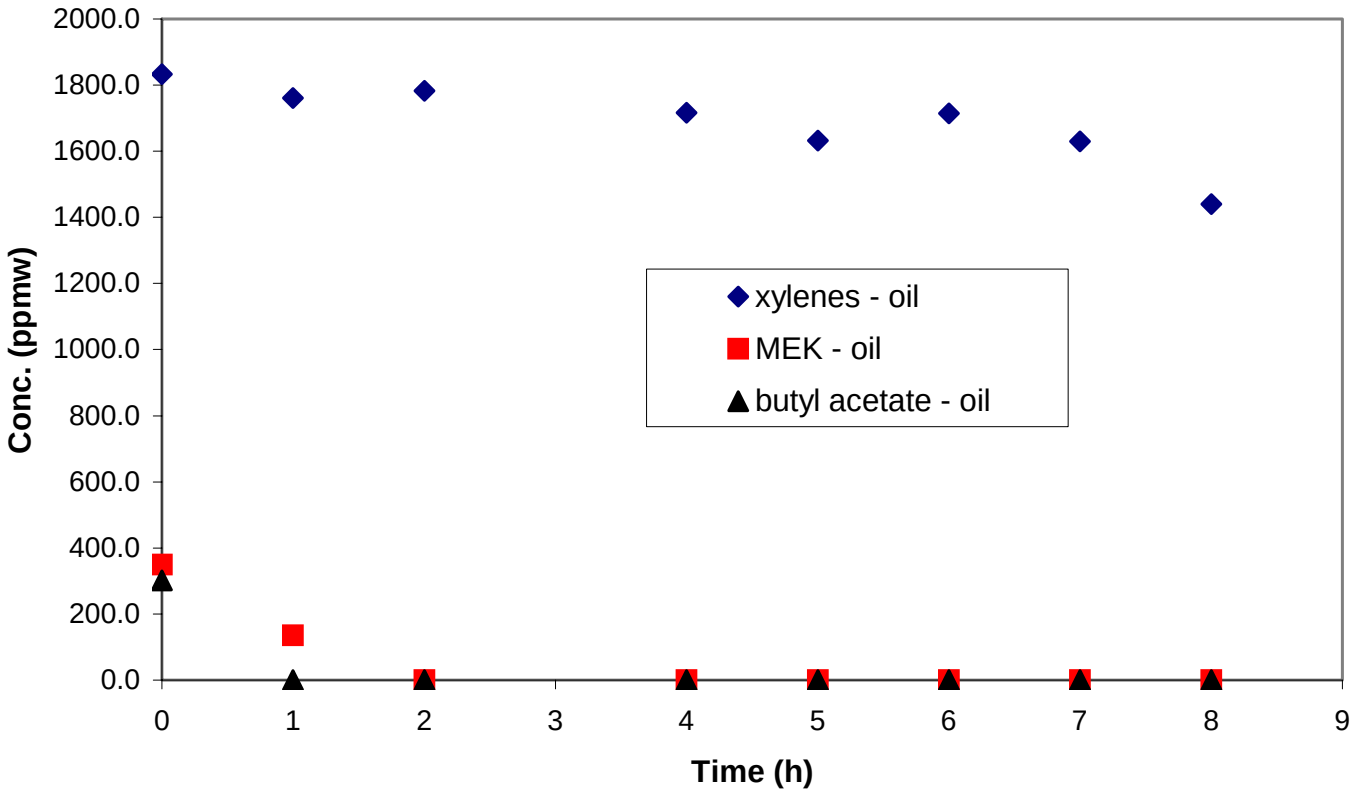

Figure B-47. SB6: Degradation of *m*-xylene, *p*-xylene, Butyl Acetate and MEK in a Staged Bioreactor

Table B-48. SB7: Degradation of VOCs in Oil Generated from Spray Booth Tests Containing BA, EB, *m*-xyl, o-xyl

Time hour	Oil MEK ppm MEK	Oil BA ppm BA	Oil EB ppm EB	Oil *m*-xyl ppm *m*-xyl	Oil *o*-xyl ppm o-xyl	Aq MEK ppm in	Aq MEK ppm out	Aq BA ppm in	Aq BA ppm out	Aq EB ppm in	Aq EB ppm out	Aq *m*-xyl ppm in	Aq *m*-xyl ppm out	Aq *o*-xyl ppm in	Aq *o*-xyl ppm out
0	0.0	256.0	105.0	129.0	355.7	0	0	0	0	0	0	0	0	0	0
1	0.0	114.1	100.7	130.4	340.0	0	0.97	0	0	0	0	0	0	0	0.414
2.08	0.0	0.0	98.1	130.9	333.7	0		4.15	3.50	0	0	0	0	0.352	0
3.08	0.0	0.0	96.4	127.0	332.5	0.81	1.76	2.63	2.54	0	0	0	0	0.348	0.364
4	0.0	0.0	94.1	124.1	328.7										
5	0.0	0.0	92.1	126.0	325.4										
6.25	0.0	0.0	91.8	129.4	324.6										
7	0.0	0.0	95.4	128.0	339.2										
23.8	0.0	0.0	91.3	124.4	328.7										

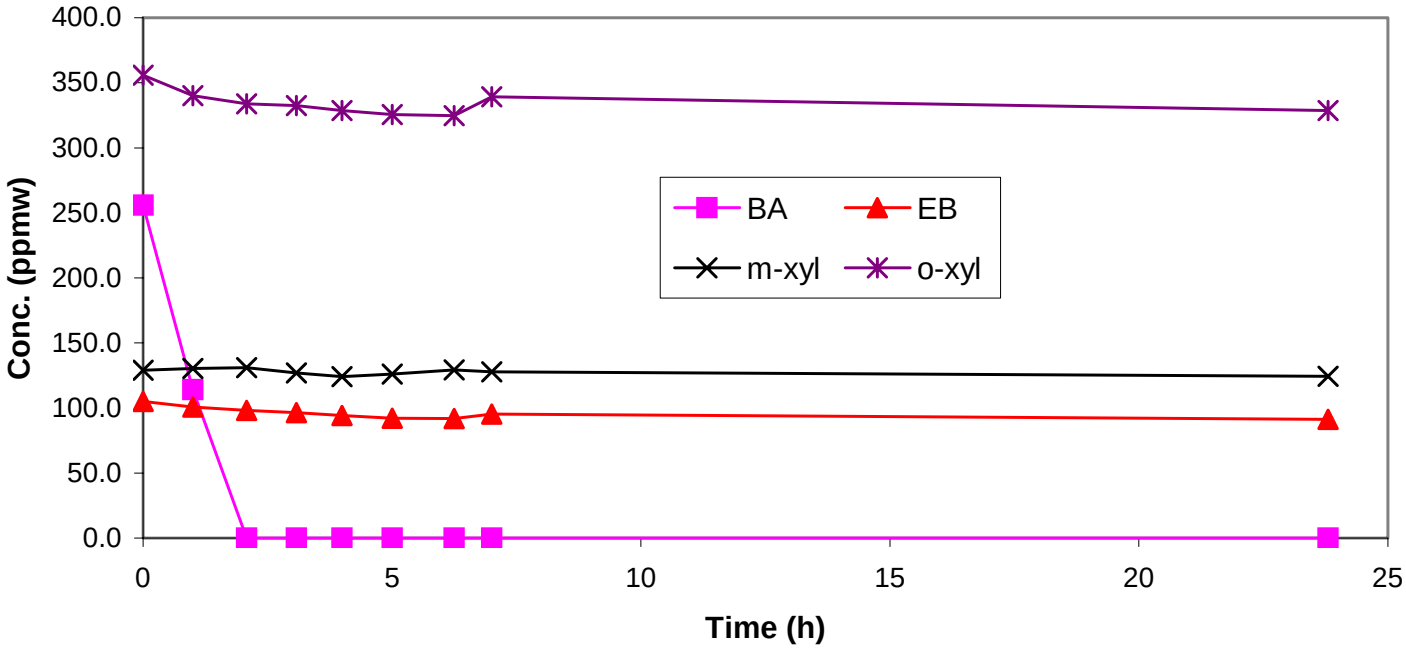

Figure B-48. SB7: Degradation of VOCs in Oil Generated from Spray Booth Tests Containing BA, EB, *m*-xyl, o-xyl

Table B-49. SB8: Degradation of VOCs in Oil Run with Paint

SB8

Oil run for 1 hour with paint

31.08.00

Time hour	Oil MEK ppm MEK	Oil BA ppm BA	Oil EB ppm EB	Oil *m*-xyl ppm *m*-xyl	Oil *o*-xyl ppm o-xyl
0	0.0	0.0	35.9	186.5	18.4
1	0.0	0.0	35.2	174.7	38.1
2	0.0	0.0	34.5	171.2	28.7
3	0.0	0.0	34.4	167.6	13.7
4	0.0	0.0	34.2	164.2	38.2
5	0.0	0.0	34.9	165.5	40.9
6	0.0	0.0	33.7	160.4	14.8
24	0.0	0.0	33.9	153.9	35.8
25.75	0.0	0.0	33.6	143.1	34.4
27.75	0.0	0.0	33.3	142.5	32.0

Oil run for 2 hours with paint

05.09.00

Time hour	Oil MEK ppm MEK	Oil BA ppm BA	Oil EB ppm EB	Oil *m*-xyl ppm *m*-xyl	Oil *o*-xyl ppm o-xyl
0	132.5	100.8	40.7	183.1	49.6
1	0.0	0.0	40.5	179.9	43.6
2	0.0	0.0	39.8	178.1	41.3
3	0.0	0.0	41.4	185.7	44.5
4	0.0	0.0	39.1	172.8	37.0
23	0.0	0.0	39.9	174.8	34.8
24	0.0	0.0	39.3	171.0	31.6
25	0.0	0.0	38.8	168.4	30.2
25.8	0.0	0.0	38.1	168.4	30.8

Oil run for 2 hours with paint

11.09.00

Time hour	Oil MEK ppm MEK	Oil BA ppm BA	Oil EB ppm EB	Oil *m*-xyl ppm *m*-xyl	Oil *o*-xyl ppm o-xyl
0	131.4	84.1	39.6	158.8	44.9
1	0.0	0.0	39.6	158.4	39.9
2	0.0	0.0	38.7	153.8	34.7
3	0.0	0.0	38.8	156.1	35.2
4	0.0	0.0	39.2	157.2	36.5
5	0.0	0.0	39.2	158.5	34.6
76	0.0	0.0	37.9	312.1	27.0

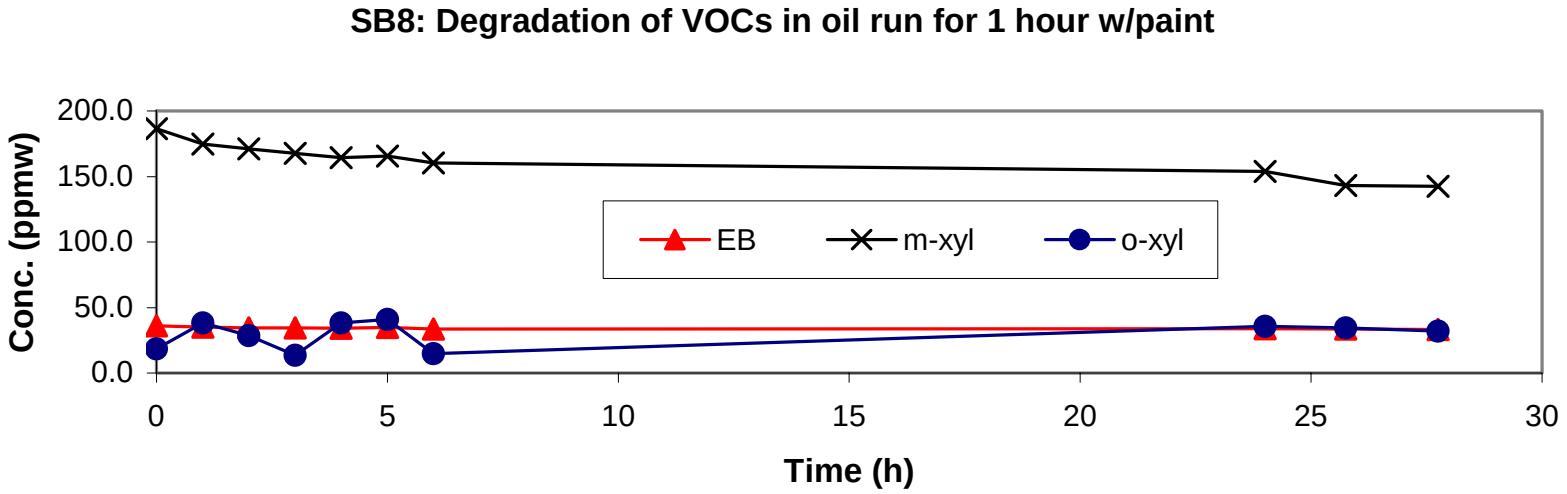

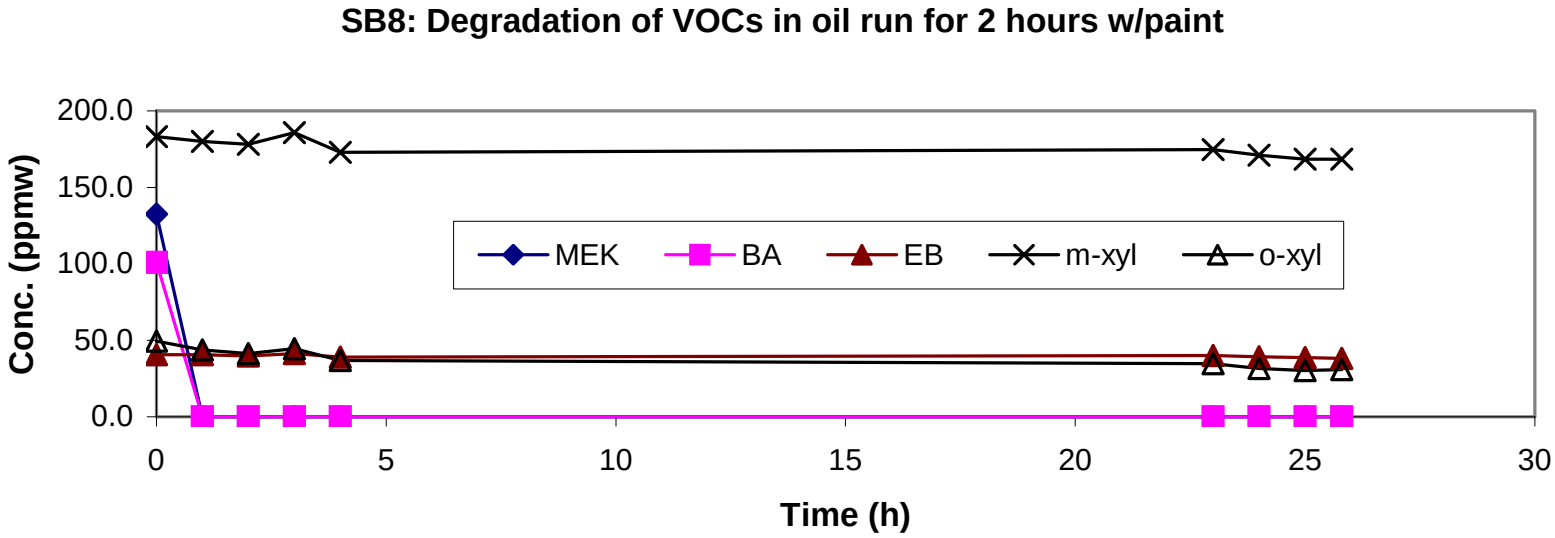

Figure B-49. SB8: Degradation of VOCs in Oil Run with Paint

APPENDIX C

PILOT SCALE DATA

Table C-1. AMT Modules; Pilot Test 1

Arrangement : Two Banks of Five Modules in Series
Oil : 5 PSIg Delivered, 5.0 Centistokes Viscosity, 3.8 L/min Oil Flow
Air : 44.5 ft^3/min

8/29/00					
Time	Inlet PPM		Time	Outlet PPM	
3:29 PM	-0.88285		3:31 PM	2.51195	
3:33 PM	-1.2429		3:35 PM	2.5634	
3:37 PM	-1.19145		3:39 PM	1.7404	
3:41 PM	50.70783		3:43 PM	61.7152	
3:45 PM	311.5931		3:47 PM	118.4495	
3:49 PM	336.0768		3:51 PM	135.9379	
3:53 PM	356.3427		3:55 PM	151.3174	
3:57 PM	324.8637		3:59 PM	155.2265	
4:01 PM	284.8976		4:03 PM	153.8892	
4:05 PM	312.0046		4:07 PM	163.3021	
4:09 PM	296.4193		4:11 PM	164.948	
4:13 PM	293.899		4:15 PM	169.0629	
4:17 PM	287.8295		4:19 PM	170.4003	
4:21 PM	281.3485		4:23 PM	171.7376	
4:25 PM	274.3017		4:27 PM	169.8345	
4:29 PM	258.9737		4:31 PM	171.3261	
4:33 PM	261.5455		4:35 PM	173.6922	
4:37 PM	359.8918		4:39 PM	191.5406	
4:41 PM	563.477		4:43 PM	221.8881	
4:45 PM	598.5051		4:47 PM	241.4339	
4:49 PM	568.6206		4:51 PM	249.3551	
4:53 PM	581.2225		4:55 PM	259.3852	
4:57 PM	570.3694		4:59 PM	271.7813	
5:01 PM	548.7662		5:03 PM	272.0899	
5:05 PM	554.2184		5:07 PM	277.9023	
5:09 PM	574.793		5:11 PM	208.8232	
5:13 PM	12.69633		5:15 PM	29.51605	
5:17 PM	5.392425		5:19 PM	41.24355	
5:21 PM	951.5129		5:23 PM	63.36118	
5:25 PM	15.06245		5:27 PM	201.5707	
5:29 PM	32.08785		5:31 PM	193.2895	
5:33 PM	34.814		5:35 PM	179.5559	
5:37 PM	35.7913		5:39 PM	168.0342	
5:41 PM	33.21948		5:43 PM	159.3929	
5:45 PM	33.52808		5:47 PM	150.7515	
5:49 PM	32.1393		5:51 PM	141.1844	
5:53 PM	31.47063		5:55 PM	135.3207	
5:57 PM	31.93355		5:59 PM	126.1135	
6:01 PM	29.51605		6:03 PM	118.861	
6:05 PM	28.02438		6:07 PM	113.5631	
6:09 PM	26.78993		6:11 PM	107.8537	
6:13 PM	18.35438		6:15 PM	50.91358	
6:17 PM	11.87338		6:19 PM	21.2348	
6:21 PM	9.301575		6:23 PM	14.34235	
6:25 PM	8.272825		6:27 PM	11.5133	
6:29 PM	7.346975		6:31 PM	10.536	

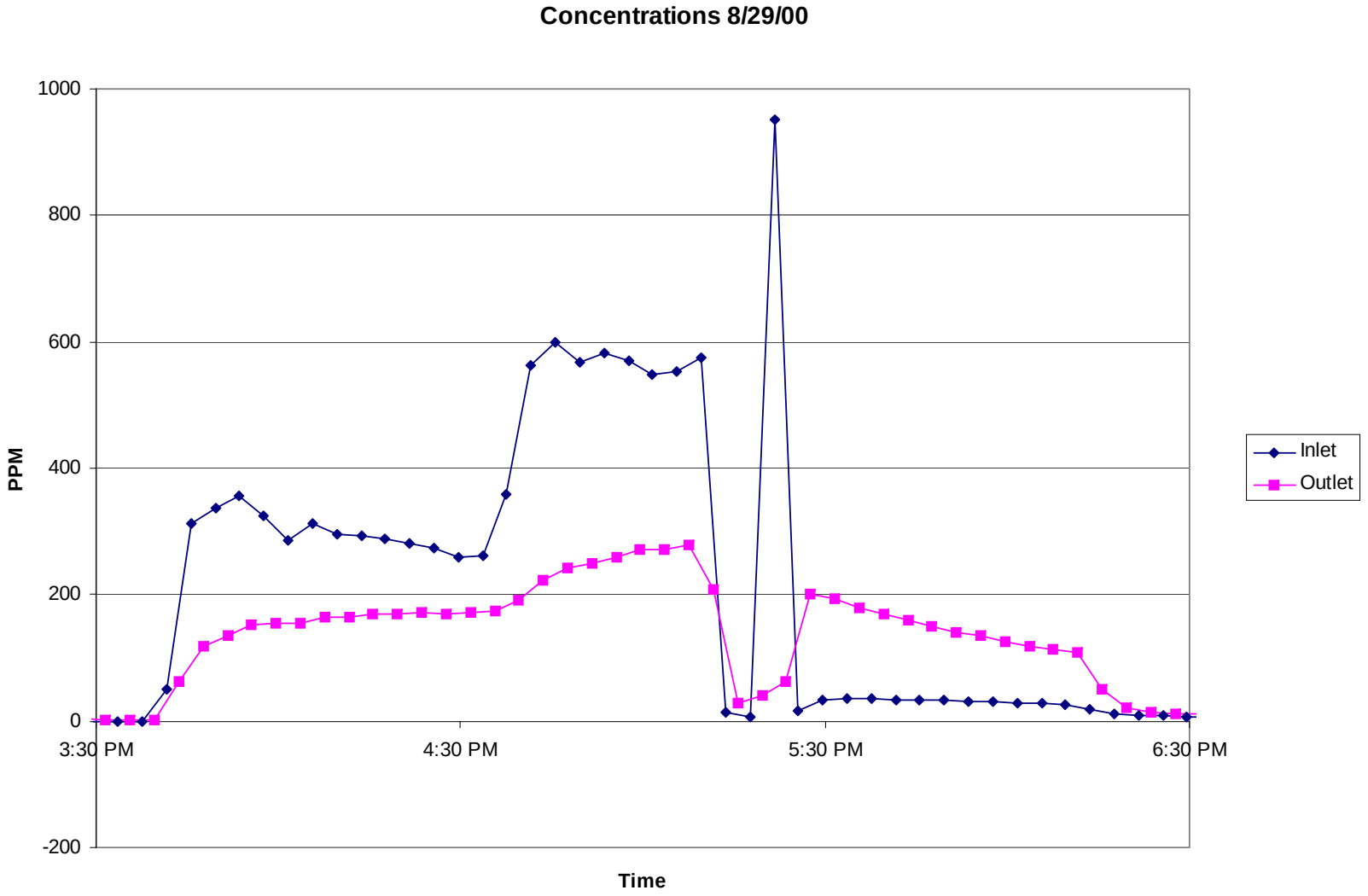

Figure C-1. AMT Modules, Pilot Test 1, 44.5 ft^3/min Air, 3.8 L/min Oil Flow

Table C-2A. AMT Modules; Pilot Test 2

Arrangement : Two Banks of Five Modules in Series
Oil : 7 PSIg Delivered, 5.0 Centistokes Viscosity, 5.5 L/min Oil Flow
Air : 44.5 ft^3/min

8/30/00 A					
Time	Inlet PPM		Time	Outlet PPM	
12:05 PM	-1.24288		12:03 PM	-0.00842	
12:09 PM	-1.29433		12:07 PM	-0.47138	
12:13 PM	-1.29433		12:11 PM	-0.26563	
12:17 PM	-1.19145		12:15 PM	-0.21418	
12:21 PM	-1.19145		12:19 PM	-0.21418	
12:25 PM	-1.5515		12:23 PM	-0.47135	
12:29 PM	-1.44865		12:27 PM	-0.31703	
12:33 PM	-1.2429		12:31 PM	-0.31703	
12:37 PM	-1.2429		12:35 PM	-0.31705	
12:41 PM	-1.19145		12:39 PM	-0.16275	
12:45 PM	-1.03713		12:43 PM	-0.11128	
12:49 PM	-1.14003		12:47 PM	-0.5228	
12:53 PM	-1.34575		12:51 PM	-0.00843	
12:57 PM	-1.50005		12:55 PM	-0.52278	
1:01 PM	-1.5515		12:59 PM	-0.41993	
1:05 PM	-1.24288		1:03 PM	-0.5228	
1:09 PM	-0.98573		1:07 PM	-0.21415	
1:13 PM	-1.50008		1:11 PM	-0.21415	
1:17 PM	-1.34578		1:15 PM	-0.16273	
1:21 PM	-1.55153		1:19 PM	-0.3685	
1:25 PM	-1.5515		1:23 PM	0.043	
1:29 PM	-0.8314		1:27 PM	-0.16273	
1:33 PM	-1.39723		1:31 PM	-0.62565	
1:37 PM	-1.55148		1:35 PM	-0.21418	
1:41 PM	-1.0886		1:39 PM	-0.05988	
1:45 PM	-1.3972		1:43 PM	-0.26558	
1:49 PM	-1.50008		1:47 PM	-0.2656	
1:53 PM	-1.3972		1:51 PM	-0.36845	
1:57 PM	-1.14003		1:55 PM	-0.0084	
2:01 PM	-1.34575		1:59 PM	-0.2656	
2:05 PM	-0.98573		2:03 PM	-0.21418	
2:09 PM	-1.2429		2:07 PM	-0.47135	
2:13 PM	-1.39723		2:11 PM	-0.41995	
2:17 PM	-1.44863		2:15 PM	-0.5742	
2:21 PM	-1.14		2:19 PM	-0.16273	
2:25 PM	-1.0886		2:23 PM	-0.47135	
2:29 PM	-2.16875		2:27 PM	-0.6771	
2:33 PM	196.6328		2:31 PM	93.24573	
2:37 PM	172.4577		2:35 PM	189.8947	
2:41 PM	-2.06588		2:39 PM	-2.37453	
2:45 PM	28.17873		2:43 PM	196.1699	
2:49 PM	-3.5575		2:47 PM	2.15195	
			2:51 PM	-3.40318	

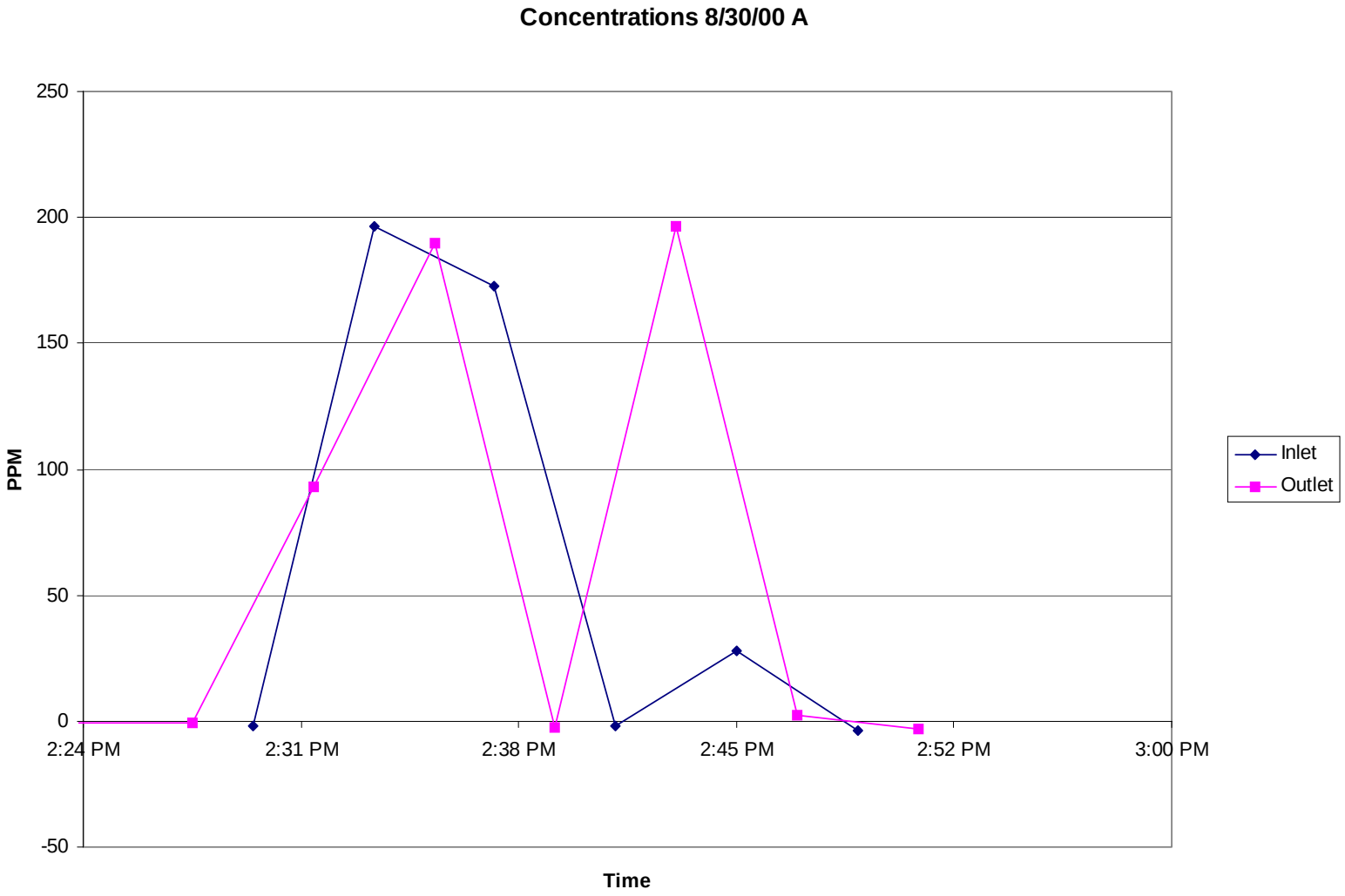

Figure C-2A. AMT Modules, Pilot Test 2, 44.5 ft^3/min Air, 5.5 L/min Oil Flow

Table C-2B. AMT Modules; Pilot Test 2B

Arrangement : Two Banks of Five Modules in Series
Oil : 7 PSIg Delivered, 5.0 Centistokes Viscosity, 5.5 L/min Oil Flow
Air : 44.5 ft^3/min

8/30/00 B					
Time	Inlet PPM		Time	Outlet PPM	
5:29 PM	-2.2202		5:32 PM	21.02905	
5:34 PM	3.38635		5:37 PM	7.44985	
5:39 PM	3.9522		5:42 PM	19.7946	
5:44 PM	22.1092		5:47 PM	9.661625	
5:49 PM	95.35458		5:52 PM	132.5945	
5:54 PM	153.4262		5:57 PM	51.89088	
5:59 PM	89.18223		6:02 PM	51.0679	
6:04 PM	1001.612		6:07 PM	465.2335	
6:09 PM	1001.715		6:12 PM	217.0531	
6:14 PM	330.4188		6:17 PM	210.572	
6:19 PM	362.4637		6:22 PM	205.7885	
6:24 PM	335.511		6:27 PM	195.3469	
6:29 PM	281.8629		6:32 PM	181.1504	
6:34 PM	257.8421		6:37 PM	171.5319	
6:39 PM	229.9121		6:42 PM	266.8949	
6:44 PM	657.9141		6:47 PM	302.9003	
6:49 PM	678.2829		6:52 PM	315.3479	
6:54 PM	643.2548		6:57 PM	328.9271	
6:59 PM	194.061		7:02 PM	95.61178	
7:04 PM	92.57703		7:07 PM	53.74258	
7:09 PM	9.250125		7:12 PM	40.2148	
7:14 PM	60.275		7:17 PM	929.0352	
7:19 PM	45.97568		7:22 PM	1.226075	
7:24 PM	-2.2716		7:27 PM	196.1184	
7:29 PM	15.57678		7:32 PM	-1.44863	
7:34 PM	-2.16873		7:37 PM	-2.37453	
7:39 PM	-1.91158		7:42 PM	-2.58023	
7:44 PM	-3.24888		7:47 PM	195.0383	
7:49 PM	6.88405		7:52 PM	4.517975	
7:54 PM	2.923475		7:57 PM	13.41645	
7:59 PM	13.51935		8:02 PM	12.69633	
8:04 PM	12.49063		8:07 PM	12.28488	
8:09 PM	12.64493		8:12 PM	11.4619	
8:14 PM	11.30755		8:17 PM	11.2047	
8:19 PM	11.41045		8:22 PM	10.69035	
8:24 PM	10.48463		8:27 PM	10.12455	
8:29 PM	9.6102		8:32 PM	9.97025	

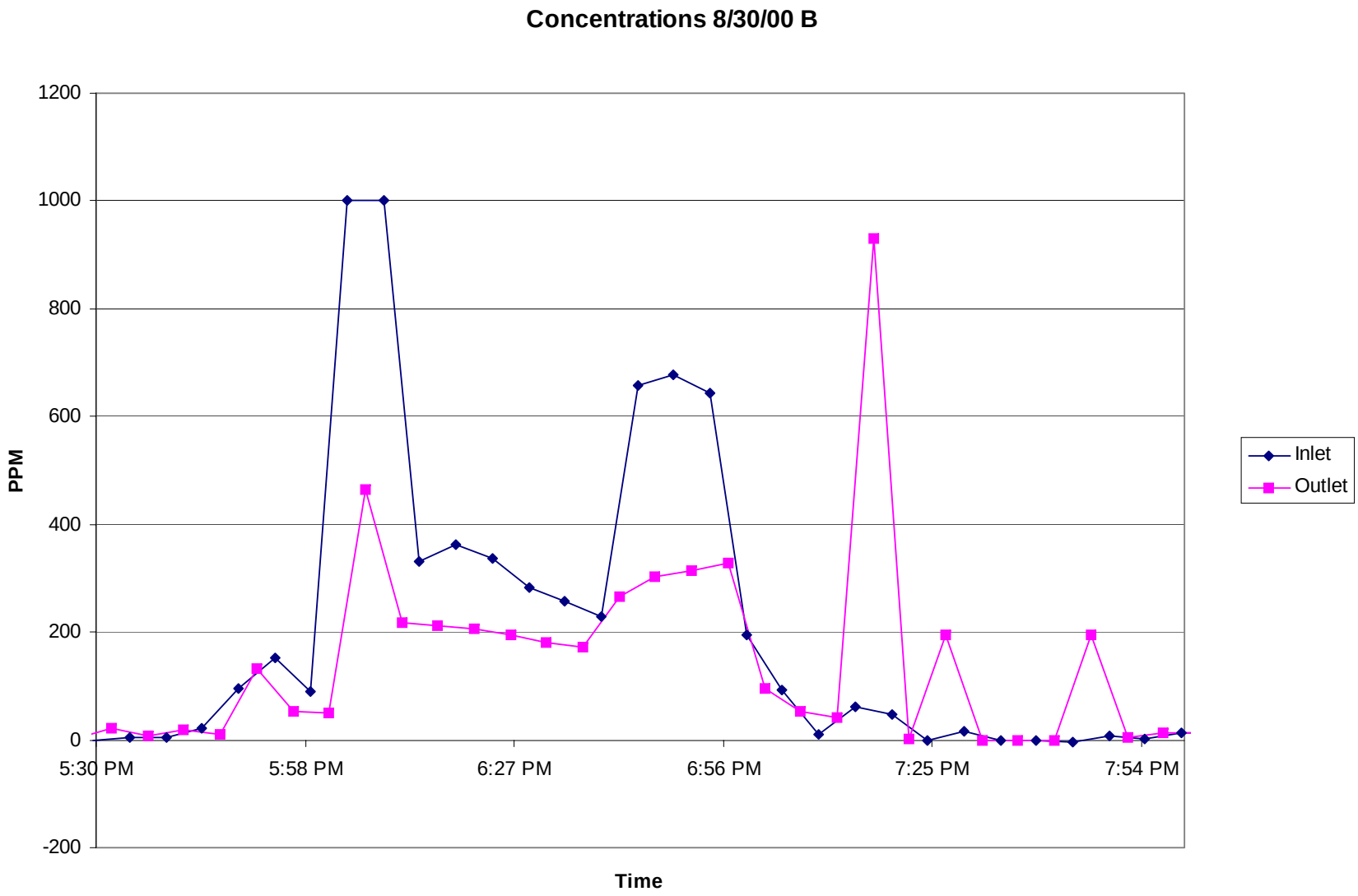

Figure C-2B, AMT Modules, Pilot Test 2A, 44.5 ft^3/min Air, 5.5 L/min Oil Flow

Table C-3. AMT Modules; Pilot Test 3

Arrangement : Two Banks of Five Modules in Series
Oil : 6 PSIg Delivered, 5.0 Centistokes Viscosity, 4.6 L/min Oil Flow
Air : 197 ft^3/min

Pilot Test 3 - CEM Data, 9/1/2000					
Time	Inlet PPM		Time	Outlet PPM	
3:59 PM	150.0315		4:02 PM	86.55898	
4:04 PM	264.4259		4:07 PM	148.0769	
4:09 PM	310.9244		4:12 PM	163.5592	
4:14 PM	308.044		4:17 PM	169.5258	
4:19 PM	34.45393		4:22 PM	33.57953	
4:24 PM	21.85203		4:27 PM	28.07583	
4:29 PM	29.36175		4:32 PM	1001.663	

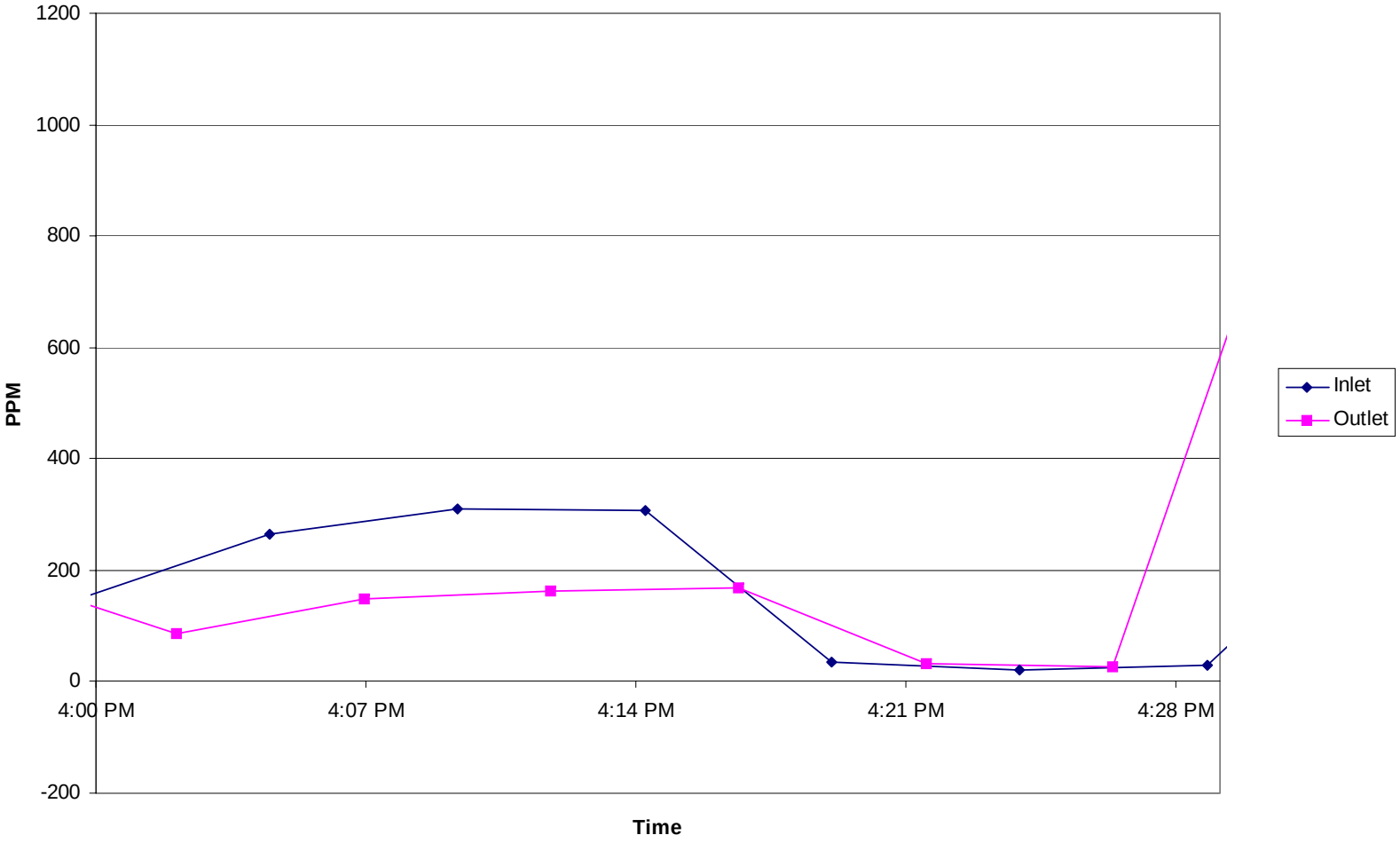

Figure C-3. AMT Modules, Pilot Test 3, 197 ft^3/min Air, 4.6 L/min Oil Flow

Table C-4. AMT Modules; Pilot Test 4

Arrangement : Two Banks of Five Modules in Series
Oil : 6 PSIg Delivered, 5.0 Centistokes Viscosity, 4.4 L/min Oil Flow
Air : 100 ft^3/min

Pilot Test 4 - CEM Data, 9/5/2000					
Time	Inlet PPM		Time	Outlet PPM	
3:34 PM	0.19735		3:37 PM	0.763125	
3:39 PM	0.557375		3:42 PM	0.968875	
3:44 PM	-0.57423		3:47 PM	0.81455	
3:49 PM	0.763125		3:52 PM	-1.8601	
3:54 PM	221.1165		3:57 PM	220.7565	
3:59 PM	221.3223		4:02 PM	-2.01443	
4:04 PM	-1.963		4:07 PM	421.4097	
4:09 PM	1002.486		4:12 PM	367.7616	
4:14 PM	221.4766		4:17 PM	-0.3685	
4:19 PM	-2.5288		4:22 PM	1001.149	
4:24 PM	219.1105		4:27 PM	220.9622	
4:29 PM	221.0136		4:32 PM	168.4971	
4:34 PM	0.608825		4:37 PM	4.312225	
4:39 PM	-3.30035		4:42 PM	-2.9403	
4:44 PM	196.2213		4:47 PM	911.804	
4:49 PM	910.9296		4:52 PM	912.8841	
4:54 PM	912.5241		4:57 PM	910.9295	
4:59 PM	911.9069		5:14 PM	908.8097	
5:17 PM	385.4817		5:19 PM	3.919225	
5:22 PM	2.898575		5:24 PM	3.306825	
5:27 PM	193.8074		5:29 PM	18.66733	
5:32 PM	-0.41845		5:34 PM	179.2634	
5:37 PM	3.000675		5:39 PM	4.5316	
5:42 PM	3.51095		5:44 PM	3.255825	
5:47 PM	3.357875		5:49 PM	3.562025	
5:52 PM	3.45995		5:54 PM	3.459925	
5:57 PM	3.306825		5:59 PM	3.51095	
6:02 PM	3.459925		6:04 PM	3.00065	
6:07 PM	2.337225		6:09 PM	2.082075	
6:12 PM	2.643425		6:14 PM	3.20475	
6:17 PM	3.613025		6:19 PM	3.20475	
6:22 PM	3.562		6:24 PM	3.562	
6:27 PM	3.61305		6:29 PM	3.30685	
6:32 PM	3.408875		6:34 PM	4.225425	
6:37 PM	4.42955		6:39 PM	7.899675	
6:42 PM	14.38068		6:44 PM	40.1516	
6:47 PM	169.5675		6:49 PM	226.8758	
6:52 PM	760.8183		6:54 PM	175.283	
6:57 PM	465.5501		6:59 PM	358.2309	
7:02 PM	74.4958		7:04 PM	336.1853	
7:07 PM	284.7966		7:09 PM	215.9041	
7:12 PM	200.8498		7:14 PM	151.6044	
7:17 PM	257.2906		7:19 PM	117.9236	
7:22 PM	157.7792		7:24 PM	144.0007	
7:27 PM	19.38175		7:29 PM	45.5099	
7:32 PM	990.1029		7:34 PM	997.0432	
7:37 PM	68.32098		7:39 PM	488.5653	
7:42 PM	18.66733		7:44 PM	47.4491	
7:47 PM	9.9409		7:49 PM	37.39588	
7:52 PM	8.409975		7:54 PM	31.27213	
7:57 PM	6.368725		7:59 PM	24.9952	
8:02 PM	6.6239		8:04 PM	34.12985	
8:07 PM	995.257		8:09 PM	167.22	
8:12 PM	50.91923		8:14 PM	59.9518	
8:17 PM	23.9746		8:19 PM	79.95613	
8:22 PM	59.59458		8:24 PM	70.51533	
8:27 PM	57.80848		8:29 PM	58.82913	
8:32 PM	46.4795		8:34 PM	46.37743	
8:37 PM	45.5609		8:39 PM	44.02998	
8:42 PM	39.3861		8:44 PM	41.73355	
8:47 PM	43.92793		8:49 PM	41.58045	
8:52 PM	41.88668		8:54 PM	42.19285	
8:57 PM	39.3861		8:59 PM	39.94743	
9:02 PM	41.42738		9:04 PM	38.87578	

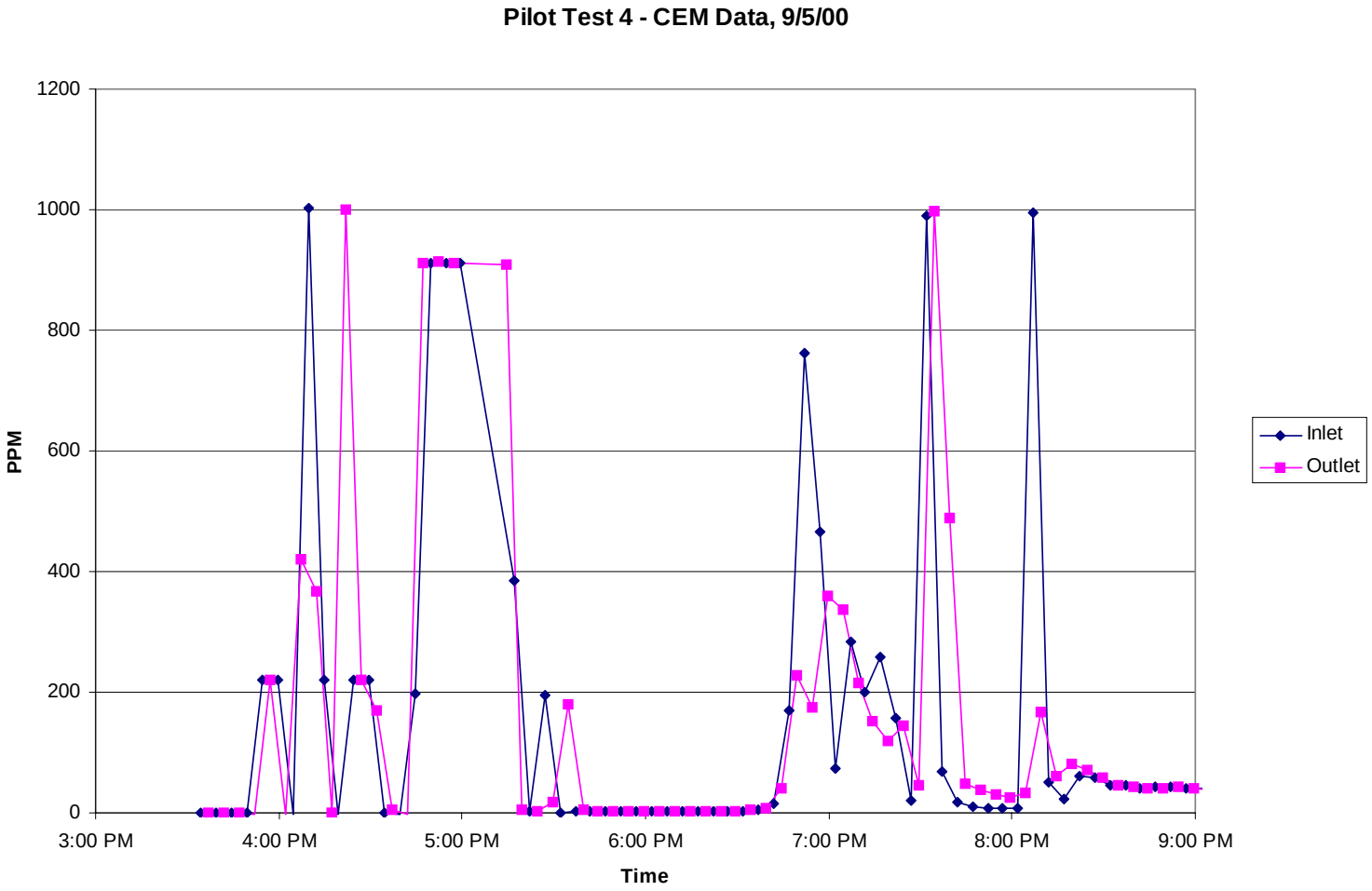

Figure C-4. AMT Modules, Pilot Test 4, 100 ft^3/min Air, 4.4 L/min Oil Flow

Table C-5. AMT Modules; Pilot Test 5

Arrangement : Two Banks of Five Modules in Series
Oil : 5.5 PSIg Delivered, 5.0 Centistokes Viscosity, 3.85 L/min Oil Flow
Air : 100 ft^3/min

Pilot Test 5 - CEM Data, 9/6/2000					
Time	Inlet PPM		Time	Outlet PPM	
7:02 PM	1.265575		6:59 PM	1.2656	
7:07 PM	32.13963		7:04 PM	1.980025	
7:12 PM	141.3981		7:09 PM	93.68363	
7:17 PM	297.1972		7:14 PM	237.4904	
7:22 PM	273.0083		7:19 PM	289.4404	
7:27 PM	372.6218		7:24 PM	269.7423	
7:32 PM	364.865		7:29 PM	399.2602	
7:37 PM	52.24605		7:34 PM	216.6185	
7:42 PM	307.7097		7:39 PM	116.8519	
7:47 PM	322.9171		7:44 PM	315.4155	
7:52 PM	65.15703		7:49 PM	311.9453	
7:57 PM	994.7977		7:54 PM	32.70095	
8:02 PM	96.03108		7:59 PM	275.9682	
8:07 PM	24.74005		8:04 PM	57.50228	
8:12 PM	16.9833		8:09 PM	19.8921	
8:17 PM	14.2276		8:14 PM	14.48273	
8:22 PM	12.6456		8:19 PM	13.00283	
8:27 PM	3.613025		8:24 PM	12.69663	
8:32 PM	2.2862		8:29 PM	91.18308	
8:37 PM	167.0669		8:34 PM	0.09185	
8:42 PM	0.908375		8:39 PM	6.9811	
8:47 PM	179.9269		8:44 PM	246.625	
8:52 PM	288.1647		8:49 PM	248.9215	
8:57 PM	271.0181		8:54 PM	284.2862	
9:02 PM	236.3167		8:59 PM	253.9736	

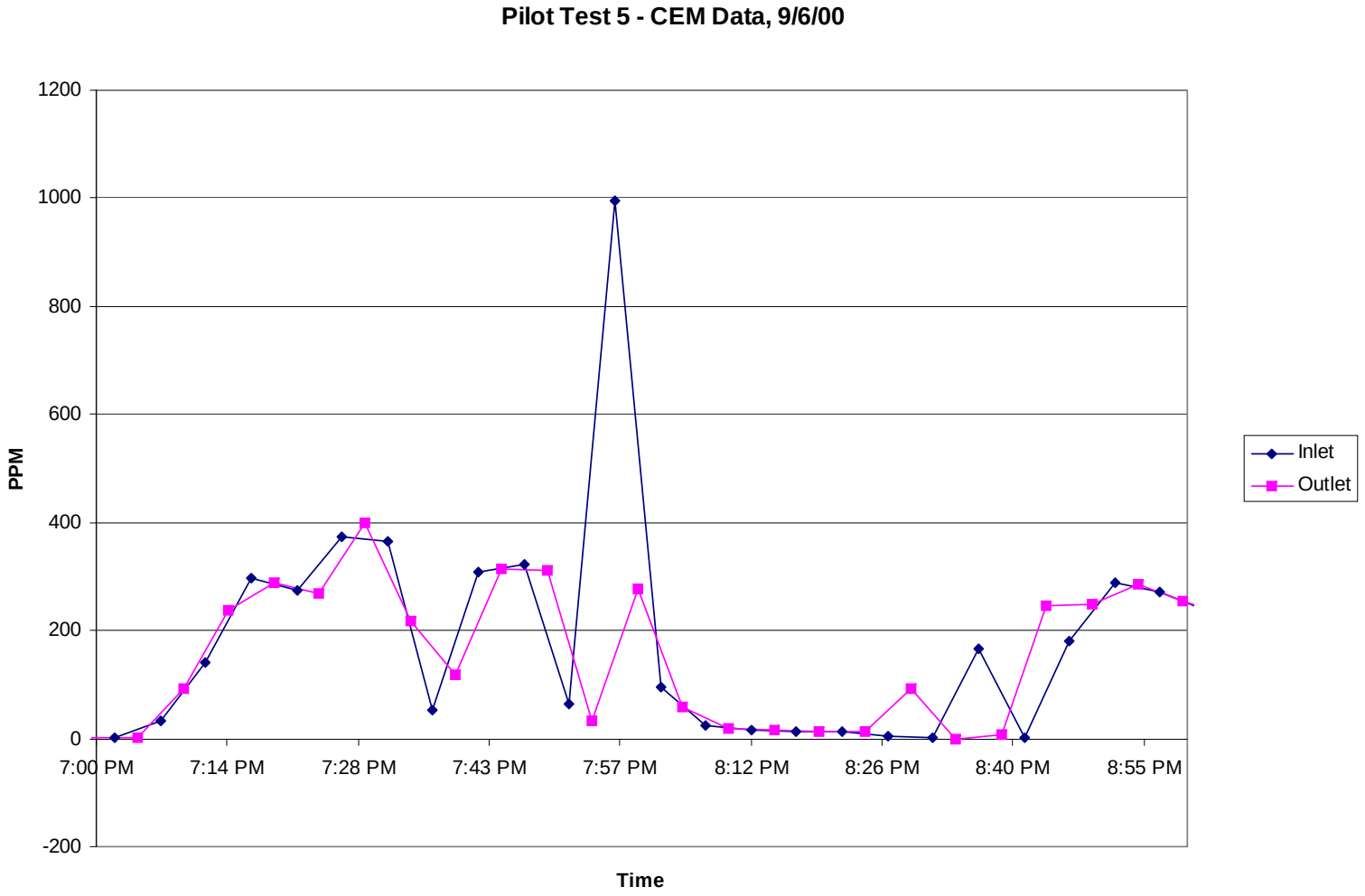

Figure C-5. AMT Modules, Pilot Test 5, 100 ft^3/min Air, 3.85 L/min Oil Flow

Table C-6 AMT Modules; Pilot Test 6

Arrangement : Two Banks of Five Modules in Series
Oil : 3.5 PSIg Delivered, 5.0 Centistokes Viscosity, 1.8 L/min Oil Flow
Air : 100 ft^3/min

Pilot Test 6 - CEM Data, 9/8/2000

Time	Inlet PPM	Time	Outlet PPM
3:29 PM	366.1821	3:32 PM	361.1989
3:34 PM	325.1082	3:37 PM	254.8396
3:39 PM	334.672	3:42 PM	247.4906
3:44 PM	320.6786	3:47 PM	247.6919
3:49 PM	295.3598	3:52 PM	229.9234
3:54 PM	276.4839	3:57 PM	89.58748
3:59 PM	33.56385	4:02 PM	50.67798

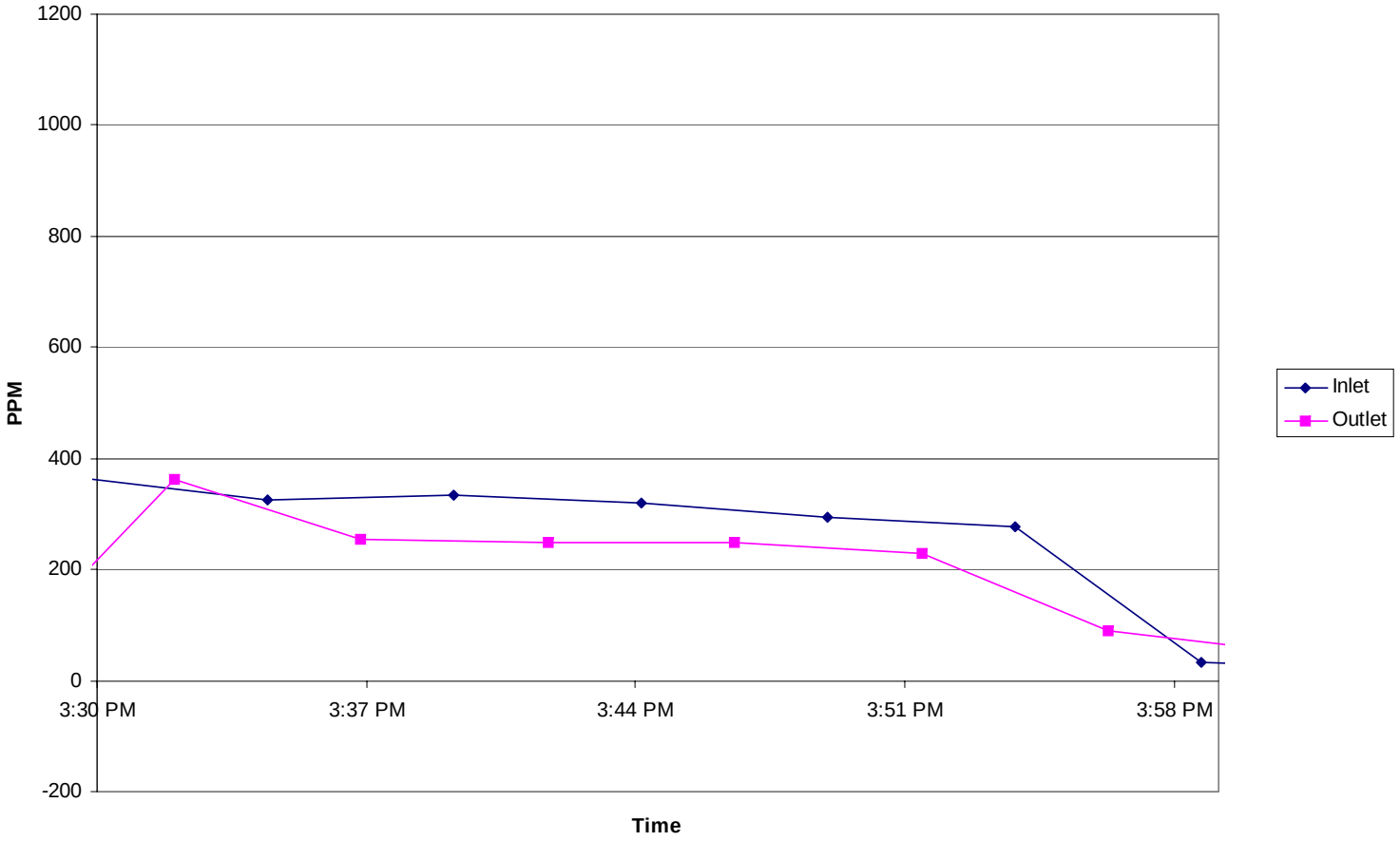

Figure C-6. AMT Modules, Pilot Test 6, 100 ft^3/min Air, 1.8 L/min Oil Flow

Table C-7 AMT Modules; Pilot Test 7

Arrangement : Two Banks of Five Modules in Series
Oil : 6.0 PSIg Delivered, 5.0 Centistokes Viscosity, 6.0 L/min Oil Flow
Air : 100 ft^3/min

Pilot Test 7 - CEM Data, 9/12/00

Time	Inlet PPM	Time	Outlet PPM
2:47 PM	225.8462	2:49 PM	183.0105
2:52 PM	234.5039	2:54 PM	187.9937
2:57 PM	229.118	2:59 PM	190.7119
3:02 PM	228.0106	3:04 PM	187.9938
3:07 PM	221.316	3:09 PM	144.4534
3:12 PM	28.42958	3:14 PM	47.70815
3:17 PM	13.32888	3:19 PM	38.4464

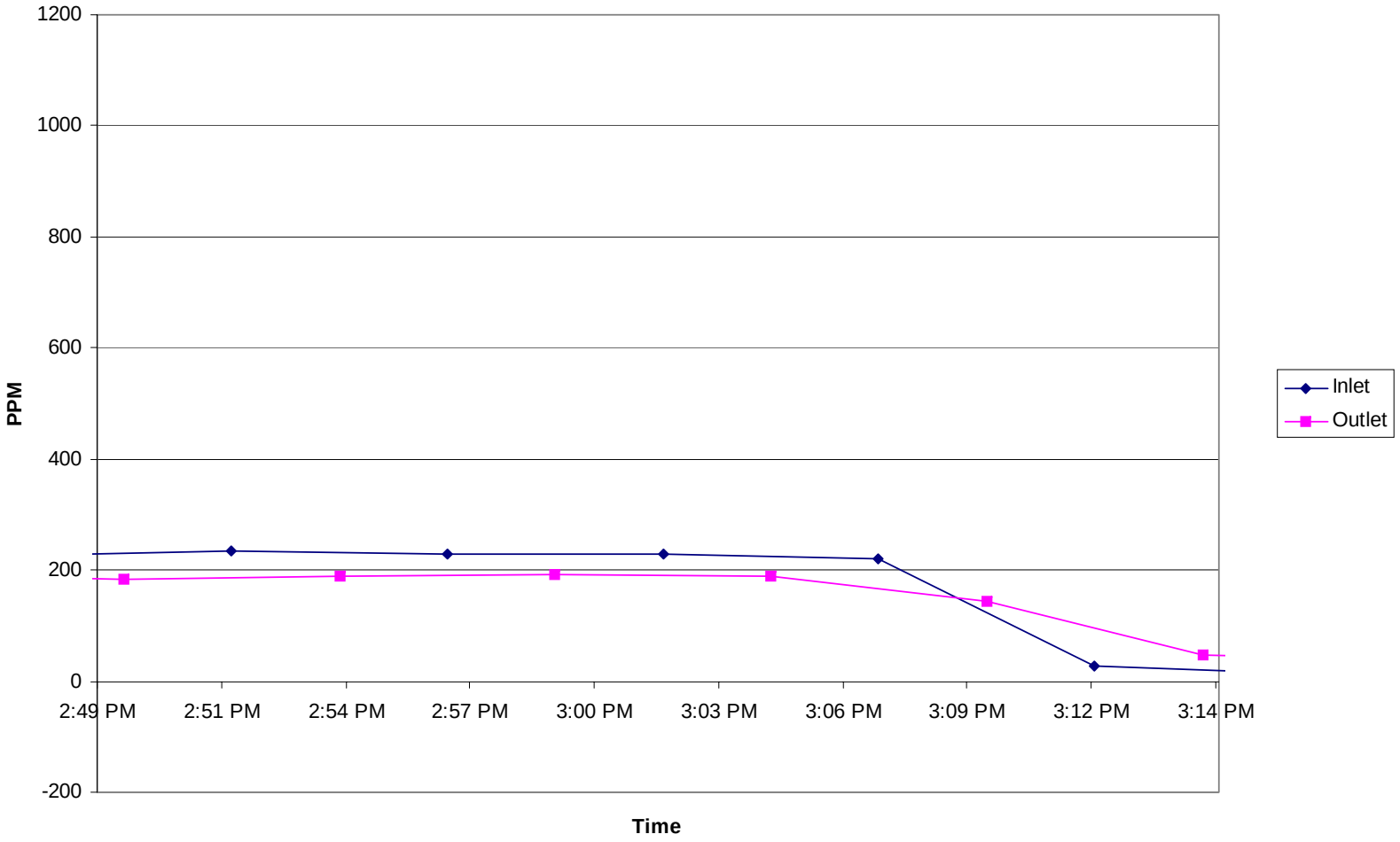

Figure C-7. AMT Modules, Pilot Test 7, 100 ft^3/min Air, 6.0 L/min Oil Flow

Table C-8 AMT Modules; Pilot Test 8

Arrangement : Two Banks of Five Modules in Series
Oil : 6.0 PSIg Delivered, 5.0 Centistokes Viscosity, 4.5 L/min Oil Flow
Air : 136 ft^3/min

Pilot Test 8 - CEM Data, 9/13/00

Time	Inlet PPM	Time	Outlet PPM
4:12 PM	-0.16108	4:09 PM	-0.1611
4:17 PM	100.8123	4:14 PM	0.090625
4:22 PM	275.9805	4:19 PM	298.984
4:27 PM	271.5007	4:24 PM	203.7992
4:32 PM	259.6215	4:29 PM	200.0743
4:37 PM	242.2556	4:34 PM	196.8025
4:42 PM	219.0509	4:39 PM	185.1246
4:47 PM	32.15445	4:44 PM	85.35928
4:52 PM	16.90273	4:49 PM	740.3273
4:57 PM	92.10428	4:54 PM	983.5494
5:02 PM	9.352375	4:59 PM	64.77195

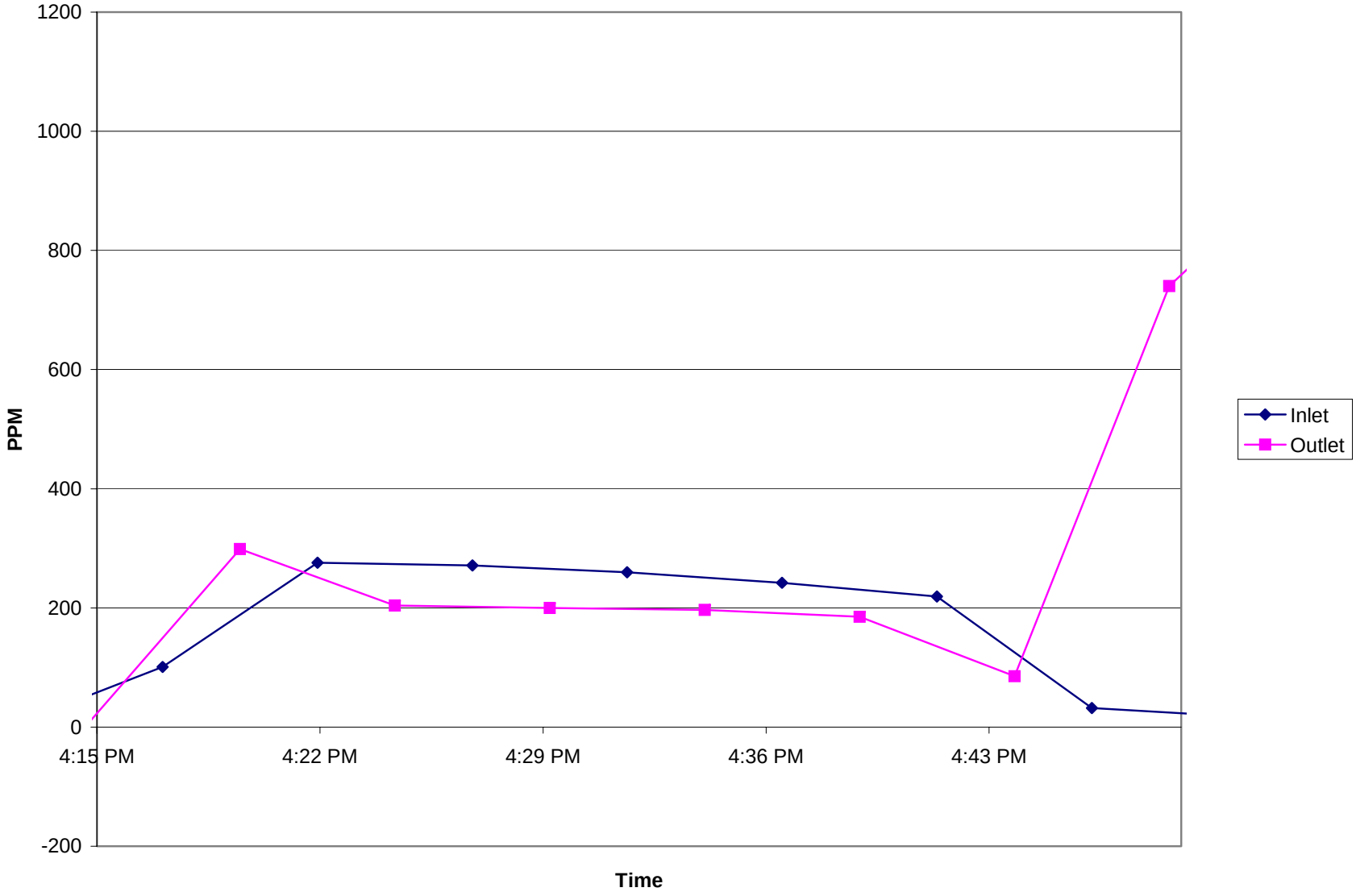

Figure C-8. AMT Modules, Pilot Test 8, 136 ft^3/min Air, 4.5 L/min Oil Flow